Exploring the adaptive capabilities of the brain following unilateral conductive hearing loss



Ana Isabel Sánchez Jiménez

Merton College, University of Oxford

A thesis submitted for the degree of

Doctor of Philosophy

Michaelmas 2023

Exploring the adaptive capabilities of the brain following unilateral conductive hearing loss

Ana Isabel Sánchez Jiménez

Merton College, University of Oxford

A thesis submitted for the degree of Doctor of Philosophy

Michaelmas, 2023

Plasticity in adulthood potentially allows the recovery of perceptual abilities following sensory impairments. Training-dependent recovery of sound localisation accuracy following unilateral conductive hearing loss has been widely used to study the adaptability of the auditory system. Previous studies have implicated the inferior colliculus (IC) in this plasticity, but have not examined whether neural correlates of training-induced plasticity are found in this midbrain structure.

To explore this question, we performed chronic electrophysiological recordings in the IC of ferrets while they were trained to adapt to unilateral hearing loss, induced by reversibly plugging one ear. We found that IC responses were initially disrupted by monaural hearing loss, which coincided with impaired localisation behaviour. With daily training, however, adaptive changes occurred in the spatial response properties of IC neurons and in the animals' localisation behaviour. Neural correlates of training-induced adaptation are therefore found in the IC, supporting its role in auditory spatial plasticity. These results also provide insight into how sound azimuth is encoded by IC neurons.

Demonstrating that training-dependent adaptation has potential therapeutic value for people with hearing disorders requires an understanding of the persistence and context dependence of this plasticity, and of the extent to which adaptation generalises to untrained sounds. By measuring the behavioural effects in ferrets of repeated periods of monaural occlusion in the same ear and then of the opposite ear, we show that adaptation leaves a "memory trace" that determines how localisation accuracy is affected when unilateral hearing loss is experienced again. To evaluate the generalisation of learning, we measured localisation accuracy after adaptation using different bandwidth stimuli presented in silence or against background noise. Our results show a positive relationship between generalisation and the degree of adaptation achieved. Finally, a virtual reality setup was developed for investigating these questions in human participants.

Acknowledgements

First and foremost, I would like to thank my supervisors, Andy King and Fernando Nodal for their constant support and guidance throughout my DPhil. Thank you, Andy, for providing me with the opportunity of joining the lab. It has been an absolute pleasure to work with such an inspiring group of people and undoubtedly, an enriching experience both personally and professionally. I am also deeply grateful to have been able to develop my scientific career under your guidance, you are an inspiration. Fernando, thank you for your constant support and trust, and for sharing your incredible expertise. Especially, thank you for your positivity and support during the hard pandemic days. You both have been exceptional mentors and have contributed to the growth of my passion for science, for that I am truly thankful.

I would also like to thank Vicky Bajo for sharing her expertise and advice and, very importantly, for the 'falcon idea'. Thank you also to Mattia Montanari for his help with the development of the virtual reality project and to Ben Willmore for his assistance with the decoding analysis. In addition, I would like to thank Sue Spires, for the help with the behavioural training and for taking such a good care of the ferrets. Thanks also go to the rest of the ANG group.

Nada de lo que soy a día de hoy habría sido posible sin el apoyo incondicional de mis padres, Pepe y Mari Feli, gracias por creer siempre en mí y hacer que crea[1]. Thank you to the rest of my family too, my brother Jose and my sister Ali, with special mention to my little nephew Hugo, seeing you grow these past few months has been a blessing.

Tim, no words could ever express how grateful I am of having you in my life. Our DPhils brought our lives together, and that is what I am most thankful for. Thank you for your love and support during these past years. I cannot wait to continue our lives together.

I would also like to thank Tim's family for welcoming me and making me feel like home, when mine was so far away.

[1]Nothing of what I am today would have been possible without the unconditional support of my parents, Pepe and Mari Feli, thank you for always believing in me and making me believe.

Thank you to my incredible friends, my daisies, Alba, Laura, Natalia, María Sanchiz and María Tormo, always there for each other unconditionally. Also thank you to my friends from Mairena, especially to Isa, for being the most amazing friend, and to Paola, my best Erasmus discovery and who convinced me to come to Oxford. I am also grateful for the amazing group of the friends that I made when I moved to the UK, my "LaCaixa" friends, they made the journey easier. Special thanks also go to my best furry friend, Firu, thank you for your unconditional love and for always receiving me with excitement even after being away for months. Finally, thank you to the Oxford University Contemporary Dance Team, it was amazing dancing with such an incredible group of talented people and achieving the first ever Varsity win with them; and to the rest of the people in Oxford who made these past years some of the best of my life.

Last but not least, I would like to thank each of the lovely ferrets that made the work for this thesis possible: Leitrim, Clare, Donegal, Cavan, Pooh, Roo, Tiger, Woozle, Gamora, Nebula, Danvers, Romanoff, Kaikoura, Onewhero, Rangitoto and Tarawera. You deserve the biggest thank you.

Contributions

Chapter 2:

Sound localisation behaviour: hardware installed by Fernando Nodal (FN). Software written by Ana Sanchez Jimenez (ASJ) adapted from scripts written by FN. Behavioural training and testing performed by Ana Sanchez Jimenez (ASJ), Susan Spires (SS), Victoria Bajo (VB) and Fernando Nodal (FN) and Linus Milinski (LM).

Electrophysiology: surgeries performed by FN, VB, ASJ. Hardware installed by ASJ and FN. Software adapted by ASJ. Recordings performed by ASJ, FN. VB.

Histology: Perfusions performed by FN and ASJ. Histological processing by FN, VB and ASJ. Identification of recording sites FN and VB.

Chapter 3:

Data analysis performed by ASJ using MATLAB scripts by ASJ. Katherine Willard (KW) wrote scripts for the analysis of head orienting data.
This chapter has been published as *Sanchez Jimenez A, Willard KJ, Bajo VM, King AJ, Nodal FR. Persistence and generalization of adaptive changes in auditory localization behavior following unilateral conductive hearing loss. Front Neurosci. 2023 Feb 1;17:1067937.*

Chapter 4 and 5:

Data processing and analysis performed by ASJ. Population pattern decoder developed by Ben Willmore (BW) and implemented by ASJ.

Chapter 6:

Development of virtual reality setup by ASJ in collaboration with Mattia Montanari (MM)

Table of contents

1. GENERAL INTRODUCTION 1

1.1. Overview: perception and plasticity 1

1.2. Basis of sound localisation 3

1.2.1. Spatial cues for sound localisation 4

1.2.2. Neural processing of spatial cues 5

1.2.3. Models of auditory space coding 11

1.3. Investigating sensory plasticity: the earplug model 15

1.3.1. Behavioural properties of adaptation to unilateral conductive hearing loss 17

1.3.2. Plasticity processes involved in adaptation 19

1.4. Neural substrates of training-induced adaptation to UCHL 23

1.4.1. The role of auditory cortex and its descending connections 24

1.4.2. Plasticity in the inferior colliculus 26

1.5. Thesis overview 29

2. METHODS 32

2.1. Overview 32

2.2. Animal welfare 32

2.3. Sound localisation behaviour 34

2.3.1. Hardware and training 34

2.3.2. Adaptation to UCHL 37

2.3.3. Testing the persistence of adaptation 38

2.3.4. Testing the generalisation of adaptation 39

2.3.5. Testing the role of dynamic and spectral cues 40

2.3.6. Head orienting responses 41

2.3.7. Statistical analysis of behaviour 42

2.4. Electrophysiology recordings 42
2.4.1. General 42
2.4.2. Surgical implantation of Neuropixels probes 43
2.4.3. Hardware and training 45
2.4.4. Recordings of Frequency Response Areas 47
2.5. Data analysis of Neuropixels recordings 48
2.5.1. Data processing 48
2.5.2. Unit selection for data analysis 50
2.5.3. Single unit detection criteria 51
2.5.4. Spatial tuning 52
2.5.5. Population decoding analysis 52
2.5.6. Histology 54
2.5.7. Statistical analysis 56
3. PERSISTENCE AND GENERALISATION OF ADAPTIVE CHANGES IN AUDITORY LOCALISATION BEHAVIOUR FOLLOWING UCHL 57
3.1. Introduction 57
3.2. Results 61
3.2.1. Effects of sound localisation training on task performance 61
3.2.2. Behavioural adaptation to UCHL 62
3.2.3. Equivalent adaptation to occlusion of each ear 66
3.2.4. Adaptive learning is partially retained when spatial cues are altered again 69
3.2.5. Adaptation to UCHL in the contralateral ear 77
3.2.6. Adaptation to UCHL generalises beyond the training stimulus 80
3.2.7. Role of spectral cues and dynamic cues in adaptation to UCHL 85
3.3. Discussion 89
4. CHARACTERISATION OF NEURAL RESPONSES IN THE INFERIOR COLLICULUS OF THE FERRET IN NORMAL HEARING CONDITIONS 97

4.1. Introduction 97

4.2. Results 99

4.2.1. Recordings in the central nucleus of the inferior colliculus 99

4.2.2. Activity in the inferior colliculus in different listening conditions 104

4.2.3. Heterogeneity of responses in the IC 107

4.2.4. Modulation of IC responses by sound localisation task variables 112

4.2.5. Decoding azimuth location from data recorded in the IC 117

4.3. Discussion 132

4.4. Appendix 140

4.4.1. Supplementary figures 140

5. NEURAL CORRELATES OF ADAPTATION TO UNILATERAL CONDUCTIVE HEARING LOSS IN THE FERRET 149

5.1. Introduction 149

5.2. Results 152

5.2.1. Alteration of spatial cue processing following the onset of UCHL 152

5.2.2. Changes in response properties of neurons in the IC caused by UCHL 154

5.2.3. Neural activity in the IC during adaptation to a monaural earplug 158

5.2.4. Re-plugging and memory trace 163

5.2.5. Recovery of contralateral preference following earplug removal 166

5.2.6. Neural correlates of adaptation using population decoding analysis 169

5.3. Discussion 186

5.4. Appendix 195

5.4.1. Supplementary figures 195

6. FUTURE APPLICATIONS 200

6.1. Introduction 200

6.2. Sound localisation in virtual reality 202

6.2.1. The virtual environment 202
6.2.2. Virtual sound localisation task programming and execution 205
6.2.3. Real-time sound spatialisation 211
7. GENERAL DISCUSSION 213
7.1. Overview 213
7.1.1. Behavioural characterisation of adaptation to UCHL 214
7.1.2. Sound location encoding in the IC 217
7.1.3. Neural correlates of adaptation to UCHL in the IC 220
7.2. Future studies 222
REFERENCES 225

Abbreviations

A1	primary auditory cortex
AC	auditory cortex
am	amplitude modulated
ANF	auditory nerve fibers
BB	broadband
BF	best frequency
BIN	nucleus of the brachium of the inferior colliculus
CIA	central inhibitory area
CN	cochlear nucleus
CNIC	central nucleus of the inferior colliculus
Cu	cuneiform nucleus
DCIC	dorsal cortex of the inferior colliculus
DCN	dorsal cochlear nucleus
Ephys	electrophysiology
ERRF	equivalent rectangular receptive field
FRA	frequency response area
FSL	fist spike latency
GBC	globular bushy cells
GLMM	generalised linear mixed model
HRTF	head related transfer function
IC	inferior colliculus
ICx	external nucleus of the inferior colliculus
ILD	interaural level difference
i.m.	intramuscular
ISI	interspike interval
ITD	interaural time difference
LCIC	lateral cortex of inferior colliculus
LNTB	lateral nucleus of the trapezoid body
LSO	lateral superior olive
MGB	medial geniculate body
MI	mutual information
MNTB	medial nucleus of the trapezoid body
MSO	medial superior olive
MUA	multi-unit activity
NB	narrowband
PAG	periaqueductal grey
RMSE	root mean square error
RP	rostral pole
SBC	spherical bushy cells
SC	superior colliculus
s.c.	subcutaneous
sd	standard deviation
SE	standard error
SPL	sound pressure level
SOC	superior olivary complex
SUA	single unit activity

UCHL	unilateral conductive hearing loss
um	unmodulated
VCN	ventral cochlear nucleus
VR	virtual reality

1. General Introduction

1.1. Overview: perception and plasticity

Sensory systems are responsible for providing information about the world that surrounds us. Each sensory modality detects and encodes changes (in e.g., wavelength, pressure, vibration) in a specific form of energy from which our brain builds a perceptual representation of the world. In addition, the information provided by the different senses (vision, touch, hearing, etc) is used to guide our behaviour to interact with the physical world and if necessary, to update its perceptual representation to maximise our probability of survival. Although much is known about the organisation of the sensory systems, much is yet to be discovered about where, when, and how the brain bridges sensation and perception.

One of the main organisational principles common to most sensory systems, most likely because of the convenience of maintaining axons orderly as they grow/develop, is the topographic preservation along each sensory pathway of their specific sensory epithelium organisation. The sensory characteristic mapped onto such topographical representation varies from one sensory system to another (location for the visual and somatosensory and frequency for the auditory). Woven into that topographical representation for each sensory modality are other sensory dimensions that lack an explicit mapping representation and normally require a computation process to arise (e.g., distance in the visual system or location in the auditory to cite only two of the most studied) [see e.g. (Linton, 2023; van der Heijden et al., 2019)].

Within each sensory system different stimulus characteristics/dimensions can be encoded as either topographic or computational representations [e.g. (King et al., 1998)]. Therefore, it is expected that the emergence and consolidation of such representations might mature at different stages of development. To complicate matters more, we as individuals do not operate in terms of physical stimulus characteristics or attributes, but in perceptual ones. These perceptual representations might or might not have a direct correlation with a physical attribute (e.g. loudness and amplitude or pitch and periodicity in the auditory system). Depending on the complexity of those relationships, distinct temporal frameworks might be required to establish such representations, but more importantly, different levels of exposure or experience might be required to refine them (Paraouty et al., 2023).

The consequences of altered sensory experience during the early postnatal life highlight the experience dependency of the emergence and consolidation of sensory and perceptual representations in the brain and led to the definition of the critical periods as periods of enhanced plasticity (Mitchell & Maurer, 2022). Neural plasticity was thought to be mainly a requisite for the immature sensory systems to produce a stable representation of the world as the sense organs grow. However, once maturity is reached, neural plasticity is still necessary to adapt any perceptual representation of the world to an ever-changing environment (Ribic, 2020). Adult experience-dependent plasticity and perceptual learning have been described in multiple instances and sensory systems in response to practice on a particular sensory task (Irvine, 2018) and as a result of altered sensory input (Kacelnik et al., 2006).

The focus of this thesis is to explore some behavioural characteristics of adult-experience plasticity and its neural basis using a well-established animal model of spatial hearing adaptation to unilateral conductive hearing loss (UCHL).

1.2. Basis of sound localisation

Hearing provides invaluable information about the identity and location of sounds in the surrounding environment and plays a critical role in animal communication and speech processing in humans. Hearing is the only omnidirectional and far-reaching sense able to alert individuals about events happening in all directions, allowing them to avoid unseen dangers or helping to guide them towards objects of interest e.g. tracking a hiding prey. Moreover, sound localisation contributes to segregating sound sources in noisy environments, allowing us to focus on a sound of interest while draining down the background noise [an effect known as spatial release from masking (Cherry, 1953)]. Unlike other sensory systems, like the visual or somatosensory systems, the location of the sound is not determined by the stimulation of spatially distributed sensory neurons at the receptor level. The biomechanical characteristics of the basilar membrane along the cochlea, where the organ of Corti sits, confers a frequency organisation on the auditory sensory epithelium, which is topographically conserved along the auditory pathway generating a tonotopic organisation. Therefore, inferring the location of a sound source relies on computations performed by the brain based on the physical interactions of sounds with the head and ears, which provide acoustic cues whose integration and spatial correlation are learnt by experience.

1.2.1. Spatial cues for sound localisation

Sound localisation is inferred by the brain after encoding and integrating different spatial acoustic cues. Two types of cues can be distinguished: (1) monaural or spectral cues that do not depend on the comparison of the signal received by both ears and (2) the binaural cues that result after the comparison of the signals between ears.

The physical interaction of a sound with the head and external ears can alter its spectral content in a direction-selective manner. One of the most prominent changes observed is the spatial-dependent attenuation of specific frequencies known as spectral notches. These notches are introduced in sounds of broad spectrum with frequency components above ~4kHz (Middlebrooks, 2015). Spectral cues are especially important for providing information about the location of sounds in the vertical plane and for the resolution of the front-back confusions at positions with equal binaural cues. Evidence of these cues was first exposed by Lord Rayleigh, who described the ability of listeners to discern between front and back when broadband sounds or speech were presented, while this discrimination was not possible using pure tones (Rayleigh, 1907).

It was Lord Rayleigh who also described the binaural cues, important for localising sounds away from the midline, i.e., in the horizontal plane. By comparing the input between the ears, the brain calculates the interaural time differences (ITD) and interaural level differences (ILD). ITDs correspond to the difference in arrival time of the sound between the two ears and are the greatest when the sound is located at 90º to the left or right. ILDs correspond to the difference in intensity, and originate from the shadowing effect of the head, which attenuates the sound arriving to the ear further away

from the sound source, as well as from the difference in the spectral filtering properties of each external ear. The significance of these cues is determined by the width of the head and the frequency of the sound (Erulkar, 1972; Rayleigh, 1907). The sound attenuation resulting in ILD occurs when the sound wavelength is shorter than the head width (for humans: > 1.3kHz) (Grothe & Pecka, 2014), thus comprising mainly high frequency sounds. By contrast, at high frequencies, ITDs become uncertain because of the phase ambiguity resulting from the sound passing through more than one cycle between the ears, compounded by the high-frequency limit on the phase locking mechanism for frequency transduction in the cochlea. Therefore, ITDs are more relevant for low frequency sounds (below ~2kHz). This constitutes the 'duplex theory' proposed by Lord Rayleigh by which ITDs and ILDs are used to localise low and high frequency sounds, respectively (Macpherson & Middlebrooks, 2002; Rayleigh, 1907).

1.2.2. Neural processing of spatial cues

A wide literature has described the processing and encoding of the acoustic spatial cues at the level of the brainstem [for review (Grothe et al., 2010)]. The cochlear nucleus (CN) is the first synaptic station in the ascending auditory pathway, receiving the input directly from the auditory nerve fibers (ANF). This brainstem structure is comprised of a variety of cell types linked to the processing of the different spatial cues and other sound features. Two main subdivisions can be distinguished, dorsal and ventral cochlear nucleus.

The dorsal division of the cochlear nucleus (DCN) receives input from the descending branch of the auditory nerve and its principal cells show response patterns that seem to be optimised for the detection of spectral notches in the sound. These cells,

known as ‘type IV’ neurons, show a pure-tone response pattern characterised by a low-threshold activation around their best frequency (BF) with a large inhibitory area at higher intensities usually centred below the BF [central inhibitory area (CIA)] (Spirou & Young, 1991). Much of the inhibitory input has been shown to be provided by the DCN ‘type II’ neurons, which converge into ‘type IV’ neurons, generating a CIA whose bandwidth is larger than the excitatory area (Spirou & Young, 1991). In the presence of notched sounds, when the centre frequency of the notch is close to the type IV neurons’ BF, the excitatory input is reduced, and these neurons get strongly inhibited, which makes them highly sensitive to spectral features such as those generated by the filtering effect of head and ears (Davis et al., 2003; Nelken & Young, 1994). ‘Type IV’ neurons project to the contralateral central nucleus of the inferior colliculus (CNIC) in the midbrain, where they target ‘type O’ neurons (Davis, 2002). ‘Type O’ neurons show a similar pure-tone response pattern to that seen in ‘type IV’ neurons in the DCN. However, they present opposite response characteristics to notched noise, showing an excitatory response to a specific notch frequency flanked by inhibition (Davis et al., 2003). This response transformation is thought to arise from additional inhibitory input onto the ‘type O’ neurons. Therefore, ‘type O’ neurons in the inferior colliculus (IC) are highly sensitive to the frequencies of notches present in the sound, like those generated by the interaction of the sound with head and ears. The pathway connecting ‘type IV’ neurons in the DCN to ‘type O’ neurons in the IC has been suggested to be involved in the encoding of spatial spectral cues (Grothe et al., 2010).

The ventral cochlear nucleus (VCN) is innervated by the ascending branch of the auditory nerve and their neurons project to the superior olivary complex (SOC), which plays a role in the encoding of the binaural spatial cues. Spherical and globular bushy

cells in the VCN show a 'primary-like' response profile characterised by a high firing rate at the stimulus onset followed by a reduced response for the rest of the sound duration (Oertel et al., 2011; Rhode et al., 1983). This response pattern makes these cells highly sensitive to the temporal structure of auditory stimuli. Neurons tuned to high frequencies are able to respond to changes to the envelope of high frequency sounds whereas, lower frequency tuned neurons are able to phase-lock to the fine structure of low frequency sounds. Therefore, the temporal precision exhibited by the bushy cell responses and their intensity dependent firing rate make them well suited for ILD and ITD processing (Grothe et al., 2010). Bushy cells project to the SOC where the binaural computations take place. The lateral superior olive (LSO) and medial superior olive (MSO) are two principal nuclei of the SOC, and they are implicated in the processing of ILDs and ITDs, respectively (Grothe et al., 2010).

Sound intensity is encoded by firing rate of VCN neurons, thus ILD computations rely on the comparison of the mean firing rate of inputs coming from the left and right VCN. This computation is performed in the LSO which receives direct excitatory input from the ipsilateral spherical bushy cells (SBC) and an inhibitory input from the ipsilateral medial nucleus of the trapezoid body (MNTB) innervated by the contralateral VCN. The temporal precision of the MNTB responses is ensured thanks to a highly specialised synaptic terminal, the calyx of Held, from the globular bushy cells. LSO neurons consequently receive excitation from the ipsilateral ear and inhibition from the contralateral ear, resulting in a subtraction computation that compares the intensity input from both ears (Grothe et al., 2010). Neurons in the LSO show strong responses to sound sources located on the ipsilateral side due to the prominence of the excitatory input provided by the near (ipsilateral) ear over the inhibitory input provided by the

(contralateral) far ear, which is attenuated by the head shadow effect. However, as the source moves contralaterally, the balance between inputs is reversed as the ipsilateral ear experiences the shadow effect as it becomes the far ear relative to the sound source and vice versa for the contralateral ear, resulting in an overall reduction of the LSO responses. This constitutes the basis of the ILD sensitivity described in LSO neurons. The ILD sensitivity function presents a sigmoid form making neurons highly sensitive to small changes in displacement along the horizontal axis (Boudreau & Tsuchitani, 1968; Park et al., 1996). More recent work has shown that principal cells in the LSO show fast onset responses, challenging the traditional association of these neurons with sustained integrative responses and suggesting an important role of timing in the generation of ILD tuning (Franken et al., 2018).

The processing of ITDs requires a highly temporally precise signal transmission since the arrival time differences are of the order of microseconds. The range of ITDs for sound localisation depends on the head dimensions, i.e., the interaural distance. Mammals, birds, and reptiles have evolved the ability to use ITDs, but because of their different evolutionary paths, their neural bases for ITD encoding are thought to be different (Grothe & Pecka, 2014). In mammals, MSO is considered the main structure involved in the processing of ITDs although, LSO neurons tuned to low frequencies have also been described to be sensitive to ITDs (Tollin & Yin, 2005). Therefore, ITD processing in the MSO is thought to be a refinement of the LSO circuit, developed in animals with good low frequency hearing (Grothe & Pecka, 2014) . The MSO acts as a coincidence detector of the bilateral excitatory inputs from the spherical bushy cells in the VCN. These VCN neurons are temporally more precise than their input from the ANF, showing enhanced synchronisation (Joris et al., 1994). MSO neurons also receive

bilateral inhibitory inputs questioning the oversimplified model of the coincidence detection mechanism. The ipsilateral source of inhibition originates in the lateral nucleus of the trapezoid body (LNTB) where globular bushy cells from the ipsilateral VCN form synapses onto glycinergic neurons. The contralateral inhibition, also glycinergic, is generated in the ipsilateral MNTB which in turn receives input from the contralateral VCN, similarly to the LSO circuitry. This inhibition has been suggested to act as a modulator of the time window for binaural excitatory inputs (Grothe & Pecka, 2014; Pecka et al., 2008). Therefore, MSO neurons are thought to integrate bilateral excitatory and inhibitory input to generate their ITD sensitivity.

Along with the DCN, LSO and MSO both project to the central nucleus of the IC (CNIC). Hence the IC is considered to be a mandatory centre for the convergence of the different ascending auditory pathways carrying information from the brainstem about the auditory spatial cues. The LSO sends excitatory connections to the contralateral IC and inhibitory projections to the ipsilateral IC. The MSO sends excitatory projections to the ipsilateral IC (Grothe et al., 2010). Most of the ascending input encoding the acoustic cues necessary for sound localisation targets the CNIC, which shows a tonotopic organisation inherited from lower structures, with increasing best frequencies (BF) dorsoventrally. Although the ascending inputs from the DCN, LSO and MSO are tonotopically organised and primarily distinct regions of the CNIC, reflecting the frequency dependence of the monaural and binaural spatial cues (Loftus et al., 2010), they have been shown to converge on individual midbrain neurons. Different encoding strategies for spatial cues in the IC have been proposed, such as the first spike latency (FSL), ongoing spike timing and spike rate (Chase & Young, 2008). Each of these firing properties can provide a neuron with information about different spatial cues, although a

dominance of ILDs has been described, showing the greatest mutual information values between this cue and IC activity (Chase & Young, 2008). Moreover, (Dorkoski et al., 2020) showed that neurons in the IC are sensitive to ITD and ILD changes independently of their BF, and that high-frequency neurons respond to both the temporal structure and the envelope of the sound. The alignment of the spatial cues has been suggested to occur in the nucleus of the brachium of the IC (BIN) (Slee & Young, 2014), which receives inputs from the CNIC, contains a partial spatial map (Schnupp & King, 1997) and projects to the superior colliculus (SC) (Nodal et al., 2005). The SC is a structure involved in reflexive acoustic head orienting responses (Lomber et al., 2001), and where an auditory space map has been described in mammals (Ito et al., 2020; King & Hutchings, 1987; Middlebrooks & Knudsen, 1984; Palmer & King, 1982).

An integrated sensitivity to ILD and ITD cues has also been described in the auditory cortex (AC) of humans (Higgins et al., 2017). The IC projects to the medial geniculate body (MGB) in the thalamus, which projects to the AC. In general, responses of neurons in the IC are characterised by a contralateral bias and heterogenous azimuth functions. Thus, auditory space is represented contralaterally and lesions in one IC result in localisation deficits in the contralateral hemifield (Jenkins & Masterton, 1982). Similarly, responses in the AC have been described to be broadly tuned and show a contralateral preference, resulting in an inhomogeneous representation of space (King et al., 2007; Stecker et al., 2005). Moreover, lesion and deactivation studies have demonstrated that, despite the extensive processing occurring at subcortical level, the AC is necessary for accurate sound localisation (Jenkins & Merzenich, 1984; King et al., 2007; Malhotra et al., 2004; Nodal et al., 2010).

1.2.3. Models of auditory space coding

Despite the vast literature describing the neural bases underlying the sensitivity to the different acoustic spatial cues involved in sound localisation along the ascending auditory pathway, how these cues are integrated to generate the perception of auditory space is still a matter of debate.

Given that the cortical representations in the visual and somatosensory systems are spatially organised, it was thought that the same would apply for auditory space coding. A topographic spatial representation was proposed by Jeffress in 1948 to be located in the IC or MGB. His model remained an influential one after gaining support from the ITD sensitivity described in the nucleus laminaris in barn owls and to a partial extent in other species, including the MSO in mammals(Schnupp & Carr, 2009). The Jeffress model proposed that ITDs are encoded by highly tuned individual neurons that evenly represent the acoustic space. According to this model, these neurons act as coincidence detectors and are innervated by axons of different lengths that therefore act as delay lines for the signals coming from each ear, thereby conferring sensitivity to ITDs that offset the interaural difference in the delay lines. Such delay lines have been anatomically described to support the ITD sensitivity in the nucleus laminaris of the barn owl (Carr & Konishi, 1988). However, anatomical studies in cats have failed to find evidence for delay lines (Karino et al., 2011; Smith et al., 1991), calling into question the existence of such a mechanism in mammals. Moreover, no topographic mapping of ITDs has been found in the MSO (Franken et al., 2015). It is important to point out that the use of ITDs for sound localisation is thought to have evolved separately in birds and mammals (Grothe & Pecka, 2014). There are also important differences between the barn owl and

other low-frequency hearing animals: (1) the barn owl uses ITDs to localise high frequency sounds (up to 9 kHz), while mammals are insensitive to time disparities in this frequency range and use ILDs instead, also (2) at high frequencies, the barn owl uses ILDs to localise in the vertical, rather than the horizontal, plane (McAlpine, 2005; McAlpine et al., 2001).

Furthermore, McAlpine et al., 2001 recorded data from low-BF neurons in the IC of guinea pigs that provided evidence against the existence of a place code in this structure. They showed that low BF neurons were often tuned to ITDs outside the physiological range, and ITD peaks varied with neuron BF along the tonotopic axis, which is inconsistent with a place code model, by which ITD peaks should vary with location independently of the frequency. Therefore, they challenged the accepted idea of a similar ITD code for mammals to that found in the barn owl, and alternatively, proposed that physiologically-relevant spatial information is conveyed by the slope of the ITD functions rather than the peaks of those functions. They found that neurons showed the greatest modulation of their responses near the interaural midline, where the slopes were the steepest, thus reconciling neural and psychophysical observations revealing that the midline is the region with greatest spatial acuity (Mills, 1958). In view of these findings, McAlpine and colleagues proposed a model by which azimuth is encoded by a comparison of two broadly tuned populations constituted by the two hemispheres, where the midline represents the transition region (two-hemispheric-channel model) (McAlpine et al., 2001).

The lack of support for a topographic representation of auditory space and the descriptions in the AC of mammals of broadly tuned neurons with a contralateral preference (Stecker et al., 2005) opened the gate to novel models of auditory spatial

coding. As in the IC, it was suggested that instead of being based on the neurons' peak responses, the spatial information is encoded in the rate of change of the responses because the slopes of azimuth functions in the AC have been described to be the steepest near the midline (Campbell et al., 2006; Stecker et al., 2005), and thus consistent with a two-channel model (azimuth encoded by the differences in two subpopulations with opposite spatial preference). Evidence for this model in humans has been shown in the planum temporale using neuroimaging techniques (Derey et al., 2016).

Importantly, the two-channel model offers an explanation for invariant sound localisation abilities with increasing sound level despite the consistent finding that the spatial sensitivity of individual neurons changes in an intensity-dependent manner. According to the two-channel model, changes in the stimulus intensity would result in an equivalent change in the firing rate of both populations that would effectively cancel each other. This is not necessarily the case for a spatial code model, where an increment in sound intensity might be expected to result in impaired localisation, thereby predicting the best accuracy at low levels, which is the opposite to that observed in psychophysical research (Stecker et al., 2005). The two-channel model also outperforms other models proposed as an alternative to the topographical model, like the panoramic model (Middlebrooks et al., 1998), which is compatible with some description in bats (Razak, 2011) . This model suggested that each neuron encodes locations throughout the full 360º of sound azimuth (panoramic neurons) with varying degrees of accuracy and sound space is conveyed by different patterns of activity in the population. Nevertheless, this model does not account for the improved acuity consistently observed in behavioural studies along the midline, suggesting that the two-channel model provides a better conciliation between neural and behavioural observations.

Lesion and deactivation studies along the auditory pathway (Jenkins & Masterton, 1982; Malhotra et al., 2004) in cats have shown that unilateral disruption above the superior olivary complex only produces contralateral deficits in sound localisation, which is hard to reconcile with a hemispheric two-channel model (Day & Delgutte, 2013). Day and Delgutte 2013 carried out a comparison of different population decoders including the already discussed two-channel model, as well as a population-vector decoder and a population-pattern decoder, using data from IC of awake rabbits. The population-vector decoder was based on the neurons' peak responses without assuming a topographical organisation, and due to the high contralateral bias and the heterogeneity in the azimuth functions of neurons in the IC, its decoding performance was very poor. The population-pattern decoder used the pattern of spike counts to decode the azimuth location while the two-channel decoder was based on the difference of the summed firing rates of the left and right channels. Both models performed accurately (former: mean error <5º, latter: 7º), although the population-pattern decoder was better. A single-channel model, a variation of the two-channel model using only the right IC, failed to predict the sound source azimuth on the contralateral side, which is not the result that would have been predicted by lesion/deactivation studies. Interestingly, the population pattern decoder could decode not only contralateral locations, but also ipsilateral locations when using data from a single side, which is also inconsistent with lesion and deactivation studies.

A variant of the two-channel model has also been proposed to explain differences in lateralisation observed in MS and stroke patients, who presented lesions at different stages of the auditory pathway. Lesions affecting fibers leading to the SOC cause large interaural differences to be perceived as small (centre-oriented), while lesions in connections leading to the IC have the opposite effect, with small interaural differences

being perceived as large (side-oriented) (Aharonson & Furst, 2001). A multi-level hierarchical model proposed by Aharonson and Furst 2001 to account for these observations suggests a neural code based on the comparison of a right and left channel at two different stages. A first level, corresponding to the SOC, would estimate the differences between left and right channel, while a second level, the IC, would estimate the similarities (Aharonson & Furst, 2001).

In conclusion, several attempts have been made to model how different regions of the brain might transform the encoding of different spatial cues into a perception of auditory space. However, how sound localisation is achieved by the brain is still a matter of controversy. The computational nature of sound localisation and specifically its dependence on the geometry of the head and ears makes sensory experience crucial for the acquisition of this ability. Consequently, sound localisation is highly susceptible to alterations in the auditory input, such as the onset of hearing loss. How sound localisation ability is altered by unilateral hearing loss and how auditory experience impacts its recovery has been extensively used as a model of the bases and functional consequences of sensory plasticity in the brain.

1.3. Investigating sensory plasticity: the earplug model

Sensory experience plays a critical role in the calibration of sensory systems. This experience-dependent plasticity is especially vital during early stages of life, when sensory systems are maturing and adjusting to changes in sensory input to reflect the statistics of the environment (Keating & King, 2013; Kumpik & King, 2019). Alterations

in input due to hearing disorders during these sensitive (or critical) periods of development could result in long-term sequelae in perceptual capabilities as a consequence of maladaptive plasticity (Popescu & Polley, 2010). Later in life, plasticity in sensory processing is still present but to a lesser extent, and is dependent on behavioural training (Irvine, 2018). This training-induced plasticity, also known as perceptual learning, is essential for improving perceptual skills but also for allowing compensation for alterations in the sensory input associated with sensory disruptions such as hearing loss.

In the context of spatial hearing a unilateral conductive hearing loss (UCHL), i.e., affecting one ear, has a detrimental impact on sound localisation processing, because of the disruption of the binaural computations due to the asymmetric and frequency dependent sound attenuation and delay in the affected ear (Keating et al., 2013; Keating et al., 2016; Moore et al., 1989). UCHL can be experimentally induced by inserting a foam earplug in one ear, producing a reversible binaural imbalance. Several studies have shown that a partial recovery of sound localisation can take place through behavioural training following the disruption caused by monaurally inserting an earplug and this has been widely used as a model for training-induced plasticity (Irving & Moore, 2011; Kacelnik et al., 2006; Strelnikov et al., 2011).

1.3.1. Behavioural properties of adaptation to unilateral conductive hearing loss

Perceptual training improves performance and provides the basis for recovering a perceptual skill following a sensory disruption (Irvine, 2018). The monaural insertion of an earplug produces an immediate disruption in sound localisation accuracy and training in a sound localisation task induces a progressive improvement in performance towards normal hearing levels, which has been reported in humans (Irving & Moore, 2011; Keating et al., 2016; Kumpik et al., 2010) and ferrets (Bajo et al., 2019; Bajo et al., 2010; Kacelnik et al., 2006; Nodal et al., 2012; Nodal et al., 2010).

There is still a controversy about the amount of training needed and its relationship with the speed of learning. One study has reported a rapid adaptation to altered binaural cues in humans within a short training session when sound intensity is fixed and visual feedback is provided (Zonooz & Van Opstal, 2019). Other work (Kumpik et al., 2010) has showed that progressive training over several days in a sound localisation task is needed to achieve adaptation to monaural occlusion in humans, reaching pre-plug performance after 1 week, while no improvement was observed if all the trials were performed during the first day of training (Kumpik et al., 2010). In this study, sound level was roved randomly to rule out any contribution of intensity cues (i.e., the head-shadow effect). Adaptation has also been observed when individuals only experience monaural hearing loss during training sessions, showing gradual improvement in sound localisation performance, despite experiencing normal binaural hearing between sessions (Keating et al., 2016). Studies in ferrets adapting to an UCHL have demonstrated that the amount of training and its frequency are key for determining the speed and level of performance

recovery. Comparison between the performance of animals with daily and one every six days training schedules showed that animals in daily routines achieved a more complete adaptation to UCHL relative to training only every six days, despite performing the same overall number of trials. Moreover, no improvement was observed after several weeks of monaural occlusion experience if training was not provided (Kacelnik et al., 2006). Altogether these studies show that training is necessary for adaptation to UCHL, and training schedule is an important factor, with the most complete adaptation being achieved by frequent training.

Orienting responses to a novel stimulus are not exclusive to a particular sensory modality and in real life scenarios a single event is often perceived by multiple senses. Consequently, it is not surprising that visual influences on spatial hearing have been widely described. During early stages of development, visual activity is involved in the calibration of auditory spatial information in the superior colliculus of mammals (King et al., 1988) and in the optic tectum of barn owls (Brainard & Knudsen, 1998), structures that contain an auditory space map. Adaptive shifts in ILD and ITD sensitivity in the optic tectum of barn owls have been described following early monaural occlusion even without vision, although shifts were smaller than in sighted animals (Knudsen & Mogdans, 1992). Moreover, recovery of normal sound localisation during development after earplug removal in these animals depends on the visual system (Knudsen & Knudsen, 1985). In adulthood, perception of auditory space has been shown to be influenced by visual activity (Woods & Recanzone, 2004). Nevertheless, adaptation to UCHL in adult ferrets has been found to be independent of visual calibration (Kacelnik et al., 2006). Ferrets reared with visual deprivation by binocular eye lid suture showed no difference in the rate of adaptation to UCHL compared to sighted animals. Further

evidence of this adaptation being guided exclusively by auditory training was provided by showing that animals experiencing UCHL only showed auditory localisation improvement when trained in an auditory but not in a visual localisation task (Kacelnik et al., 2006). Consistent with this work, Carlile and Blackman 2014 showed that humans experiencing distorted spectral cues by wearing moulds in their ears adapted to use these modified cues to perform elevation judgements both inside and outside the visual field, once more suggesting that the recalibration of the auditory system was independent of the visual input (Carlile & Blackman, 2014). Although vision is not necessary for this process of adaptation to occur, it does seem to facilitate it, as suggested by a better improvement in performance in humans after audiovisual training relative to auditory training only (Keating & King, 2015; Strelnikov et al., 2011).

1.3.2. Plasticity processes involved in adaptation

Two different bases have been suggested to underlie the adaptation to UCHL. Spatial cue remapping suggests that adaptation is achieved by adjusting neuronal sensitivity to the altered binaural inputs, thus associating the modified input to locations in space previously associated to other binaural cue values. Alternatively, spatial cue reweighting proposes that individuals rely more heavily on spatial information provided by unaltered cues and play down or ignore the information provided by altered cues, i.e., the spectral cues provided by the open ear would be more reliable than the altered binaural cues that result from wearing the earplug.

The mapping of the values of the acoustic cues to different sound locations is experience dependent as has been described during development in the barn owl

(Knudsen et al., 1984). Electrophysiology work shows that this remapping is associated with adaptive shifts of binaural cues in the optic tectum (Gold & Knudsen, 2000a; Mogdans & Knudsen, 1992). Moreover, barn owls raised with a monaurally fitted filtering device also show frequency-dependent changes in tuning for binaural cues in the optic tectum (Gold & Knudsen, 2000a). In mammals, adaptation to monaural earplugging is thought to rely mainly on cue reweighting. The ability to relearn to localise sounds by relying on the unaltered spectral cues provided by the open ear has been demonstrated in juvenile ferrets raised with an earplug, and this is associated with increased sensitivity to these cues in the primary auditory cortex (A1) (Keating et al., 2013). Importantly, evidence for reweighting does not exclude the possibility of a remapping mechanism. A study in ferrets demonstrated that cue remapping can be used by these animals to adapt to monaural earplugging (Keating et al., 2015). This study showed that ferrets reared with an earplug can localise narrowband sounds, which do not provide reliable spectral cues due to the limited frequency components, implying that animals are able to perform the task without relying on unaltered cues. Moreover, recordings in A1 in these ferrets showed a systematic shift in ILD sensitivity, which suggests that a remapping mechanism of the altered cues is also possible in mammals during early stages of life (Keating et al., 2015). Therefore, remapping and reweighting are not mutually exclusive and can be found in the same species depending on the available spatial cues.

Studies in humans suffering from single-sided deafness also suggest that accurate sound localisation is possible, although considerable interindividual variability has been reported (Agterberg et al., 2014; Slattery & Middlebrooks, 1994; Van Wanrooij & Van Opstal, 2004). Slattery and Middlebrooks 1994 showed that some individuals with congenital single-sided deafness were able to localise sounds in the azimuth better than

normal-hearing controls wearing an earplug, implying developmental plasticity in integration of the different acoustic cues. A later study in monaural listeners showed that their azimuth localisation performance was highly affected by stimulus level relative to normal hearing controls, suggesting a dependence on the attenuation effect of the head, although some individuals also relied on unaltered spectral cues for sound localisation (Van Wanrooij & Van Opstal, 2004). The use of spectral cues provided by the intact ear has been shown to play a role in the ability of single-sided deaf people to localise in the azimuth plane (Agterberg et al., 2014; Ausili & Snapp, 2023; Van Wanrooij & Van Opstal, 2004). However, some variability is found in the ability of these listeners to use them (Agterberg et al., 2014; Van Wanrooij & Van Opstal, 2004).

Both adaptive processes, remapping and reweighting, have also been described following the onset of monaural hearing loss in the adulthood in mammals, and in contrast to the plasticity that occurs earlier in life, their acquisition is dependent on training in a sound localisation task. Similar to the results from developmental research in ferrets (Keating et al., 2013, 2015), work in adult human participants suggests that different mechanisms of adaptation take place depending on the availability of different spatial cues (Keating et al., 2016). Up weighting of spectral cues as an adaptation strategy in these individuals was evidenced by a reduced improvement in sound localisation when the spectrum of the sound was randomised, which made spectral localisation uncertain, relative to cue-rich broadband stimuli with a flat spectrum. Nevertheless, improvement was still observed when individuals were trained using low- and high- frequency pure tones. This is indicative of changes in binaural sensitivity since narrowband stimuli, such as pure tones, lack spectral localisation cues, which rely on the comparison of sound energy across frequency components (Keating et al., 2016). Therefore, remapping and

reweighting seem to be general plasticity mechanisms that occur in development and in the adult life. Moreover, they can emerge together in the same individual depending on the available cues (Keating et al., 2016).

Further work in adult ferrets which similarly adapted to a UCHL through training in a sound localisation task has demonstrated that reweighting of spatial cues also plays an important role in adaptation in these animals. A drop in performance was observed after adaptation to UCHL when the open ear was fitted with a mould, which modified the spectral cues (Kacelnik et al., 2006). Further evidence for cue reweighting is provided by the absence of behavioural aftereffect following earplug removal, with normal (i.e., pre-plug) localisation performance found straightaway. Thus, it seems cue reweighting could be context-specific, providing an effective mechanism for a rapid adaptation to the prevalent hearing conditions. Nevertheless, adaptation to UCHL through training is a progressive and relatively long process that leaves a memory trace, evidenced by a reduced drop in performance after a subsequent UCHL (Bajo et al., 2019; Kacelnik et al., 2006). Further research is necessary to understand how long this memory persists and whether the direction of adaptation to UCHL affects adaptation when hearing loss affects the other ear. This could be relevant for understanding the impact on hearing of clinical conditions such as otitis media with effusion, which can be recurrent and affect one or both ears (Hogan et al., 1997).

Furthermore, a key feature in understanding the effectiveness of perceptual learning is determining its generalisation to untrained stimuli. The research investigating training-induced adaptation to UCHL, referenced above, has traditionally been performed in highly controlled experimental conditions in which individuals learn to localise single noise bursts presented in isolation in quiet conditions. This scenario lies quite far from

the complex listening environments we encounter in our daily lives, where people suffering from hearing loss struggle to segregate sound sources impacting their speech intelligibility. It is then important to investigate the extent of generalisation achieved with sound localisation training, especially looking towards a possible implementation of this regime as a therapeutic treatment to improve auditory spatial awareness in people suffering from asymmetric hearing loss.

In summary, both persistence and generalisation of the adaptation to monaural hearing loss are essential parameters to examine if we are to determine the effectiveness of sound localisation training. This behavioural characterisation constitutes one of the research questions addressed as part of this thesis. Together with this, we will also explore the possible neural substrates underling this process of adaptation at the level of the auditory midbrain, where the integration of the localisation cues initially takes place.

1.4. Neural substrates of training-induced adaptation to UCHL

The training-induced recovery of sound localisation ability following UCHL in adult individuals has been widely described behaviourally and has been used as a model for perceptual learning. Nevertheless, the neural substrates underlying this plasticity remain unknown. Many studies addressing this research question have pointed at the importance of the AC and its descending connections to the IC in this process.

1.4.1. The role of auditory cortex and its descending connections

The AC is necessary for normal sound localisation, as indicated by lesion (Heffner & Heffner, 1990; Jenkins & Merzenich, 1984; Nodal et al., 2010) and inactivation studies (Malhotra et al., 2004; Smith et al., 2004). This suggests that AC could also be involved in the training-induced plasticity that accounts for the recovery of sound localisation following unilateral hearing loss. This hypothesis is further supported by electrophysiology work providing evidence for changes in the AC in adult mammals during perceptual learning (Dahmen & King, 2007; Polley et al., 2006; Recanzone et al., 1993).

Lesion and deactivation studies have provided evidence for a causal role of AC in auditory plasticity. Sound localisation plasticity has been shown to be impaired when different parts of the AC were lesioned bilaterally (Nodal et al., 2010). A cohort of ferrets with bilateral lesions in the AC (primary and secondary areas) were unable to recalibrate sound localisation following the monaural insertion of an earplug when they were trained in a sound localisation task using relatively long noise bursts, even though the animals' ability to localise these sounds in normal hearing conditions was conserved. What is more, lesions restricted to A1 showed a similar phenotype, suggesting the crucial role of A1 in this process of learning. Later work involving selective deactivation of different auditory cortical areas in ferrets revealed that inactivation of any auditory area resulted in some disruption in learning relative to control animals, indicating that other cortical areas, as well as A1, might be involved. The biggest effect was observed with the deactivation of higher-level areas (Nodal et al., 2012). Together, these studies highlight the role of different auditory cortical areas in sound localisation plasticity.

An imperative question arising from these observations was whether the adaptation to UCHL is just a cortical phenomenon or requires the intervention of subcortical nuclei where the integration of localisation cues takes place. Bajo et al., 2010 demonstrated that cortico-collicular projections from A1 to the IC in the midbrain are necessary for adult ferrets to recalibrate sound localisation following UCHL. In this study, chromophore-targeted laser photolysis was used to selectively kill cortico-collicular cells labelled retrogradely with fluorescence microbeads injected in the IC. The loss of two-thirds of the layer 5 cells, without affecting other cortical layers impaired the training-induced adaptation to UCHL without affecting normal sound localisation (Bajo et al., 2010). This suggests that interactions between cortical and subcortical structures are necessary for auditory plasticity.

The emergence of optogenetics provided the temporal specificity necessary to explore the role of the AC at different stages of learning. Using this technique, Bajo et al., 2019 investigated the contribution of A1 during training and learning retrieval. They expressed Archaerhodopsin unilaterally in the high-frequency region of left A1 of ferrets and supressed cortical activity during each stimulus presentation. Disruption of activity in A1 unilaterally did not affect sound localisation in normal hearing conditions. However, following monaural occlusion, impaired ability to adapt was found when cortical activity was suppressed optogenetically during sound presentation. Subsequent training without cortical inactivation resulted in improved learning which was unaffected when another period of training with laser inactivation was provided (Bajo et al., 2019). This suggests that the retrieval of the auditory memory resulting from the training-induced learning is not dependent on A1 and thus its consolidation might occur somewhere else.

Altogether these studies provide growing evidence for the crucial role for A1 in sound localisation plasticity. However, optogenetic work suggests that the consolidation of this learning resides in a different structure receiving projections from this cortex (Bajo et al., 2019). As described above, the essential role of the cortico-collicular pathway has also been demonstrated (Bajo et al., 2010). Therefore, it has been proposed that the IC could be the centre for the consolidation of training-induced plasticity, and thus neural changes linked to sound localisation recalibration might be expected to be found there.

1.4.2. Plasticity in the inferior colliculus

The IC in the midbrain is a key structure in the processing of auditory information. It is considered a mandatory centre for the convergence of the different ascending auditory pathways, which carry information about the auditory spatial cues (Grothe et al., 2010). The IC is also the target of a profuse descending input from the auditory cortex, which is thought to influence the processing of information in the IC (Bajo & King, 2012). Therefore, the confluence of ascending and descending connections in the IC suggests that this structure could be a centre for spatial auditory plasticity.

Corticofugal connections target many structures in the auditory pathway, including the MGB, the IC, the SOC and the CN and its influence even reaches the cochlea via the olivocochlear efferent pathway [reviewed in (Terreros & Delano, 2015)]. In particular, the cortico-collicular projection connecting A1 with the IC is necessary for the auditory plasticity involved in the recovery of sound localisation ability following the unilateral insertion of an earplug (Bajo et al., 2010). How IC responses are altered by UCHL and how they might change with learning is currently unknown.

Studies using electrical stimulation have shown that cortical activity influences the responses of neurons in the IC. Electrical stimulation of the AC in bats resulted in an overrepresentation in the IC of the best frequencies (BF) of the neurons stimulated in the cortex (Yan & Suga, 1998). Further research showed that the cortical influence in the IC is not limited to the frequency sensitivity, but it also modulates the neurons' responses to other stimulus characteristics such as duration (Ma & Suga, 2001), intensity (Yan & Ehret, 2002) and spatial sensitivity (Zhou & Jen, 2005). This modulation is also strongest when the BF differences between AC and IC are smallest (Ma & Suga, 2001; Yan & Ehret, 2002; Yan & Suga, 1998; Zhou & Jen, 2005). This is in consonance with anatomical evidence showing a topographical organisation of the cortico-collicular connections, by which cortical neurons with specific frequency tuning would be influencing the activity of frequency-like collicular neurons (Andersen et al., 1980; Bajo et al., 2007; Herbert et al., 1991; Saldaña et al., 1996; Winer et al., 1998). Moreover, inactivation of the AC by cooling in anaesthetised guinea pig resulted in an alteration of ILD sensitivity in the IC (Nakamoto et al., 2008), further supporting the modulation of activity in the IC by top-down influences.

Changes in ILD and ITD sensitivity appear in the external nucleus of the IC (ICx) of young barn owls raised with an earplug (Gold & Knudsen, 2000b; Mogdans & Knudsen, 1993). Adaptive shifts in ILD sensitivity also appear in the optic tectum (Knudsen & Mogdans, 1992) whose primary source of input is the ICx. Furthermore, signs of experience-dependent plasticity have been shown in the auditory space map of the optic tectum in adult barn owls (Bergan et al., 2005). Notwithstanding the differences previously described between the sound localisation mechanisms found in birds and mammals (Grothe & Pecka, 2014), neural and behavioural correlates of remapping have

also been found in mammals (Keating et al., 2014; Popescu & Polley, 2010; Thornton et al., 2021), suggesting that the sites of plasticity might not differ as much as previously thought between these groups of animals. Thus, these findings further point to the auditory midbrain as a place for auditory plasticity.

The optic tectum is the avian homolog of the superior colliculus (SC) in mammals, which is a midbrain structure that receives input from the IC and has been shown to contain a representation of the auditory space (Ito et al., 2020; King & Hutchings, 1987; Middlebrooks & Knudsen, 1984; Palmer & King, 1982). This structure is implicated in head-orienting behaviour (Lomber et al., 2001), a reflexive behaviour involved in sound localisation. Head orienting responses are highly correlated with voluntary approach-to-target responses (Nodal et al., 2008) and are influenced by cortical activity as evidenced by lesion studies (Nodal et al., 2010). Descending projections from AC to the SC have been described (Bajo et al., 2010b) that could mediate the cortical effect on normal head orienting behaviour. As with the approach to target responses, the head orientation behaviour is also altered following UCHL, producing a bias in the head movement towards the open ear. Sound localisation training results in a recovery of both approach-to-target responses and head orienting behaviour, returning to close to pre-plug head movements (Kacelnik et al., 2006; Nodal et al., 2012). This adaptation in orienting behaviour is also dependent on modulation from the auditory cortex (Nodal et al., 2012) and, more precisely, it is influenced by the cortico-collicular projections (Bajo et al., 2010). Hence, the training-induced recovery of head orienting movements, a subcortically mediated behaviour, is in turn dependent on cortical input, further supporting the role of subcortical processing, under the influence of the cortex, as the neural substrate for auditory plasticity.

In summary, there is growing evidence that points to the inferior colliculus, a midbrain structure that serves as a confluence for top-down and bottom-up signals, as a centre for the consolidation of spatial auditory plasticity. Nevertheless, how neural responses vary in this nucleus throughout training-induced adaptation to monaural hearing loss remains as an unanswered question which constitutes a central focus in this thesis research.

1.5. Thesis overview

As part of this thesis, we aimed to behaviourally characterise the persistence and generalisation of training-induced adaptation to monaural hearing loss. For this project, we trained a cohort of ferrets in an approach-to-target sound localisation task and tested their ability to localise sounds after several periods of UCHL in the same or the opposite ear interleaved with normal hearing periods. We also assessed the generalisation of this learning by testing the ability of ferrets that had adapted to a UCHL to localise different types of sounds in silence or in the presence of background noise. Generalisation of auditory learning to complex listening environments is key to determining its effectiveness and thus an important aspect to consider for the design of training protocols as a rehabilitation strategy for people suffering from hearing loss. In relation to this, the possibility of reproducing listening environments that resemble those we find in daily life is currently limited by the experimental setups, which usually consist of a few speakers placed around the subject inside a soundproof chamber. To overcome this, as part of this thesis, we developed a setup using virtual reality (VR) to test sound localisation ability in

humans. VR is a tool that allows us to get rid of the physical constraints of current experimental conditions and explore any possible listening scenario. The use of VR also makes training accessible much more widely, which constitutes a great advantage for the future implementation of training protocols as a therapy approach.

The study of training-induced adaptation to monaural hearing loss induced by plugging one ear is not only relevant from a clinical point of view. Due to the computational nature of sound localisation, earplugging has been widely used as model to study sensory plasticity. In particular, it has been used to study neural substrates of plasticity. Accumulative evidence points at the role of subcortical processing, in particular, the IC, under the influence of the AC via corticofugal connections, as a key site for the consolidation of auditory spatial plasticity. Neural responses in the IC have not yet been characterised during adaptation to UCHL to test this hypothesis. Here, we performed electrophysiological recordings in ferrets using high count and density recording probes (Neuropixels) to record neural activity in the IC bilaterally. These recordings were performed in awake animals while they were trained in a sound localisation task in both normal hearing conditions and while adapting to an earplug. Using an animal model allows us to carry out invasive recordings of spiking activity extracellularly to track responses of neurons and ultimately correlate their neural activity with the same individual's behaviour. In particular, ferrets are a great animal model for auditory research, not only for their ability to learn complex behaviours but also for their low-frequency hearing that, unlike rodents, resembles that in humans. This is especially important in the context of sound localisation since binaural cues are frequency specific. Ferrets also have a prolonged lifespan relative to rodents, allowing long-term behavioural

studies such as training for several periods of earplugging without the risk of appearance of age-related hearing loss.

2. METHODS

2.1. Overview

Fifteen adult female ferrets (*Mustela putorius*), sourced from Marshal BioResources (United Kingdom), aged 6 months old approximately at the start of the experiments were used. All procedures were approved by the Committee on Animal Care and Ethical Review at the University of Oxford and licensed by the Home Office under the Animals (Scientific Procedures) Act (1986). All ferrets were trained in an approach-to-target sound localisation task to explore the adaptation to unilateral conductive hearing loss (UCHL) induced by plugging one ear. Eleven ferrets were used to further characterise the behavioural process of adaptation by determining its generalisation to a variety of stimuli and listening conditions and also the persistence of learning across different periods of earplugging. A further four ferrets were used to explore the neural correlates of this adaptation by implanting recording electrodes (Neuropixels 1.0) and recording chronically the neural activity during the adaptation process.

2.2. Animal welfare

Ferrets were housed in a large pen in groups of 6 -7 individuals with *ad libitum* access to food and water. To ensure a healthy life cycle, seasonal variations in the housing conditions were introduced (summer: 15/9 h light/dark daily cycle and 21-24ºC and

winter: 8/16 light dark cycle and 17-20ºC). The environment was enriched with objects with which the ferrets could play, as well as beds and shelters at different height levels accessible through a tubing system.

Prior to the start of behavioural training, the animals underwent an otoscopic examination and a tympanogram to confirm the absence of any disease of the external and middle ear. During periods of behavioural testing, the animals were housed in standard laboratory cages (L x W x H: 76.2 x 76.2 x 86.4 cm) in groups of up to 3 individuals with *ad libitum* access to dry food and controlled access to water. Ferrets had access to water twice daily while they performed the behavioural task, where water was used as a reward contingent on their performance. Each behavioural testing session lasted typically 20-30 min, the exact duration depended on the willingness of animals to perform the task as each trial was voluntarily initiated by the animals and the number of trials per session was not capped. The ferrets' weight and water intake were closely monitored to ensure the animals' welfare. The body weight was recorded daily in the morning and compared to the weight at the start of the testing period (baseline) to control the animal's weight loss. A drop in the body weight of 10% relative to the baseline resulted in the provision of extra water (10ml approx.) at the end of the day, together with a supplemented diet. Although no animal reached a reduction in their weight of more than 15% relative to the baseline, this would have resulted in the suspension of the behavioural testing and the resumption of *ad libitum* access to water until the animal's weight recovered. The daily intake of water was measured for each animal and if it was below the estimated daily need of 60ml/kg (based on daily measurements made on ferrets with free access to water in the animal facility at the University of Oxford), extra water was provided in the form of pureed food, comprised of mashed food pellets and water.

2.3. Sound localisation behaviour

2.3.1. Hardware and training

Ferrets were trained by positive reinforcement in an approach-to-target sound localisation task. Training was performed in a circular arena (Ø 140 cm) located inside a soundproof chamber. The testing arena was equipped with 12 loudspeakers (FRS 8, Visaton, Crewe, United Kingdom) and water spouts distributed around the perimeter with a 30º separation. Target sounds were presented from these loudspeakers to test the ferrets' sound localisation ability. Moreover, an overhead speaker was placed over the centre of the arena to present a background noise when required (Figure 2-1A). Auditory stimuli were produced using MATLAB (MathWorks, United States) and presented using an RX8 multi I/O processor and two SA-8 power amplifiers (Tucker-Davies Technologies (TDT), Alachua, FL, United States). The output of each loudspeaker was digitally matched and flattened across sound frequencies within the range 0.25-30 kHz.

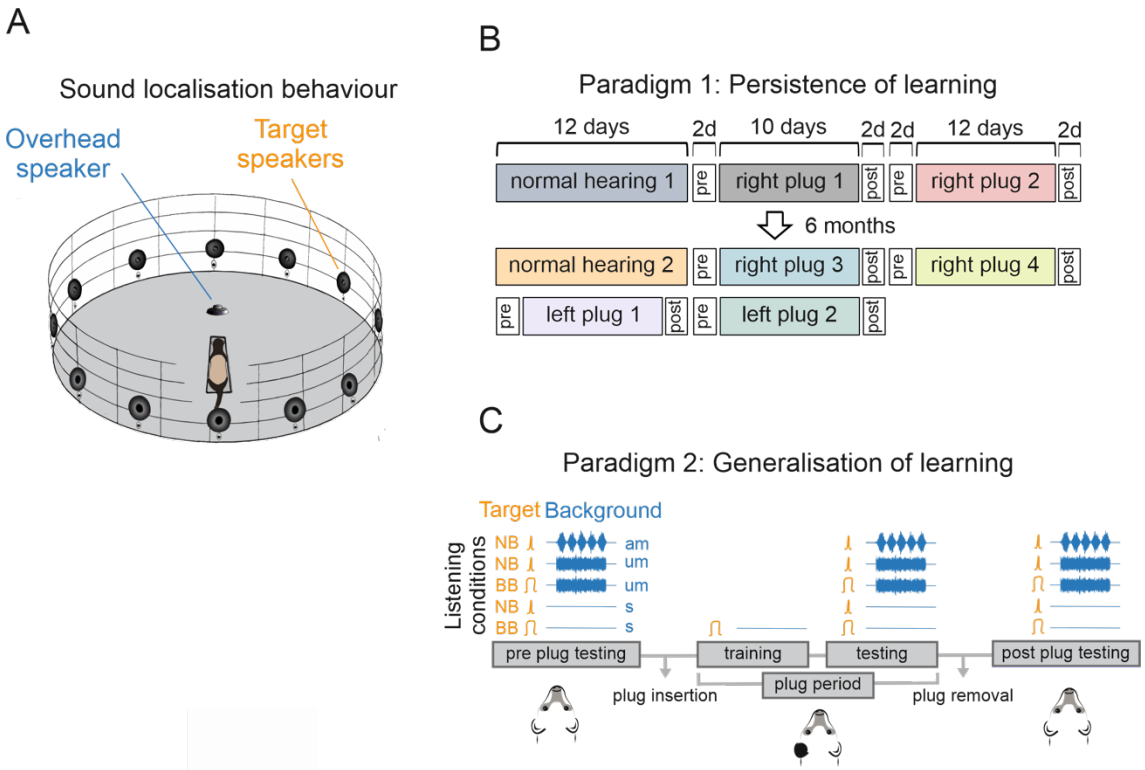

Figure 2-1. Behavioural training setup and paradigms. (A) Schematic of the circular testing arena with 12 loudspeakers and reward ports located at 30° intervals around the perimeter and a central platform on which the animal stands facing position 0° in order to trigger each stimulus presentation. A loudspeaker located above the central platform is also shown, used to generate background noise. (B) Timeline of behavioural testing to explore the persistence of adaptive learning over multiple periods of monaural occlusion interspersed by periods of normal binaural hearing. These animals were first trained to adapt with the right ear plugged and then with the left ear plugged. (C) Timeline indicating the different combinations of target and background sounds used for behavioural training and testing to explore the generalisation of learning. The two types of target sounds [broadband (BB) and narrowband (NB) noise] are depicted in orange and three possible backgrounds [silence (s), unmodulated BB noise (um), and BB noise amplitude modulated at 5 Hz (am)] are shown in blue.

Ferrets were trained to stand on a platform at the centre of the testing arena facing the loudspeaker at 0º location and lick a waterspout for a variable amount of time (300-500ms) to trigger the presentation of a target sound from one of the twelve surrounding loudspeakers. An infrared beam located at the back of the platform, and one located in

the proximity of the waterspout were used to determine that the animal was in the correct position when triggering the sound presentation. The animal then had to approach the location of the loudspeaker that presented the sound to receive a reward from its associated waterspout, each equipped with an infrared beam to detect the response. Only correct responses were rewarded (typically 150–250 µl of water depending on the animal and matched across all reward spouts). An incorrect response was followed by a "correction trial," whereby the same sound was presented from the same location as in the previous unsuccessful trial. As in our previous work, up to two correction trials were allowed. Exceptionally, the number of corrections trials was increased to three if the performance was very low in order to maintain the animal's motivation. If correction trials elicited incorrect responses, an "easy trial" was triggered, in which the same sound was presented continuously until a response was made. Data from correction and easy trials were not included in the analysis in the behaviour chapter. All trials were included for the analysis of electrophysiology data.

We also obtained a more absolute measure of localisation accuracy by tracking the ferret's head movement using a reflective strip attached to the midline of the animal's head. A high-speed camera located above the central platform captured the reflectance of the head-strip for 1 s from the onset of the target sound. The image acquisition rate was 60 frames per second (FPS) for the first part of the study (Imaging Source DMK21BF04) and 500 FPS for the second part of the study, following an upgrade to a high-speed camera (DMK 37AUX287).

2.3.2. Adaptation to UCHL

All animals were trained and tested on the approach-to-target sound localisation task in a quiet background (hereafter referred to as "silence") for 1–2 months until they showed a stable level of performance before the ear-plugging experiment started. Sound localisation accuracy was measured using single bursts of broadband noise (low-pass cut-off frequency 30 kHz) in blocks of constant stimulus duration (2000, 1000, 500, 200, 100, and 40 ms). Within each block, we pseudorandomly varied both the stimulus location across the 12 loudspeakers and its level over a 56–84 dB SPL range in steps of 7 dB. In implanted animals, training up to a consistent level of performance was carried out before the implantation surgery.

A reversible UCHL was induced by inserting an earplug (E-A-R Classic 3M) into the external auditory meatus and securing this in place with a silicone mould (Otoform KC, Dreve Otoplastik GmbH, Unna, Germany) placed in the concha of the external ear. Earplug insertion and removal were performed under sedation (medetomidine hydrochloride 0.1 mg/kg i.m., Domitor Orion Pharma, Reading, United Kingdom). An otoscopic examination was performed and a tympanogram (Kamplex KLT25 Audiometer, P.C. Werth, London, United Kingdom) was obtained both before insertion and after removal of an earplug to check the health status of the external and middle ear. No abnormalities were detected. Sedation was reversed with atipamezole hydrochloride (0.5 mg/kg s.c., Antisedan, Orion Pharma, Reading, United Kingdom). The acoustical effects of these earplugs have been characterised in previous studies in our laboratory in ferrets (Keating et al., 2013; Moore et al., 1989) and humans (Keating et al., 2016; Kumpik et al., 2010). We did not determine whether their properties changed during each

period of monaural occlusion as this would have involved sedating the animals to remove and reposition the earplugs.

As in previous work (Bajo et al., 2019; Bajo et al., 2010; Kacelnik et al., 2006), we trained ferrets to adapt to an earplug using 1000-ms long broadband noise bursts as the target stimuli on a background of silence. Ferrets will recover their sound localisation accuracy when trained with target noise bursts as short as 40 ms in duration (Kacelnik et al., 2006), but the much higher scores achieved with longer stimuli make it easier to investigate individual differences when the stimulus conditions are changed and have been used in all the previous studies carried out on the neural circuit basis for training-dependent adaptation (Bajo et al., 2010; Bajo et al., 2019; Nodal et al., 2010). Individual ferrets wore an earplug in one ear for typically ≥10 days, until their performance stabilised over three consecutive days, typically at a mean score of ≥70% correct across all 12 loudspeaker locations. We then removed the earplug and measured their localisation accuracy again.

2.3.3. Testing the persistence of adaptation

To explore the persistence of the adaptive learning with one ear occluded, one group of 4 ferrets was subjected to several periods of unilateral conductive hearing loss interspersed within variable periods of normal binaural hearing (Figure 2-1 B).

Once their localisation performance under normal hearing conditions had been measured using broadband noise bursts as target sounds in silence, a temporary UCHL was induced by inserting an earplug in the right ear. Target sound levels and locations

were pseudorandomised as described above. This first period of right ear occlusion (right plug 1) was followed by 7 days of normal hearing and then by another period of right ear occlusion (right plug 2) [data from right plug 1 and right plug 2 were reported in Bajo et al., 2019 as part of the control group in that study]. After a 6-month-long break in which the ferrets experienced normal hearing conditions, localisation performance was measured during two further periods of right ear occlusion (right plug 3 and right plug 4). Finally, two periods of left ear occlusion were conducted (left plug 1 and left plug 2) (Figure 2-1 B).

2.3.4. Testing the generalisation of adaptation

A second group of 7 ferrets was used to explore whether the adaptive learning induced by training animals whilst wearing an earplug to localise broadband noise target sounds on a silent background extended to other stimuli and acoustic conditions that were not available during training.

The sound localisation performance of the animals was measured using different stimuli before, during and after occlusion of one ear. As before, adaptation to the earplug was achieved by training the animals to localise 1000-ms broadband noise burst targets presented in silence, after which the animals were tested using different stimuli and background sounds with the earplug still in place. The target sound was either broadband (BB) noise (low-pass cut-off at 30 kHz) or one-octave wide narrowband noise (NB) centred on 16 kHz. The duration of the target sound was again 1000 ms, and its level and location were pseudorandomly varied as before. These stimuli were presented either in

silence (s) or in the presence of continuous background noise presented from an overhead loudspeaker. The background noise consisted of a broadband stimulus (low-pass cut- off at 30 kHz), whose envelope was either unmodulated (um) or amplitude modulated (am) at 5 Hz. The combination of these targets and backgrounds produced five different testing conditions: BBs, NBs, BBum, NBum, and NBam (Figure 2-1 C). The combination of broadband target sounds presented in an amplitude-modulated background (BBam) was discarded as a testing condition, because no difference was observed in localisation accuracy between modulated and unmodulated backgrounds with this target sound in normal hearing conditions. Broadband target sounds were therefore only presented in silence (BBs) or with an unmodulated background (BBum).

2.3.5. Testing the role of dynamic and spectral cues

To explore the extent to which dynamic spatial cues that might be provided by the movement of the head during stimulus presentation and the spectral cues available at the non-occluded ear contribute to adaptation to UCHL, we included additional sessions with different sound durations and limited bandwidth sounds during daily sound localisation training with an earplug in place. Ferrets (n = 4) were trained to localise 1000-ms broadband noise bursts in silence in the same fashion as described in previous sections. Every 2 days, we interspersed broadband and narrowband sounds (1/6-octave bandwidth centred at 15 kHz frequency to restrict the cues to ILDs) (Keating et al., 2015) at two different durations (200 and 1000 ms), with each of these 4 stimulus types being presented with equal probability. The level of the broadband noise bursts was pseudorandomised as

described previously, whereas the level of the narrowband stimuli was kept constant at 84 dB SPL, except for 10% of the trials in which it was 56 dB SPL. Incorrect responses to the broadband target sounds were followed by correction and easy trials, whereas no correction or easy trials were provided after an incorrect response on the narrowband trials. This was done to ensure that the animals did not learn a different strategy when localising these stimuli that might have interfered with the normal adaptation process with broadband targets. However, all correct responses were rewarded to maintain the motivation of the animals.

2.3.6. Head orienting responses

The angular position of the head-strip in each video frame was used to produce head movement traces. Trials in which <10% of consecutive frames contained measurable data were rejected. The start of a head turn was defined as a movement exceeding a threshold speed of 50 deg/s in the same direction (initial direction) over at least three consecutive frames. The timing of the last frame before a change in this initial direction was taken as the end of the head turn. The final head bearing was defined as the mean head angle calculated over the three frames before the end of the head movement. For the learning generalisation experiment, traces were down-sampled to 50 FPS to make the data analysis comparable to the learning persistence experiment (Figure 2-1 B), in which the sample rate was 60 FPS.

2.3.7. Statistical analysis of behaviour

The rate of adaptation for each of the periods of monaural occlusion was computed by fitting regression lines to the percentage of correct responses across training day, with the shaded areas in the figures representing 95% confident intervals. The probability of making a correct response was compared across animals, hearing conditions (unilateral earplug or no earplug), and stimulus characteristics using a linear mixed model with a Bernoulli- distributed data, probit link function. Final head bearings were compared using repeated measures ANOVA. Data normality was checked using Q-Q plots and applying the Shapiro–Wilk test. All statistical tests were performed using RStudio (RStudio: Integrated Development for R. RStudio, Inc., Boston, MA, United States) or SPSS (IBM, SPSS Inc., Armonk, NY, United States).

2.4. Electrophysiology recordings

2.4.1. General

Electrophysiological data were recorded from four ferrets using Neuropixel 1.0 probes, which were chronically implanted in the animals' brain. Each probe allowed us to record neuronal signals from 384 dual-band low-noise recording channels simultaneously. In three ferrets (F2108, F2109, F2111), probes were implanted bilaterally in the inferior colliculus (IC), with a dorsoventral approach, to cover the whole tonotopic axis of the central nucleus of the IC. One ferret (F2110) was implanted with one probe in the left IC

with the same approach as before and another in the left primary auditory cortex (A1) with a tangential trajectory to the surface, aiming to record the neural responses along the tonotopic axis of A1 rather than at a single location across the cortical layers.

2.4.2. Surgical implantation of Neuropixels probes

In preparation for the surgery, anaesthesia was induced with Domitor (medetomidine hydrochloride, 0.022 mg/kg, i.m., Orion Pharma) and Narketan (ketamine hydrochloride, 5 mg/kg, i.m., Vetoquinol). Once the animals were intubated and artificially ventilated anaesthesia was then maintained with IsoFlo (isoflurane, 1–3% with 100% oxygen as a carrier, Abbott Laboratories) and the effects of Domitor reverted by the administration of Antisedan (atipamezole hydrochloride, 0.06 mg/kg, s.c., Orion Pharma). At the start of the surgery, the ferrets also received a dose of Atropine (0.06 mg/kg, s.c., Hameln Pharmaceuticals) to reduce pulmonary secretions, Amoxicillin/clavulanic acid (Co-amoxiclav, MSD Sandoz) antibiotic to prevent infections, Metacam (meloxicam, 0.2 mg/kg, s.c., Boehringer Ingelheim) and Vetergesic (buprenorphine hydrochloride, 0.03 mg/kg, s.c., Alstoe Animal Health) for analgesia, Dopram (doxapram hydrochloride, 0.2 mg/kg, s.c., Norbrook Laboratories) to prevent respiratory depression, and Dexamethasone (Dexadreson, MSD Animal Health) to reduce brain oedema. Heart rate, respiratory rate, oxygen saturation and CO_2 levels were always monitored. The body temperature of the animal was measured using a rectal probe and maintained using a BearHugger warming up device at 38-39º and an electrical heating blanket. A cannula inserted in the radial vein was used to provide a solution of glucosate serum (0.9% sodium chloride, pH 7.2–7.4, plus 5% glucose) at a rate of 3.0–5.0 mL/h and to administer a dose

of antibiotic every 2 hours. The eyes were protected using Viscotears liquid gel (Carbomer, Bausch + Lomb).

A midline scalp incision was made and the temporal muscles retracted to expose the skull, which was scrapped cleaned ahead of performing the craniotomies. In the first surgery (F2110), two craniotomies were performed, one over the left auditory cortex (AC) and the other anterior to the cerebellar tentorium, exposing the posterior part of the occipital cortex which was aspirated to reveal the underlying IC. In the craniotomy over the left AC, the dura was punctured to allow the implantation of a Neuropixels 1.0 probe. The probe was implanted with a tangential approach to A1 aiming to cover the tonotopic axis. The second probe was implanted with a dorsoventral orientation, in the central nucleus of the IC covering also the tonotopic axis. The other three animals (F2108, F2109 and F2111) had craniotomies performed bilaterally over the cortex overlying the IC. In two of the animals (ferrets F2109, F2111) the exposed occipital cortex in the left craniotomy was aspirated to reveal the IC where the electrode was implanted. Equivalent coordinates were used for the implantation of the recording probe in the right IC. In the last surgery (ferret F2108), a different implantation approach was used by which we recorded electrical activity in the brain as the recording probes were being implanted to target each IC. In this case, no cortex was aspirated and the anaesthesia was maintained using Domitor and Narketan in saline throughout the surgery, to avoid the reduction of neural responses in the brain commonly associated with IsoFlo anaesthesia. Once the probes were in place and the craniotomies sealed with silicone (Kwik-Sil™, World precision Instruments), the probes were secured using bone cement and electrically grounded to previously implanted bone screws that also provided extra fixation for the bone cement in addition to the adhesive (SuperBond, Sun Medical) applied over the skull.

A rigid cylindric enclosure (max. dimensions D x H: 3 x 4 cm) with a narrowed base was placed around the exposed part of the probes to protect them and secured using bond cement. These enclosures had a removable cap to provide access to the probes during recording sessions. Finally, the scalp was sutured around the enclosure.

The postoperative analgesic protocol consisted of 2 days of treatment with Vetergesic (0.1 mg kg/ml, s.c.) twice a day and 7 days of oral Metacam (2 mg/kg orally). Profilactic antibiotic (Synulox (0.1 mL/kg, s.c.) was administered for 7 days.

Approximately 2 weeks after the surgery the recordings were started. None of the probes implanted in animal F2109 worked after the implantation, so the electrophysiological data presented here were recorded in three animals (F2108, F2110 and F2111). For animal F2110, neural data recorded during a first period of monaural earplugging were noisy due to a problem with the ground for one of the probes, which introduced electrical noise in both probes. After fixing the ground, data were collected for a second period of earplugging in the IC, while the probe in the AC stopped working. Therefore, the data presented in the results section were obtained exclusively from the IC in all animals.

2.4.3. Hardware and training

We recorded electrophysiological data from freely moving ferrets (n=3) while they performed a sound localisation task. To track the neural changes associated with learning-induced adaptation to monaural earplugging, recordings were performed daily throughout training while the animals wore an earplug. Additionally, data were recorded in normal hearing conditions, both prior to the earplug insertion as well as after restoring normal

binaural hearing post earplug removal (see 2.3.1 and 2.3.2 for a detailed description of the behavioural paradigm).

Additional recordings were performed in all the ferrets at the end of the adaptation experiment under anaesthesia with Domitor (medetomidine hydrochloride, 0.022 mg/kg, i.m.) and Narketan (ketamine hydrochloride, 5 mg/kg, i.m.), with the earplug in place and after earplug removal. Anesthetised animals were placed at the central platform in the same arena used for behavioural testing while sounds were presented from different azimuthal locations around the animal in the same manner as when the behavioural task was being performed, to compare the properties of responses in the IC between the awake and anaesthetised conditions.

Each ferret was implanted with two Neuropixels 1.0 probes which allowed us to record single and multi-unit activity from 768 recording channels simultaneously (384 channels per probe). Recordings were performed using SpikeGLX, which registered the neural data streams from an Imec Onebox (IMEC Leuven, Belgium) connected to the animal's implants. Task-related events, including triggering of sound presentation and licking at the peripherical spouts, were input into a PXIe – 6341 board (National Instruments (NI), United Kingdom). MATLAB (MathWorks, United States) was used to control the task and save the task variables, such as intensity or location of the presented sound, while SpikeGLX recorded the timing of task-related events, such as the time of the sound presentation or the animals' response, which could be aligned to neural events offline. Twelve analogue channels (0-11) in the PXIe – 6341 board recorded the timing of the animals' responses at each of the individual waterspouts associated with the twelve loudspeakers in the arena. A thirteenth channel (analogue 12) registered the timing of the sound presentations and analogue 13 was used to record a 1 Hz square wave, which was

common to all data streams and used to align neural and task events during the data processing.

At the beginning of any recording session, the Neuropixels probes were connected to the headstages that were in turn connected to the control unit by an interface cable. A pulley system with a weight allowed the interface cable to extend and retract to allow the free movement of the animal in the arena without being any interference from the cable. The length and flexibility of the cable allow it to extend and retract without adding tension to the head of the animals.

2.4.4. Recordings of Frequency Response Areas

To characterise the frequency tuning of the recorded units, 100-ms pure tones at different frequencies (499Hz to 30kHz) and intensities (10 to 90 dB SPL in steps of 10dB) were presented from the loudspeaker at 0 degrees (in front of the animal) to anaesthetised ferrets. Each frequency/intensity pair was presented 10 times, resulting in 2700 sound presentations per recording session. Frequency response areas (FRA) were computed by summing activity in the first 50 ms following sound onset for each frequency-level combination and the resulting spike matrix was smoothed.

2.5. Data analysis of Neuropixels recordings

2.5.1. Data processing

The raw data were processed using the ecephys_spike_sorting pipeline for recordings in SpikeGLX (https://github.com/jenniferColonell/ecephys_spike_sorting.git). This pipeline processes comprises data pre-processing, spike sorting, post-processing and quality assessment.

Raw data were filtered and denoised using CatGT[1]. By default, as per recommended by the developer due to its robustness against outlier values, a global common average referencing (gblcar) was used along with a time shift (tshift) to account for the fact that not all channels are sampled simultaneously and to temporally align all the channels. Exceptionally, for a subgroup of sessions that contained high frequency artefacts due to external electrical noise, the gbldmx (global demux common average referencing) filter was used instead of gblcar, which performs common average referencing using groups of channels that are digitised at the same time. This latter filter deals better with high frequency noise, since using a smaller group of channels results in larger correction factors. For sessions where noise was not present, no substantial difference was observed between the two filters.

Spike sorting was performed using Kilosort 3.0 (Pachitariu et al., 2023). Any electrical event or spike was matched against a series of templates that differ in their characteristics, e.g. amplitude and the distance between peaks, and were accordingly

[1] https://billkarsh.github.io/SpikeGLX/#catgt

grouped and assigned into different clusters, a conceptual representation of a neural unit (unit for short), or neuron. The close proximity of the recording sites within the electrode allows a single spike to be potentially recorded by different channels. To prevent the overestimation of recorded units at different recording sites with different template characteristics, the algorithm takes into account the timing of spikes at close recording sites and the geometry of the recording sites on the probe to estimate the changes in amplitude with distance. Additionally, tracking the activity over time in all channels allows the correction of drifting activity due to the minute relative movements between the probe and the brain. Spike sorting was followed by a Kilosort postprocessing step which removed spike duplicates that can emerge from the sorting process. This step is necessary since Kilosort sometimes fits spike templates to the residual of other spikes, resulting in units that contain duplicated spikes. Moreover, because Kilosort does not present any constraints on template shape, a further processing step consisted of identifying noise templates, which were those that could not physically correspond to the voltage change associated with a neuron's action potential because of an abnormal spatial spread, an abnormal shape (no peak and trough) or having multiple peaks. Clusters with noise templates were assigned to the *noise clusters* category.

Additional steps consisted of extracting the mean waveform of each of the units using Cwaves and computing a series of metrics (e.g. firing rate, interspike interval (ISI) violation and amplitude cut-off) that are useful for assessing the quality of the sorting output, by providing measurements for each individual unit.

Finally, the temporal alignment between the neural and task events was achieved using the tool Tprime, which aligns both streams using a common signal consisting of a 1 Hz square wave generated from the Imec Onebox.

2.5.2. Unit selection for data analysis

The output of the spike sorting process stores the timings of all the spikes grouped in different clusters classified as *good* or *noise*. The g*ood* cluster category comprises both single and multi-unit activity, while *noise* clusters correspond to those identified by the 'Noise Clusters' module as 'non-physiological' based on the template shape. However, this classification is not perfect, giving some false negatives, i.e., clusters that were classified as *good* but are actually *noise*. Removing these clusters is crucial to avoid contamination, which can alter the results during the data analysis.

Regardless of their classification, any cluster could also be classified based on whether it showed a response to sound presentation or not (i.e., responsive and non-responsive). We defined a unit as responsive when it showed a significant difference in firing rate within a 100 ms window after the onset or offset of a sound relative to an equivalent window prior to the presentation of the sound. We observed that *noise* clusters, overall, did not show any change in firing rate associated with the stimulus presentation (i.e., they were non-responsive). Conversely, *good* clusters showed both profiles, responsive and non-responsive. Manual curation of some example sessions showed that the majority of the *good* responsive units were actually good units, while most of the non-responsive *good* clusters had been misclassified and were actually noise.

Therefore, since our main interest focuses on understanding how the activity of auditory units changed throughout learning, only clusters that were responsive to sounds and were originally classified as *good* were considered for the analysis. The results reported in this thesis are based on the activity of these units. These criteria were applied

uniformly to all recording sessions, which provided an objective way of selecting good units for analysis while avoiding the subjectivity of the manual selection of units.

2.5.3. Single unit detection criteria

The number of extracted clusters varied substantially across sessions, but the number of responsive units was relatively constant, and was around a hundred units per hemisphere.

These units corresponded to both single (SUA) and multi-unit activity (MUA). Single units were identified using the following criteria: (1) firing rate above 0.5 Hz, (2) waveform amplitude higher than 70 μV (peak amplitude – trough amplitude), and (3) less than 30% of missing spikes computed by fitting a Gaussian distribution to the amplitude of the spikes. The missing tail of the distribution corresponds to the undetected spikes that fell below the threshold for detection. A cut-off parameter indicates where the distribution is truncated, and this value serves as a proxy for the percentage of missing spikes (estimate of a false negative rate). A fourth criterion for identifying single units was provided by estimating a false positive rate ($\mathbf{f}_I{}^p$), calculated using the formula $r = 2(T_R - T_C)N^2(1 - \mathbf{f}_I{}^p)\,\mathbf{f}_I{}^p\,/T$ (Hill et al., 2011), where r is the number of refractory period violations, T_R is the refractory period (set to 1 ms for the units recorded in the IC), T_C is the censored period (set to 0.16 ms and corresponding to the spike duplicate detection threshold), N is the number of spikes, and T is the total length of the recording. The solution to this equation is the root of a quadratic equation, and when the output is an imaginary number, the number of violations is too high, so the $\mathbf{f}_I{}^p$ is set to 1 and the unit is rejected as a single unit.

2.5.4. Spatial tuning

We found no systematic difference in the spatial responses of single and multiunit activity, therefore all were included in all analyses, as has been done in other studies (Lee & Middlebrooks, 2011). Thus, we will use the terms 'unit', 'neuron' and 'cluster' interchangeably. To determine the sharpening of the spatial tuning we computed the equivalent rectangular receptive field (ERRF) for each unit (Lee & Middlebrooks, 2011). This was calculated by determining the area under the rate-azimuth function computed for the first 50 ms after sound onset. Then the width of a rectangle with equivalent area and peak rate was computed as a measure of the tuning width, which was transformed into degrees by multiplying by 30. To obtain the direction of the tuning we used trigonometry to extract the centroid of the azimuth-rate function.

2.5.5. Population decoding analysis

Different decoding approaches were used. A pattern classifier adapted from Meyers, 2013 was trained using the spike trains from units recorded in the IC in either a single or both hemispheres. Data were binned into 100 ms bins with 50 ms overlap, and were then split into training and test sets using 10 cross-validation splits. This method was used to predict the actual target azimuth in awake and anaesthetised conditions and the compressed azimuth, for which locations were grouped into four quadrants (northeast NE, southeast SE, southwest SW and northwest NW). In both cases, the azimuth was estimated using the maximum correlation coefficient between the predicted and actual target azimuth.

For the spike-pattern decoding model, we divided spikes from each simultaneously recorded unit into 25 ms bins (optionally normalising each neuron's spikes so the sum of all of its spikes across trials is equal to 1), and collated responses for each trial, giving a tensor of neuronal responses, Xthu, where t is the trial number, h is the bin number within that trial, and u is the unit number. The opponent-coding model was similar but all spikes from each side of the brain were collapsed into a single time-varying spike rate.

We then created a target vector, yt, where t again corresponds to trial number. Depending on the quantity to be decoded, yt was the left-right location of the sound source (between -1 and 1), the front-back location of the sound source (between -1 and 1), the azimuth of the sound source (-180 to +180 degrees) or the sound level (dB SPL).

We used a linear model to produce $\hat{y}_t$, an estimate of, yt, by linearly decoding the neuronal responses:

$$\hat{y}_t = a_0 + \sum_{h,u} X_{thu} \cdot k_{hu}$$

We optimised the model parameters a0 and khu to minimise the mean square error between $\hat{y}_t$ and yt, subject to L2 regularisation, using glmnet (https://glmnet.stanford.edu/articles/glmnet.html). The trials were divided into non-overlapping sets of 12 trials (with the last set containing any extra trials), and each of these was used as the test set for one 'fold' of the data. For each fold, the model was trained only on the trials that were not part of the test set for that fold, so that the training and test sets were non-overlapping in every case. For each fold, the model was evaluated

on the test data by measuring the mean square error (or correlation coefficient) between $\hat{y}_t$ and yt.

To test the models' performance at decoding azimuth, we used trigonometry to convert the left-right (sine of the azimuth angle) and back-front (cosine of the azimuth angle) model predictions into azimuth values and compared these with the actual target stimulus azimuth.

2.5.6. Histology

Once the behavioural and neural recording data were acquired, animals were euthanised and their brains recovered to identify the location of the recording probes.

Animals were euthanised under sedation (Domitor: medetomidine hydrochloride, 0.022 mg/kg, i.m., Orion Pharma) by an intraperitoneal injection of pentobarbital sodium (Euthatal, 400 mg/kg, IP, Merial Animal Health). Once respiration had ceased, animals were perfused transcardially using 500ml of saline (0.9% NaCl) to wash out the blood from the circulatory system, followed by two litres of paraformaldehyde (4%) in 0.1M phosphate buffer ((PB), pH = 7.4).

The brain was removed from the cranium following the direction of the probes to minimise any physical damage caused by the extraction. For example, in case F2111 (Figure 4-1 C, D), small mechanical lesions were observed in the most dorsal part of the IC without any associated gliosis, suggesting that they were caused at the time of brain extraction because of the different directions of the probes. After removing the meninges, the brain was placed in a cryoprotective sucrose solution (30% sucrose in 0.1M PB) for 3 days or until it sank. The brain was blocked and the region containing the auditory

midbrain was sectioned at 45-µm thickness in the coronal plane using a freezing microtome (Leica SM2000 R sliding microtome, Leica Biosystems, Milton Keynes, UK). All sections containing the area of interest (the IC) were collected in six serial series, mounted on gelatinised slides and, once dried, stained for Nissl substance.

Sections were immersed for 10 min in cresyl violet acetate (0.5%, 61123, Fluka, Buchs, Switzerland) and then washed with distilled water for 30 seconds. To remove unspecific staining, sections were serially immersed for 1 minute each in an increasing concentration of ethanol (ETOH) solutions: ETOH (50%), ETOH (70%), acidic ETOH (1% glacial acetic acid in 95% ETOH) and ETOH (× 2, 100%). Following differentiation, to reduce unspecific background staining, slides were then serially immersed in chloroform (100%) for 20 seconds, ETOH (× 2, 100%) for 2 minutes and Xylene (× 3, 100%) for 3 minutes for complete dehydration. Finally, slides were cover-slipped using mounting medium (Entellan, Merck, Darmstadt, Germany).

Anatomical subdivisions of the IC were identified in each section and drawn under the microscope (DMR Leica Microsystems, Heerbrugg, Switzerland) fitted with a camera lucida and later superimposed to digital photographs for illustration purposes. IC subdivisions were identified based on previous descriptions of cell morphology and density in different species, included the ferret, as delineated in the ferret atlas (Radtke-Schuller, 2018). The location of the probes was readily apparent under the microscope from the physical lesion left in the tissue and the associated gliosis, characterised by a much denser Nissl staining of small cells at the tip of the electrode or along the track of the probe (Figure 4-1 D&E). The serial sections allowed reconstruction of the location of the probe along its length when the direction of the probe did not match the plane of sectioning. For illustrative purposes (Figure 4-1), the full length of the probe was

superimposed onto a photographed representative section where a significant length of the probe was observed.

2.5.7. Statistical analysis

The effect of stimulus parameters (sound location and intensity) on the sound-evoked activity (50 ms window from sound onset) was computed using a negative binomial generalised linear mixed effects model (glmmPQL). A negative binomial was used since prior inspection of the data showed overdispersion. Normalised firing rates, spatial tuning width, and centroids were compared using statistical tests, which were performed using RStudio (RStudio: Integrated Development for R. RStudio, Inc., Boston, MA, United States). Data normality was checked using the Shapiro–Wilk test.

3. Persistence and Generalisation of Adaptive Changes in Auditory Localisation Behaviour Following UCHL

3.1. Introduction

Sensory experience plays a vital role in calibrating neural circuits in the brain, so that they can be optimised to the prevailing sensory conditions. The experience-dependent plasticity of the maturing brain enables the processing that takes place within those circuits to adjust to growth-related changes in sensory inputs and to be matched to the statistics of the environment during sensitive periods of development (Keating & King, 2013; Kumpik & King, 2019). Plasticity in later life allows perceptual skills to improve with practice and affords a capacity to compensate for altered inputs associated with sensory disorders (Irvine, 2018; Kumpik & King, 2019).

In the auditory domain, the recovery of sound localisation accuracy in mammals experiencing a unilateral conductive hearing loss (UHCL) has been widely used as a model for training-dependent plasticity (Keating & King, 2015). Sound localisation is achieved by the computation of binaural and monaural spatial cues that result from the way sounds interact with the head and external ears (Grothe et al., 2010). Interaural time differences (ITDs) and interaural level differences (ILDs) provide the primary basis for localising sounds in the horizontal plane, and the relationship between these binaural cues and directions in space is altered by occluding one ear, resulting in much less accurate localisation judgments. Previous work has shown that adult humans and ferrets can be trained to adapt to this monaural hearing perturbation, thereby substantially recovering their localisation accuracy (Kacelnik et al., 2006; Keating et al., 2016; Kumpik et al., 2010). This entails plasticity in the way monaural and binaural cues are used to localise sound (Keating & King, 2015), which is dependent on the functional integrity of auditory cortical circuits (Bajo et al., 2019; Bajo et al., 2010; Nodal et al., 2010).

Adaptation to monaural hearing loss can be achieved by reweighting the different localisation cues—with greater reliance placed on the unchanged monaural spectral cues available at the open ear—or through compensatory changes in binaural cue sensitivity (Kacelnik et al., 2006; Keating et al., 2016; Kumpik et al., 2010; Zonooz & Van Opstal, 2019). In addition, when a fixed sound level was used, the localisation responses of adult humans wearing an earplug in one ear became more dependent during training on spatially ambiguous monaural head-shadow cues (Zonooz & Van Opstal, 2019). The absence of an aftereffect when the earplug is removed, i.e., post-plug localisation performance is indistinguishable from the normal-hearing pre-plug condition (Bajo et al., 2019; Kacelnik et al., 2006; Keating et al., 2016; Kumpik et al., 2010; Zonooz & Van

Opstal, 2019) has been interpreted as the result of reweighting. Cue reweighting may provide a particularly effective strategy for adapting to asymmetric hearing loss because this helps to maintain accurate sound localisation under different hearing conditions without the need of drastic neural changes.

Spatial cue reweighting is therefore thought to be context specific, arising from changes in the relative reliability of different localisation cues (Keating & King, 2015; Van Wanrooij & Van Opstal, 2007). Although the lack of aftereffect could be interpreted as an indication of a transient process, the process of adapting to a monaural occlusion appears to leave a memory trace that can be retrieved when the same ear is re-plugged (Bajo et al., 2019). It is not known how long this memory trace is retained or whether the previously learned strategy for adapting to UCHL is ear specific. This is likely to be important in clinical conditions, such as otitis media with effusion (Hogan et al., 1997), where recurrent hearing loss is often experienced.

The extent to which perceptual training generalises to untrained stimuli determines its therapeutic value. Previous studies have assessed adaptation to UCHL by presenting target sounds against a silent background in order to maximise learning. However, more naturalistic listening conditions can change abruptly as we navigate our daily lives, as do the target sounds we need to attend to. Therefore, determining whether auditory spatial learning generalises beyond the training stimulus and to more complex listening environments is crucial for designing effective training protocols as part of rehabilitation strategies for hearing-impaired individuals.

In this chapter, I address both the persistence and generalisation of auditory adaptive learning. Our results show that the cue reweighting that occurs when adult ferrets are first trained with abnormal auditory spatial cues takes place more readily when

subsequent periods of monaural occlusion are experienced, indicating that the effects of learning persist for at least several months. However, adaptation to conductive hearing loss in one ear appears to reduce the capacity of the auditory system to compensate for occlusion of the contralateral ear. We also show that the training-dependent recovery in localisation accuracy does generalise to other acoustic conditions and that the degree of adaptation correlates with the generalisation of learning.

3.2. Results

3.2.1. Effects of sound localisation training on task performance

Ferrets were trained in an approach-to-target sound localisation task in which the animal self-triggered the presentation of a broadband sound from one of the 12 surrounding loudspeakers. The ferret reported the location of the presenting loudspeaker by approaching it and correct responses were rewarded with water (Chapter 2 Section 2.3.1). Over the course of collecting behavioural data on the sound-localisation task, we observed little change in the performance of the ferrets (n = 4) under normal hearing conditions (i.e., during the testing runs carried out without an earplug) (Figure 3-1). The accuracy of their responses on the approach-to-target task improved as the duration of the broadband target sound was increased (from 47.8 ± 3.4% correct for 40 ms to 96.1 ± 1.5% correct for 2,000 ms) (GLMM, $p < 0.0001$) (Figures 3-1). Despite extensive testing, which included several periods of monaural occlusion, their performance across different stimulus durations remained very stable when normal binaural inputs were available, other than a small reduction in percentage correct scores at intermediate target durations (100– 500 ms) (GLMM, $p = 0.001$) (Figure 3-1 A). The lack of improvement in localisation accuracy over time for broadband stimuli providing access to the full range of spatial cues suggests that no perceptual learning had taken place over the course of these sessions. Furthermore, the consistent performance across different stimulus locations (Figure 3-1 B) gave no indication of any long-lasting change in the way these cues were processed and integrated under normal hearing conditions, despite the ferrets

experiencing several intervening periods during which they learned to adapt their behaviour to conductive hearing loss in one ear.

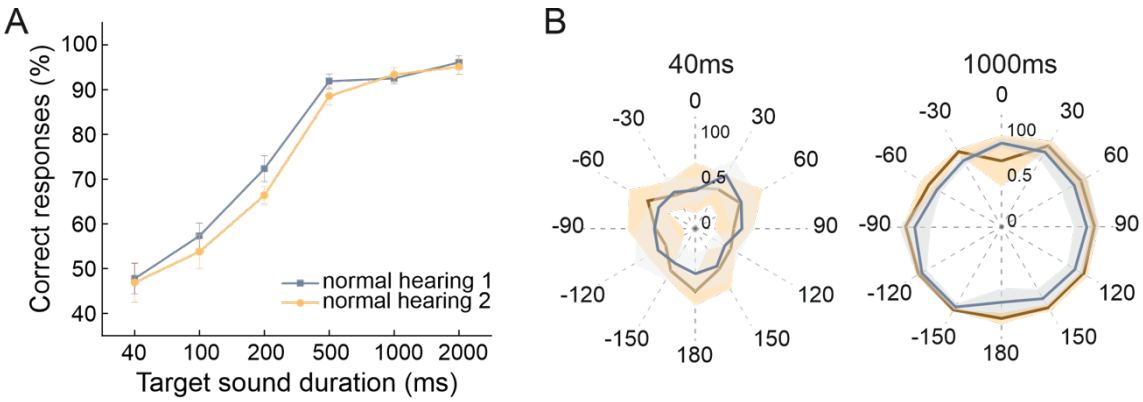

Figure 3-1. Stability of ferret sound localisation performance over time when normal spatial cues are available. (A) Localisation performance (percentage of correct trials averaged across all 12 target locations, sound levels and ferrets (n=4)) at different sound durations for two normal hearing periods (>300 trials at each sound duration in each of the two periods) separated by 6 months during which two 10-day periods of training-induced adaptation to monaural occlusion in the right ear took place. Error bars show the standard error of the mean. (B) Spatial distribution of the percentage correct scores from both normal hearing periods for the 40- and 1000-ms broadband noise bursts. Lines represent the means and shaded areas the standard error of these scores across animals.

3.2.2. Behavioural adaptation to UCHL

The approach-to-target responses of one cohort of ferrets (n = 7) are shown in Figure 3-2 A. They localised 1000-ms broadband noise busts with a consistently high level of accuracy when normal binaural and monaural spatial cues were available, with their performance declining from ~95% in the last pre-plug session to ~30% correct when one of their ears (the left in this case) was first occluded. The ferrets initially mis-localised almost every stimulus presented in the frontal region of the hemifield ipsilateral to the earplug (see polar plots at the top of this figure). Over the first few days of monaural

occlusion, a gradual improvement in performance occurred at all other locations, including those on the side of the open ear, which was then followed by a recovery in localisation accuracy at the frontal ipsilateral locations. This pattern of adaptation was remarkably consistent across animals.

We also measured the accuracy of the ferrets' sound-evoked head orienting movements, as these are thought to involve different neural circuits from those required for the approach-to-target responses (Isa et al., 2021; Lomber et al., 2001; Nodal et al., 2012; Thompson & Masterton, 1978) (Figures 3-2 B,C). Data from one example ferret (F2005) show that when the earplug was inserted, the initial head turns made following sound presentation were clearly biased toward the side of the open ear, independent of the location of the target (Figure 3-2 B, first 3 plug days). Adaptation of the head orienting movement then occurred with training on the sound-localisation task, which was manifested as a gradual recovery in orienting responses toward the side of the plugged ear for stimulus locations on that side (Figure 3-2 B, last 3 days). It should be noted, however, that the degree of adaptation varied between animals and was generally not complete, as shown by the undershoot in the responses made in that hemifield by ferret F2005 on the last 3 plugging days (Figure 3-2 C). This mirrors the asymmetry in the approach-to-target behaviour at the corresponding stage (Figure 3-2 A). As with the approach-to-target responses, the metrics of the head turns measured on the days after earplug removal resembled the pre-plug data (Figure 3-2 B).

Adaptation of the head orienting responses was quantified for each ferret as the area between a plot of the average final head bearing versus target location across all animals prior to earplug insertion and the final head bearing measured for individual animals on the side of the occluded ear in the last 3 days of training (Figure 3-2 C). This

was then compared to the adaptation index derived from the approach-to-target behaviour, which was computed as the ratio between the percentage correct responses in the last 3 days of monaural occlusion and the 3 days prior to earplug insertion. The comparison of these two measures for individual animals revealed that they were highly correlated (slope significantly different from zero; $R^2 = 0.94$, $p < 0.001$) (Figure 3-2 D), with the ferrets that achieved the highest percentage correct scores also showing greatest adaptation of the head orienting responses, as reflected by a smaller difference between pre-plug and adapted final head bearing.

Importantly, given that the initial head orienting responses were generally completed within 200-300 ms of stimulus onset (Figure 3-2 B), it is unlikely that the very similar adaptation in the approach-to-target behaviour can be attributed solely to the animals tracking the source of the 1000 ms noise bursts as they approached the loudspeakers.

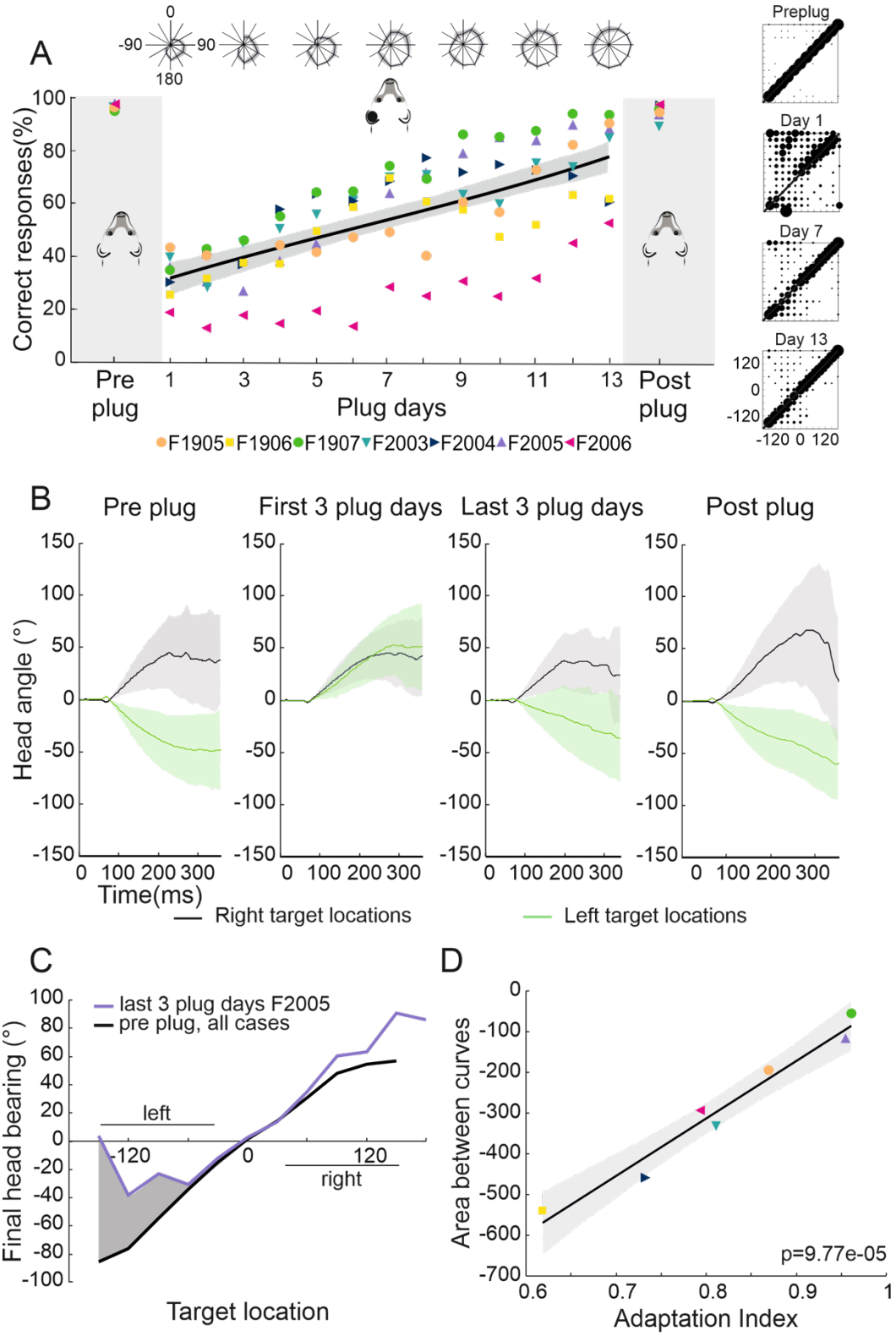

Figure 3-2. Adaptive changes in approach-to-target and head orienting responses over the course of monaural occlusion. (A) Percentage correct scores for the approach-

to-target behaviour. Different symbols indicate individual ferrets. Their mean scores over 3 days prior to earplug insertion and 3 days after earplug removal are highlighted by the grey regions on either side of the scores obtained for each day of training with the left ear occluded, which for these animals lasted 13–16 days (days 1–13 only are shown). The black line and shaded area represent the linear regression and the 95% confident intervals for the data obtained with the earplug in place. The polar plots at the top show the mean ± S.E. score across animals at different target locations for every 2 days of training. The stimulus-response plots on the right show the distribution of response locations selected (y-axis) as a function of target location (x-axis) before and at three different time points after earplug insertion. (B) Mean ± S.E. changes in head angle for left (green) and right (black) target locations for ferret F2005 (measured at 500 FPS and low-pass filtered at 50 Hz for plotting). Positive values correspond to rightward turns and negative values correspond to leftward turns of the head. Plots from left to right correspond to the 3 days before earplug insertion, the first 3 days with the ear plugged, the last 3 days with the ear plugged, and the 3 days following earplug removal. Occluding the left ear disrupted head orienting responses made to locations on the left, which progressively recovered as approach-to-target performance improved with training. (C) Mean final head bearing, [computed as the mean angle of the last-three frames before the end of the head turn, which is defined when a change from the original direction is detected (Chapter 2 Section 2.3.6.)], versus target location before earplug insertion averaged across all animals (black) and for the last 3 days of earplug adaptation for the example animal F2005 (purple). The shaded region represents the area between the two curves on the side of the occluded ear, computed as an index of adaptation of the head orienting responses. (D) Relationship between the adaptation index (ratio of the percentage correct scores on the last 3 days of plugging and before earplug insertion), which reflects recovery with training of the approach-to-target behaviour, and adaptation of the head orienting responses (the area between the head orientation curves, as in panel C) for all seven animals shown in panel (A).

3.2.3. Equivalent adaptation to occlusion of each ear

Before investigating the persistence of adaptation by examining the effects of further exposure to UCHL in either the same or the contralateral ear, it was first necessary to show that ferret localisation behaviour adapts equally well to occlusion of either the left or the right ear. This is illustrated in Figure 3-3 for the sound-evoked head orienting responses recorded from two groups of ferrets, one of which was plugged in the left ear

(the animals used in Figure 3-2) and another in the right ear. In the normal hearing (pre-plug) sessions, the final head bearing of the ferrets varied systematically with the target location out to ±150° azimuth (Figure 3-3 A). As previously reported (Nodal et al., 2008), we observed an increasing undershoot in the final head bearing for progressively more eccentric targets (Figure 3-3 B). There was no difference in the accuracy of the responses to targets in the left and right hemifields or in the absolute slope of the regression lines fitted to these data (GLMM, $p = 0.055$; Table 1).

The head-orienting responses were affected in the same way by plugging either the left ear in one group of ferrets (Figures 3-3 C, D) or the right ear in the other group (Figures 3-3 E, F) (Kruskal-Wallis chi-squared = 1259.2, df = 3, $p<0.001$, post-hoc pairwise comparison head bearing error in the first 3 days on the side ipsilateral to the earplug, right earplug vs left earplug $p = 0.078$; head bearing error in the first 3 days on the side contralateral to the earplug, right earplug vs left earplug $p = 0.160$). The final head bearing was initially biased toward the side of the open ear, i.e., to the right when the left ear was plugged (Figure 3-3 C) and to the left when the right ear was plugged (Figure 3-3 E). Although the size of the head orienting errors across locations remained unchanged on the side of the open ear, much larger errors were made on the contralateral side, as indicated by the steeper slope of the linear fits to these data (Figures 3-3 D, F and Table 1). This asymmetry in performance between the left and right hemifields then declined with training, as illustrated by the adaptive changes in head-orienting behaviour for one example animal (F2005) in Figure 3-2 B.

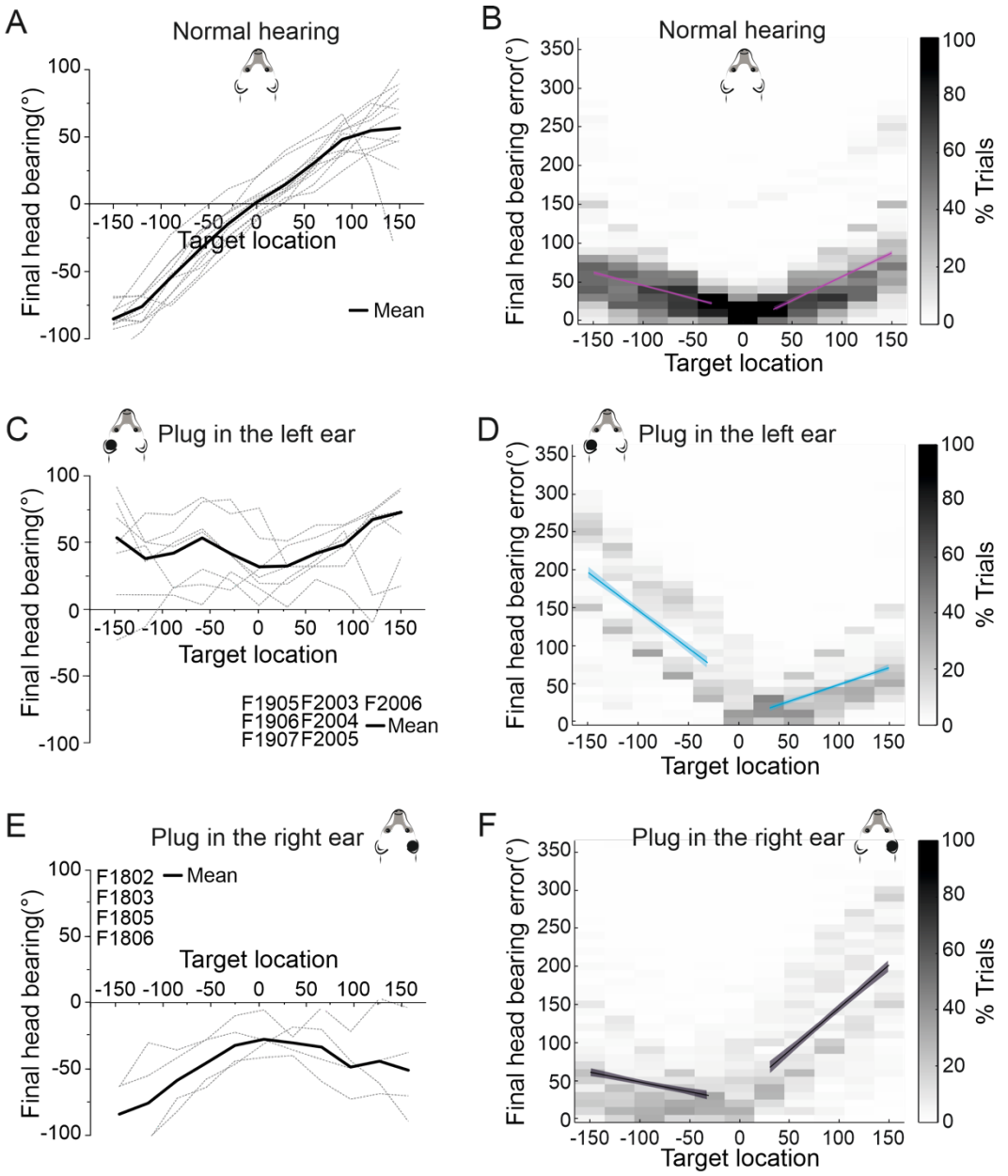

Figure 3-3. Effect of plugging either the left or the right ear on the accuracy of sound-evoked head-orienting responses. (A) Average final head bearing versus target location in normal hearing conditions for each of the animals (grey dashed lines) that participated in this study. Positive values correspond to targets on the right and rightward head movements, and negative values to targets on the left and leftward movements. The solid line represents the mean across animals. (B) Mean final head bearing errors versus target location in normal binaural hearing conditions for all animals. Linear regressions and their 95% confidence intervals are fitted independently for right and left target locations (magenta lines). (C) Mean final head bearing versus target location in the first 3 days with the left ear occluded. (D) Mean final head bearing errors versus target location in the first 3 days with the left ear occluded. Linear regressions and their 95% confidence intervals are fitted independently for right and left target locations (blue). (E) Mean final head

bearing versus target location in the first 3 days with the right ear occluded. (F) Mean final head bearing errors versus target location in the first 3 days with the left ear occluded. Linear regressions and their 95% confidence intervals are fitted independently for right and left target locations (black/grey).

TABLE 1. Parameters of the fitted regression lines for head bearing errors in Figure 3-3.

y = a + bx

		R^2	a (intercept)	b (slope)	p_b	tStat (b)
Preplug	Left side	0.17	11.96	-0.333	<0.0001	$t_{(2049)}$= -20.220
	Right side	0.28	-4.00	0.610	<0.0001	$t_{(1822)}$= 26.674
Right ear plugged	Left side	0.05	22.69	-0.258	<0.0001	$t_{(854)}$= -7.102
	Right side	0.34	33.55	1.124	<0.0001	$t_{(833)}$= 20.829
Left ear plugged	Left side	0.34	47.17	-1.000	<0.0001	$t_{(762)}$=-19.805
	Right side	0.26	3.86	0.449	<0.0001	$t_{(777)}$= 16.784

3.2.4. Adaptive learning is partially retained when spatial cues are altered again

Previous work has suggested that adaptation to the altered cues resulting from monaural occlusion leaves a "memory trace," since a second period of ear-plugging has a smaller impact on localisation accuracy (Bajo et al., 2019; Kacelnik et al., 2006). Here, we explored further how this spatial learning, and its memory or retrieval, are affected by multiple periods of monaural occlusion and their relative timing. To that aim, the interval between the training periods was varied, as was the ear that was plugged.

The ferrets in this group (n = 4) first experienced four periods of right ear occlusion, separated by short (7 days) or long (6 months) periods of normal binaural hearing. To determine whether they were then able to adapt to a different set of altered spatial cues, we subsequently measured their performance when the contralateral left ear was occluded instead (see Figure 2-1 B for timeline). We modelled adaptation to an earplug by fitting a linear regression line, for which the independent term (a) is inversely proportional to the initial disruption caused by insertion of the earplug and the slope (b) represents the rate of adaptation (Table 2). Plugging the right ear for the first time (right plug 1) resulted in the most dramatic loss of sound localisation accuracy from 97.6 ± 1.2% correct to 28.9 ± 9.3%, as indicated by the lowest value of the intercept (a = 10.366). Sound localisation accuracy recovered with twice-daily training and the highest rate of adaptation (b = 6.4) was observed during this first period of monaural occlusion (Figure 3-4 A). On all three subsequent occasions that the same ear was plugged, a smaller initial drop in performance was observed (Figure 3-4 and see intercepts in Table 2). Although less adaptation was therefore required, the animals' performance improved at a slower rate (smaller slopes) than during the first adaptation period, each time reaching a mean score of 70– 80% correct after 10 days of monaural occlusion. All adaptation slopes were, however, statistically significant from zero (Table 2), indicating that the ferrets were relearning to accommodate the altered spatial cues after each period of normal binaural experience.

Despite the similar pattern of adaptation in the second, third and fourth periods of right ear occlusion, differences were observed based on the interval between the plugging runs. The right plug 2 and right plug 4 runs were preceded by a short period (7 days) of normal binaural hearing following a prior period of monaural occlusion (right plug 1 and

right plug 3, respectively) and had the smallest initial localisation errors when the earplug was first inserted and lowest slope values (Figures 3-4 A, B, D, E and Table 2). This, therefore, suggests a greater retention of the previously learned adaptation. By contrast, the third period of right ear occlusion (right plug 3) was preceded by 6 months of normal hearing, and the adaptation profile more closely resembled that for right plug 1, i.e., a larger initial drop in performance (lower intercept value) and faster rate of adaptation (higher slope) than in the right plug 2 and right plug 4 runs (Figures 3-4 C, E and Table 2). In other words, the behavioural effects of each episode of UCHL depended on the animals' preceding binaural experience.

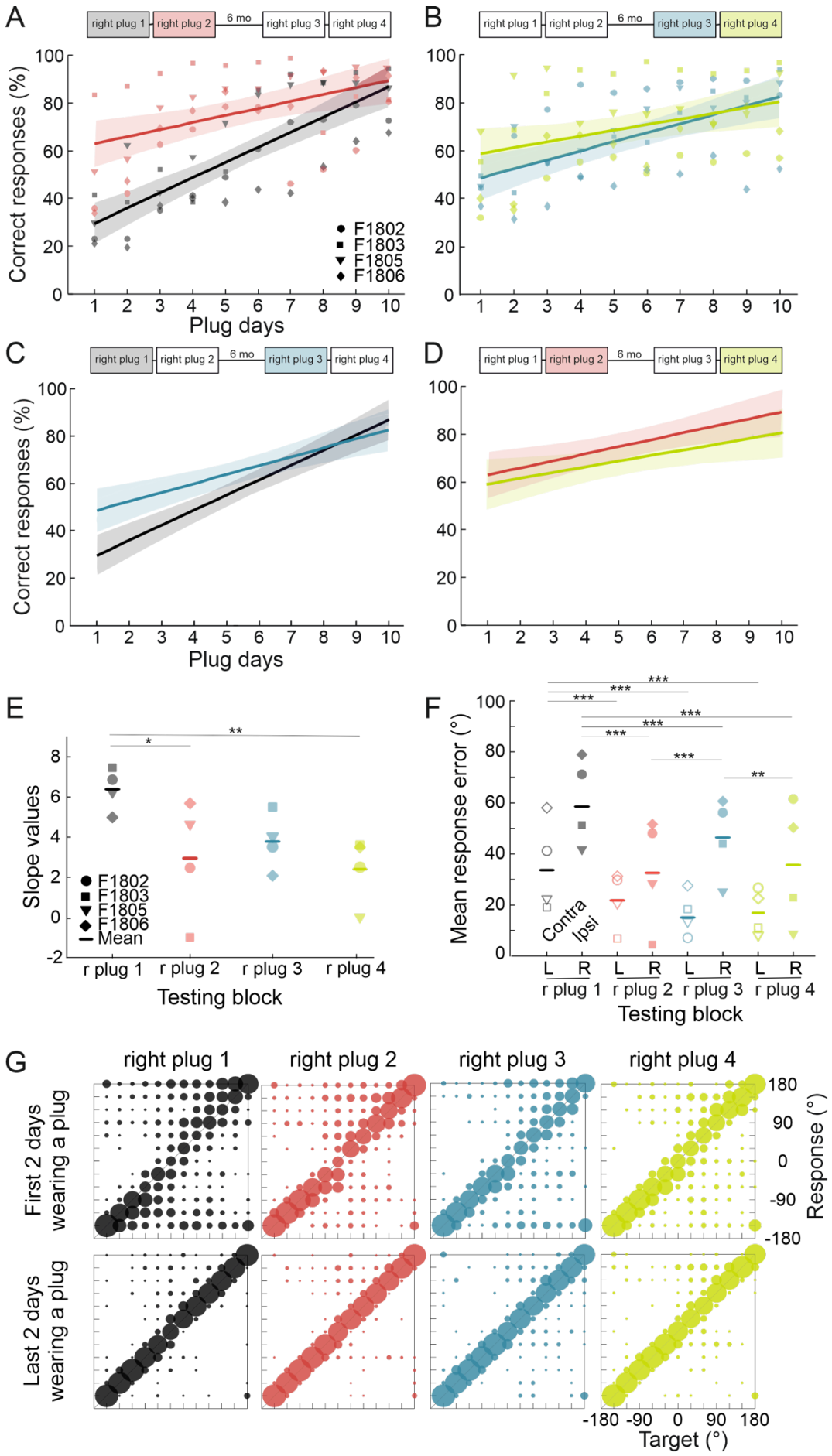
A
right plug 1
right plug 2
6 mo
right plug 3
right plug 4
Correct responses (%)
Plug days
F1802
F1803
F1805
F1806
B
C
D
E
Slope values
Mean
r plug 1
r plug 2
r plug 3
r plug 4
Testing block
F
Mean response error (°)
Contra
Ipsi
L
R
G
First 2 days wearing a plug
Last 2 days wearing a plug
Response (°)
Target (°)

Figure 3-4. Effect of repeated occlusion of the same ear on adaptive learning. (A) Regression lines (shaded areas indicate 95% confidence intervals) and individual animal scores during the first (right plug 1, black line and grey symbols) and second (right plug 2, red line and symbols) periods of right ear occlusion, which were separated by 7 days of normal binaural hearing. (B) Regression lines and individual performance for the third (right plug 3, blue line and symbols) and fourth (right plug 4, green line and symbols) periods of right ear occlusion, which were also separated by 7 days of normal binaural hearing. A longer interval of 6 months separated the right plug 2 and right plug 3 runs. (C) Comparison of regression lines for the right plug 1 and right plug 3 runs, which were each preceded by long periods (~6 months) of normal binaural hearing. (D) Comparison of regression lines for the right plug 2 and right plug 4 runs, which were each preceded by 7 days of normal binaural hearing following the right plug 1 and right plug 3 runs, respectively. (E) Individual animal and mean regression slopes for all four periods of monaural occlusion. (F) Mean response error magnitude in the initial 2 days of each period of right ear occlusion (right plug 1 to 4). Errors are shown separately for ipsilateral (R, right) and contralateral (L, left) target locations. Midline locations (0° and 180°) were not included in this analysis. Asterisks represent statistical significance of paired comparisons (*$p < 0.05$, **$p < 0.01$, and ***$p < 0.001$). (G) Response probabilities versus target location for the initial 2 days (top row) and the final 2 days (bottom row) of each of the four periods of right ear occlusion. For the numerical values and statistical analysis, refer to the main text.

The distribution of the localisation errors produced by monaural occlusion was not homogeneous across target locations and was always greater in the hemifield ipsilateral to the occluded right ear. This pattern was apparent at the start of all 4 ear-plugging runs (Figures 3-4 F, G top row), and partly reflects mis-localisation of sounds presented on the side of the earplug to the opposite side (right-to-left errors were initially twice as high as left-to-right errors). However, in contrast to the first and third periods of right ear occlusion, the difference between the mean response errors in the left and right hemifields for the right plug 2 and 4 runs was not significant (GLMM, $p = 0.126$, $p = 0.99$, respectively) (Figure 3-4 F), providing further evidence that the amount of prior normal binaural experience determines how the brain responds behaviourally to each episode of UCHL.

The spatial pattern of errors also provides insights into the potential basis for the recovery of sound localisation accuracy at different stages during the adaptation process. Localisation errors on the side of the open left ear were consistently low at the start of the second, third and fourth periods of right ear occlusion (Figures 3-4 F, G), which could reflect a rapid switch to the use of monaural cues provided by the open ear. A greater and more gradual improvement in performance was found on the side of the plugged ear (Figure 3-4 G) and over this time the incidence of both left-right and front-back errors declined. This could be due to a more gradual remapping of the abnormal binaural cues to compensate for the effects of the earplug. Further support for this interpretation is provided by the observation that performance reaches ≥70% correct after a similar number of days irrespective of previous earplug experience and adaptation, the time elapsed between the periods of monaural occlusion, or the initial impact of plugging the ear on localisation performance.

TABLE 2. Parameters of the fitted regression lines during earplug adaptation.

	y = a + bx				
	R^2	**a (intercept)**	**b (slope)**	**p_b**	**tStat (b)**
Right plug 1	0.633	10.366	6.377	5.06e-10	$t_{(38)}$= 8.2695
Right plug 2	0.198	54.064	2.939	0.00234	$t_{(38)}$= 3.2623
Right plug 3	0.337	37.354	3.775	5.07e-05	$t_{(38)}$= 4.5681
Right plug 4	0.122	51.785	2.395	0.0154	$t_{(38)}$= 2.5363
Left plug 1	0.474	20.61	3.541	5.43e-07	$t_{(38)}$= 6.0149
Left plug 2	0.442	33.301	3.524	1.71e-06	$t_{(38)}$= 5.6525

The primary auditory cortex (A1) has previously been shown to play an essential role in adapting to an earplug in one ear but is not required for retrieval of the memory trace that facilitates adaptation during a second period of monaural occlusion (Bajo et al., 2019). This raises the possibility that adaptive learning is consolidated in circuits that lie downstream from the cortex. The disruptive effects of auditory corticocollicular lesions on adaptation (Bajo et al., 2010) suggest that midbrain areas that are known to be more directly involved in the control of head orienting behaviour may be important for the retrieval of learning. We therefore also examined the impact of a second period of monaural occlusion on the accuracy of the sound-evoked head movements.

In contrast to the start of the first period of right ear occlusion (right plug 1), where a marked left-right asymmetry was observed in the size of the head orienting errors due to the animals consistently turning toward the side of the open ear, these responses were more symmetrically distributed to appropriate sides of the midline at the start of the second period of right ear occlusion (right plug 2) (Figures 3-5 A, B and Table 3). In both cases, head orienting accuracy had partially recovered toward pre-plug values by the last 3 days of ear-plugging, with all the animals now responding to the appropriate side of space (Figures 3-5 C, D). This pattern of adaptation in head orienting behaviour across the two periods of right ear occlusion is consistent with that seen for the approach-to-target responses in showing that previous experience with altered spatial cues enables the ferrets to more readily adapt to a second period of UCHL in the same ear. The head orienting data therefore support the possibility that retrieval of learning following a short period of normal hearing involves subcortical circuits.

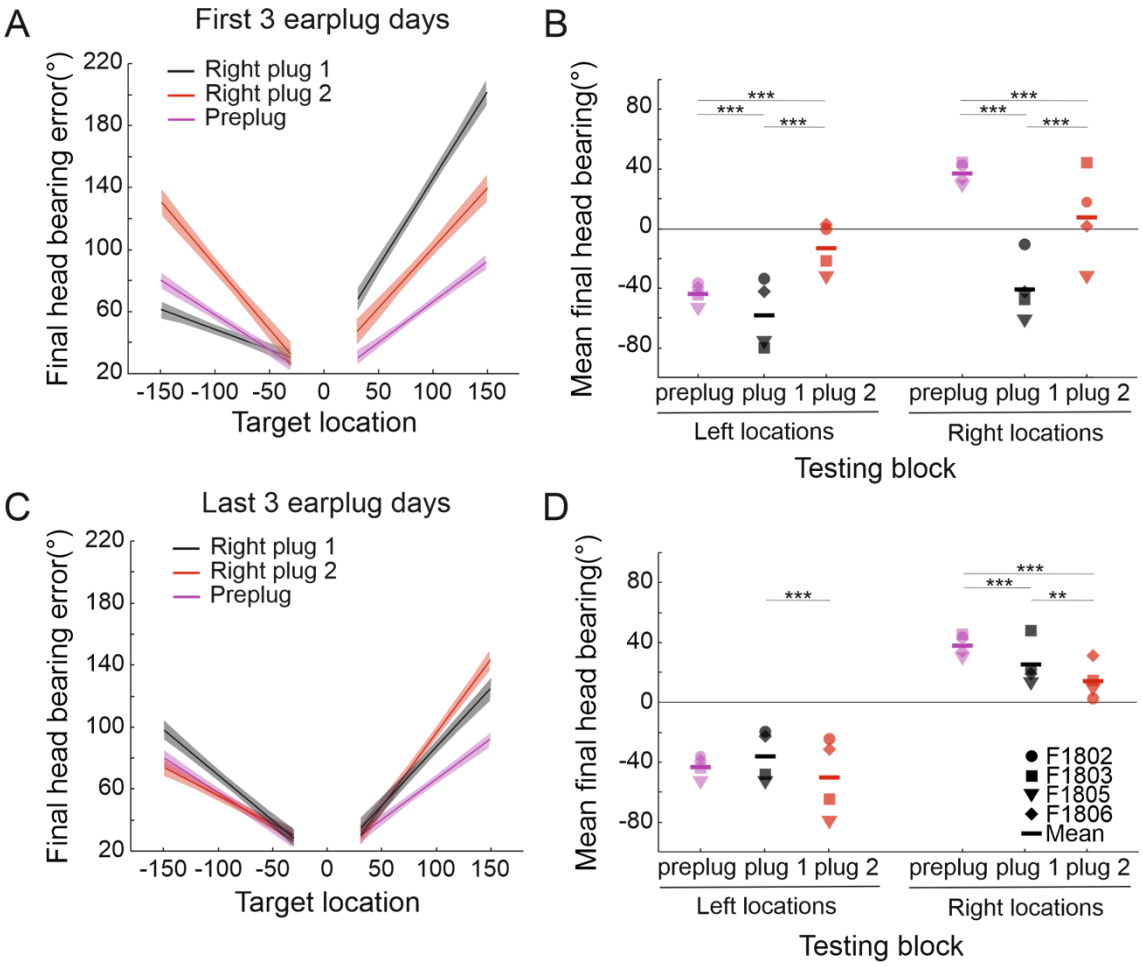

Figure 3-5. Persistence of adaptation in the sound-evoked head orienting responses. (A) Linear regression fits and their 95% confidence intervals for the mean final head bearing errors in the first 3 days of the right plug 1 and 2 runs (black and red lines, respectively). For comparison linear fits for preplug responses are shown in magenta. (B) Mean final head bearing shown separately for left and right target positions in the first 3 days of the right plug 1 and 2 runs. Midline locations (0° and 180°) were excluded. Note that the head orienting responses were no longer as biased toward the side of the open left ear at the start of the second period of right ear occlusion. (C) Linear regression fits and their 95% confidence intervals for the mean final head bearing errors in the pre-plug responses (magenta lines) and in the last 3 days of the right plug 1 and 2 runs (black and red lines, respectively). (D) Mean final head bearing shown separately for left and right target positions in the last 3 days of the right plug 1 and 2 runs. (**p < 0.01, ***p < 0.001).

TABLE 3. Parameters of fitted regression lines for head bearing errors (Figure 3-5).

			$y = a + bx$				
			R^2	a (intercept)	b (slope)	p_b	tStat (b)
First 3 days	Preplug	Left side	0.14	12.84	-0.449	<0.0001	$t_{(992)}$= -12.946
		Right side	0.21	14.34	0.520	<0.0001	$t_{(977)}$= 16.388
	Right plug 1	Left side	0.05	22.69	-0.258	<0.0001	$t_{(854)}$= -7.102
		Right side	0.34	33.55	1.124	<0.0001	$t_{(833)}$= 20.829
	Right plug 2	Left side	0.27	7.30	-0.824	<0.0001	$t_{(494)}$=-13.763
		Right side	0.24	23.19	0.779	<0.0001	$t_{(529)}$= 13.058
Last 3 days	Right plug 1	Left side	0.22	10.38	-0.587	<0.0001	$t_{(716)}$= -14.299
		Right side	0.27	12.00	0.752	<0.0001	$t_{(641)}$= 15.414
	Right plug 2	Left side	0.12	19.15	-0.364	<0.0001	$t_{(849)}$=-10.885
		Right side	0.35	1.21	0.950	<0.0001	$t_{(837)}$= 21.099

3.2.5. Adaptation to UCHL in the contralateral ear

We next examined whether ferrets that had learned to localise accurately following occlusion of one ear also exhibit similar adaptive plasticity when the direction of the binaural imbalance is reversed by plugging the other ear. The same group of ferrets that had experienced four periods of right ear occlusion now had their left ear plugged (Figure 3-6). This resulted in an initial drop in localisation accuracy to ~30% correct, the same as that seen when the right ear was plugged for the first time (Figures 3-6 A, B).

All the ferrets then exhibited a gradual improvement in performance with training, but they did so at a slower rate than in the equivalent first right ear plug run and recovered to a much lower level after 10 days of training with the left earplug in place (Figures 3-6

B, D and Table 2). A further difference in localisation accuracy between right plug 1 and left plug 1 was revealed by comparing the responses to sounds presented in the left and right hemifields. In the first left earplug run, localisation accuracy at the end of the adaptation period was significantly worse on the side of the plugged ear than on the side of the open ear (repeated measures ANOVA: effect of side, $p = 0.01$), whereas no difference between the left and right hemifields was found for the first right earplug run ($p = 0.139$) (Figures 3-6 E, F). This is not because of any inherent difference in the capacity of the auditory system to adapt to conductive hearing loss in the two ears (Figure 3-3), nor is it likely to reflect any residual bias toward the side of the previously open ear since this declined as the ferrets adapted and disappeared when the earplug was removed. Rather, it appears to reflect the prior experience of the ferrets in repeatedly adapting to occlusion of the right ear.

A week after removing the earplug from the left ear, this ear was occluded for a second time (left plug 2). As with repeated plugging of the right ear, this resulted in a much smaller initial deficit than when the animals first received an earplug in the left ear (Figure 3-6 A and Table 2), and their performance then improved with training at approximately the same rate as in left plug 1 (Figures 3-6 A, D) and right plug 2 (Figures 3-6 C, D). However, the animals localised less accurately at the end of the second period of left ear occlusion than after equivalent training with the right ear plugged (Figure 3-6 C), due to their poorer performance on the left side, ipsilateral to the earplug, relative to the right side (repeated measures ANOVA, $p = 0.003$) (Figure 3-6 E). These results therefore show that learning to localise sound with one ear occluded interferes with the capacity to subsequently adapt to conductive hearing loss in the other ear and that this effect persists over more than one period of monaural occlusion.

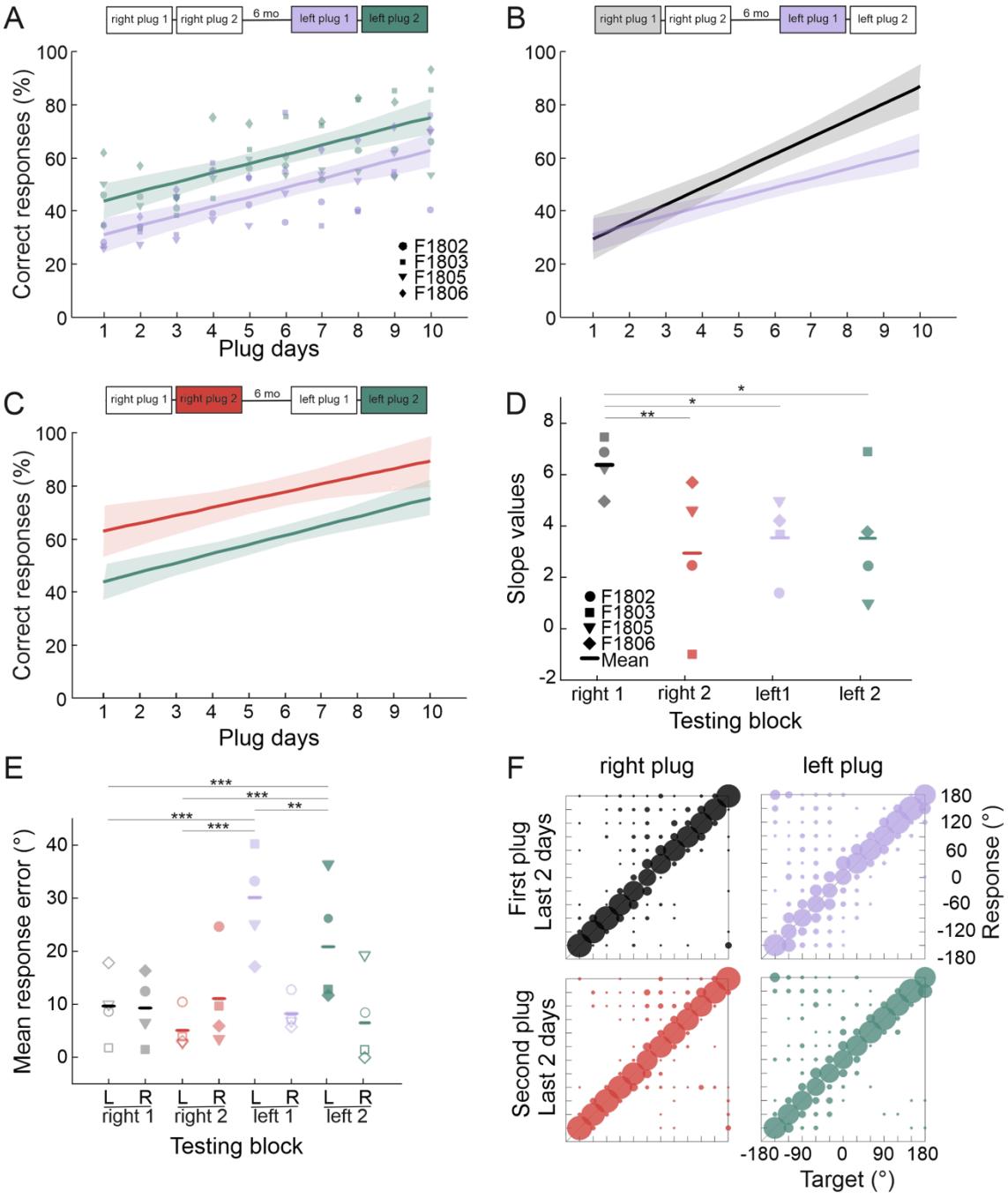

Figure 3-6. Effect of occluding the other ear following adaptation to UCHL. (A) Regression lines (shaded areas indicate 95% confidence intervals) and individual animal scores during the first (left plug 1, purple line and symbols) and second (left plug 2, green line and symbols) periods of left ear occlusion, which were separated by 7 days of normal binaural hearing. Unlike the right plug 1 and right plug 2 runs (Figure 3-4 A) previously experienced by these animals, the slopes of the linear fits to these data were very similar. (B) Comparison of the regression lines for the right plug 1 (black/grey) and left plug 1 (purple) runs. Although the ferrets performed at the same level when each ear was first plugged, much less adaptation was seen when the hearing loss was experienced in the left

ear following adaptation to right ear occlusion. (C) Comparison of the regression lines for the right plug 2 (red) and left plug 2 (green) runs. The slopes are very similar, but the difference in intercepts indicates less overall improvement in localisation accuracy when the left ear was occluded. (D) Individual animal and mean regression slopes for the fits shown in panels (A–C). (E) Mean response error magnitude in the final 2 days of each of these periods of monaural occlusion (right plug 1 and 2, left plug 1 and 2). Errors are shown separately for target locations ipsilateral (filled symbols) and contralateral (open symbols) to the side of the earplug. Midline locations (0° and 180°) were not included in this analysis. Asterisks represent statistical significance of paired comparisons (*$p < 0.05$, **$p < 0.01$, and ***$p < 0.001$). (F) Response probabilities versus target location for the final 2 days of the first right and left (top row) and the second right and left (bottom row) periods of monaural occlusion.

3.2.6. Adaptation to UCHL generalises beyond the training stimulus

To explore the extent to which the improvement in localisation accuracy following adaptation to UCHL generalised beyond the standard broadband noise training paradigm, we tested the performance of a group of ferrets using a combination of different target sounds and acoustic backgrounds before and after they had been trained to adapt to an earplug. The target sounds were either broadband noise (BB), for which all acoustic spatial cues would have been available, or narrowband noise (NB) with a one-octave bandwidth centred on 16 kHz, selected to reduce the availability of binaural cues and to provide limited access to high-frequency spectral localisation cues (Carlile, 1990; Keating et al., 2013). The target sounds were either presented in silence (s) or against a background of continuous broadband noise presented from an overhead speaker (Chapter 2 Figure 2-1 A), whose amplitude was either unmodulated (um) or modulated at 5 Hz (am) to add temporal structure to it (Chapter 2 Figure 2-1 C).

After measuring their localisation accuracy with all combinations of targets and acoustic backgrounds (Figure 3-7 A, Normal hearing), the animals were plugged in the

left ear and trained as usual using 1000-ms BB targets. Once they reached the adaptation criterion, the animals were retested on the above combination of target and acoustic backgrounds while still wearing the earplug (Figure 3-7 A, Plugged testing).

Under normal hearing conditions and in a silent acoustic background, the ferrets localised the BB targets almost perfectly (96.4 ± 0.76%) and the NB target sounds slightly less well (88.9 ± 1.13%) (GLMM, $p < 0.001$, Table 4), particularly for posterior sound locations (Figure 3-7 A, Normal hearing, Table 5). Reducing the bandwidth of the stimulus led to an increase in the incidence of both front-back errors (sounds presented in the frontal hemifield that were mis-localised into the posterior ipsilateral hemifield or vice versa; BB target, 0.94 ± 0.83%; NB target 1.99 ± 1.30%; paired sample t-test, $df = 6$, $p = 0.039$) and left-right errors (BB target, 0.23 ± 0.23%; NB target 0.81 ± 0.51%; paired sample t-test, $df = 6$, $p = 0.043$). Sound localisation accuracy was also degraded to a small but significant extent in the presence of both types of background noise (GLMM, $p = 0.019$, Table 4).

Following training with one ear plugged, the ferrets showed the usual substantial recovery in their ability to localise BB noise bursts. Nevertheless, their sound localisation accuracy across all stimuli was lower than that measured under normal hearing conditions prior to plugging one ear (Figures 3-7 A, B and Table 4, GLMM, hearing condition, $p < 0.001$). This was particularly the case for the NB targets, with a greater difference in performance between BB and NB targets when one ear was occluded than prior to ear-plugging (GLMM, $p < 0.001$), as indicated by the greater distance to the identity line for the data from the NB targets in Figure 3-7 B. The difference in localisation performance with target bandwidth was also apparent from the incidence of front-back errors (BB target, 3.82 ± 2.92%; NB target 10.42 ± 6.22%; paired sample t-test, $df = 6$, $p = 0.002$)

and left-right errors (BB target, 2.78 ± 2.43%; NB target 8.27 ± 6.19%; paired sample t-test, df = 6, p = 0.011). Following adaptation to monaural occlusion, the ferrets localised NB targets significantly worse on the side of the plugged ear (GLMM effect of target location, $p < 0.001$; odds ratio −0.385 relative to the best localised locations) (Figure 3-7 A, Plugged testing).

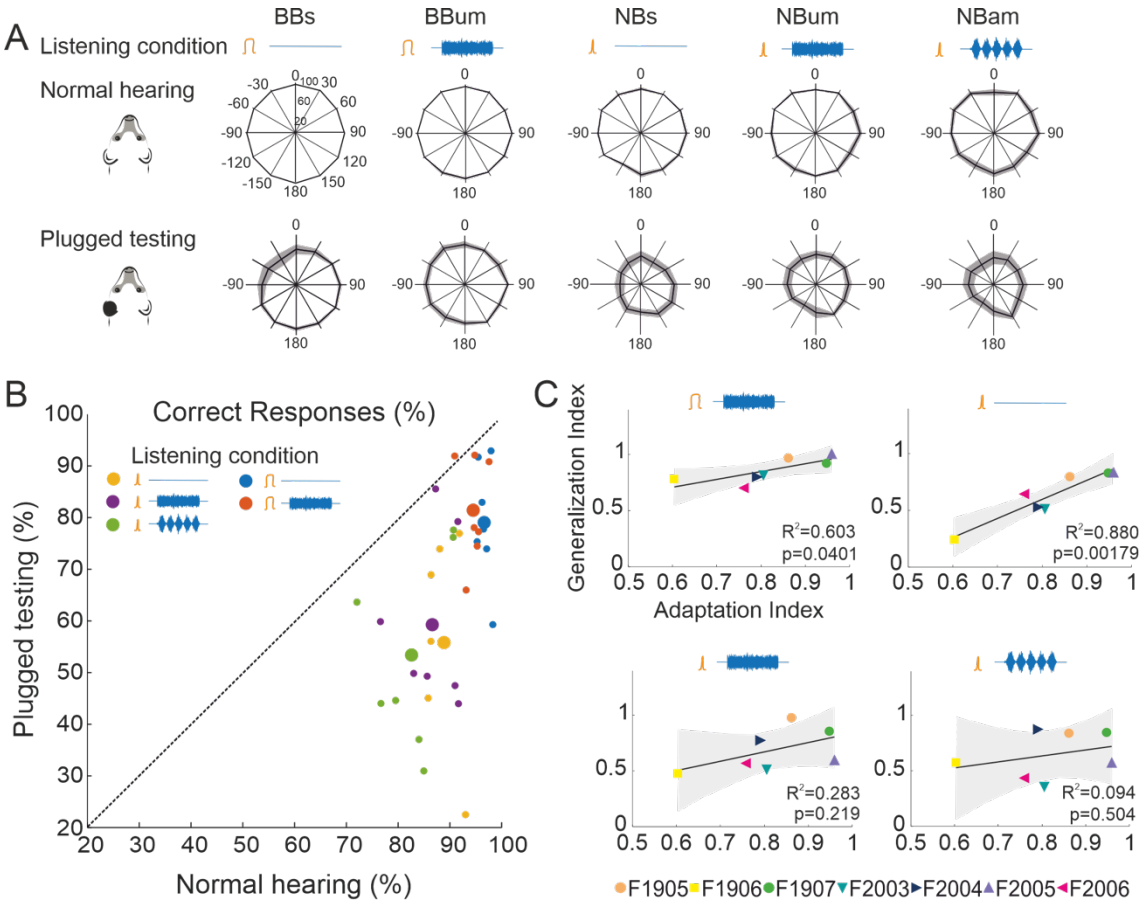

Figure 3-7. Generalisation of training-dependent adaptation. (A) Spatial distribution of mean (±S.E.) percent correct scores for each target and background combination (from left to right: BBs, BBum, NBs, NBum, NBam) under normal listening conditions (top row) and after adaptation to an earplug in the left ear ("Plugged testing", bottom row). (B) Mean percent correct scores for all target and background combinations under normal hearing conditions and after adaptation with one ear plugged. Large circles are the mean values and the small circles represent individual animals. Almost all values fall below the diagonal identity line, indicating more accurate responses with normal binaural inputs. Responses to BB targets (blue, red symbols) were closer to the identity line and therefore

showed less difference between the two hearing conditions. (C) Relationship for each stimulus type (shown at the top of the panels) between the adaptation index (the ratio of the percent correct scores for BB noise in silence in the final 3 days of adaptation to monaural occlusion and the preplug scores) and the generalisation index (the ratio of the percent correct scores for each stimulus type measured with the earplug in place at the end of the adaptation run and the corresponding preplug scores).

TABLE 4. Generalised linear mixed model comparing different stimuli.

			Normal hearing					Adapted hearing				
P value/odds			**BBs**	**BBum**	**NBs**	**NBum**	**NBam**	**BBs**	**BBum**	**NBs**	**NBum**	**NBam**
Reference	**Normal hearing**	**BBs**	-	-0.171	-0.610	-0.728	-0.915	-1.080	-0.924	-1.740	-1.613	-1.799
		BBum	**	-	-0.439	-0.556	-0.744	-0.909	-0.753	-1.569	-1.441	-1.628
		NBs	***	***	-	-0.117	-0.305	-0.470	-0.314	-1.130	-1.003	-1.189
		NBum	***	***	**	-	-0.188	-0.352	-0.196	-1.012	-0.885	-1.071
		NBam	***	***	***	***	-	-0.165	-0.009	-0.825	-0.698	-0.884
	Adapted hearing	**BBs**	***	***	***	***	***	-	0.156	-0.660	-0.533	-0.719
		BBum	***	***	***	***	0.816	***	-	-0.816	-0.689	-0.875
		NBs	***	***	***	***	***	***	***	-	0.127	-0.059
		NBum	***	***	***	***	***	***	***	***	-	-0.186
		NBam	***	***	***	***	***	***	***	0.081	***	-

Target: BB, broadband noise; NB, narrowband noise (one octave bandwidth, centred on 16 kHz). Background: s, silence; um, unmodulated noise; am, amplitude-modulated noise. $**p < 0.01$ and $***p <$ on grey background are p values ** p<0.01, *** p<0.001; numbers on white background are odds ratios.

Surprisingly, we found an improvement in performance in the presence of background noise for BB target sounds after the animals had adapted to the earplug (GLMM, $p < 0.001$, odds ratio = 0.156) (Figures 3-7 A, B). This is also reflected by the greater value of the generalisation index, the mean performance following adaptation relative to that obtained under normal hearing conditions (Figure 3-7 C and Table 6). We observed a significant correlation between the degree of adaptation and generalisation: ferrets that

showed more complete recovery in their performance with training also localised BB targets against background noise more accurately, indicating that they were able to effectively segregate these sound sources despite the presence of a conductive hearing loss in one ear.

TABLE 5. Sound localisation accuracy for different stimuli.

	%Correct responses Normal hearing / After adaptation				
Ferret#	**BBs**	**BBum**	**NBs**	**NBum**	**NBam**
F1905	96.2 / 82.9	94.8 / 92.0	86.3 / 68.9	87.2 / 85.4	90.6 / 76.1
F1906	98.2 / 59.2	95.2 / 74.4	93.0 / 22.5	91.6 / 44.0	76.6 / 44.0
F1907	97.9 / 92.8	97.5 / 90.7	91.8 /76.8	91.5 / 79.1	90.6 / 77.5
F2003	96.4 / 77.7	94.6 / 78.0	91.0 / 47.5	90.9 / 47.5	84.9 / 31.0
F2004	95.2 / 75.3	95.5 / 77.2	85.8 / 45.0	76.5 / 59.8	72.0 / 63.6
F2005	95.4 / 91.6	91.0 / 91.8	88.0 / 73.9	83.0 / 49.8	79.5 / 44.6
F2006	97.1 / 73.9	93.1 / 65.9	86.3 / 56.0	85.6 / 49.3	84.0 / 37.0

Target: BB, broadband noise; NB, narrowband noise (one octave bandwidth, centred on 16 kHz).
Background: s, silence; um, unmodulated noise; am, amplitude-modulated noise.

Greater inter-animal variability in performance was found with NB than BB target sounds (Figures 3-7 A–C and Table 6). Ferrets that adapted more to the earplug when trained with BB sounds also localised NB targets in silence more accurately. Although they localised less accurately than with BB noise (Figures 3-7 A, B), the significant correlation between the adaptation index and the generalisation index (Figure 3-7 C) suggests that sufficient spatial information that formed the basis for adapting to UCHL remained in these NB stimuli. The addition of background noise weakened this relationship,

particularly when it was amplitude modulated, suggesting that background noise has a more disruptive effect on the transfer of learning when more limited spatial cues are provided by the target stimuli.

TABLE 6. Adaptation and generalisation indices.

Ferret#	Adaptation index BBs	Generalisation index BBum	NBs	NBum	NBam
F1905	0.86	0.97	0.80	0.98	0.84
F1906	0.60	0.78	0.24	0.48	0.57
F1907	0.95	0.93	0.84	0.86	0.85
F2003	0.80	0.82	0.52	0.52	0.36
F2004	0.79	0.81	0.52	0.78	0.88
F2005	0.96	1.01	0.84	0.60	0.56
F2006	0.76	0.71	0.65	0.57	0.44
Mean ± sd	0.82 ± 0.12	0.86 ± 0.11	0.63 ± 0.22	0.69 ± 0.19	0.64 ± 0.21

3.2.7. Role of spectral cues and dynamic cues in adaptation to UCHL

The lack of an aftereffect following earplug removal is consistent with a primary adaptation strategy to UCHL in which the animals learn to rely more on the intact monaural spectral cues provided by the non-occluded ear than the normally dominant but now distorted binaural cues. However, adaptive changes in binaural cue sensitivity appear to contribute as well, as shown by the recovery in localisation accuracy observed in humans when pure tones are interspersed during training with one ear occluded (Keating et al., 2016). Our finding that adaptation of sound localisation in the horizontal plane is

initially restricted to the side of the open ear, with improvements in performance on the plugged side occurring later during the period of monaural occlusion also supports the possibility that more than one process may underlie this training-dependent plasticity.

An additional factor that needs to be considered is that the relatively long training stimulus (1000 ms noise bursts) may have allowed the animals to sample dynamic spatial cues as they were approaching the perceived sound source location. As noted earlier, the very similar pattern of adaptation observed in the head orienting responses (Figure 3-2), which have a latency of ~100–200 ms (Nodal et al., 2012; Nodal et al., 2008), strongly suggests that adaptation relies primarily on the spatial information available at the onset of the target sound. Nevertheless, the extent of the adaptation has been shown to increase with the stimulus duration (Kacelnik et al., 2006), which could reflect greater integration time or multiple sampling of the available localisation cues.

To gain a better understanding of the processes underlying training-dependent adaptation to UCHL, we interspersed sessions in which high-frequency narrowband sounds [1/6 octave bandwidth centred on 15 kHz, as in (Keating et al., 2015)] were presented during the adaptation training with broadband noise. These sounds were designed to eliminate monaural spectral cues and ITDs, leaving only narrowband ILDs available. In addition, the stimuli in these trials were either 200 ms or 1000 ms in duration to determine whether more adaptation occurred with the longer duration sounds.

As expected, the pre-plug scores showed that the ferrets localised high-frequency narrowband targets less accurately than the broadband sounds at stimulus durations of both 1000 ms (Figure 3-8 A) and 200 ms (Figure 3-8 B). Including different stimulus types and durations within the training block did not interfere with the expected adaptation to BB noise stimuli, with the percentage correct scores increasing throughout

the period of monaural occlusion for both target durations (GLMM testing day, $p < 0.001$) (Figures 3-8 A, B). By contrast, no improvement in performance was seen over time for NB targets that had a duration of either 1000 ms (GLMM, testing day, $p = 0.071$) (Figure 3-8 A) or 200 ms (GLMM, testing day, $p = 0.341$) (Figure 3-8 B).

The sound-evoked head movements measured for these animals (combined across target locations in each hemifield for the first 3 days of monaural occlusion and plotted separately for BB and NB stimuli in Figures 3-8 C, D, respectively) were very similar at each of the two stimulus durations used. These averaged measurements demonstrate that the head began to move near the end of the 200-ms noise bursts, and this movement continued during the longer stimulus until the animal left the central start platform [which typically occurs at ~600 ms after stimulus onset (Kacelnik et al., 2006; Nodal et al., 2008)]. Although the metrics of the head turns were little affected by stimulus duration, they differed with the bandwidth of the stimulus in a similar way to the approach-to-target response accuracy shown in Figures 3-8 A, B.

These results therefore indicate that that 1/6-octave bandwidth noise bursts centred at 15 kHz do not contain sufficient spatial information to support the adaptive improvements in localisation performance that take place during the training runs with BB noise. Furthermore, localisation accuracy was reduced for both BB (GLMM, target duration, $p < 0.001$) and NB (GLMM, target duration, $p < 0.001$) stimuli when the duration used was too short for the animals to be able to use dynamic cues to any degree, suggesting that the ferrets may benefit from re-sampling the longer stimuli during and after the initial head turn. Nevertheless, some adaptation still took place with 200-ms noise bursts so long as they were sufficiently broadband to provide access to other

auditory spatial cues (Figures 3-8 A, B). Adaptive learning does not therefore depend on head movements, though it is possible that they enhance this process.

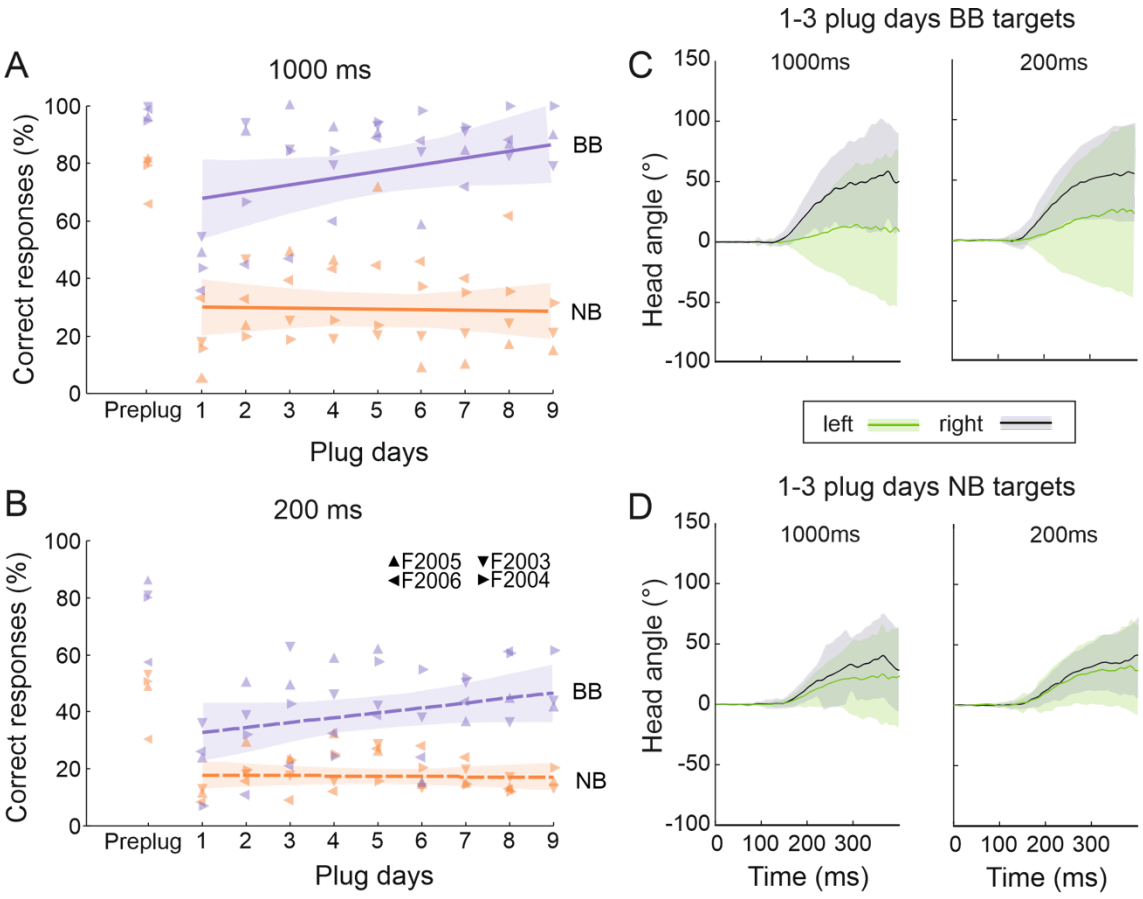

Figure 3-8. Role of dynamic and spectral cues in adaptation to UCHL. (A) Percentage of correct responses for 1000-ms broadband noise (purple, BB) and 1/6 octave narrowband noise bursts with a centre frequency of 15 kHz (orange, NB) over the course of daily training with one ear occluded. Coloured lines are linear regressions, and the shaded areas correspond to the 95% confidence intervals. The symbols represent individual animals. (B) Same as panel (A) but for stimuli with a duration of 200 ms. (C) Change in the mean (±S.E.) horizontal angle of the head over time following BB target onset at time 0 ms. These measurements were taken at the start (days 1–3) of the ear-plugging run, combined across target locations in the left (green) and right (black) hemifields, and are plotted separately for 1000 ms (left) and 200 ms (right) noise bursts. (D) Same as panel (C) but for NB target sounds.

3.3. Discussion

Perceptual learning enables auditory perceptual skills to be improved with practice or training (Irvine, 2018), and allows abnormal inputs to be accommodated in ways that are likely to be important in the treatment of hearing disorders (Glennon et al., 2020; Kumpik & King, 2019). Plasticity in the processing of auditory spatial information is essential for calibrating neural circuits through experience with the available cues, which vary with individual differences in the geometry of the head and external ears and change over time, particularly as these structures grow but potentially also following hearing loss. While this plasticity is most pronounced during development, many studies have shown that the adult brain can learn to utilise abnormal auditory space cues (Carlile, 2014; Mendonca, 2014). We used a well-established paradigm for investigating the adaptive capabilities of the auditory system by temporarily plugging one ear in order to induce a reversible binaural imbalance, so that we could explore the retention and retrieval of learning and its generalisation beyond the standard stimuli conditions used for training.

The earplugs we used disrupt binaural localisation cues by attenuating and delaying the sound at the occluded ear (Keating et al., 2013; Keating et al., 2016; Moore et al., 1989). The attenuation is frequency dependent and will therefore also distort the spectral cues available at the occluded ear, leaving the spectral filtering provided by the open ear as the only unchanged acoustic cue. Following an immediate decline in localisation accuracy in the horizontal plane, we found that performance steadily improved with daily training toward the pre-plug scores, as shown in previous studies in ferrets (Bajo et al., 2019; Bajo et al., 2010; Kacelnik et al., 2006; Nodal et al., 2012; Nodal et al., 2010) and humans (Keating et al., 2016; Kumpik et al., 2010). Although an

improvement in localisation accuracy in monaurally plugged human subjects has been observed over the course of a single training session when the sound level was fixed and visually guided feedback provided (Zonooz & Van Opstal, 2019), other work in humans has shown that training has to be spread out over several days rather than compressed into a single block on 1 day in order for adaptation to occur (Kumpik et al., 2010). While this suggests that learning to localise sound after disrupting the cues in this fashion requires a period of consolidation between training sessions, daily training in monaurally occluded ferrets has been shown to produce faster and more complete adaptation than in animals that were trained every sixth day and which therefore experienced altered spatial cues over a longer period (Kacelnik et al., 2006). Related to this is the finding that human participants who have one ear plugged only during sound localisation training sessions that took place approximately every 3 days still show a gradual improvement in performance from one session to the next despite receiving normal binaural inputs in the intervening periods (Keating et al., 2016). These findings highlight the key role of training in the rapid adaptation to altered spatial cues, confirming that it represents a form of perceptual learning.

Compensatory changes in binaural cue sensitivity have been reported in adult humans who adapt to the presence of an earplug in one ear (Keating et al., 2016; Zonooz & Van Opstal, 2019) and have also been observed at a neurophysiological level in animals following several weeks of monaural occlusion during development (Keating et al., 2015) or in adulthood (Thornton et al., 2021). Nevertheless, the absence of an after-effect in the localisation responses following earplug removal suggests that the auditory system primarily adapts by giving greater weight to the unchanged monaural spectral cues provided by the open ear. This conclusion is supported by the immediate reduction in

percentage correct scores produced by inserting a mold in order to reshape the external ear contralateral to the earplug (Kacelnik et al., 2006) and by the greatly reduced adaptation observed when spectral cues were disrupted during training by randomising the spectrum of the sounds (Keating et al., 2016). Monaural spectral cues also appear to contribute to the ability to localise sounds in the horizontal plane of at least some humans who are deaf in one ear (Agterberg et al., 2014; Slattery & Middlebrooks, 1994; Van Wanrooij & Van Opstal, 2004). Our results provide additional evidence for the importance of spectral cues in adaptation to unilateral hearing loss. While the ferrets exhibited an improvement in accuracy when trained to localise broadband noise stimuli, which provide access to the full range of acoustic spatial cues, no improvements were seen with narrowband sounds (1/6-octave bandwidth noise bursts centred at 15 kHz) presented during the training to restrict access to high-frequency interaural level differences.

Following earplug removal, the auditory system switches back to relying more on binaural cues for azimuthal localisation. This is shown by our finding that subsequently re-plugging the same ear again degrades localisation accuracy [see also (Bajo et al., 2019; Kacelnik et al., 2006)]. A capacity to alternate between different sets of cues has also been demonstrated in adult humans who experience altered spectral cues by wearing ear moulds for several weeks (Carlile & Blackman, 2014; Hofman et al., 1998; Trapeau et al., 2016; Van Wanrooij & Van Opstal, 2005; Watson et al., 2017). These manipulations impaired elevation responses, which then recovered as the participants learned to localise with their new ears, but when the moulds were removed, restoring normal spectral cues, they were immediately able to localise as accurately as they did prior to insertion of the moulds. Furthermore, upon reinsertion of the moulds approximately 1 week later, localisation performance was found to be no different from that measured at the end of

the previous accommodation period (Carlile & Blackman, 2014). This suggests that after learning to localise with the moulds in place, humans are able to interchangeably use their original own-ear spectral cues and the abnormal spectral cues they have adapted to. Brief periods of training with inappropriate spectral cues provided by using virtual auditory displays with non-individualised head-related transfer functions also result in improvements in localisation performance that have been shown to persist for at least several weeks (Mendonça et al., 2013; Zahorik et al., 2006).

The effects of occluding one ear are different, however, with our results showing that additional training is required to achieve the same level of adapted performance whenever the same ear was re-plugged, with the magnitude of the initial drop in performance positively correlated with the duration of prior normal experience and greatest at the start of the first ear-plugging run. Thus, although it takes longer for the brain to adjust to the altered spatial cues resulting from monaural occlusion than to revert to normal inputs, previous ear-plugging experience leaves a "memory trace" so that less adaptation is required when the cues are changed again in the same manner. This was particularly the case for locations ipsilateral to the open ear, suggesting that upweighting of monaural spectral cues is facilitated by prior experience.

Switching the UCHL to the contralateral ear also resulted in an impairment in localisation accuracy that partially recovered with training. However, the localisation performance of the ferrets improved to a significantly lesser extent than when the hearing loss was previously experienced on the other side. This is consistent with evidence that ferrets raised with one ear occluded adapt by changing the relative weighting of the spectral cues in opposite directions for each ear (Keating et al., 2013). If this also happens when the animals adapt to a UCHL in adulthood, these opposing changes in cue weighting

would then need to be reversed when the earplug is switched to the other ear. Alternatively, any remapping of binaural cues that accompanies adaptation to monaural conductive hearing loss, and which may account for the more gradual improvements observed at frontal regions ipsilateral to the occluded ear, is also likely to hinder the capacity of the brain to recover localisation accuracy when the side of the hearing loss is changed.

In these experiments, we measured the accuracy of the ferrets' head orienting responses following sound presentation, as well as the target location they approached to receive a reward. Our previous work has shown that restricted lesions (Nodal et al., 2010) or reversible deactivation (Nodal et al., 2012) of the auditory cortex impair approach-to-target behaviour whilst preserving the accuracy of the initial sound-evoked head orienting responses, which are likely to be more dependent on midbrain circuits (Isa et al., 2021; Lomber et al., 2001). Nevertheless, the initial head turn and subsequent selection of target location are both components of the animals' behavioural response to sounds presented from different directions and are dependent on the same spatial cues. Indeed, it has previously been reported that when ferrets with normal hearing approach an incorrect target location, the preceding head turn is more closely correlated with that response than with the target location (Nodal et al., 2008).

We observed a very similar pattern of training-dependent plasticity for each measure of sound localisation, including the partial retention of learning when abnormal spatial cues are again experienced by re-plugging the same ear. Since silencing the primary auditory cortex impairs adaptation but not the retrieval of previous learning (Bajo et al., 2019), it is likely that the latter involves downstream circuits. Although we cannot rule out the involvement of other brain areas, such as the striatum, our previous

demonstration that the descending auditory corticocollicular pathway is essential for adaptive plasticity of both head-orienting and approach-to-target behaviour (Bajo et al., 2010) suggests that the midbrain may be involved in the retention of learning. Recording studies will be required to identify exactly where and how spatial information is stored to allow the partial retrieval of localisation accuracy from one period of monaural occlusion to the next. It is interesting to note, however, that these findings are consistent with the reverse hierarchy theory of perceptual learning (Ahissar & Hochstein, 2004), whereby learning proceeds in a top-down fashion from higher to lower levels of processing, where the relevant stimulus features are represented more precisely.

Adaptation of the head-orienting responses also allowed us to address the potential contribution of sensorimotor behaviour to auditory localisation plasticity (Aytekin et al., 2008; Carlile et al., 2014; Parseihian & Katz, 2012; Zahorik et al., 2006). Head turning accuracy is likely to depend on the spatial cues available at the onset of the target sound and is not affected by its duration (Nodal et al., 2012). Our finding that adaptive changes in head-orienting responses during initial and subsequent periods of monaural occlusion mirrored those seen for the approach-to-target behaviour suggests that head movements are not necessary for training-dependent plasticity to occur. This is supported by our finding that approach-to-target accuracy showed some recovery with one ear occluded when the duration of the broadband noise bursts was reduced to 200 ms, which is close to the head-orienting latency. Partial adaptation to UCHL has also been observed in ferrets for 40-ms broadband noise bursts (Kacelnik et al., 2006), and human participants wearing a plug in one ear can re-learn to correctly identify the target loudspeaker location without first turning toward it (Kumpik et al., 2010).

Although these findings indicate that head movements do not play an essential role in adjusting auditory localisation to compensate for a conductive hearing loss in one ear, the recovery in accuracy is more complete when longer duration noise bursts are used for training [see also (Kacelnik et al., 2006)], suggesting that movement of the head may benefit adaptation by allowing multiple sampling of the stimulus. No improvement was observed, however, when 1/6- octave narrowband noise bursts of either 200 or 1000 ms duration were presented during the training, suggesting that even when head movements during sound presentation were possible, these stimuli provide insufficient spatial information to provide a confident assessment of target location and therefore support learning. While this highlights the importance for adaptation to UCHL of using a broadband stimulus so that the full range of localisation cues is available, it seems likely that further training with narrowband sounds would eventually lead to a remapping of high-frequency ILDs (Keating et al., 2015; Keating et al., 2016).

Investigating the generalisation of perceptual learning to untrained stimulus properties can provide valuable insights into the neural substrates of learning and retrieval (Dosher et al., 2013; Wright & Zhang, 2009). In terms of adaptation to UCHL, generalisation is clearly important if this form of training-dependent plasticity is to be relevant clinically to users of cochlear implants and hearing aids. In this respect, previous studies of adaptation to abnormal spatial cues in humans are promising in demonstrating that improvements in performance do transfer to untrained sound types (Mendonça et al., 2013; Watson et al., 2017) and locations (Mendonça et al., 2013; Watson et al., 2017; Zahorik et al., 2006; Zonooz & Van Opstal, 2019), and to reverberant conditions (Watson et al., 2017). Zonooz & Van Opstal, 2019 reported that while adaptation to monaural ear-plugging leads to a generalised increase in azimuth accuracy, this was accompanied by

degraded elevation responses, though individuals with single-sided deafness can benefit from monaural spectral cues for localisation in both dimensions (Van Wanrooij & Van Opstal, 2004).

Our results show that the adaptation achieved after training ferrets to localise broadband noise with one ear occluded was positively correlated with their ability to generalise this performance improvement to untrained octave band noise. These narrowband stimuli would have provided high-frequency binaural cues and a subset of the directional spectral features produced by the filter properties of the head and ears (Keating et al., 2013). While these cues were sufficient to support the generalisation of adaptation when the narrowband target sounds were presented in silence, the addition of background noise degraded the performance of the ferrets both before and after learning. However, when broadband target sounds were used, the spatial learning resulting from training ferrets with one ear plugged in quiet conditions was preserved when the animals were subsequently tested in a noisy environment. Indeed, following adaptation to monaural occlusion, they achieved significantly higher scores when background noise was added than in a silent background, raising the possibility that localisation training may enhance the perception of targets in noise when hearing is perturbed. This indicates that the benefits of daily training for hearing-impaired individuals may translate to listening conditions that more closely resemble those of real-world environments.

4. CHARACTERISATION OF NEURAL RESPONSES IN THE INFERIOR COLLICULUS OF THE FERRET IN NORMAL HEARING CONDITIONS

4.1. Introduction

The inferior colliculus (IC), located in the midbrain, constitutes one of the main centres for the processing of auditory information in the auditory pathway, and, as such, is thought to play an important role in sound localisation. The IC receives direct ascending input from the contralateral dorsal cochlear nucleus (DCN), a subdivision of the cochlear nuclei, the first synaptic station of the auditory nerve fibers. DCN has been suggested to play a role in the encoding of spectral notches (Grothe et al., 2010; Nelken & Young, 1994), one of the most prominent features of the directional filtering introduced by the

external ear. The IC also receives input from the superior olivary complex bilaterally, where binaural differences in intensity and time are computed (Grothe et al., 2010). Therefore, the IC is the first station in the auditory pathway where multiple parallel ascending inputs encoding spatial information converge, suggesting its involvement in sound localisation. Moreover, the IC projects to the superior colliculus (SC), where a map of space has been described in mammals (Ito et al., 2020; King & Hutchings, 1987; Middlebrooks & Knudsen, 1984; Palmer & King, 1982).

How the different spatial cues are integrated, in the first instance in the IC, to generate a reliable representation of sound source location is still a matter of controversy. Many studies have investigated the spatial sensitivity of IC neurons, mainly focusing on the sensitivity to binaural cues (e.g. McAlpine et al., 2001; Chase & Young, 2008; Dorkoski et al., 2020). However, a substantial proportion of these studies were performed under anaesthesia or, occasionally, in unanaesthetised, head-restrained animals. In this study, we recorded neural activity bilaterally from the IC in ferrets while they performed a sound localisation task. This approach has allowed us to characterise spiking activity from units in the IC in response to sounds presented from different azimuths. We also recorded from the same animals under anaesthesia in order to more fully characterise their response properties and to facilitate a comparison with previous studies. Finally, we used population decoding analyses (Day & Delgutte, 2013) to explore the possible basis by which sound source location could be encoded by activity in the IC.

4.2. Results

4.2.1. Recordings in the central nucleus of the inferior colliculus

Histological sections confirmed that recordings were performed in the IC (Figure 4-1). The left probe in animal F2108 (top left panel in Figure 4-1) was located rostrally in the IC and therefore most of the recordings were assigned to the lateral cortex of the IC (LCIC). All the other probes targeted the central nucleus (CNIC) (red labelled in Figure 4-1) with a dorsoventral trajectory, and therefore were oriented along the tonotopic axis (Figure 4-2). This meant that some of the most dorsal recoding sites were located in the dorsal cortex (DCIC) (labelled green in Figure 4-1), which lies above the CNIC. The left probe in ferret F2111 was an exception, however, entering directly into the CNIC (Figure 4-1 C). All probes spanned the whole dorsoventral dimension of the CNIC, covering approximately 2 mm of the recording sites (see Figure 4-1 F for comparison across animals and penetrations). Therefore, the recorded units spanned the full tonotopic range. In some instances, the probes' trajectory continued beyond the IC for a short distance, extending into the cuneiform nucleus, which has been associated with gait initiation (Takakusaki et al., 2016). The probe in the left IC of ferret F2111 extended the furthest into this nucleus (~500μm).

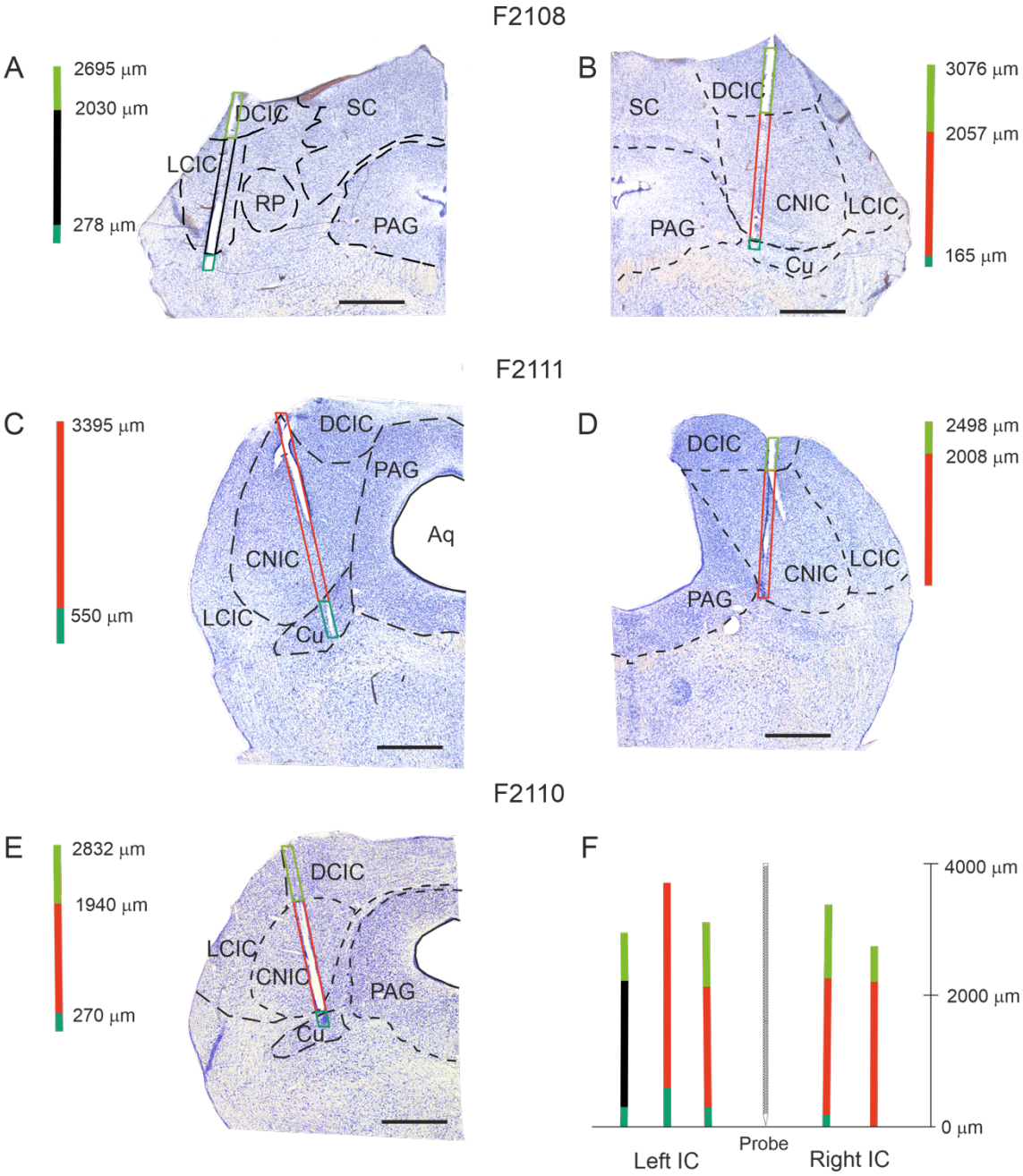

Figure 4-1. Anatomical location of recording probes in the IC. Photographs of coronal sections (45µm thick) stained for Nissl substance showing the lesions caused by the recording probes. (A & B) left and right IC of ferret F2108. (C & D) left and right IC of ferret F2111 (E) left IC of ferret F2110. (F) Comparison across probes of the length of each penetration, colour coded by brain region (red CNIC, light green DCIC, black LCIC and dark green Cu). Anatomical boundaries and probe tracks are superimposed using dashed lines and colour-coded rectangles, respectively. Calibration bars 1mm. Abbreviations: Cu, cuneiform nucleus; SC, superior colliculus; PAG, periaqueductal

grey; RP, rostral pole of the IC; DCIC, dorsal cortex of the IC; CNIC, central nucleus of the IC; LCIC, lateral cortex of the IC.

To aid the assignment of the recorded units to specific brain regions, we examined the electrophysiological properties of the units by computing their frequency response areas (FRA) along the length of the probes. As expected, clusters showed a topographic organisation, with a distribution from low to high preferred frequencies along the dorsoventral axis, constituting the tonotopic axis that characterises the CNIC (Merzenich & Reid, 1974). This tonotopy was even observed for clusters located in the DCIC (Figure 4-2 FRA). In both awake and anaesthetised, states, responses of the clusters to free-field stimuli, presented at 12 different locations separated by 30º along the azimuth, showed heterogeneous tuning that was heavily biased towards the contralateral hemifield, independently of their location along the probe/characteristic frequency (Figure 4-2 Spatial Responses). This heterogeneity and contralateral dominance have previously been described in the CNIC (Delgutte et al., 1999).

The estimated location within the IC based on the neural activity registered along the probes was further confirmed by the histological reconstructions. For example, in animal F2111, no clusters responding to pure tones under anaesthesia were described at the deepest ~500μm (Supplementary Figure 4-1, Supplementary Figure 4-2 FRA), suggesting that the tip of the probe was not located in the IC. Histologically, this was confirmed as the lesion left behind by the probe showed that the deepest part of it was located in the cuneiform nucleus (Cu Figure 4-1 C). Moreover, recordings carried out while the animal was performing a sound localisation task showed a delayed modulated response in this deep region uncharacteristic of responses in the IC (Supplementary

Figure 4-2, third row Awake panel). On the right side of the brain in the same animal, we found that FRA responses displayed a tonotopic gradient below ~2100μm (Supplementary Figure 4-1), close to the limit between CNIC and DCIC according to the histology. In animal F2108, a clear dorsoventral tonotopy was observed on both sides (Supplementary Figure 4-1), despite the left probe being located in the rostral portion of the lateral cortex instead of the central nucleus. No change in the tonotopic arrangement of the clusters across the length of the probes was observed because of the histological boundaries delineated between the LCIC and the CNIC, and so all clusters from this penetration were considered for further analyses, along with those whose location was confirmed to be in the CNIC. For all probes, clusters recorded over a distance of ~2mm showed a tonotopic organisation.

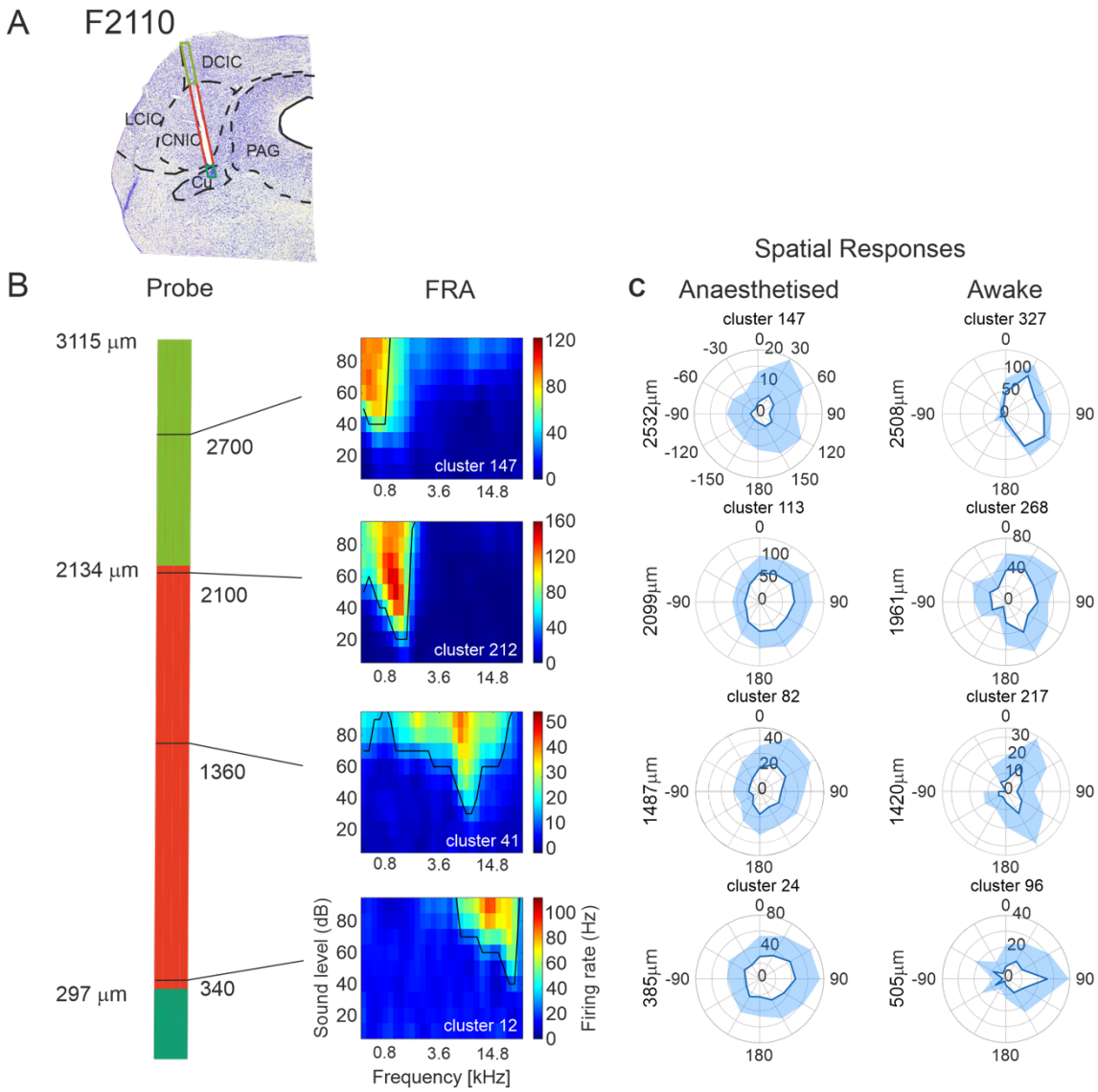

Figure 4-2. Tonotopic organisation and spatial sensitivity along a recording probe. (A) Coronal section of the left IC for animal F2110 showing the location of the recording probe (same as in Figure 4-1 E). (B) Colour-coded (see legend for Figure 4-1) schematic of the probe shown in A. The numbers indicate the distance from the tip of the probe in micrometres. The panels show the frequency response areas (FRA) in response to 100 ms pure tones presented at different intensities for four example clusters at different depths along the probe specified by the lines connecting the plots with the probe. The most dorsal one (top panel) was located in the DCIC and the deepest three were located at different depths across the CNIC. (C) Polar plots show the mean (+ sd) firing rate (spikes/s) of different clusters in anaesthetised (left column) and awake (right column) conditions in response to 1000 ms broadband noise presented from loudspeakers positioned 70 cm away at different angular locations spanning 360º in azimuth. The depth of each cluster

(distance from the tip of the probe) is specified by the number on the left of each polar plot.

4.2.2. Activity in the inferior colliculus in different listening conditions

Several response patterns were observed across all recordings that were dependent on the stimulus type. For recordings carried out under anaesthesia using 100-ms pure tones to characterise the FRA, three main types of response profiles were observed. Spiking activity could be: (1) locked to the onset of the stimulus (17.75% of units averaged across animals), (2) sustained throughout the presentation of the stimulus (21.47%) or (3) locked to both the onset and the offset of the stimulus (37.93%), with the latter being the most commonly observed pattern (Figure 4-3 A-C, Supplementary Figure 4-3). However, in response to 1000-ms broadband noise bursts, offset responses were infrequently observed in either anaesthetised or awake conditions, and often associated with clusters showing a suppressed response to the stimulus (e.g. clusters 88 and 99 in Supplementary Figure 4-4). Responses to broadband noise were often characterised by sustained spiking activity throughout the sound presentation, followed by a suppression at the offset of the sound (Figure 4-3 B-C).

Despite the similarities in the firing patterns between anaesthetised and awake recordings in response to broadband sounds, we also found some important differences in the responses recorded in different brain states. Responses recorded under anaesthesia showed a much prolonged suppression of activity following the end of the sound presentation (Figure 4-3 B) than those recorded in awake ferrets. Neural activity recorded

in awake animals while they performed a sound localisation task was characterised by a greater diversity of response patterns along the probe than in the anesthetised condition, as well as greater baseline activity (Figure 4-3 C). The greater activity observed in awake behaving animals, which was not associated with the stimulus, could be due to noise produced as a result of the animal's movement or other task related factors. Interestingly, during the behavioural task, we observed a suppression of activity prior to the sound presentation, which was not present in the anaesthetised recordings (Kruskal-Wallis chi-squared = 111.6, df = 2, $p<0.001$ (Figure 4-3 B-D). This suppression was even observed when only single units were analysed (Kruskal-Wallis chi-squared = 57.61, df = 2, $p<0.001$). We hypothesise that this suppression could be task related and reflect preparatory activity prior to self-initiated triggering of the trial or anticipation of the sound stimulus, which could result in an enhanced behavioural performance by increasing the neural gain.

In both anaesthetised and awake conditions, units responded with a contralateral preference (Figure 4-2, Spatial responses). However, a difference in the sharpness of tuning was observed (Wilcoxon signed-rank test W = 213578, $p<0.001$), with units exhibiting a larger ERRF under anaesthesia (awake lower quartile (Q1) = 109º, median = 150º, upper quartile (Q3) = 197º, anaesthetised Q1 = 139º, median = 187º, Q3 = 223º) (Figure 4-3 E). This difference was also present when the analysis was restricted to single units (Wilcoxon signed-rank test W = 35100, p = 0.004. Awake Q1 = 108º, median = 152º, Q3 = 210º, anaesthetised Q1 = 127º, median = 170º , Q3 = 222º).

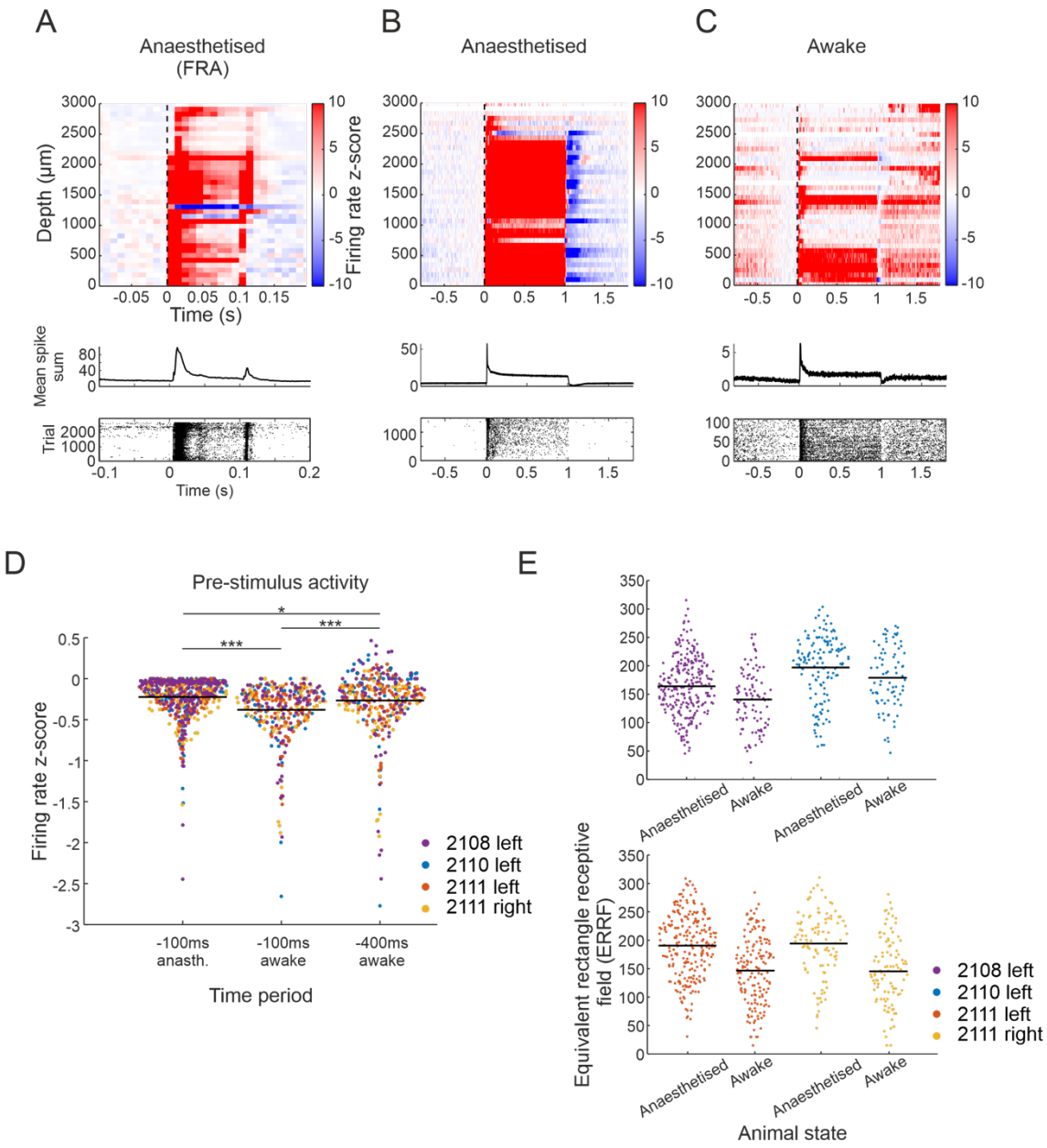

Figure 4-3. Comparison of IC responses to different stimuli in anaesthetised and awake ferrets. (A) Top panel: neural activity recorded under anaesthesia in an example animal (F2110 left IC) in response to 100-ms pure tones. Activity is shown for different recording sites along the probe and is aligned relative to the onset of the sound presentation indicated by the vertical dashed line. Red represents an increase in the firing rate z-score (baseline: 195 ms presound presentation) and blue, suppression. Bottom panel: Peristimulus time histogram (PSTH) and raster plot illustrating the response to sound presentation averaged across all recorded units. (B) Activity recorded under anaesthesia in the same ferret in response to broadband noise averaged across locations. Otherwise as in A. (C) Activity recorded in the same ferret while awake and behaving in response broadband noise averaged across locations. (D) Swarm plot showing the firing rate z-scores computed for 100 ms windows at different time points prior to presentation

of noise stimuli [100 ms before stimulus in anesthetised (-100ms anaesth.) and 100 ms and 400 ms before stimulus in awake (-100ms and -400ms respectively)] in awake and anaesthetised conditions for all probes (F2108 right IC was not recorded in anaesthetised conditions due to failure of the probe; therefore awake recordings from that probe were not included in this analysis). Each dot corresponds to a cluster and the black line indicates the mean across clusters from all probes. (E) Swarm plots showing the distribution of clusters recorded on different probes according to their equivalent rectangular receptive fields (ERRF) computed for a 50 ms window after sound onset in anaesthetised and awake behaving conditions (F2108 right IC was not recorded under anaesthesia due to failure of the probe; therefore this probe is not included in the figure) (* $p<0.05$, *** $p<0.001$).

4.2.3. Heterogeneity of responses in the IC

Focusing on activity recorded in the IC of awake behaving ferrets in response to 1000-ms noise bursts, we found considerable variability between clusters in their response profiles. Clusters were classified into six main types based on their spiking activity in response to stimulus presentation (Supplementary Figure 4-5), four of which exhibited excitatory responses while two were characterised by suppression of baseline activity. Excitatory responses were defined by an increase in the firing rate following stimulus onset of at least 1.5 times relative to that measured prior to sound presentation. This increase in firing could be confined to the onset of the stimulus, constituting the so-called ‘onset only’ type, or it could continue throughout the presentation of the stimulus. Clusters that showed a persistent increase in firing rate beyond the onset of the sound were further classified into three different response profiles. When the onset response was followed by a decrease in activity back to pre-sound rate followed, in turn, by an increase in activity throughout the duration of the stimulus, the cluster was classified as ‘onset with rebound’ type. A decrease in activity following the onset response which was still

significantly above the pre-sound rate and maintained until the offset of the sound constituted the 'onset-sustained' type. In some cases, this sustained component was not significantly different from the pre-sound rate, but pre-sound activity was significantly higher than post-sound, thus it was still considered 'onset-sustained'. 'Onset-sustained' responses resemble primary-like responses described in bushy cells in the ventral cochlear nucleus (Rhode et al., 1983), cells that provide the inputs to the superior olivary complex and are therefore involved in the processing of binaural cues. Finally, when the increase in activity at the onset of the sound was maintained at a similar rate during the full presentation, it was classified as 'sustained' response (Figure 4-4 A).

In the awake state and under normal hearing conditions, a minority of clusters showed suppressed responses to sound (7.48 ± 4.99 %), characterised by a decrease in the firing rate following the stimulus onset relative to preceding activity. This suppressive response could be further classified into two categories based on whether the suppression was limited to the sound onset or maintained throughout the duration of the stimulus, constituting the types 'suppressed onset' and 'suppressed sustained' respectively (Figure 4-4 B).

All six different response types, excitatory and suppressed, were found on all probes (Figure 4-4- C). The two most common response types were 'onset-sustained' (34.19 ± 9.43%) and 'sustained' (25.87 ± 6.35%) (Figure 4-4 C). In the right IC of ferret F2111, a large proportion of clusters (37.99%) were unclassified, but when restricting the analysis to clusters below the border at 2000μm from the probe tip, to limit clusters to the CNIC, this proportion was reduced (17.3%), with 'onset sustained' and 'sustained' becoming the most common response types (28.29% and 25.05%, respectively). In comparison with the awake recordings, responses under anaesthesia also showed a

predominantly sustained or onset-sustained profile, although the percentage of onset-sustained responses was much higher (64.60±4.71%) and was the predominant response type recorded with all probes. We further explored in the awake recordings whether these response types had a specific anatomical distribution within the IC and, thus, whether they were related to the units' preferred sound frequency, which was previously confirmed to have a dorsoventral distribution from low to high frequency along the probe/tonotopic axis. A sparse distribution of the different types was observed along the depth of the probe, with none of them being confined to any specific anatomical region overall (Figure 4-5 A-B). In the right IC of animal F2111 we observed that 'onset-sustained' units were located below the ~2000 μm border, where anatomically the CNIC was found and also consistent with the FRA recordings showing a tonotopic organisation (Figure 4-5 B). Although those response types were found using all clusters, single and multi-unit, to ensure that none of the response types were arose erroneously from the contribution of different units in the multi-unit clusters, we performed the same analysis using single units only for animal F2108. The same response types and similar distribution (data not illustrated) were found, demonstrating that none of the firing patterns were the result of possible multi-unit activity.

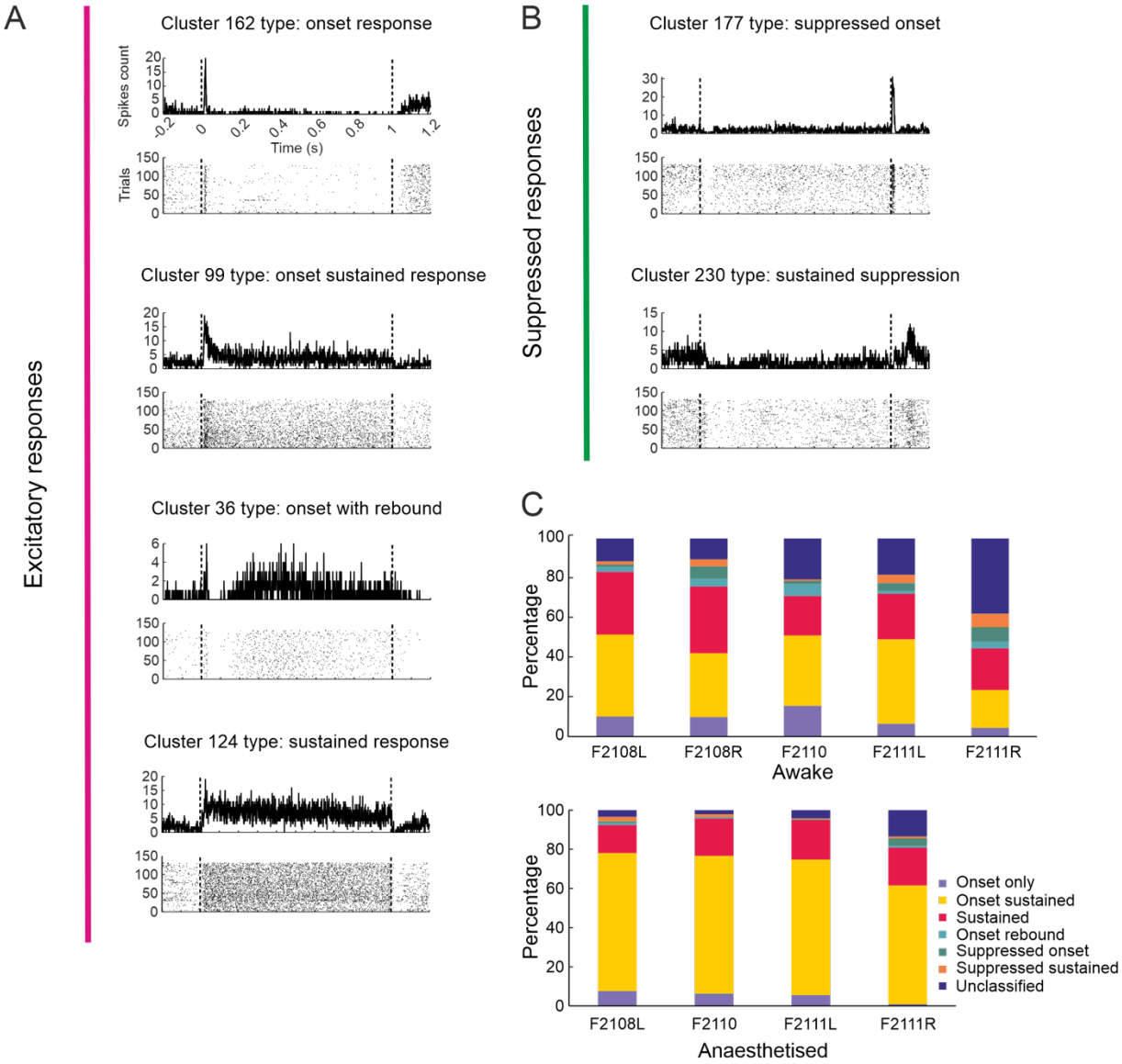

Figure 4-4. Response types in the IC. (A). Example PSTHs and raster plots illustrating four different types of excitatory responses in the IC that were defined by their response profiles. Clusters were recorded in the left IC of ferret 2108 in response to 1000-ms bursts of broadband noise presented at different azimuths while the animal performed a sound localisation task. The onset and offset of the stimulus are indicated by the vertical dashed lines. (B) Example PSTHs and raster plots depicting two different types of inhibitory responses recorded in the IC. Clusters were obtained from the same recording session as in A. (C). Stack plots showing the percentage of each response type found in the IC of awake behaving animals (averaged across sessions in each animal) and anaesthetised animals (single session for each animal) in normal hearing conditions (F2108 right IC was not recorded under anaesthesia due to failure of the probe; therefore, this probe is not included in the figure).

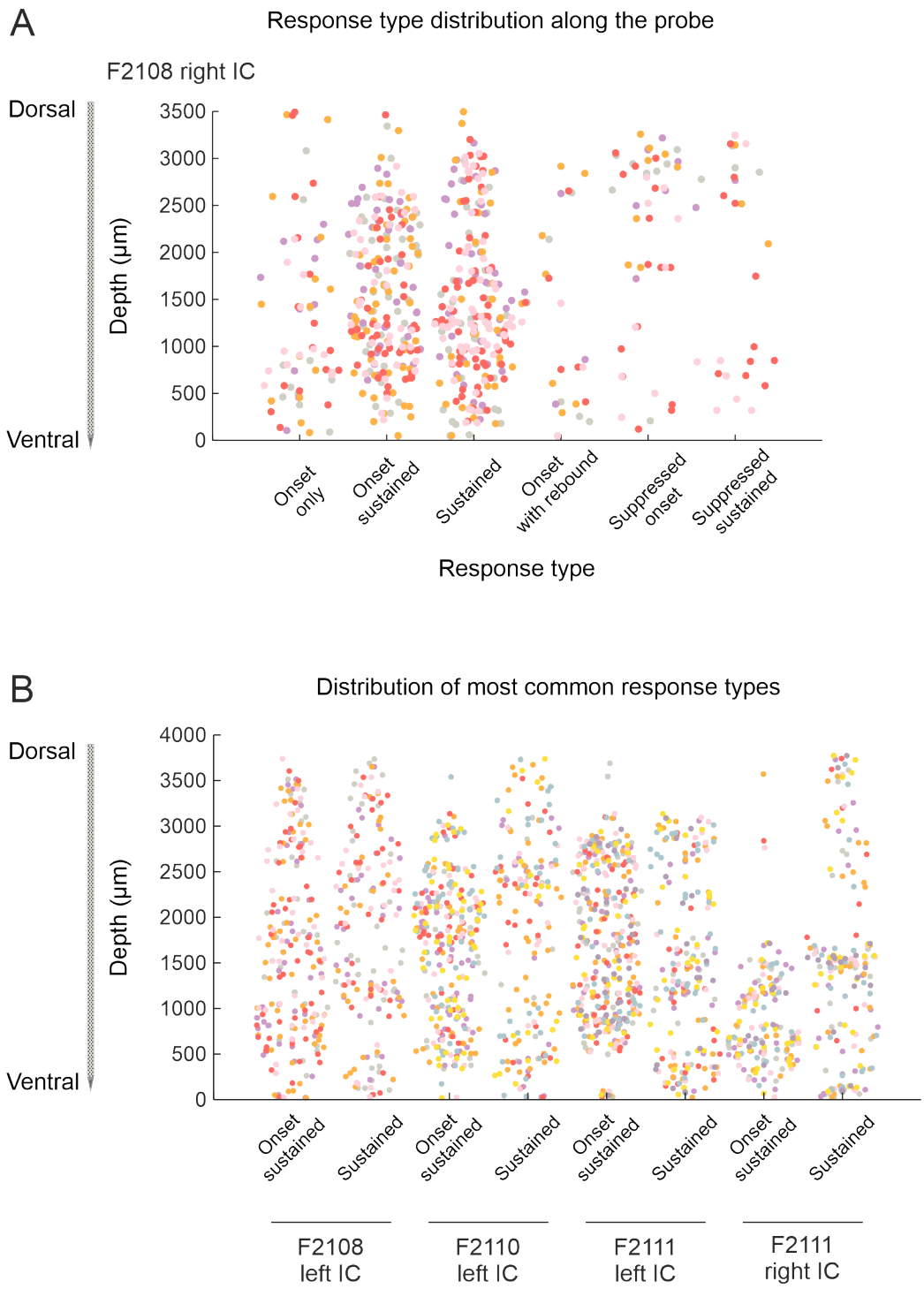

Figure 4-5. Distribution of response types along the depth of the probe in awake recordings. (A) Swarm plot indicating the distribution of clusters along the probe according to their response type for an example animal (F2108 right IC). Each colour corresponds to clusters for a single recording session in the awake animal while executing a sound localisation task. (B) Distribution of clusters by depth for the two most common

response types for each probe. Each colour corresponds to clusters from a single recording session in the awake animal while executing a sound localisation task. Note that depth refers to the distance from the tip of the probe, which had a dorso-ventral trajectory.

4.2.4. Modulation of IC responses by sound localisation task variables

We studied the spatial responses of units in the IC while the animals were engaged in a sound localisation task (see Chapter 2). Sound sources were spaced at 30º intervals around the circumference of the arena, which had a radius of 70 cm. Azimuth-response functions were produced from the average firing rate at each of the 12 loudspeaker locations while the animal stood at the centre of the arena (Figure 4-6 A-B). Despite the contralateral preference of the IC units, the azimuth functions were quite heterogeneous (Figure 4-6 A-B). This predominantly contralateral preference was found in both the left and right IC (mean centroid left IC: 55.19º, mean centroid right IC: -45.19º, averaged across animals), although in all animals and probes, a minority of units exhibited an ipsilateral preference (Figure 4-6 C). The right IC of animal F2111 showed a more heterogeneous distribution of spatial responses and a less clear contralateral preference (F2111 right IC mean centroid: -11.9º, 44.82% ipsilateral units and 55.18% contralateral units) (Figure 4-6 C). Reducing the number of clusters in this animal to those located below the border (at ~2000μm from the probe tip) between the CNIC and the DCIC, only slightly changed the proportions of ipsilateral and contralateral units towards a greater contralaterality (42.29% ipsilateral units and 57.71% contralateral units). Characterisation of the spatial responses of IC units in the same animals while anaesthetised revealed a contralateral

preference in all probes, including in the right IC of animal F2111 (Supplementary Figure 4-6).

During the sound localisation task, the intensity of the sounds presented was varied from 56-84 dB SPL in 7 dB steps. To explore how the responsiveness, spatial tuning sharpness and location preferences were affected by stimulus intensity, we compared the azimuth functions obtained with stimuli of lower (56-63 dB SPL) and higher (77-84 dB SPL) intensities. While the overall spatial preference changed relatively little (mean centroid low vs high intensity per animal: F2108 left IC 45.33° vs 36.99°, F2108 right IC -50.95° vs -64.31°, F2110 left IC 38.22° vs 50.94°, F2111 left IC 46.07° vs 42.33°, F2111 right IC -2.21° vs 4.90°), we observed a broadening of the azimuthal functions with increasing sound intensity (Wilcoxon signed-rank test $W = 7618660$, $p<0.001$), as determined by the computation of the equivalent rectangular receptive fields (ERRF) for each recorded unit (Figure 4-6 D) (low intensity sounds Q1 = 67.5º, median = 105º, Q3. = 146.25º, high intensity sounds Q1 = 74.6º, median = 113.75º, Q3 = 154.5º).

To further characterise the effects of sound location and intensity on evoked spiking activity recorded in the IC of awake behaving ferrets we used a mixed effects model (glmmPQL) (Table 4-1). The model revealed that sound-evoked activity in the IC significantly increased with sound intensity (Table 4-1). Sound location also significantly modulated evoked activity. Using the location at 0º as the reference category, neural activity was significantly greater for sounds presented in the contralateral hemifield and lower for sounds in the ipsilateral hemifield (Table 4-1), in keeping with the predominantly contralateral distribution of the centroids. However, when taking 60° or -60º as the reference, the closest locations in the task to the computed mean centroid in

each hemisphere, no significant differences were observed in evoked activity relative to other proximal locations in the same hemifield, such as ± 30° or ± 90°. This is consistent with the observed broad spatial tuning of units in the IC. Within the contralateral hemifield, none of the locations showed a significantly different firing rate relative to that measured at -60º azimuth. In the ipsilateral hemifield, only responses at 120º were significantly different from those at 60º location ($p = 0.0161$). As expected, sound-evoked activity was significantly different between hemifields (Table 4-1). Responses at both 0º (front) and 180º (back) locations were significantly different from those at 60º and -60º, and activity at 180º was significantly lower than that at the 0º location, indicating that differences between front and back positions can be found in the spiking activity in the IC units.

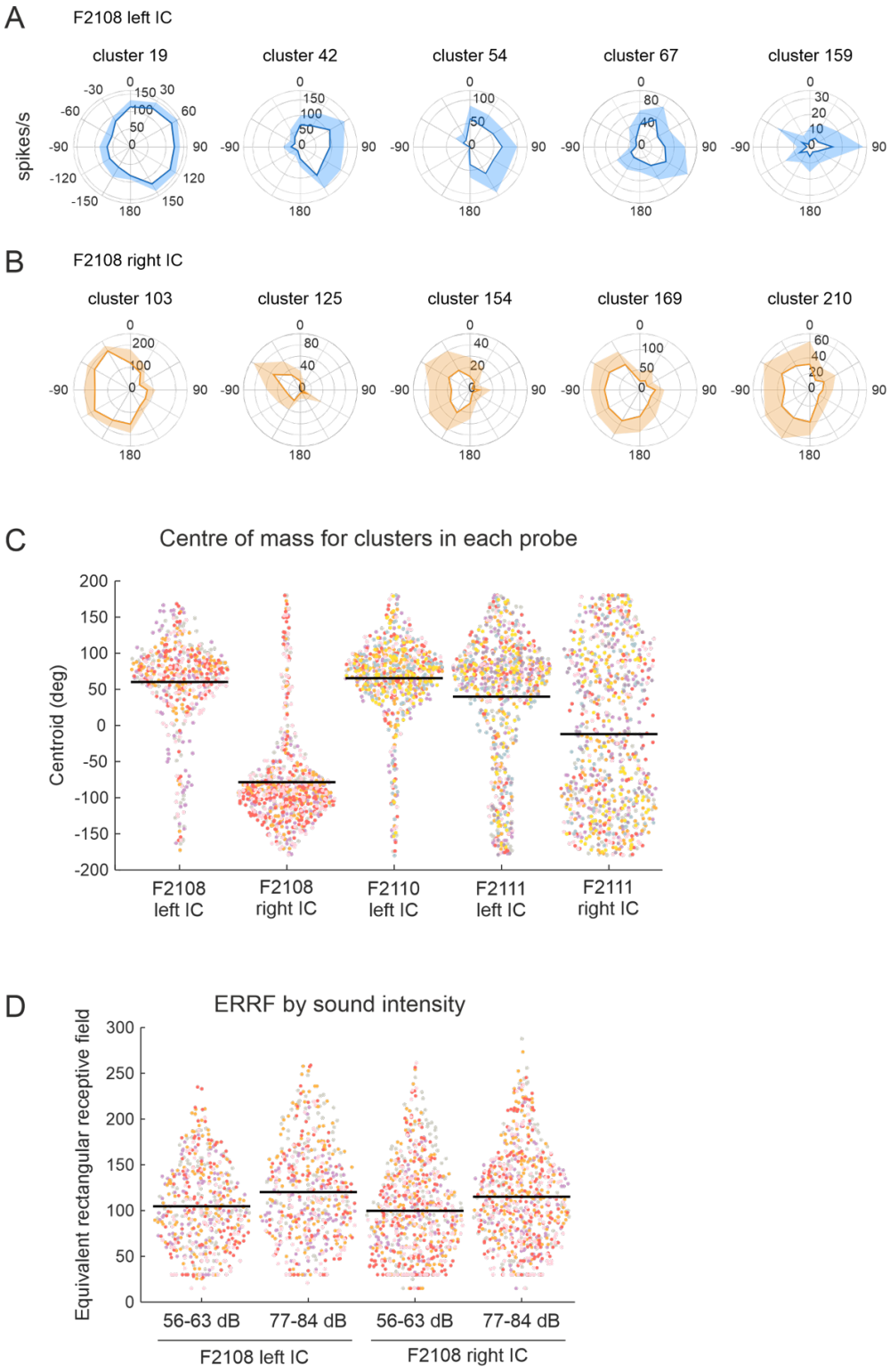

Figure 4-6. Spatial tuning of units in the IC recorded in awake animals. (A) Polar plots illustrating the firing rate (mean+sd) (spikes/s) of example units in the left IC of animal F2108 in response to 1000-ms bursts of broadband noise presented from 12 loudspeakers location around the animal. Clusters correspond to a recording session in

which the animal was performing a sound localisation task in normal hearing conditions. (B) Same as in A with example clusters extracted from recordings in the right IC of animal F2108. (C) Swarm plots describing the distribution of clusters according to their spatial preferences for each probe. Spatial preferences are defined as the centre of mass of the corresponding firing rate polar plot for each cluster. Each dot is a cluster, and each colour represents a different recording session carried while the animal was awake and performing a sound localisation task. (D) Swarm plots illustrating the distribution of clusters based of their ERRF estimated for low (56-63 dB SPL) and high (77-84 dB SPL) intensity sounds in an example animal (F2108). Each dot represents a cluster, and each colour is a different recording session.

Table 4-1. GLMMPQL measuring effect of location and sound intensity on sound evoked activity in the IC.

Reference: Location 0 º INTENSITY 56 DB SPL	**Value**	**Std. Error**	**Df**	**T-value**	**P-value**
Location -150	0.2234157	0.04216518	151920	5.29858	0.0000
Location -120	0.2511615	0.04174345	151920	6.01679	0.0000
Location -90	0.1620043	0.04202034	151920	3.85538	0.0001
Location -60	0.1671323	0.04366200	151920	3.82787	0.0001
Location -30	0.2022016	0.04615274	151920	4.38114	0.0000
Location 30	-0.2795938	0.04894652	151920	-5.71223	0.0000
Location 60	-0.3783349	0.04740991	151920	-7.98008	0.0000
Location 90	-0.4259112	0.04550728	151920	-9.35919	0.0000
Location 120	-0.2534427	0.04557590	151920	-5.56089	0.0000
Location 150	-0.3897436	0.04228916	151920	-9.21616	0.0000
Location 180	-0.1802158	0.04799535	151920	-3.75486	0.0002
Intensity 63	0.0261818	0.04537179	151920	0.57705	0.5639
Intensity 70	0.2192572	0.04824571	151920	4.54459	0.0000
Intensity77	0.1336552	0.03709386	151920	3.60316	0.0003
Intensity 84	0.2188453	0.05247052	151920	4.17082	0.0000
Reference: LOCATION 60	**Value**	**Std. Error**	**Df**	**T-value**	**P-value**
Location -150	0.6017506	0.04891209	151920	12.30270	0.0000
Location -120	0.6294964	0.04854921	151920	12.96615	0.0000
Location -90	0.5403392	0.04879308	151920	11.07410	0.0000
Location -60	0.5454672	0.05021174	151920	10.86334	0.0000
Location -30	0.5805365	0.05240365	151920	11.07817	0.0000
Location 0	0.3783349	0.04740991	151920	7.98008	0.0000
Location 30	0.0987412	0.05487578	151920	1.79936	0.0720
Location 90	-0.0475763	0.05182383	151920	-0.91804	0.3586
Location 120	0.1248922	0.05187369	151920	2.40762	0.0161
Location 150	-0.0114087	0.04903624	151920	-0.23266	0.8160
Location 180	0.1981192	0.05402823	151920	3.66696	0.0002

Reference: LOCATION - 60	Value	Std. Error	Df	T-value	P-value
Location -150	0.0562834	0.04529170	151920	1.24269	0.2140
Location -120	0.0840292	0.04489767	151920	1.87157	0.0613
Location -90	-0.0051280	0.04516142	151920	-0.11355	0.9096
Location -30	0.0350693	0.04903264	151920	0.71522	0.4745
Location 0	-0.1671323	0.04366200	151920	-3.82787	0.0001
Location 30	-0.4467261	0.05167076	151920	-8.64563	0.0000
Location 60	-0.5454672	0.05021174	151920	-10.86334	0.0000
Location 90	-0.5930435	0.04842130	151920	-12.24757	0.0000
Location 120	-0.4205750	0.04847343	151920	-8.67640	0.0000
Location 150	-0.5568759	0.04541975	151920	-12.26066	0.0000
Location 180	-0.3473481	0.05076602	151920	-6.84214	0.0000

Negative locations correspond to positions contralateral to the hemisphere of the recorded IC. Positive locations correspond to positions ipsilateral to the hemisphere of the recorded IC.

4.2.5. Decoding azimuth location from data recorded in the IC

As discussed in the previous section, the neural activity of IC units was modulated by the stimulus location and intensity while animals preformed a sound localisation task. In order to explore whether the behavioural performance of the animals could be accounted for by the activity of the recorded IC units, we used a population decoding analysis. Because the animals performed almost perfectly in every session, it was not possible to explore whether neural activity in the IC was modulated not only by the actual stimulus location, but also by the perceived location (behavioural choice, i.e., the animal's response location). Thus, the decoding analysis was exclusively focused on predicting the actual stimulus location.

We used a pattern classifier (Meyers, 2013) to predict the location of the sound in each trial from the spiking activity recorded in the IC. To avoid introducing a bias because

of the different number of clusters recorded in each IC, we balanced the number of left and right units by randomly removing clusters from the side with the greatest number. The pattern classifier was trained using the spiking activity from both hemispheres recorded for a period of 1400 ms in each trial (comprising a 1000 ms window corresponding to the sound duration plus 200 ms before and after sound presentation) which was divided into 100 ms bins with 50 ms overlap. Data were split into training and test sets over multiple cross-validation sets and classification accuracy was reported for test trials. The decoding accuracy was close to chance (~8%) for time bins before stimulus presentation. However, it increased shortly after the sound was presented, reaching its peak around 100-150ms after the onset (example session: F2108 peak: 44.6% accuracy, F2111 peak: 61.95% accuracy) (Figure 4-7, A blue lines).

We also tested the capacity of the pattern classifier to decode the stimulus location using the activity from a single IC. We found that similarly to the combined activity of the two IC, the classification accuracy increased shortly after sound presentation (example session: F2108: right IC peak: 43.6%, left IC peak: 28.25%; F2111: right IC peak: 50.22%, left IC peak: 45.48%). The peak accuracy exceeded chance regardless of whether stimulus location was decoded from only one or both ICs, indicating that the patterns of spikes from a single IC are informative about the azimuthal location of the stimulus. Nevertheless, the decoding accuracy was higher when activity from both sides was combined (Figure 4-7 A) but did not match the behavioural performance of the animals themselves, as we will discuss later.

We also observed some differences in the decoding performance between left and right IC. In animal F2111, both hemispheres showed similar levels of decoding accuracy shortly after the onset of the stimulus. In the left IC of this ferret, decoding accuracy

progressively declined after 150 ms into the stimulus presentation, which is a similar latency to the head orienting movement, after which the relative location of the sound in head-centred coordinates would change. In contrast, decoding performance based on the activity of the right IC kept rising after 150 ms, reaching its peak at around 500 ms into the stimulus presentation and stayed substantially above chance level throughout the whole presentation. This result could be due to the absence of an overall contralateral preference in this hemisphere of ferret F2111, with a more balanced number of contralateral-preferring and ipsilateral-preferring units (see Section 4.2.4.). In animal F2108, decoding performance was better in the right IC than in the left IC. In the right IC, decoding performance peaked at 150 ms after sound onset and then progressively declined back to close to chance levels, as we observed for the left IC in animal F2111. Decoding in the left IC in F2108 showed a lower accuracy peak than in the right IC, and was also delayed, reaching its highest value 250ms into the sound presentation before returning to close to chance level (Figure 4-7 A). The difference in decoding accuracy between the two sides of the auditory midbrain in this animal could be related to the different probe locations, the right probe being in the CNIC, while the left was in the LCIC (see Section 4.2.1), although for both probes most of the units showed a clear contralateral bias.

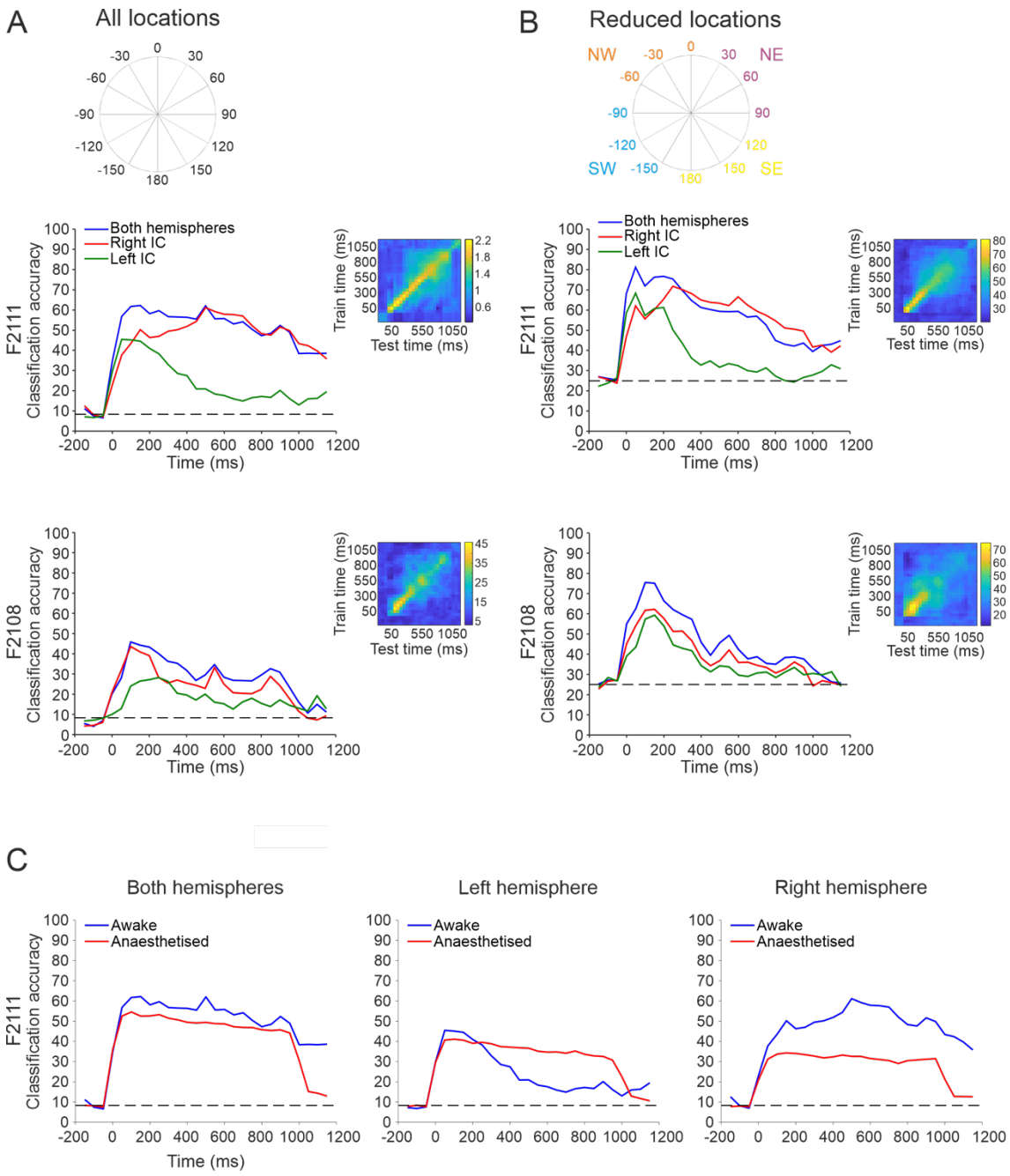

Figure 4-7. Estimation of sound azimuth by a pattern classifier. (A) Output of the decoding analysis for the prediction of the actual sound azimuth (12 locations) from activity recorded in the IC from two animals, F2111(top) and F2108 (bottom) while they were awake and engaged in a sound localisation task. The accuracy of sound azimuth decoding is plotted at each time bin for when the model was trained, combining activity from both hemispheres (blue) or with data recorded from a single hemisphere (red: right IC, green: left IC). Temporal cross-training matrices on the right show the accuracy of decoding when the model was trained using the data combined from both hemispheres at one given time bin and tested at the same or a different time bin. (B) Same as A but for a

reduced number of azimuth locations, for which sound locations were compressed into only 4 different locations: NW, northwest; NE, northeast; SE, southeast, and SW, southwest. (C). Comparison of decoding accuracy between awake and anaesthetised conditions based on IC recordings in ferret F2111 using the same range of stimulus locations in each case. Accuracy is plotted across time for three different data sets: both hemispheres combined, left IC only and right IC only.

With this analysis we have shown that activity in the IC can be used to infer the stimulus location. However, decoding accuracy was far from the behavioural performance showed by the animals (94.55% averaged across animals), reaching levels of accuracy between 40-65%. This suboptimal accuracy could be due to the broad spatial tuning of neurons in the IC that greatly exceeded the 30° separation between the sound source locations. When we subdivided the full 360° range of azimuths into 4 quadrants and grouped the sound locations into [northwest (NW), northeast (NE), southwest (SW) and southeast (SE)], thereby reducing the locations to be predicted from 12 to 4, the prediction accuracy improved considerably. For the combined activity of both ICs, the classification accuracy was around 80% (F2108 peak: 75.3%, F2111 peak:81.2%), still short of the behavioural performance. In both cases, decoding accuracy peaked at around 100-150 ms after sound presentation and declined thereafter. For ferret F2111, similar results were found as in the analysis based on all 12 stimulus locations. Both hemispheres reached a similar peak (right IC peak: 62.05%; left IC peak: 68.35%) and decoding accuracy then progressively declined in the left IC, but increased in the right IC (Figure 4-7 B). In animal F2108, the temporal structure of the classification accuracy was very similar for both hemispheres in this analysis, but was consistently higher in the right IC than on the left side (right IC peak: 61.98% left IC peak: 58.35%) (Figure 4-7 B).

We also tested the temporal cross-generalisation of the pattern classifier for the combined activity of the two hemispheres in the full and reduced locations analyses. With this analysis, we tested whether the classifier generalises across time by training and testing it at different time points. Temporal cross-training matrices (Meyers, 2013) showed that the highest correlation between training and test times occurs along the diagonal in all cases (Figure 4-7 A-B), suggesting that the pattern classifier does not generalise across time. In other words, spatial information may be encoded differently across time, which is indicative of a dynamic population code. Moreover, in the reduced locations analysis the highest classification accuracy scores were achieved within the first 300 ms of sound presentation, suggesting that this is the most informative part about the location of the stimulus (Figure 4-7 B). This result is less evident for the full locations analysis, especially for animal F2111 (Figure 4-7 A).

Although the classifier failed to reach the animals' behavioural accuracy, is still possible that the animal's sound localisation is based on the information conveyed by the IC units if we consider a possible head-orienting-related decoding strategy, with a dynamic reduction over time in the number of locations. Following sound onset and in absence of head movement, the initial decoding of neural activity based on the first ~150ms could reduce the uncertainty about the location of the stimulus by initiating a head movement in that direction. Subsequent decoding of neural activity over a more focused/reduced set of locations might then result in an improved location decoding. Behavioral data has previously shown that head movement accuracy does not change with stimulus duration, whereas the accuracy of the approach-to-target does (Nodal et al., 2008). It could be that the behavioral performance is the result of the cumulative decoding performance over time, rather than simply reflecting its peak value.

To conclude the analysis of this pattern classifier, we compared the prediction performance from the awake recording data in animal F2111, using all stimulus locations, with that based on the recordings obtained under anaesthesia in response to the same stimuli. We observed that classification accuracy was lower for anaesthetised recordings when using the combined IC activity or each side individually (both peak: 54.55 %, right IC peak: 33.73%, left IC peak: 40.68%) relative to the accuracy in awake recordings. Under anaesthesia, decoding accuracy was higher in the left IC than in the right IC, and the decoding scores were also more stable across time, which is possibly explained by the absence of head movement. Moreover, the latency of the decoding accuracy peaks was similar in awake and anaesthetised conditions (Figure 4-7 C).

Because the decoding of sound azimuth with this pattern classifier failed to reach the animals' performance in the task, even when the auditory space was reduced from 12 to 4 possible locations, we built a population pattern decoder that estimated the left-right and back-front locations separately and then combined these (using trigonometry, see Supplementary Figure 4-7 for details) to produce the decoded azimuth. The pattern decoder was trained using combined activity from the two hemispheres spanning 1400ms around the sound presentation on each trial (1000ms of sound presentation, to match the stimulus duration that the behaviour is based on, plus 200ms before and 200ms after the stimulus), binned this time in 25ms bins. Data were split into training and test sets for 24 cross-validation runs and average decoding accuracy was reported for the test set. As with the previous classifier, the number of units in each hemisphere was equalised by randomly removing units from the side with most units. Additionally, the order of the trials was randomised.

As before, with this pattern decoder we estimated sound azimuth from the recorded IC activity as a method of investigating how informative units in the IC are about sound source location. But with this model we could take a step further, since it allowed us to explore the contribution of each unit at each time point in the decoding of the relevant variable. The inspection of the units' weights across time, as shown by the kernels in (Figure 4-8 A), provided further insight into how the model achieved the decoding, i.e. how informative each unit (magnitude of the weight) was at each time point and in which direction (positive or negative weight).

The pattern decoder was used to predict sound location in the back-front and left-right axes separately, as well as the intensity of the stimulus (Figure 4-8 A). Inspection of the kernels revealed that the activity at the onset of the stimulus was the most informative part for the decoding of location in the left-right axis, as evidenced by the peak in the sum of absolute weights (Figure 4-8 A). This result resembles what we observed with the previous decoder. The early period of the stimulus (~200ms) is the only part of the trial in which only static localisation cues are available as the head movement has not yet been initiated. After this window, the ferret turns the head towards the perceived target, which may provide further dynamic sound localisation cues. Estimations of the population pattern decoder when training was limited to the first 200ms after sound onset resembled those observed with full trial duration, further indicating that the onset of the trial provides the most information for the decoding of target location (Supplementary Figure 4-8). Kernel inspection also showed that units in the left hemisphere, corresponding to the top half rows in the kernels, were more informative about locations on the right (positive weights, yellow), while right IC units, the bottom half rows, were more indicative of leftwards positions (negative weights, blue) (Figure 4-

8A, Supplementary Figure 4-8A). This observation agrees with the contralateral preference found in the spatial tuning of units in the IC and suggests that the model is taking advantage of the oppositely tuned populations for decoding the left-right axis, as proposed by the hemispheric two-opponent model (McAlpine et al., 2001). Conversely, the exploration of the output kernels for the decoding of location in the back-front axis did not show a clear temporal structure or a difference in decoding between the left and right hemispheres. With regard to sound intensity, which was also varied across trials, the sum of absolute weights showed a peak at the onset of the stimulus followed by a sustained increased weighting, indicating that neural activity was informative about the sound level throughout the sound presentation (Figure 4-8 A).

The performance of the pattern decoder was consistently higher when sound location was estimated for the left-right axis relative to the back-front axis (Figure 4-8 B, C), as evidenced by values in Figure 4-8 C falling below the identity line, indicating that the error was greater for back-front decoding relative to left-right decoding in each of the recording sessions. This was also observed when decoding was restricted to the first 200ms after sound onset (Supplementary Figure 4-8 B, C), as would be expected since it is this time window that is the most informative about left-right decoding, as indicated by the weights. The distance to the identity line was smaller for sessions recorded in animal F2111 compared to animal F2108; this could be related to the reduced contralaterality observed in the IC responses of animal F2111, which could result in an improved back-front representation, ultimately reducing the error. In any case, the enhanced performance of decoding in the left-right axis in all cases can be explained by the bias shown by the left and right hemispheres towards the right and left hemifields, respectively, and points at a hemispheric two-channel model for encoding sound location at this level of the

auditory system. Nevertheless, the back-front decoding performance suggests that the pattern of spikes recorded in the IC was also somewhat informative about location in this axis.

From the estimation of sound location in each of the axes, the decoded azimuth location could be computed using trigonometry (Supplementary Figure 4-7). We found that with this approximation, the decoding of azimuth was highly accurate, with a comparable performance to that observed in the animals' behaviour (Figure 4-8 B, Supplementary Figure 4-8 B). This indirect decoding of sound azimuth was consistently better than the performance achieved when the same pattern decoder was trained to decode the sound azimuth directly (Figure 4-8 D, Supplementary Figure 4-8 D), as evidenced by values falling below the identity line, indicating a greater error for that condition.

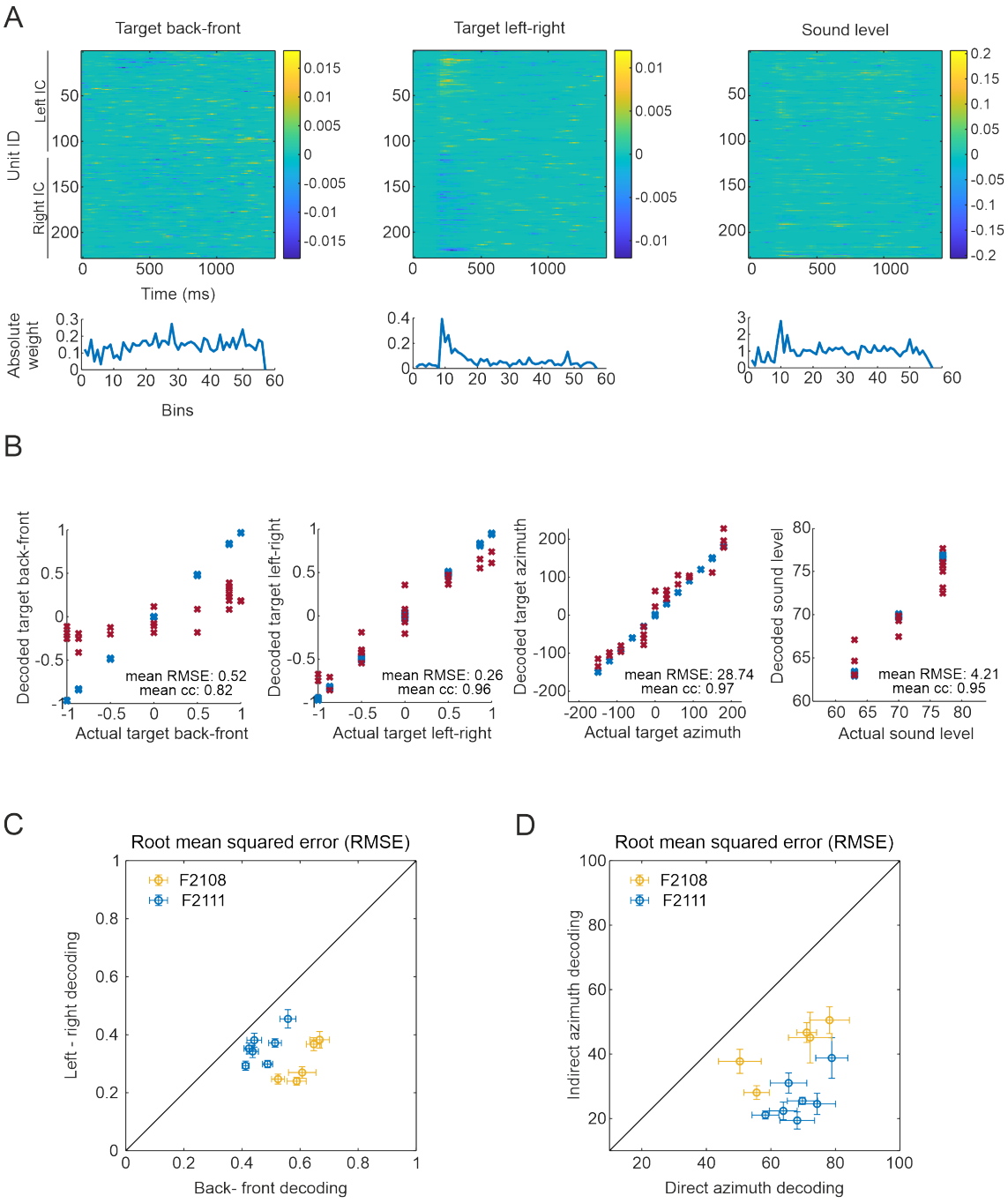

Figure 4-8. Sound location decoding by a population pattern decoder from data recorded bilaterally in the IC. (A) Kernels showing the weight of each recorded unit across time, indicating how informative each unit is about the decoded variable at each time bin. Weights are plotted over a 1400ms window (encompassing the 1000-ms sound duration plus 200 ms before and after this). Units were sorted by side (left IC – top half of each plot, right IC – bottom half). The weighting of units across time is plotted for the decoding of back-front location, left-right location, and sound intensity. For back-front decoding, yellow is indicative of 'front' and blue of 'back'; while for left-right decoding,

yellow indicates 'right' and blue 'left'. Below each kernel, the sum of the absolute weights is plotted for each time bin, indicating changes in the units' decoding weights across time. Data used to train the model were obtained from a single session of bilateral recordings in the IC in ferret F2108 while it was awake and engaged in a sound localisation task. (B) The values estimated by the decoder for each variable are plotted against the actual values. Results are plotted for back-front [circular space was compressed into a linear space going from back (-1) to front (1)], left-right [circular space was compressed into a linear space going from left (-1) to right (1)], azimuth (extracted from back-front and left-right decoding), and sound intensity decoding. Estimates are shown for the training set (blue) and the testing set (red) for an example fold. The mean correlation coefficient (cc) and root mean square error (RMSE) across folds are indicated at the bottom of each plot. The dataset used to train the model was the same as for panel A. (C) RMSE for back-front and left-right decoding for different recording sessions in animals F2108 and F2111 (mean±SE, across folds). All sessions shown were performed while animals were awake and performing a sound localisation task. Data from the two hemispheres were combined to train the decoder. All values that fall below the diagonal identity line indicating better decoding accuracy along the left-rightaxis. (D). RMSE for direct and indirect estimations of sound azimuth in different recording sessions in animals F2108 and F2111 (mean±SE, across folds). Recordings were the same as in C. For indirect sound azimuth decoding, the azimuth location was estimated from left-right and back-front decoding by applying trigonometry. For the 'direct' condition, the decoder was trained to directly decode the azimuthal location. All values fall below the diagonal identity line, indicating greater accuracy of indirect azimuth decoding.

To further test the hypothesis of a hemispheric two-channel model, we built a variant of the pattern decoder that collapsed the activity of each hemisphere into a single "unit", by averaging spiking activity across all recorded units in each IC in order to preserve their temporal firing patterns. Therefore, the collapsed two-channel decoder predicted sound location based on the activity of just two collapsed units, one per hemisphere, corresponding to each of the channels with opponent tuning proposed by the model. The comparison of decoding accuracy between the pattern decoder and the collapsed two-channel decoder revealed that the estimation of sound location in the left-right axis was very similar between the two models, as evidenced by values falling close to the identity line in (Figure 4-9 left-right decoding). Despite the great simplification of the collapsed model, these results suggest that the activity of two opponent units, or channels, is enough

to decode sound location in the left-right axis to a comparable degree to a pattern decoder which uses the activity of hundreds of units recorded on each side of the brain. This result therefore supports the hemispheric two-opponent channel model as a code for computing sound location. However, when azimuth decoding was compared between these two models, the pattern decoder exhibited consistently better performance, as shown by the values falling below the identity line, indicating a greater decoding error of the collapsed model (Figure 4-9 azimuth decoding). This was accompanied by a similar result in the decoding of back-front location (Figure 4-9 back-front decoding). Altogether, these findings indicate that beyond the information about sound location provided by the opponent contralateral tuning found in the IC, the heterogeneity in the pattern of spikes produced by the neurons provides further information about sound location that contributes to a higher accuracy in azimuth decoding.

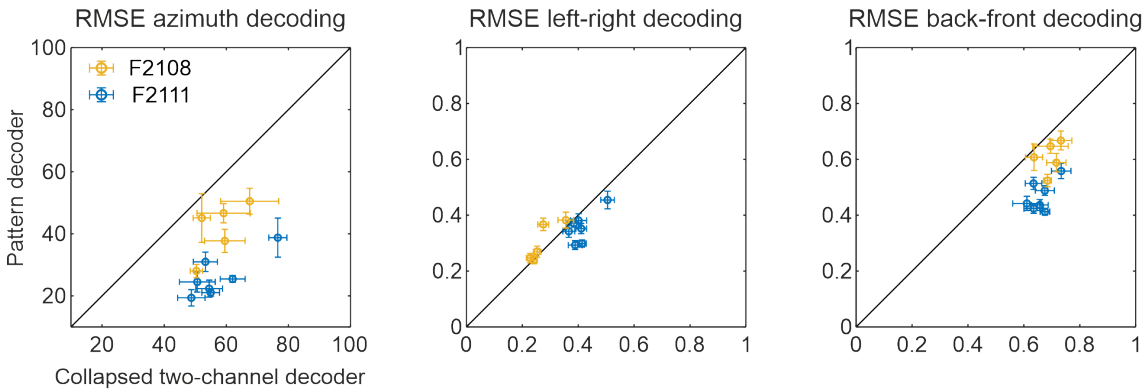

Figure 4-9. Comparison of decoding performance between a pattern decoder and a collapsed two-channel decoder. The decoding accuracy of azimuth (left panel), left-right (middle panel) and back-front (right panel) locations are compared for two different decoding approaches. The pattern decoder was trained using the pattern of spikes of simultaneously recorded units in both ICs. The collapsed two-channel decoder was a variant of the pattern decoder for which the activity of units in each hemisphere was averaged and then collapsed into a single unit with time varying spikes. The RMSE is

shown for each decoder and decoding variable (mean±SE, across folds) for different recording sessions in animals F2108 and F2111. Distance and position of values relative to the diagonal identity line allows a comparison in the performance between the two decoding methods.

To conclude this analysis, we explored the decoding accuracy of the pattern decoder when it was trained using activity from a single IC. We found that the decoder was able to accurately estimate sound azimuth (Figure 4-10A). However, as before the back-front decoding was worse (higher RMSE) than left-right decoding (Figure 4-10 B). The right IC of animal F2111 showed the greatest similarity between the decoding in each axis i.e., the shortest distance to the diagonal identity line. It was also this IC that lacked a clear contralateral dominance, supporting the previously proposed hypothesis of improved back-front performance when contralaterality is not so marked. Sound azimuth decoding performance was computed separately for the left and right sides of space to further characterise how accurately each IC encodes sound locations in the contralateral and ipsilateral hemifields. Despite the contralateral sound preferences observed for most units, surprisingly, we found that for both right and left ICs, the decoding of azimuth locations in the right hemifield was worse relative to the left hemifield.

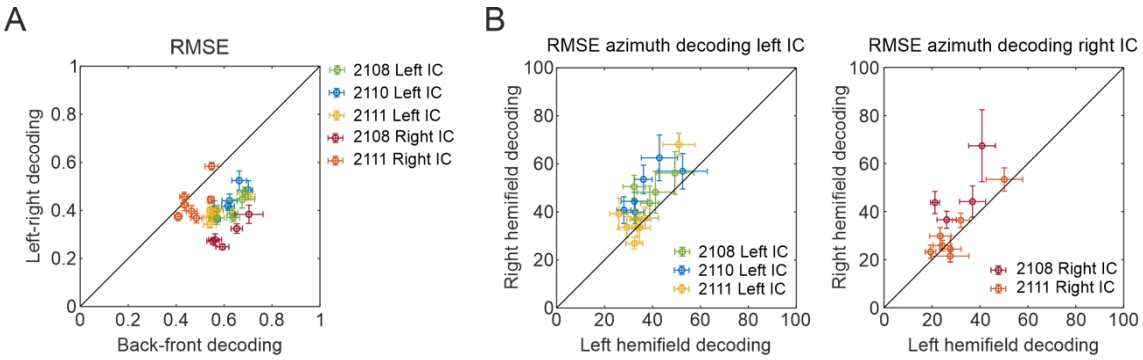

Figure 4-10. Decoding performance of a pattern decoder trained with data from individual ICs. (A) The accuracy of back-front and left-right decoding are compared for estimations obtained by training the pattern decoder with data collected from either the left or the right IC in F2108, F2110 and F2111. RMSE (mean±SE, across folds) is shown for different recording sessions in each animal and distance and location of values relative to the identity line allow a comparison between back-front and left-right decoding. (B) Accuracy of azimuth location decoding is compared between the right and left hemifields (RMSE, mean±SE) when the model was trained only with left IC data (left panel) or only with right IC data (right panel), to show how accurately each IC represents locations in the ipsilateral and contralateral hemifields.

4.3. Discussion

The IC is thought to be a key processing hub in the auditory pathway. Given that ascending pathways encoding different auditory localisation cues converge in the IC, this midbrain nucleus is widely thought to play an important role in sound localisation processing (Grothe et al., 2010). Many studies have aimed to characterise the spatial response properties of IC neurons to ultimately try to understand how sound location is represented [e.g.(Chase & Young, 2008; Day & Delgutte, 2013; McAlpine et al., 2001)]. However, these studies have traditionally been performed under anaesthesia and, occasionally, in unanaesthetised head-restrained animals. The majority of studies have also focused on characterising IC sensitivity to individual spatial cues (e.g. measuring ILD or ITD sensitivity) [e.g. (Chase & Young, 2008; Dahmen et al., 2010; Dorkoski et al., 2020) and only some studies have measured azimuth tuning, often restrained to the frontal hemifield [e.g. (Day & Delgutte, 2013)].

In our study, we used high density recording probes to perform recordings bilaterally in the IC in awake ferrets while they were engaged in a sound localisation task. This approach allowed us to record activity in the IC in response to broadband sounds presented from in 12 different locations distributed throughout the full 360º of azimuth. Multiple strategies for encoding spatial information have been proposed, including place, rate and temporal codes (Day & Delgutte, 2013; Jeffress, 1948; McAlpine et al., 2001). To investigate these coding strategies in the context of our sound localisation task, we measured the spatial sensitivity of large numbers of IC neurons and built different neural models to estimate whether the sound localisation behaviour can be accounted for by the information encoded at the level of the IC in the same animals.

Most of the recordings were performed in the CNIC, the area of the IC where parallel ascending inputs encoding the different spatial cues have been shown to converge (Grothe et al., 2010). In one case, the recording probe was located in the LCIC for which the recording of FRAs showed a similar tonotopy as in the CNIC. Some of the recording sites also covered the DCIC, which may be important given that a recent volumetric calcium imaging study in mice has shown that the DCIC and CNIC contribute to sound location coding (Boffi et al., 2022).

Most of the units recorded in all probes showed an excitatory response to sound presentation, and only a limited number of units showed a suppressive response. The characterisation of the temporal response patterns revealed a large variety of response types. The most common type was 'onset sustained', characterised by a high firing rate at the onset of the stimulus followed by a reduced and sustained firing for the rest of the sound duration. The second most common type was 'sustained', which showed a more constant firing rate throughout the duration of the stimulus. A similar characterisation of temporal firing patterns has been described in the cochlear nucleus (CN) by (Rhode and Oertel 1983). The CN is the first synaptic station in the auditory pathway, and it sends direct input to the contralateral IC from the dorsal division (DCN), involved in the processing of spectral cues. The ventral division (VCN) projects to the superior olivary complex (SOC), a brainstem structure involved in the processing of binaural cues, which ultimately sends connections to the IC. In the VCN, bushy cells have a 'primary-like' response profile, which is equivalent to that described as 'onset sustained' in our study. This temporal profile makes neurons highly sensitive to the temporal structure of the auditory stimulus, crucial for the computation of binaural cues. Also in the VCN, multipolar/T stellate cells show 'chopper' response profiles, which resemble the

'sustained' response type that we observed in the IC. This response makes multipolar/T stellate cells sensitive to the sound spectrum and they have been shown to project to the ipsilateral DCN, lateral superior olive (LSO) and the IC (Oertel et al., 2011). Therefore, the different response patterns that we observed in the IC in response to broadband sounds resemble those described in brainstem auditory structures.

Some differences were observed in the firing patterns when activity was recorded under anaesthesia in response to pure tones. In this condition, units most commonly showed a clear response to the onset and offset of the sound, while a peak of activity at the offset of the sound was uncommon when the stimulus was broadband noise in awake recordings. In that case, offset activity was limited to units showing a suppressive response to sounds. Sound offset responses have previously been described in the IC and one of the mechanisms proposed to underlie them is a post-inhibition rebound, which would agree with that observed with broadband stimuli. This mechanism has been suggested in the DCN (Hancock & Voigt, 1999; Kopp-Scheinpflug et al., 2018). However, offset responses in the IC have also been shown to be driven by excitatory input directly inherited from the brainstem (Kasai et al., 2012; Kopp-Scheinpflug et al., 2018). Studies exploring the role and basis for these offset responses have mainly been conducted in response to pure tones, therefore further studies will be necessary to understand how the nature of the stimulus affects offset activity in neurons in the IC.

Recording neural activity in ferrets engaged in a sound localisation task allowed us to investigate the spatial response properties of IC units during active listening. To describe how these properties compare to those recorded under anaesthesia, we also performed recordings in response to the same stimuli as those presented in the task while the animals were anaesthetised. It is well known that anaesthesia can alter the response

properties of auditory neurons (Zurita et al., 1994), including binaural sensitivity in the IC (Kuwada et al., 1989). A direct comparison between states was important to determine how anaesthesia affects neural activity in the IC, since most of the literature on spatial responses in the IC is based on recordings in anaesthetised animals.

The width of the spatial tuning, computed as the ERRF, was highly variable in both conditions, and it was sharper in units recorded in awake behaving animals relative to those recorded under anaesthesia. Similar results were described in recordings in the AC by (Mickey & Middlebrooks, 2003) where the median tuning width spanned between 150º for single-units and 180º for multi-units in awake cats, but from 270º - 350º for multi-unit activity recorded in A1 in anaesthetised animals (Middlebrooks et al., 1998). In our study, the difference in median width values was smaller (150º in awake recordings and 187º under anaesthesia). This might be due to differences between the IC (present study) and the AC (Middlebrooks et al., 1998), or to differences in the approaches used to compute tuning width in each study. In any case, both studies point at an effect of anaesthesia on the width of spatial tuning. Further evidence of differences between brain states was provided by our population decoding analysis. Neural activity recorded in the awake condition was more informative about sound location than that recorded under anaesthesia, as evidenced by an improved decoding accuracy.

A significant reduction of the normalised firing activity prior to sound presentation was also observed in the awake state relative to under anaesthesia. Because awake animals were involved in a sound localisation task in which all trials were self-initiated, this reduction in neural activity prior to stimulus onset could be an effect of attention, motivation, or expectation about the timing of the upcoming task. This possibility is supported by previous findings showing that reward and behavioural context

can alter IC activity in primates (Metzger et al., 2006) and that trial outcome can even be decoded from pre-stimulus activity in mice performing a sound-detection task (Lee et al., 2023). Together, these findings indicate that some differences exist in neural activity in the IC between the awake and anaesthetised states, and thus the state in which recordings are performed is an important factor to consider in future studies.

We found that the activity of ferret IC units was strongly modulated by sound azimuth, in both awake and anaesthetised animals, with the majority showing a strong contralateral preference. This contralaterality has been previously described (Aitkin et al., 1984; Day & Delgutte, 2013; Kuwada et al., 2011) and partially reflects the input from the LSO, a brainstem nucleus involved in the processing of ILDs which sends contralateral excitatory and ipsilateral inhibitory projections to the IC (Grothe et al., 2010). Additionally, the IC receives ipsilateral excitatory input from the medial superior olive (MSO), involved in ITD processing, and contralateral excitatory input directly from the DCN, suggested to be involved in the encoding of spectral cues, with both pathways also contributing to the contralateral representation of auditory space in the IC. How information encoding the different spatial cues is integrated in the IC to ultimately decode sound location is still a matter of debate and several models have been proposed.

In this study, we used a population decoding analysis to explore how spatial information is represented by neural activity in the IC. We trained a decoder using the spiking activity of units recorded in both ICs recorded during the sound localisation task. We found that the estimation of sound azimuth based on the pattern of spikes was highly accurate. This agrees with similar results reported by Day and Delgutte 2013, who compared different decoding approaches and reported that the ‘population pattern’ decoder outperformed other decoders. As part of that study, Day and Delgutte 2013 also

tested a 'two-channel difference' decoder that estimated sound location based on the comparison of the summed activity in each hemisphere. This decoder was based on the hemispheric two-channel model proposed by McAlpine et al., 2001, which suggests that sound location is determined by the comparison of broadly tuned neural populations with opponent spatial preference in each hemisphere. In the study by Day and Delgutte (2013), the two-channel decoder also showed a highly accurate decoding performance, with a mean error of 7º, relative to a < 5º mean error reported for the 'population pattern' decoder.

We developed our own two-channel decoding approach by collapsing unit activity in each hemisphere. In our case, and differently to the Day and Delgutte 2013 study, the decoder still had access to information about the change in spiking activity over time. With our collapsed two-channel decoder, we also found that sound location was decoded accurately, especially in the left-right axis, although its performance was consistently worse than that of the population pattern decoder. The hemispheric two-channel model presents some advantages relative to other proposed models in that it reconciles neural and psychophysical findings, since this model predicts that the greatest neural sensitivity based on firing rate (steepest slope) would occur across the midline, where the highest spatial acuity has been described in humans (Mills, 1958) and where ferrets localise short-duration sounds most accurately (Nodal et al., 2008). Additionally, this code would be stimulus level independent since the firing rate of both populations would change together with sound intensity. In our experiments, we found that increasing the sound intensity produced an overall broadening of the spatial tuning of units in the IC. However, varying sound intensity from trial to trial did not affect decoding accuracy for any of the models and does not alter the accuracy of sound localisation behaviour in ferrets (Nodal

et al., 2008). In a later study, (Day & Delgutte, 2016) showed that sound level changed the mutual information (MI) between sound azimuth and the spike rate of cat IC neurons, but did not affect the median MI of the population.

A key difference between our study and that by Day and Delgutte 2013 is that their dataset was restricted to the frontal hemifield. In our study, we recorded IC responses to sound presented over the full 360º azimuth range, so we were able to compare the decoding accuracy of back-front position relative to left-right position in the IC. Our population pattern decoder showed higher accuracy for left-right estimation than for back-front, which is consistent with a model in which sound location is computed by comparing the activity of two populations biased to the left and right, respectively, as proposed by the hemispheric two-channel model. Our model also shows that the onset of the sound is the most informative part of the stimulus, providing a possible explanation for the observation that changing the duration of the stimulus has been shown to have no effect on the MI between final head bearing and target location or on the incidence of left-right errors in the approach-to-target responses made by ferrets (Nodal et al., 2008). On the other hand, front-back errors are more susceptible to a reduction in the sound duration (Nodal et al., 2008).

Our decoder also showed that estimating sound azimuth based on an extrapolation from back-front and left-right decoding more closely predicted the behavioural results than a direct estimation. This observation challenges other proposed models such as the panoramic model (Middlebrooks et al., 1994), which suggests that cortical neurons can encode all locations in space to different degrees and that stimulus location is encoded by different patterns of neural activity. A panoramic model would not offer a ready explanation for the observed difference between back-front and left-right decoding.

Some authors have proposed that the two-channel code could be implemented in each hemisphere independently in the auditory cortex (Keating et al., 2015; Stecker et al., 2005), as both contralateral and ipsilateral units have been described, similarly to what we found in each IC. Indeed, decoding ILDs from the activity of ferret cortical neurons that prefer contralateral versus ipsilateral values can account for the accuracy with which the animals localise high-frequency narrowband noise bursts (Keating et al., 2015). To further explore whether the combination of activity from intrahemispheric contralateral-preferring and ipsilateral-preferring IC populations is necessary to decode sound azimuth, we trained a pattern decoder using only data collected from a single hemisphere. The decoder was able to estimate sound location accurately although it showed a greater error than when trained with data from both ICs. Surprisingly, we found that the decoding of the right hemifield degraded relative to the left hemifield independently of the side of the IC. The role of opponent coding in representing sound-source location in a behaviourally-relevant way therefore remains unclear (Middlebrooks, 2021). Day and Delgutte 2013 also showed that when the 'population pattern' decoder was trained with data from one side, it was able to accurately decode sound azimuth. However, they found greater decoding accuracy for locations ipsilateral to the IC, which is inconsistent with lesion studies in cats (Jenkins & Masterton, 1982).

4.4. Appendix

4.4.1. Supplementary figures

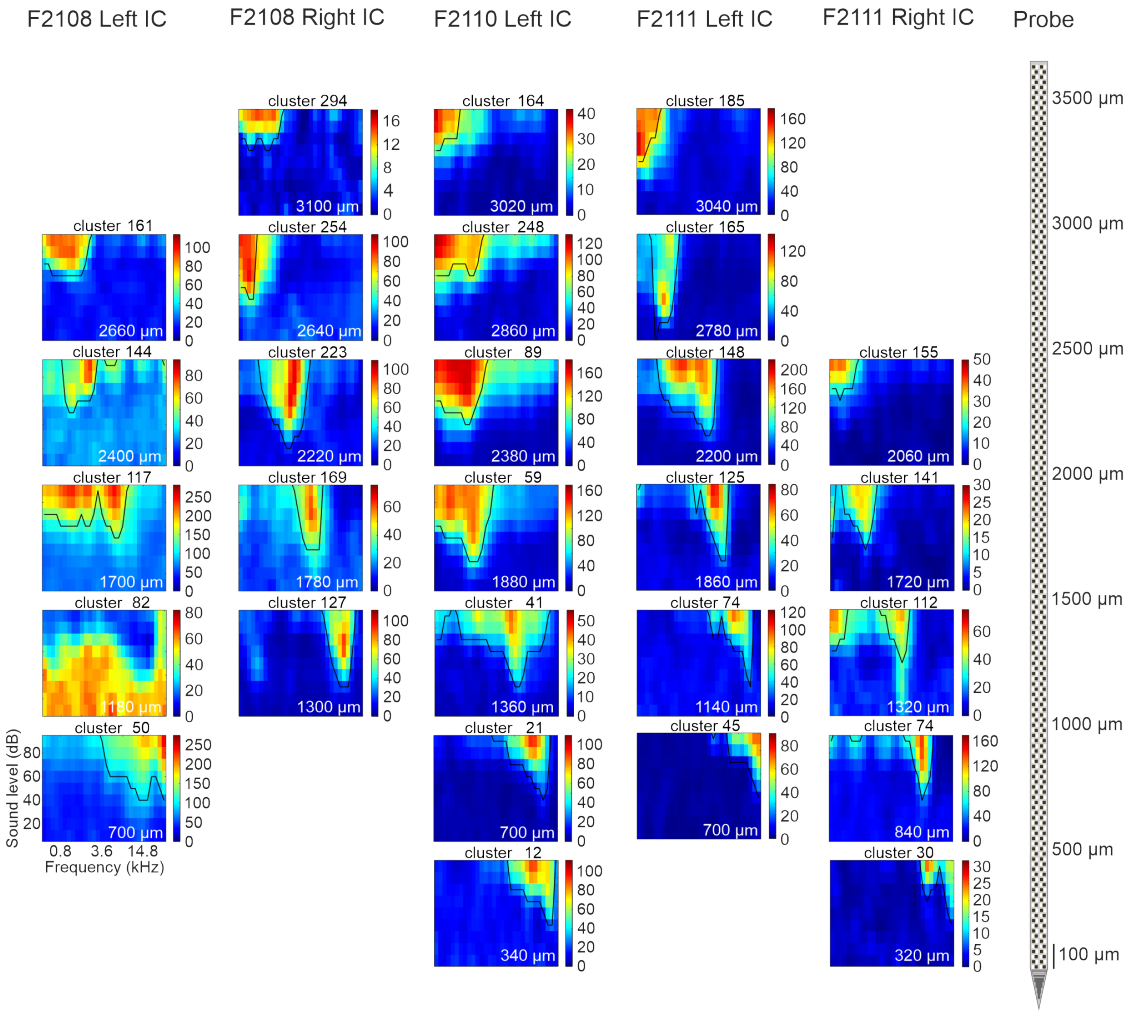

Supplementary Figure 4-1. Tonotopy by depth in all probes. Frequency response areas (FRAs) are shown for example clusters in all probes at different depths along the probe. For each 500µm interval, the FRA for an example cluster is displayed per probe and they are ordered by depth (numbered as distance from the tip of the probe) and positioned relative to the schematic of the probe located on the right in the figure. The specific depth for each cluster is specified in white.

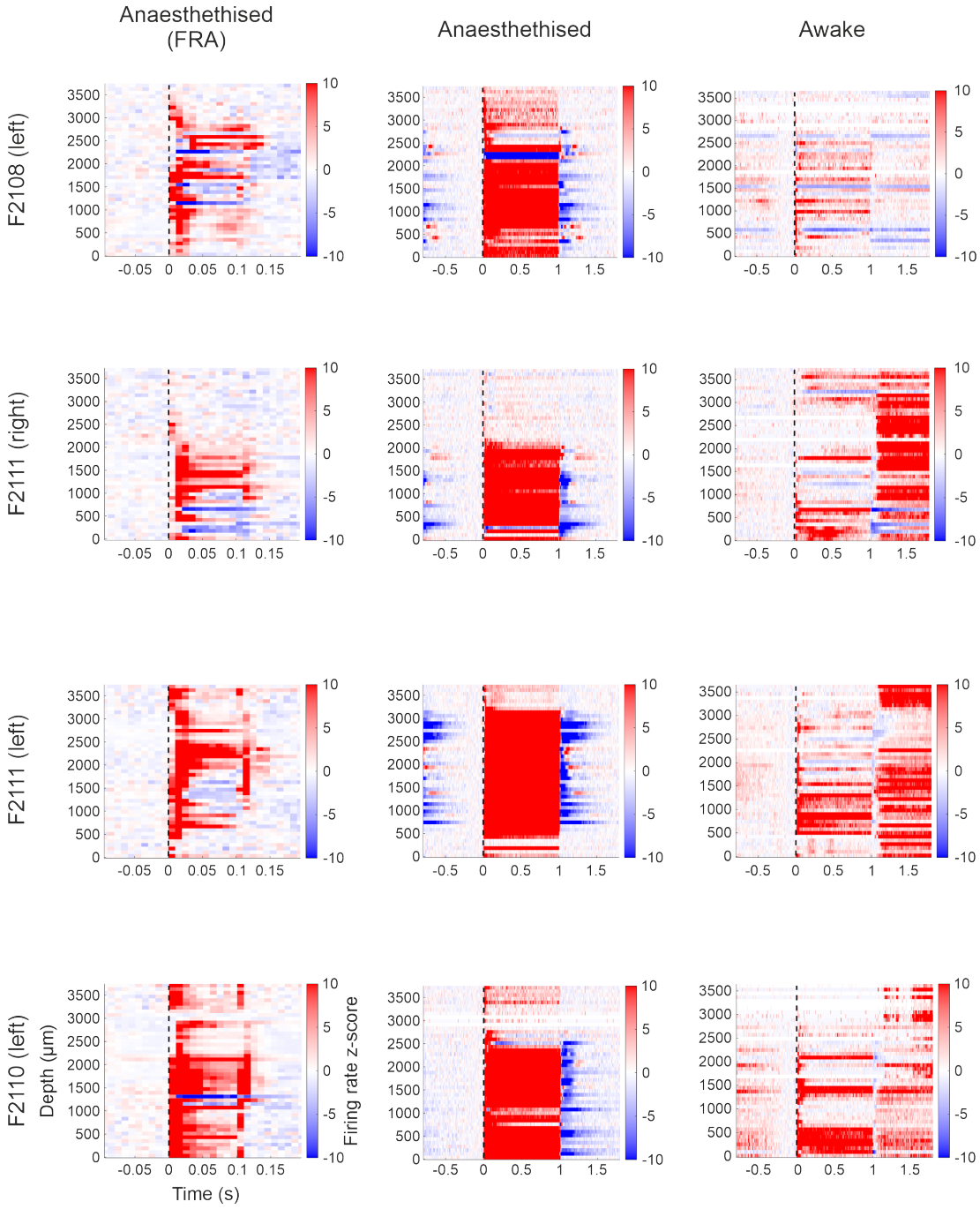

Supplementary Figure 4-2. Probe activity in different brain states. Firing rate z-score is illustrated along the recording probe aligned relative to the onset of the stimulus indicated by the vertical dashed line. Red and blue represent an increase and decrease in activity, respectively. Each row of plots corresponds to a specific side and animal while each column represents a listening condition. Recordings in F2108 right IC were not made under anaesthesia in response to broadband sounds due to failure of the probe, therefore this probe is not included in the figure.

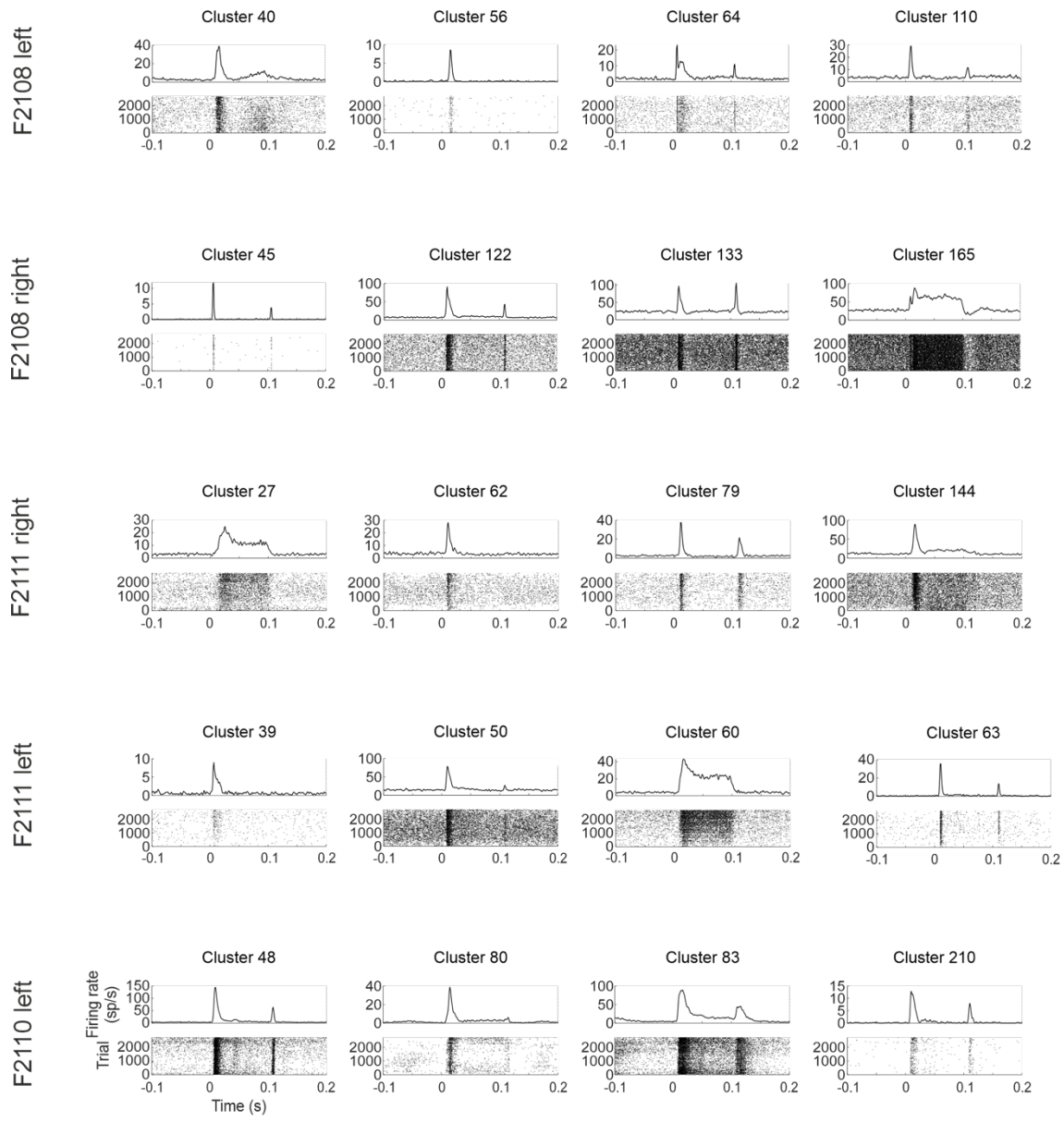

Supplementary Figure 4-3. Responses to pure tones under anaesthesia. Peristimulus time histograms (PSTHs) and corresponding raster plots are shown for clusters by animal and side recorded in the IC under anaesthesia in response to 100 ms pure tones presented from the loudspeaker located in front of the animal.

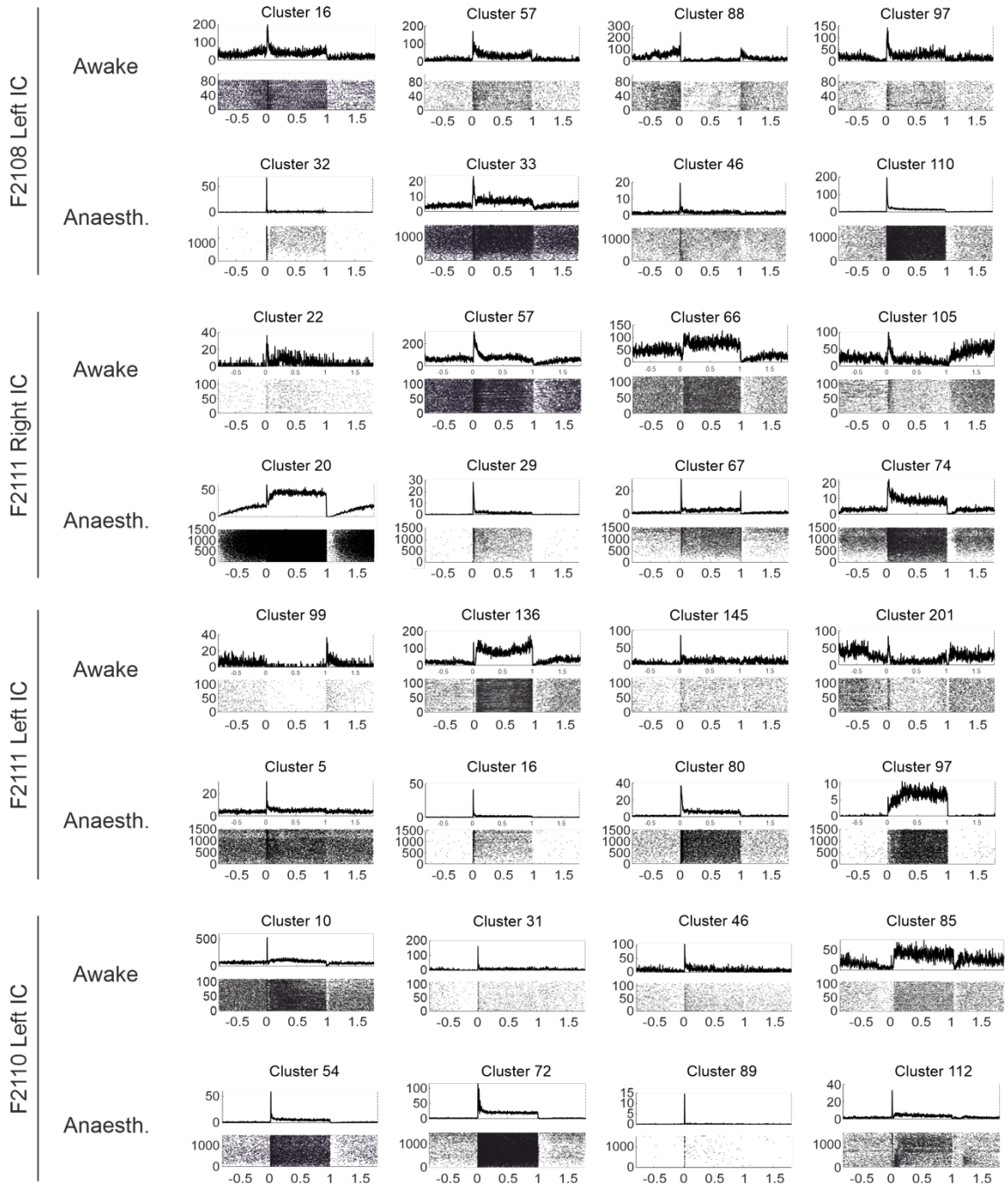

Supplementary Figure 4-4. Responses to broadband sounds under anaesthesia and in awake behaving animals. Example PSTHs and raster plots are shown for clusters grouped by animal and side recorded in the IC. In each group, the top row corresponds to recordings in awake behaving animals in response to 1000 ms broadband sounds and the bottom row corresponds to recordings performed under anaesthesia in response to the same stimuli. F2108 right IC was not recorded in anaesthetised conditions due to failure of the probe, therefore this probe is not included in the figure.

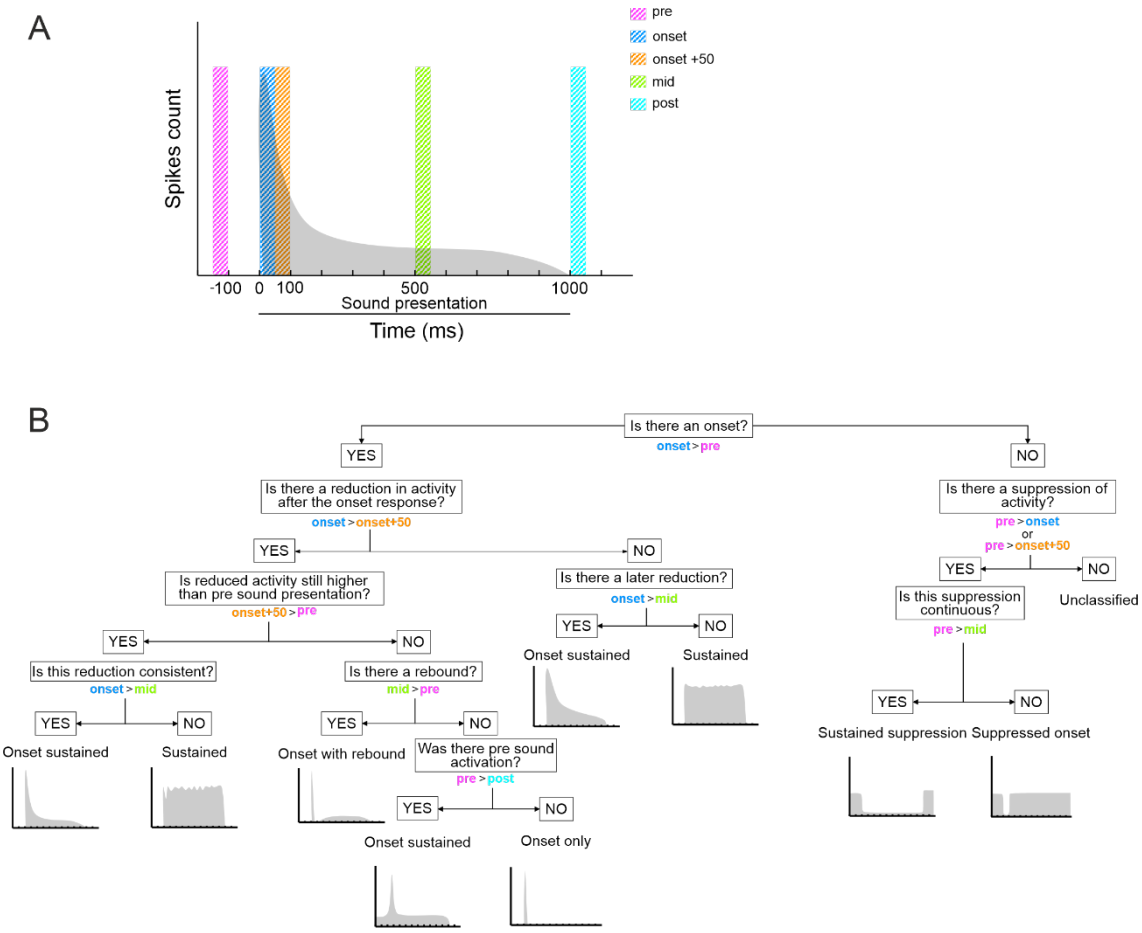

Supplementary Figure 4-5. Decision tree for classification of response types in the IC. (A). Representation of a dummy PSTH in which the periods of activity that were compared to characterise the different response types in the IC are marked using coloured bars. Five different 50ms periods were compared, one before sound presentation (pre), one after sound offset (post) and three at different type points during the stimulus presentation (onset, onset+50, mid). (B) Pipeline illustrating the comparisons between the periods of activity shown in A and the order in which they were made to classify clusters into six different response types: onset-sustained, sustained, onset with rebound, onset only, sustained suppression and suppressed onset. The number of spikes in each 50 ms period was compared using a t-test and it was determined to be significantly different when $p<0.05$. Moreover, firing rates were compared to determine the direction of the difference when this was significant. A dummy PSTH is shown at the bottom of each branch illustrating the appearance of the cluster's response classified as the indicated category.

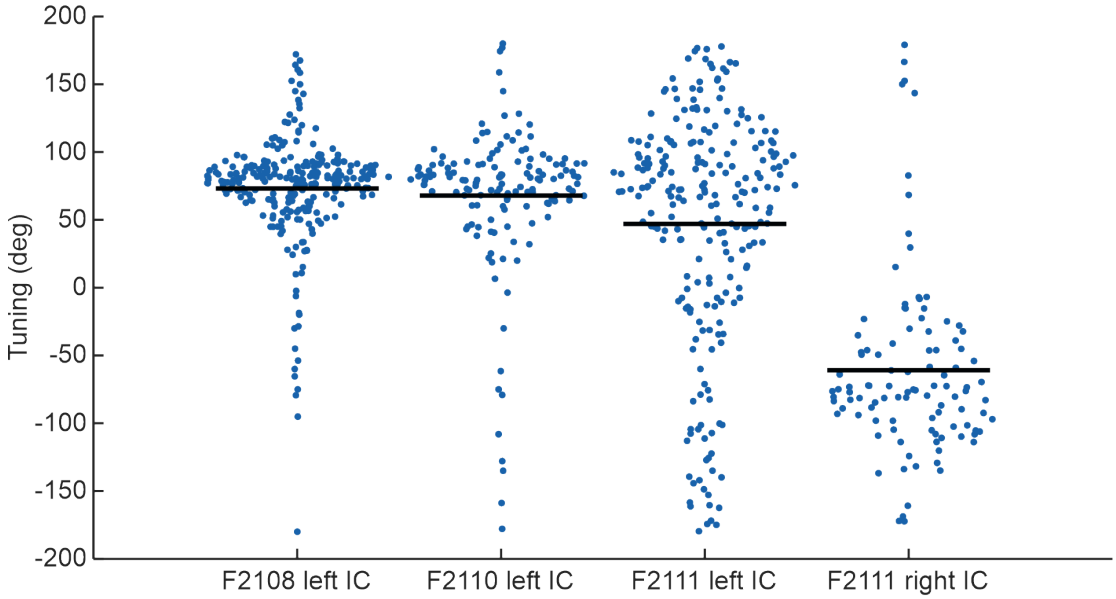

Supplementary Figure 4-6. Distribution of clusters according to their spatial preferences in anaesthetised conditions. The spatial preference for each cluster is defined as the centre of mass of the firing rates computed by sound location. All clusters were extracted from a single recording session for each animal and brain side performed under anaesthesia in response to 1000ms broadband bursts of sound. Each dot represents a cluster, and the black lines indicate the mean. F2108 right IC was not recorded in these conditions due to failure of the probe, therefore this probe is not included in the figure.

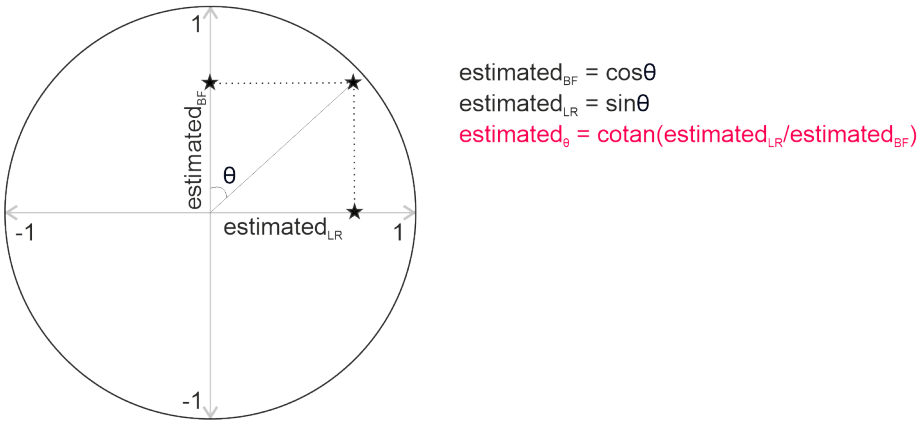

Supplementary Figure 4-7. Estimation of azimuth from back-front and left-right estimations. Using basic principles of trigonometry, the azimuth angle (Θ) is calculated using the cotangent function (cotan(y/x)) from the estimated left-right value (y = sine of Θ), and the estimated back-front value (x = cosine of Θ) given by the population pattern decoder.

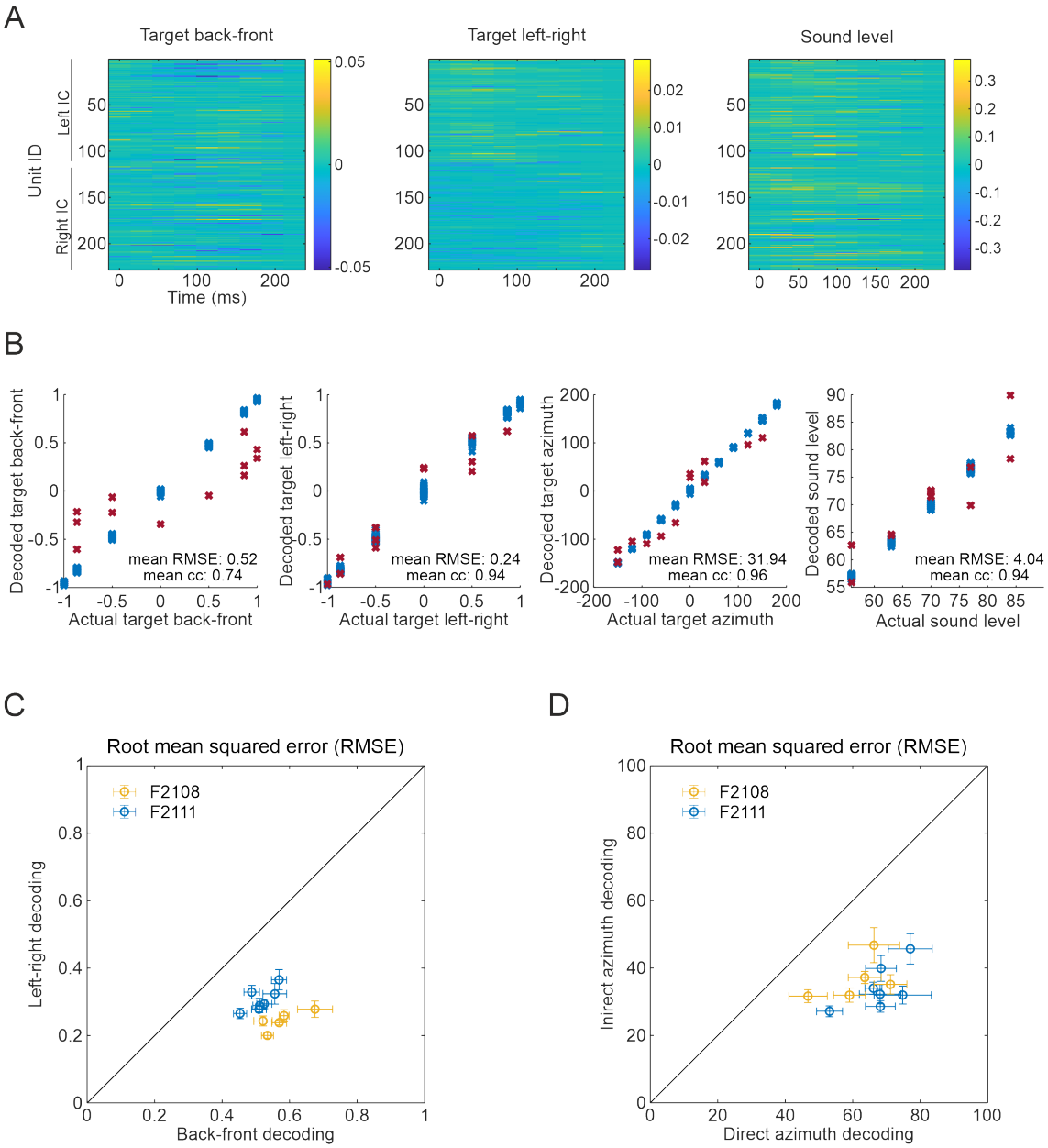

Supplementary Figure 4-8. Sound location decoding by a population pattern decoder from data recorded bilaterally in the IC with a reduced time window restricted to 200ms after sound onset where head movement was not present. (A) Kernels showing the weight of each recorded unit across time, indicating how informative each unit is about the decoded variable at each time bin. Weights are plotted over a 200 ms window from sound onset. Units were sorted by side (left IC – top half of each plot, right IC – bottom half). The weighting of units across time is plotted for the decoding of back-front location, left-right location, and sound intensity. For back-front decoding, yellow is indicative of 'front' and blue of 'back'; while for left-right decoding, yellow indicates 'right' and blue 'left'. Data used to train the model were obtained from the same

session of bilateral recordings in the IC in ferret F2108 as in Figure 4-8. (B) The values estimated by the decoder for each variable are plotted against the actual values. Results are plotted for back-front, left-right, azimuth (extracted from back-front and left-right decoding), and sound intensity decoding. Estimates are shown for the training set (blue) and the testing set (red) for an example fold. The mean correlation coefficient (cc) and root mean square error (RMSE) across folds are indicated at the bottom of each plot. The dataset used to train the model was the same as for panel A. (C) RMSE for back-front and left-right decoding in a 200ms window for different recording sessions in animals F2108 and F2111 (mean±SE, across folds). All values fall below the diagonal identity line indicating better decoding accuracy along the left-right axis. (D) RMSE for direct and indirect estimations of sound azimuth in a 200ms window in the same sessions as in C in animals F2108 and F2111 (mean±SE, across folds). For indirect sound azimuth decoding, the azimuth location was estimated from left-right and back-front decoding. For the 'direct' condition, the decoder was trained to directly decode the azimuthal location. All values fall below the diagonal identity line, indicating greater accuracy of indirect azimuth decoding.

5. Neural Correlates of Adaptation to Unilateral Conductive Hearing Loss in the Ferret

5.1. Introduction

One way to further understand how spatial information is encoded in the brain is to alter the spatial cues and examine how well decoding from neural responses can account for changes in the animals' behaviour. Unilateral conductive hearing loss (UCHL) experimentally induced by plugging one ear is a way to achieve this. This was the approach taken by Keating et al. (2015), who showed that the localisation errors predicted by decoding ILDs from A1 activity using an opponent coding model matched the behavioural performance of normal ferrets and those raised with one occluded ear.

In adulthood, adaptation to UCHL can be induced by training in a sound localisation task resulting in the partial recovery of spatial hearing. Thus, this model of auditory plasticity constitutes an ideal scenario to explore how the processing of auditory spatial information is altered when spatial cues are disrupted and how the encoding of sound location is affected by the adaptation process.

Two different processes have been suggested to underlie this adaptation: reweighting and remapping. The former refers to an upweighting of the unaltered spectral cues provided by the non-occluded ear during the computational integration of the different cues. The latter involves an adjustment of new localisation cues values to different locations in space. Studies in ferrets during development have provided evidence that both processes are used by these animals to adapt to UCHL (Keating et al., 2013; Keating et al., 2015). In adult humans, correlates of both processes have also been described (Keating et al., 2016), further demonstrating that they can co-occur in the same individual and are not mutually exclusive.

The neural substrates of auditory plasticity remain largely unknown but growing evidence points to the role of the IC under the influence of the AC in this process. Bilateral lesions of the AC have been shown to impair recalibration of sound localisation ability following UCHL (Nodal et al., 2010), indicating its importance in auditory plasticity. Further research has also demonstrated that not only the AC but also its projection to the IC is necessary for this recalibration (Bajo et al., 2010), pointing to the interaction of cortical and subcortical structures as the basis for auditory plasticity. The controlled optogenetic inactivation of the primary auditory cortex (A1) showed that it is necessary for learning, but indicated that learned information retrieval occurs independently of A1, suggesting that learning consolidation might be occurring somewhere else in the brain. Altogether, this evidence indicates that the IC is likely to play a key role in auditory plasticity as a centre for the consolidation of learning.

The IC is considered a mandatory synaptic station for ascending input containing auditory spatial information. But it is also the recipient of extensive descending projection from the AC, which has been implicated in auditory plasticity. The sensitivity and tuning

properties of IC neurons have been shown to be modulated by the AC, raising the possibility that the IC could be a centre for the consolidation of auditory plasticity under the influence of the AC. Evidence from developmental studies showing that the binaural response properties of IC neurons are altered by raising animals with altered spatial cues supports this idea (Gold & Knudsen, 2000b; Moore & Irvine, 1981; Popescu & Polley, 2010; Thornton et al., 2021). However, recordings in the IC are necessary to investigate whether any changes happen in this structure that are associated with and potentially responsible for adaptation to UCHL.

In this study, we chronically implanted ferrets with recording probes bilaterally in the IC and we recorded activity across weeks while animals were trained in a sound localisation task to induce adaptation to UCHL. This allowed us to explore the effects of monaurally plugging one ear on activity in the IC and investigate any neural correlates of sensory recalibration.

5.2. Results

5.2.1. Alteration of spatial cue processing following the onset of UCHL

Electrophysiological data were recorded from the IC of three ferrets (over 6 months old) while they were performing a sound localisation task. These were the same animals from which IC data were obtained under normal hearing conditions and reported in Chapter 4. Here, we explored the alterations in neural activity in the IC caused by a UCHL, which was experimentally induced by inserting an earplug in one ear. Moreover, we were able to track changes in neural processing while the animals adapted to this condition through training in the sound localisation task.

The central nucleus of the IC (CNIC) is a site for the convergence of auditory inputs encoding monaural spectral cues and binaural cues, necessary for localising sounds. The insertion of an earplug in one ear attenuates and delays the sound reaching the cochlea in that ear, which should cause a reduction of activity in the ipsilateral monaural neurons along the auditory brainstem, including the type IV units in the DCN, and an imbalance of the binaural inputs to neurons in the superior olivary complex. This imbalance will considerably alter the encoding of both binaural localisation cues. On the one hand, the encoding of ILDs in the LSO depends on the comparison of the monaural inputs from the two ears that are intensity (rate coded) dependent. On the other hand, in mammals, the encoding of ITDs is based on the temporally precise summation of inputs from both ears, which transforms the temporal code into a rate code (Brand et al., 2002).

As demonstrated in Chapter 4, the majority of neurons in the IC show a contralateral preference. This results from the integration of excitatory input from the contralateral LSO, inhibitory input from the ipsilateral LSO, excitatory input from ipsilateral MSO and excitatory input from the contralateral DCN, just to name the principal inputs carrying spatial information, although other ascending inputs from VNLL and DNLL are also integrated in the IC activity (see Chapter 1 for more details).

The LSO is a brainstem nucleus involved in the encoding of ILDs, which in turn receives excitatory input from the ipsilateral VCN and inhibitory input from the contralateral VCN, resulting in a subtractive computation of firing rates that reflects the differences in level between the sounds arriving at the two ears. Insertion of an earplug in one ear would be expected to reduce the excitatory input from the VCN in the hemisphere of the plugged ear to the ipsilateral LSO, while the inhibitory input from the contralateral VCN would be intact. The opposite should occur for the contralateral LSO. This would result in altered inputs from both LSOs arriving at each IC. It would be expected that the IC ipsilateral to the plugged ear would receive a reduced inhibitory input from the ipsilateral LSO and an increased excitatory input from the contralateral LSO, producing an overall increase in excitatory drive. On the contrary, the contralateral IC would be expected to receive a reduced contralateral excitation and an increased ipsilateral inhibition, resulting in an overall suppression of activity (Figure 5-1). These predictions were borne out in our recordings from the IC in ferrets (N=2) after the insertion of an earplug. We observed that activity in the IC contralateral to the plugged ear was suppressed overall in response to sound presentation. In contrast, responses in the IC ipsilateral to the plugged ear were enhanced (Figure 5-1). These results confirm the

expected alteration in neural processing produced at the onset of UCHL, which is associated with a disruption in the ability to localise sounds.

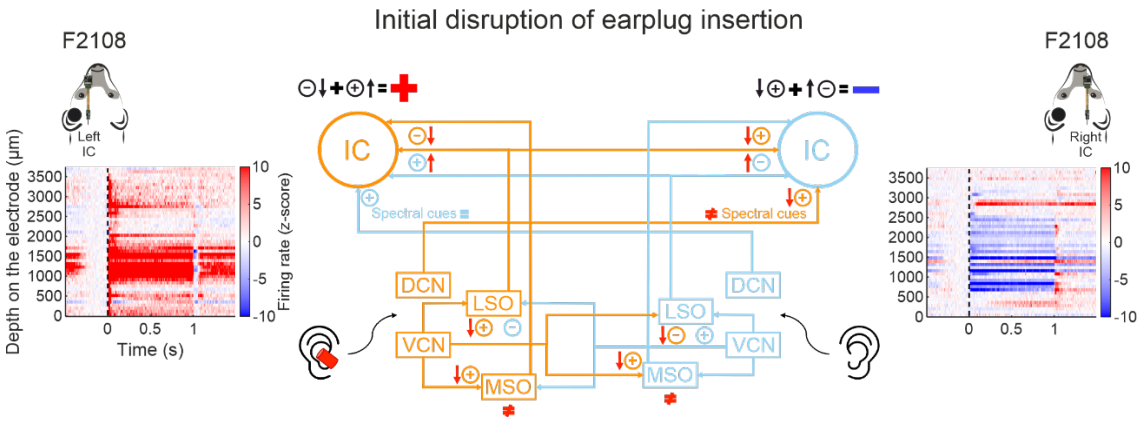

Figure 5-1. Alterations in neural processing derived from the insertion of an earplug. The central diagram shows the main ascending inputs to the inferior colliculus carrying information relevant for sound localisation and how their activity would be altered by unilaterally earplugging the left ear (+ excitatory connection, - inhibitory connections, arrows indicate expected changes in activity relative to normal hearing). The panels on the sides illustrate the overall firing activity (firing rate z-score) along the probes in the left and right inferior colliculus for ferret F2108, recorded following the insertion of an earplug in the left ear. Activity was recorded in response to 1000ms broadband sounds while performing a sound localisation task. Sound onset is indicated by the vertical dashed line.

5.2.2. Changes in response properties of neurons in the IC caused by UCHL

In normal hearing conditions, responses of neurons in the CNIC show a contralateral preference as determined by the centroid of firing rates versus sound location (Figure 5-2 preplug). The binaural imbalance produced by the earplug resulted in the loss of the

contralateral preference characteristic of the IC, which is shown by a displacement of the average centroid towards zero and an increase in the standard deviation (Figure 5-2 early plug). This is indicative of a more equal distribution of units showing ipsilateral and contralateral preference for each IC.

To fully characterise the changes in spatial sensitivity of units, in addition to changes in their preferred direction, it is necessary to consider the sharpness of their tuning computed as the equivalent rectangular receptive field (ERRF). The range of the units' ERRF did not change with the insertion of the earplug, however, we did observe an increase in the mean ERRF, suggesting that as a population, IC units became more broadly tuned because of the UCHL. These changes in the preferred direction towards zero and reduced sharpness of tuning associated with the insertion of an earplug were most pronounced in cases F2108 and F2110 (Figure 5-2), which showed the clearest contralateral preference before the insertion of the earplug (Chapter 4). For animal F2111, which exhibited less overall contralateral preference, the magnitudes of the changes were not so pronounced (Figure 5-2). In this animal, as reported in Chapter 4 Section 4.2.4., in contrast to the other ferrets, the right IC did not present a clear contralateral preference in normal hearing conditions, instead showing a similar proportion of units with contralateral and ipsilateral tuning. Moreover, the left IC, although still having a clear contralateral preference, included a greater proportion of ipsilaterally tuned units than in the other animals (% of ipsilateral units in the left IC F2111: 23.39%, F2110: 8.29%, F2108: 11.60%). Following the insertion of an earplug in the ear ipsilateral to the relative IC, the change in average centroid and ERRF was very limited and in the case of the right IC, it was in the opposite direction to that observed in the other cases (Figure 5.2).

Despite the reduced effect of earplugging on these two descriptive variables of neural responses in the IC of ferret F2111, the induction of UCHL greatly disrupted the ability of this animal to localise sound, just as did in the other two ferrets. This is shown by the reduction in the percentage of correct responses relative to normal hearing conditions (Figure 5-2). Assuming that the recorded units were located in roughly equivalent regions of the IC, this indicates that the impairment in localisation caused by a UCHL cannot be simply explained by the mean changes observed in their preferred direction and sharpness of tuning. This suggests that sound localisation accuracy cannot be inferred – at least in the IC – from a simple change in the units' tuning properties.

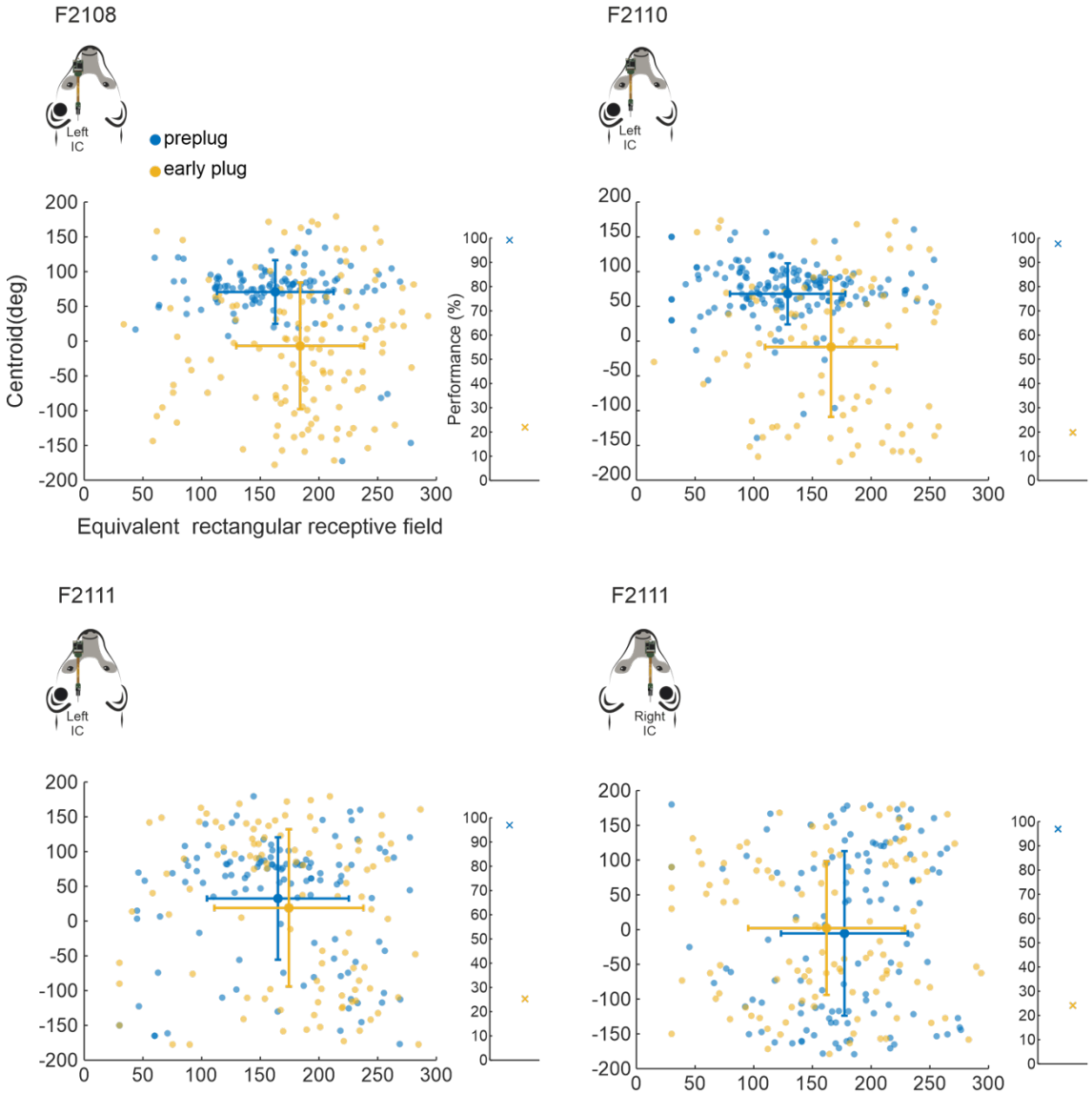

Figure 5-2. Changes in spatial tuning following insertion of an earplug. Each panel shows data recorded from a the IC ipsilateral to the side of the plugged ear in one animal during sound localisation testing. The scatter plot shows the centroid of spatial tuning, computed as the centroid of the firing rates versus sound location; and the sharpness of the tuning, computed as the ERRF. Data are plotted for an example session prior to earplug insertion ('preplug', blue) and for an example session at the initial stage of the earplugging period ('early plug', yellow). Dots represent individual units recorded in that session and the crosses correspond to the mean and standard deviations. The behavioural performance (% correct) of the animal in the corresponding sessions is indicated in the plots located to the right of each scatter plot (all trials included). The diagrams of the

ferret head indicate the animal ID, the side of the brain from which the recordings were made and the ear that was plugged.

5.2.3. Neural activity in the IC during adaptation to a monaural earplug

Training in a sound localisation task progressively induces adaptation to UCHL, as evidenced by the improvement in the task performance (see Chapter 3 Section 3.2.2.). Ferrets with chronically-implanted probes in the IC were trained to localise broadband noise bursts in a silent background (Chapter 2 Section 2.3.2.) after the insertion of an earplug on one side with the aim of inducing such adaptation. In addition, we recorded neural data in the IC during training sessions to track changes in neural activity associated with this plasticity.

Despite undergoing surgery to implant the recording probes, which caused some damage in the tissue, and the animals being tethered during the behavioral task, implanted ferrets adapted within the range of non-implanted ferrets, although their percentage scores were closer to the lower limit of this range (Figure 5-3).

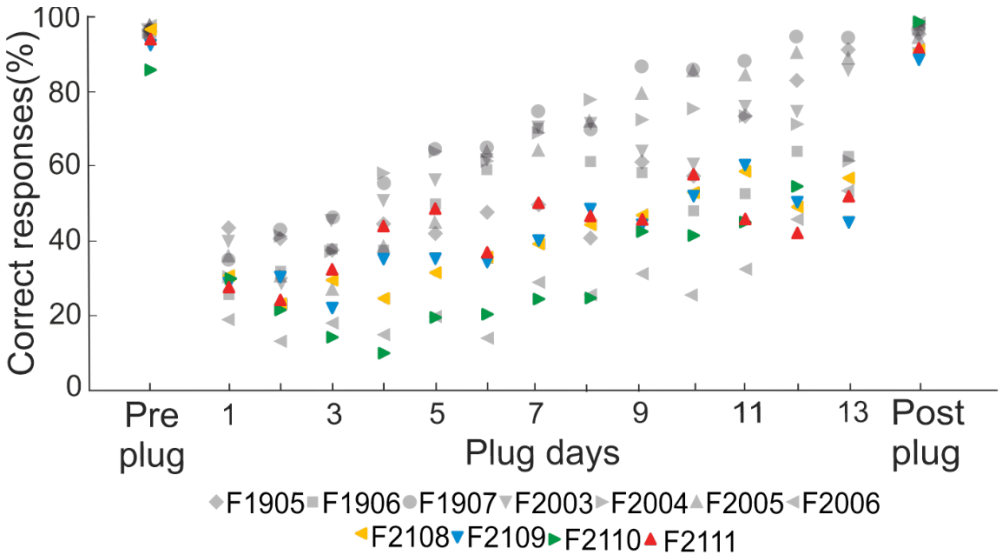

Figure 5-3. Adaptation of implanted ferrets to a UCHL. Performance is shown as percentage correct scores before the insertion of the earplug in the left ear (pre plug), for each of 13 days on which the animals were tested while wearing an earplug in the left ear, and after earplug removal (post plug). Only the first 13 days are shown but animals were tested for longer. Animals with probe implants are represented by the coloured symbols. Grey symbols indicate the performance of animals trained in the same conditions without head implants (data from Chapter 3 Section 3.2.2.).

To explore whether any neural correlates of adaptation to UCHL are found in the IC, we qualitatively compared neural responses across sessions using three main features: sound-evoked firing rate, the preferred direction of tuning determined by the centroid, and the sharpening of turning determined by the ERRF. Plugging the left ear resulted in a significant suppression of activity in the contralateral IC, indicated by the decrease in the normalised evoked firing rate compared to that measured prior to earplug insertion (e.g., case F2108, Kruskal-Wallis chi-squared = 154.92, df = 5, $p < 0.001$) (Figure 5-4). In the ipsilateral IC, no overall change of evoked activity was observed after earplug insertion

relative to normal hearing conditions (in the same example case, F2108, Kruskal-Wallis chi-squared = 3.2798, df = 5, p = 0.65).

The improvement in behavioural performance with training was not matched by a recovery of the overall evoked firing rate, with the contralateral IC remaining mainly suppressed (F2108, Kruskal-Wallis chi-squared = 154.92, df = 5, p < 0.001, pairwise comparisons preplug vs plug sessions p < 0.001) (Figure 5-4).

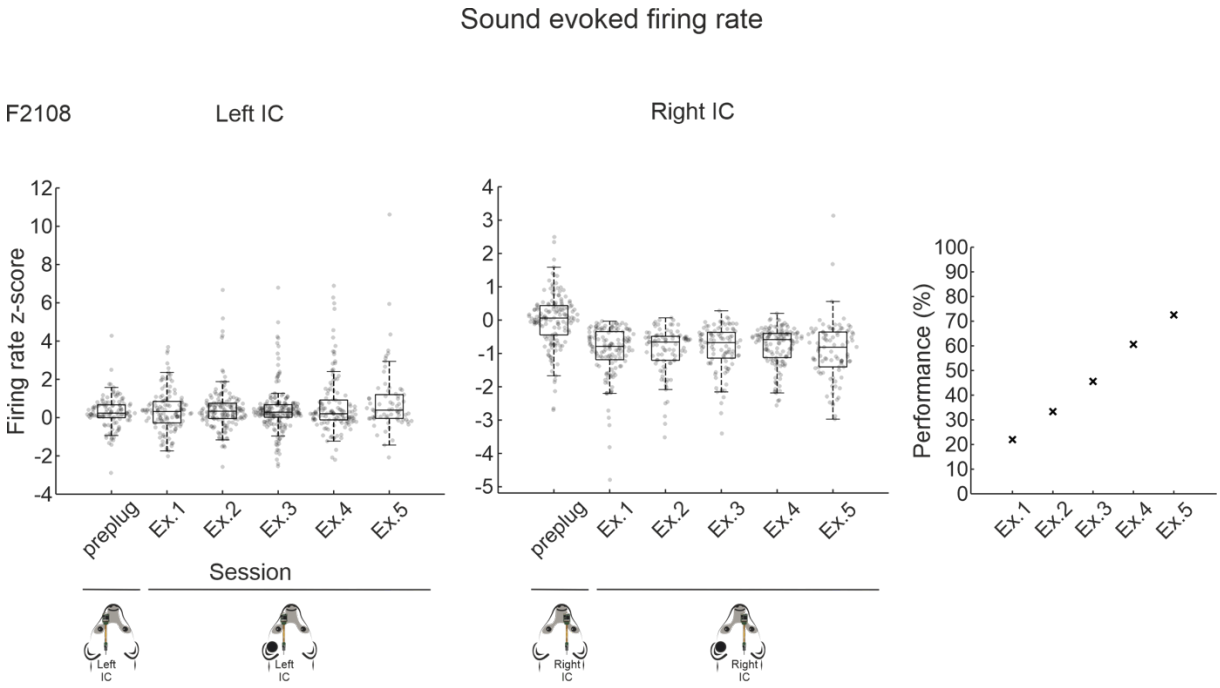

Figure 5-4. Evoked firing rate during adaptation to UCHL. (A) Normalised firing rate is shown for units recorded in the left IC of example animal F2108. Firing rate was extracted from a 50ms window following the onset of a sound presentation and recordings were performed in response to self-initiated 1000-ms broadband noise bursts while the animal carried out a sound localisation task. The distribution of firing rates across the recorded neurons is shown for different sessions throughout the adaptation period: prior to earplug insertion (preplug) and five example sessions going from early to late during the earplugging period, which lasted for 2 weeks. The exemplar sessions were chosen according to their behavioural performance, shown in the left panel, to cover the range of

adaptation. Grey dots correspond to individual clusters recorded in each session. The overlaid boxplots indicate the median (central line) and the 25th and 75th percentiles (bottom and top edges of the box). (B) As in A, but for the right IC. (C) Behavioural performance indicated as percentage correct scores for the sessions represented in A and B. All trials were included.

Because training-dependent recovery of behavioural performance after insertion of an earplug is a gradual process, we compared the spatial tuning of units recorded during an early-plug session and a late-plug session corresponding to the session in which the most accurate localisation behaviour was reached while wearing an earplug. In cases F2108 and F2111, the best late-plug session was taken from a second period of left earplugging, since this is where the highest percentage correct scores were reached. Because evoked activity in the IC contralateral to the plugged ear was suppressed, we could only estimate the spatial sensitivity for ipsilateral IC units. A consistent reduction in the mean ERRF was observed for all animals in the late session relative to the early earplug session (averaged across animals, early plug ERRF Q1 = 132.22º, median = 181.88º, Q3 = 218.65º; late plug ERRF Q1 = 111.91º, median = 172.24º, Q3 = 212.51º), showing a shift towards pre plug values. This reduction was significant (Wilcoxon signed-rank test W = 106550, p = 0.03), but it has to be noted that there was considerable overlap in the ERRF distributions between the two sessions (Figure 5-5).

Given the sustained suppression of activity in the contralateral IC, it appears that the behavioural improvement is primarily associated with modest, but significant, changes in spatial sensitivity in the IC ipsilateral to the plugged ear. It is worth noting that this IC primarily represents locations on the animal's right (the side of the open ear)

where most of the behavioural improvement occurs during the early stages of monaural occlusion.

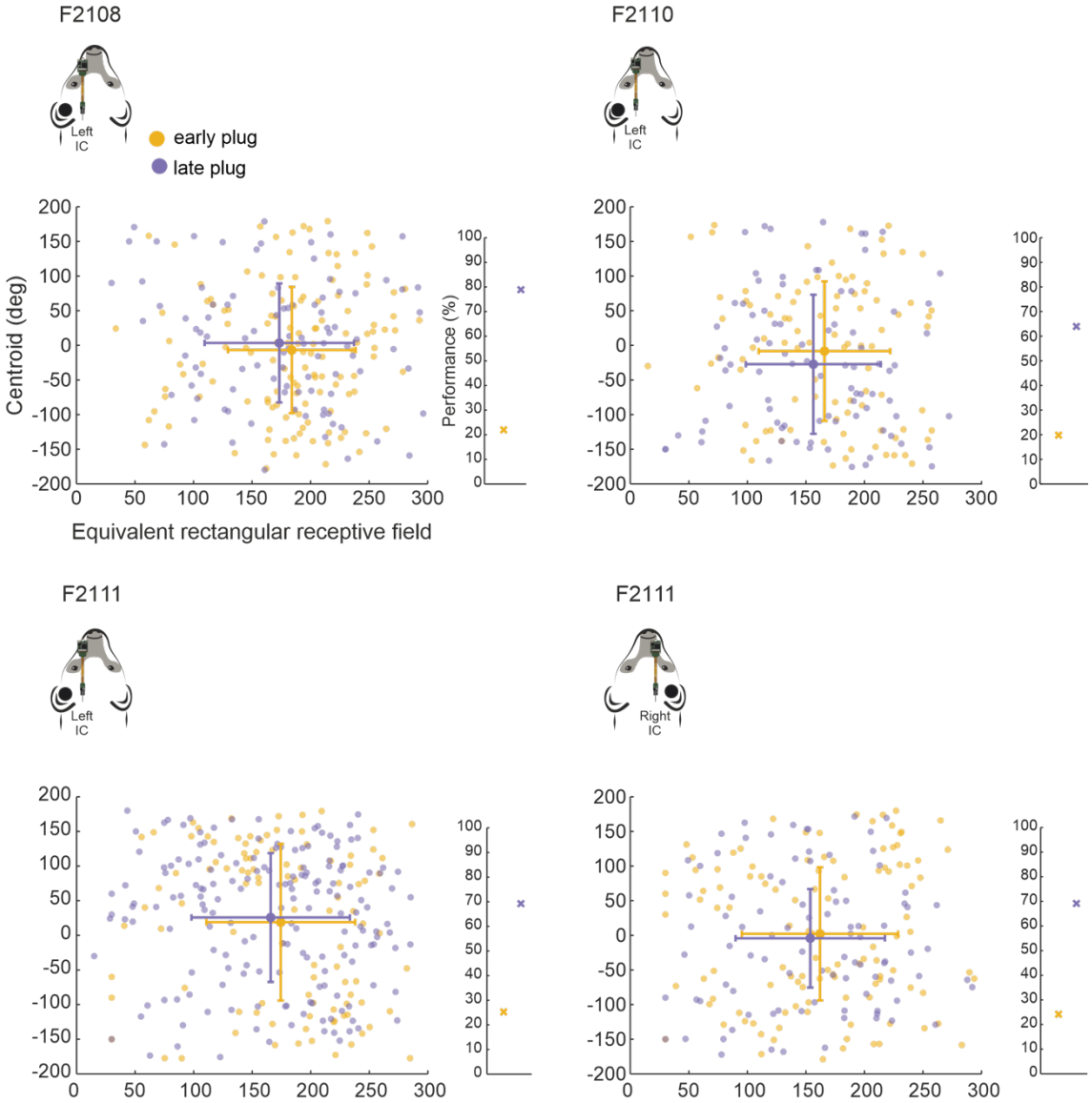

Figure 5-5. Changes in spatial tuning between early and late earplug sessions. Each panel shows data recorded from the IC ipsilateral to the side of the plugged ear in one animal during sound localisation testing. The scatter plot shows the centroid of spatial tuning, computed as the centroid of the firing rates versus sound location; and the sharpness of the tuning, computed as the ERRF. Data are plotted for an example session at the initial stage of the earplugging period ('early plug', yellow) and for the session with the best behavioural performance ('late plug', purple) achieved with the earplug in place (for F2108 and F2111 (left plug), sessions with best behavioural performance were taken from the end of a second period of earplugging). Dots represent individual units recorded

in each session and the crosses correspond to the mean and standard deviations. The behavioural performance (% correct) of the animal in the corresponding sessions is indicated in the plots located to the right of each scatter plot (all trials included). The diagrams of the ferret head indicate the animal ID, the side of the brain from which the recordings were made and the ear that was plugged.

5.2.4. Re-plugging and memory trace

Training-induced adaptation to UCHL leaves a memory trace. Previous studies (Bajo et al.,2019; Kacelnik et al., 2006) and the present work (Chapter 3) have shown that reinserting an earplug in the same ear after the first period of earplug adaptation produces a smaller drop in sound localisation accuracy, suggesting that the initial training-induced plasticity achieved leaves a memory trace that can be retrieved at the onset of a second period of UCHL. This memory trace is ear selective as only re-plugging the same ear leads to such an effect whereas plugging the other ear ("reverse occlusion") does not.

Here we explored whether the spatial sensitivity changes observed in the IC after the insertion of an earplug varied because of previous earplug experience by comparing the changes induced between two periods of earplugging in the same ear. In two of the animals, F2108 and F2111, the reinsertion of an earplug in the same ear following a first period of adaptation in the left ear resulted in a smaller decline in localisation accuracy, as expected (Figure 5-6). The same loss of contralateral preference was observed at the start of this second period of left earplugging (Wilcoxon signed-rank test $W = 44152$, $p = 0.56$) when compared to preplug spatial tuning (Figure 5-6 A, B). However, the ERRF was less affected in the second period of earplugging compared to the first (across animals, ERRF early plug 1 Q1 = 145.95°, median = 187.36°, Q3 = 223.21°; ERRF early

plug 2 Q1 = 103.51°, median = 169.55°, Q3 = 221.84°) (Wilcoxon signed-rank test W = 48205, p = 0.0078) (Figure 5-6 A, B). This sharper spatial tuning measured at the start of the second period of left earplugging may partially explain the smaller decrease in sound localisation accuracy, possibly by contributing to improved population encoding of sound source location than in the first earplugging period.

The normalised sound-evoked firing rates revealed an increase in the dispersion of firing rates during the second period of earplugging in the IC ipsilateral to the plugged ear in ferret F2108, although no significant difference was found among the selected sessions (Kruskal-Wallis chi-squared = 0.80541, df = 3, p = 0.85) (Figure 5-6 C). On the contralateral side, evoked activity was overall suppressed throughout the first and second earplugging periods in animal F2108, but the mean firing rate was significantly higher in the first session of the second earplugging period than in the first session of the first earplugging period (Figure 5-6 D). In animal F2111, a significant difference in the distribution of firing rates was observed between preplug and second earplugging sessions in the IC ipsilateral to the plugged ear (Kruskal-Wallis chi-squared = 10.158, df = 3, p = 0.0178) (Figure 5-6 E). Interestingly, as in F2108, the suppression of IC activity on the contralateral side was significantly reduced at the start of the second period of earplugging relative to the early first earplugging period (Kruskal-Wallis chi-squared = 11.71, df = 3, p = 0.008) (Figure 5-6 F). This suggests that there might be some compensation for the binaural imbalance as a result of the animals' previous earplugging experience, which may also contribute to the smaller initial deficit in localisation accuracy seen in the behavioural data obtained at the start of the second period of monaural occlusion.

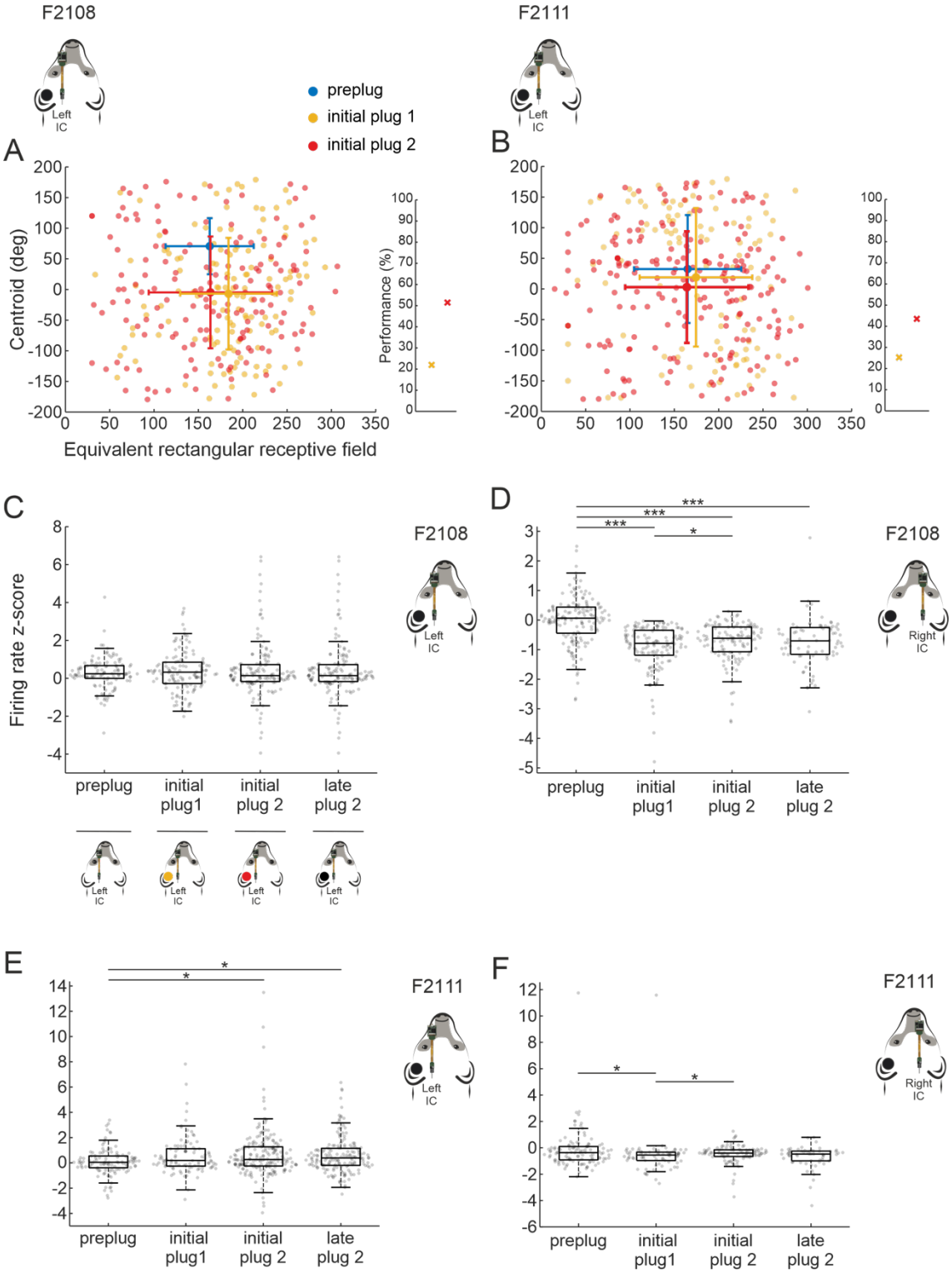
F2108
F2111
preplug
initial plug 1
initial plug 2
Left IC
A
B
Centroid (deg)
Performance (%)
Equivalent rectangular receptive field
C
D
Firing rate z-score
preplug
initial plug1
initial plug 2
late plug 2
Right IC
E
F

Figure 5-6. Differences in IC response properties between two consecutive periods of earplugging. (A) Scatter plot showing the centroid of spatial tuning, computed as the centroid of the firing rates versus sound location; and the sharpening of the tuning, computed as the ERRF, of units recorded in the inferior colliculus ipsilateral to the plugged ear in animal F2108. Individual dots correspond to units from two different earplugging sessions. Data are illustrated for a session from the initial stage of the first earplugging period (initial plug 1 – yellow) and for a session from the initial stage of the second period of earplugging (initial plug 2 – red). Crosses indicate the mean and standard deviations. As a reference, mean and standard deviations are also plotted for a session prior to the first earplugging period (preplug – blue). The behavioural performance (% correct score across all loudspeaker locations) of this animal for the initial plug 1 and 2 sessions is shown in the plot to the right of each scatter plot (all trials included). The diagram of the ferret head shows the animal ID, that recordings were performed in the left IC, and that the left ear was plugged in both periods of earplugging. (B) Same as in A but for animal F2111. (C) Normalised evoked firing rate recorded from the left IC of animal F2108 in response to self-initiated 1000 ms broadband noise bursts while performing the sound localisation task. The firing rate was computed for a 50-ms window from the sound onset. Data are presented for a preplug session, initial sessions in the first and second earplugging periods (also shown in A), and a session at the end of the second earplugging period. Grey dots correspond to individual units recorded in each session. The boxplots indicate the median (central line) and the 25th and 75th percentiles (bottom and top edges of the box, respectively). (D) Normalised firing rate for the same sessions as in C but for recorded in the right IC, contralateral to the side of the plugged ear, of ferret F2108. (E, F) As in C and D, respectively, but for animal F2111. (* $p<0.05$, *** $p<0.001$)**.**

5.2.5. Recovery of contralateral preference following earplug removal

As we reported in the previous sections, monaural insertion of an earplug causes units in the IC to lose their contralateral preference due to the imbalance in inputs between the ears. This partially recovers as the animals' localisation accuracy improves with training (see Figure 5-7 for units in the IC of animal F2108 for early and late plugging sessions), but not to the extent that would appear to be required to account for the improvement in behaviour. If a full remapping of binaural cues was to be implemented at the level of the

IC, one might expect the neurons found there to show quasi-normal spatial properties despite the persistence of the altered spatial cues. That this is not the case suggests that additional plasticity, perhaps beyond the IC, is necessary.

Removal of the earplug resulted in a recovery of sound localisation performance close to preplug levels, indicating a lack of any after-effect (Figure 5-7). Moreover, electrophysiologically we observed a recovery of the contralateral preference in both hemispheres as a consequence of reinstating balanced inputs at each ear (Figure 5-7, postplug).

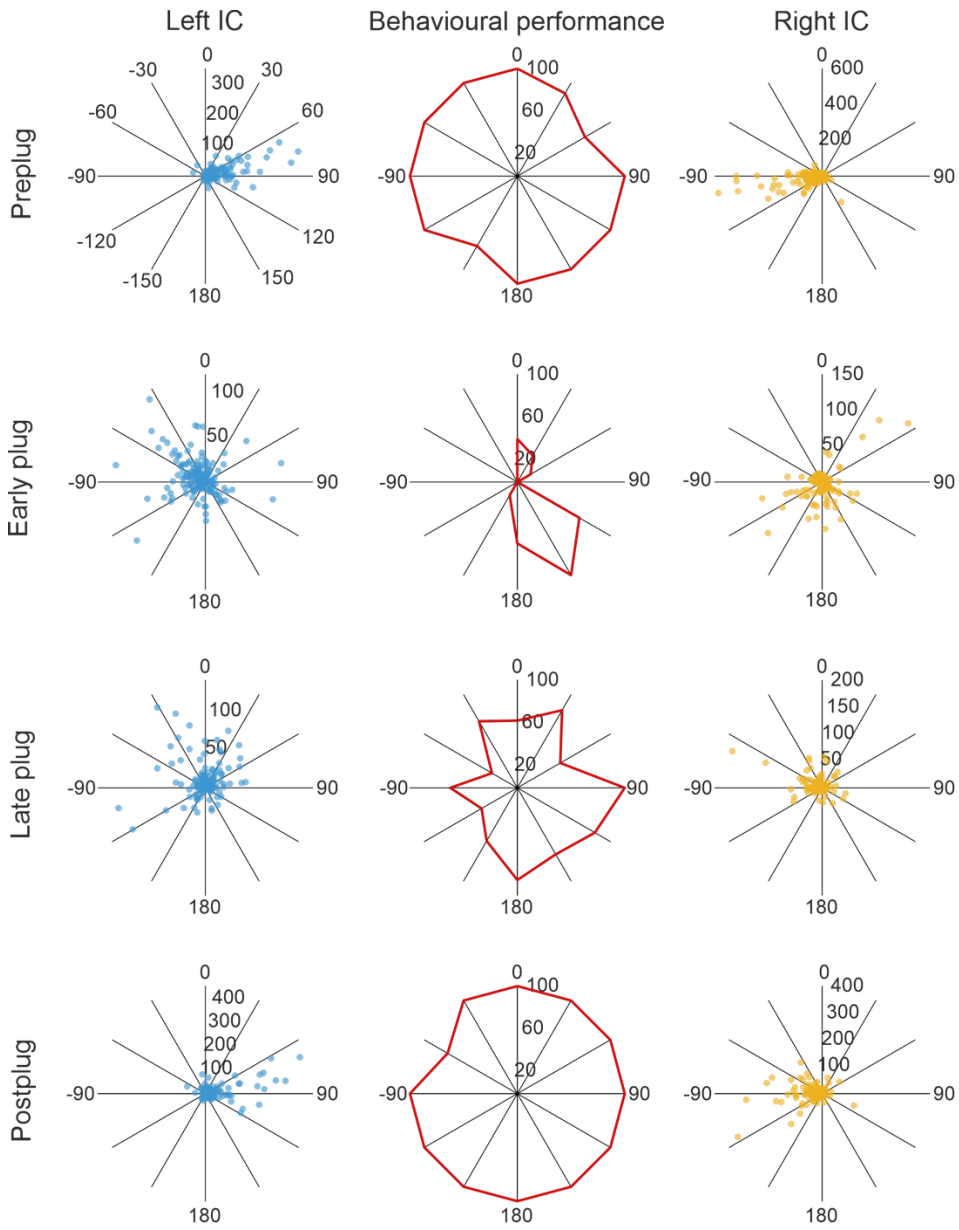

Figure 5-7. Changes in animal behaviour and spatial preferences in the inferior colliculus during adaptation to UCHL. Each polar plot in the left column illustrates the mean centroid of clusters from an example recording session in the left IC of animal F2108. The middle column shows the behavioural performance (percentage correct score) per location at different stages of adaptation. In the right column, as in the left, polar plots show the mean centroid for IC clusters, this time recorded in the right hemisphere of animal F2108. Each row of polar plots corresponds to a different stage in the adaptation to UCHL: (1) session prior to earplug insertion (2) initial disruption due to UCHL induced by plugging the left ear (3) session in the late stage of adaptation to UCHL, and (4) session after earplug removal.

5.2.6. Neural correlates of adaptation using population decoding analysis

We used population decoding analysis to further explore how the representation of sound source location in the IC changed with UCHL and whether any neural correlates of adaptation could be observed. We trained the population pattern decoder described in Chapter 4 using the data collected in the IC of ferrets while they adapted to UCHL. The population pattern decoder was trained with spiking data collected for all sound presentations during a session, including correction and easy trials, in which the sound was presented from the same location repeatedly. To avoid any bias in the training of the decoder, we randomised the trial order. In normal hearing conditions, correction and easy trials were rare since animals achieved almost perfect accuracy in the task. Thus, the randomisation of trial order in this condition did not make a great difference to the performance of the decoder, as indicated by the error values falling close to the identity line when decoding performance was compared with and without randomisation (Supplementary Figure 5-1, Normal Hearing, left panel).

With the onset of UCHL and the consequent drop in the animals' performance, correction and easy trials became more common. In this condition, trial randomisation consistently improved the performance of the decoder, as shown by the error values mainly falling on the 'not randomised' side of the identity line in Supplementary Figure 5-1 (Hearing Loss, left panel), which indicates a greater decoding error. For reproducibility, in all analyses, the trial order was randomised regardless of the hearing condition. Similarly, to avoid bias towards a particular hemifield, when the decoder was

trained with data combined from both hemispheres, the number of units from each side was equalised. However, the decoding accuracy was very similar with and without equalisation, both in normal hearing condition and after UCHL (Supplementary Figure 5-1).

The onset of UCHL disrupted activity in the IC, as described in previous sections, and altered the capacity of the population pattern decoder to estimate sound source location. Both back-front and left-right decoding were degraded when UCHL was experienced (Figure 5-8 A), relative to normal hearing conditions (Figure 4-8 B). Consequently, azimuth location decoding, estimated from those two approximations, was degraded too. Inspection of units' weights across time did not show any clear temporal structure for the location, back-front or left-right variables (Figure 5-8 B), contrary to what was observed in normal hearing conditions, especially for left-right (Figure 4-8 A). Therefore, the increased weights described at the onset of the stimulus in the decoding of left-right location in normal hearing conditions (Chapter 4 Section 4.2.5.) were not present when UCHL was induced, indicating that the onset of the stimulus was no longer informative about sound source location in the left-right axis. This is further illustrated by the absence of a peak in the sum of absolute weights during UCHL relative to normal hearing (Figure 5-8 B). However, some temporal structure was still observed for the decoding of sound level.

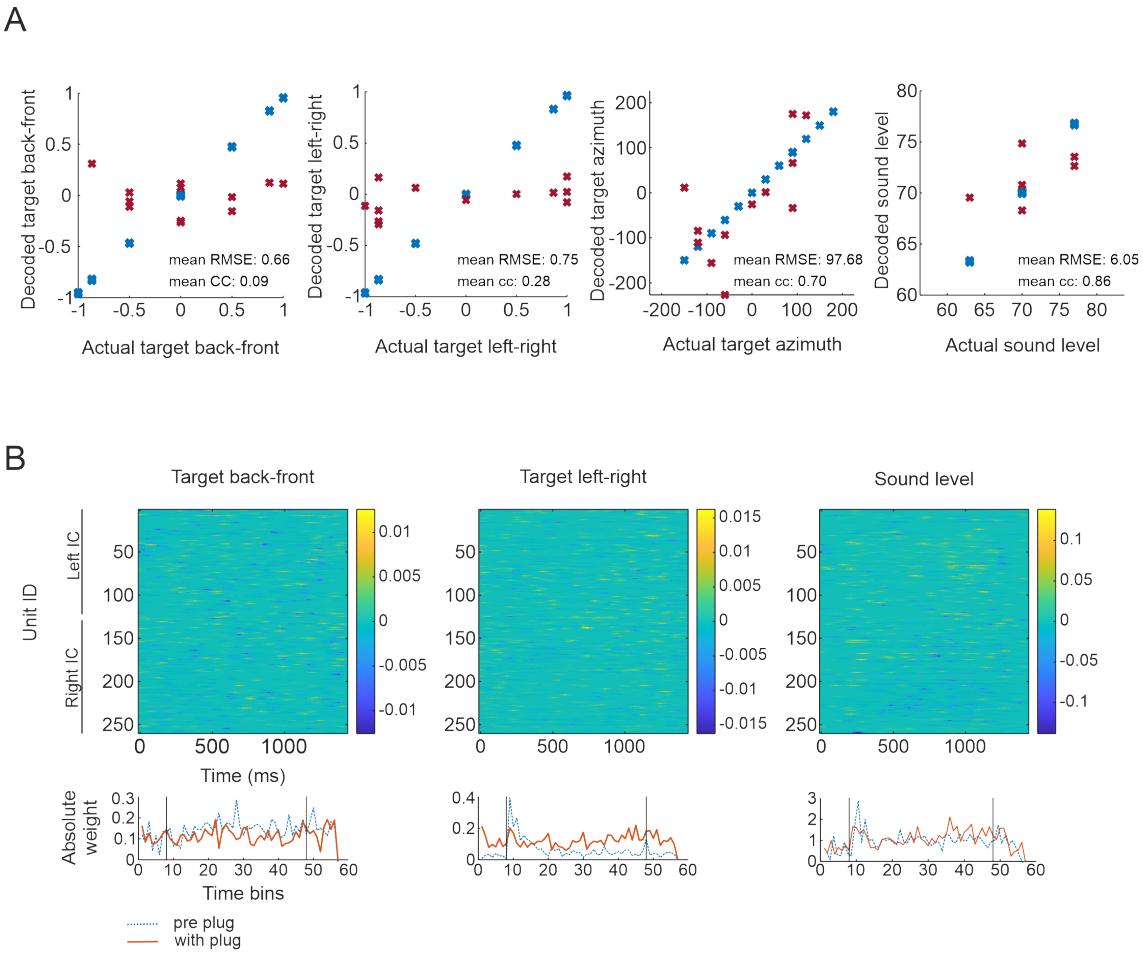

Figure 5-8. Pattern decoder accuracy on the first day of earplugging. (A) Estimated values for four parameters are plotted against the actual values for the training set (blue) and testing set (red) for an example fold. The four different variables plotted from left to right are back-front, left-right, azimuth and sound level decoding. The mean correlation coefficient (cc) and root mean square error (RMSE) are indicated at the bottom of each plot. The output was obtained from training a pattern decoder with data recorded bilaterally in the IC of an example ferret F2108 while it was awake and engaged in a sound localisation task in the first session after the insertion of an earplug in the left ear. The dataset consisted of spiking activity from IC units for 1400-ms windows encompassing the 1000-ms duration noise bursts plus 200ms before and after this for each sound presentation. (B) Kernels indicating the weight of each IC unit across time are plotted for a 1400-ms window binned in 25-ms bins. Weights (colours) indicate how informative each unit is about the decoded variable. Kernels are shown for three variables, from left to right: back-front, left-right, and sound level decoding. Data to produce the kernels were the same as for panel A. The sum of the absolute weights is plotted for each kernel (solid orange line). For comparison, the summed absolute weights are plotted for the decoding output of a session before the insertion of the earplug (dotted blue line, same as Figure 4-8 A).

To explore whether any changes in the encoding of sound source location occurred in the IC as animals adapted to UCHL with training, we trained the population pattern decoder independently from each behavioural session, i.e. with no information about previous or subsequent sessions. Therefore, a reduction in the decoding error as the sessions progressed would be indicative of the population becoming more informative about sound source location. In two out of the three tested ferrets [(F2108 (Left plug 1) and F2110 (Left plug)], we observed a reduction in the decoding error with the progression of sessions. No significant change was found in animal F2111 (Left plug and Right Plug), as indicated by fitted regression lines (Table 5-1).

Table 5-1. Parameters of the fitted regression lines for decoding accuracy across training sessions with an earplug.

	y = a + bx				
	R^2	**A (intercept)**	**b (slope)**	**p_b**	**tStat (b)**
F2108 Left plug 1	0.279	79.972	-0.54416	0.00113	$t_{(30)}$= -3.6019
F2108 Left plug 2	-0.0628	68.355	-0.079963	0.819	$t_{(15)}$= -0.23236
F2110 Left plug	0.367	74.198	-0.51153	0.00018319	$t_{(29)}$= -4.2859
F2111 Left plug	0.0459	49.82	-0.39741	0.14151	$t_{(26)}$= -1.5163
F2111 Right plug	-0.0405	62.578	-0.11859	0.708	$t_{(21)}$= -0.3799

A significant reduction in the azimuth decoding error across sessions during adaptation to UCHL was observed in animal F2108 during the first period of earplugging in the left ear (Table 5-1, Figure 5-9 A right panel). This improvement was primarily explained by a reduction in the decoding error of location in the left-right axis (Figure 5-9 A, middle panel), whereas no change was observed for decoding the back-front axis (Figure 5-9 A, left panel). Thus, this trend was indicative of neural changes in the IC that made the population activity more informative about sound source location in the left-right axis, which could be related to a recalibration/remapping process associated with adaptation to UCHL. Importantly, adaptation to UCHL is accompanied by an improvement in head-orienting accuracy. Therefore, to explore whether the improvement observed in decoding accuracy is due to the effect of changes in the acoustic cues on IC activity as the direction of the head relative to the sound source changes, we performed the same analysis restricting the training of the decoder to a 200ms window from sound onset. However, we observed a similar improvement in decoding accuracy when only a shorter time window was considered (Supplementary Figure 5-2 A), in which head movement is not present, highlighting the importance of the initial part of the stimulus. Nevertheless, we cannot rule out the possible contribution of dynamic cues provided by the head movement to the adaptation process. In fact, decoding performance over the first 200 ms was not as good as when the full stimulus duration was considered, which is further supported by the model weights not being zero after the initial 200 ms period. This is consistent with the finding that normal-hearing ferrets show an improvement in sound localisation approach-to-target accuracy with increasing stimulus duration without any changes in the head orienting response (Nodal et al., 2008). Together, these decoding results are

indicative of progressive changes in the IC responses during training-induced adaptation (Supplementary Figure 5-2 A).

To explore the underlying basis for this improvement, we compared the sum of units' absolute decoding weight across time in early and late training sessions. For the last five sessions in this earplug period, the sound duration was increased from 1000ms to 2000ms to maximise further improvement in the performance of the animal. Thus, for comparability, the change in weight sum across time was compared between the average of the last three sessions in which 1000-ms noise bursts were presented and the average of the first three sessions. We found an increase in the absolute weight in left-right decoding at the onset of the stimulus in these late earplugging sessions relative to early earplugging sessions, while no clear change was observed in the temporal structure of back-front decoding (Figure 5-9 B). This indicates that, with training, spiking activity in the IC at the onset of the stimulus became more informative about sound location in the left-right axis, resembling what we found for normal hearing conditions (Chapter 4 Section 4.2.5.) and indicating that changes in neural activity in the IC may be associated with adaptation to UCHL. This increase in the absolute weight was accompanied by a partial reappearance of the bimodal distribution of weights [(positive (yellow) and negative (blue)] by hemisphere observed in pre-plug conditions (Supplementary Figure 5-2 B), with an increase in negative weights in the right IC in the late plugging stage, which was absent after first inserting the earplug. When the sum of weights was explored separately for the right and left IC, the increase in weight at the stimulus onset was found for both hemispheres, although it was also more prominent for the right IC, contralateral to the plugged ear (Figure 5-9 B, right panel). This is the region of space where sound

localisation accuracy recovers during the later stages of the earplugging period (Chapter 3 Section 3.2.2.).

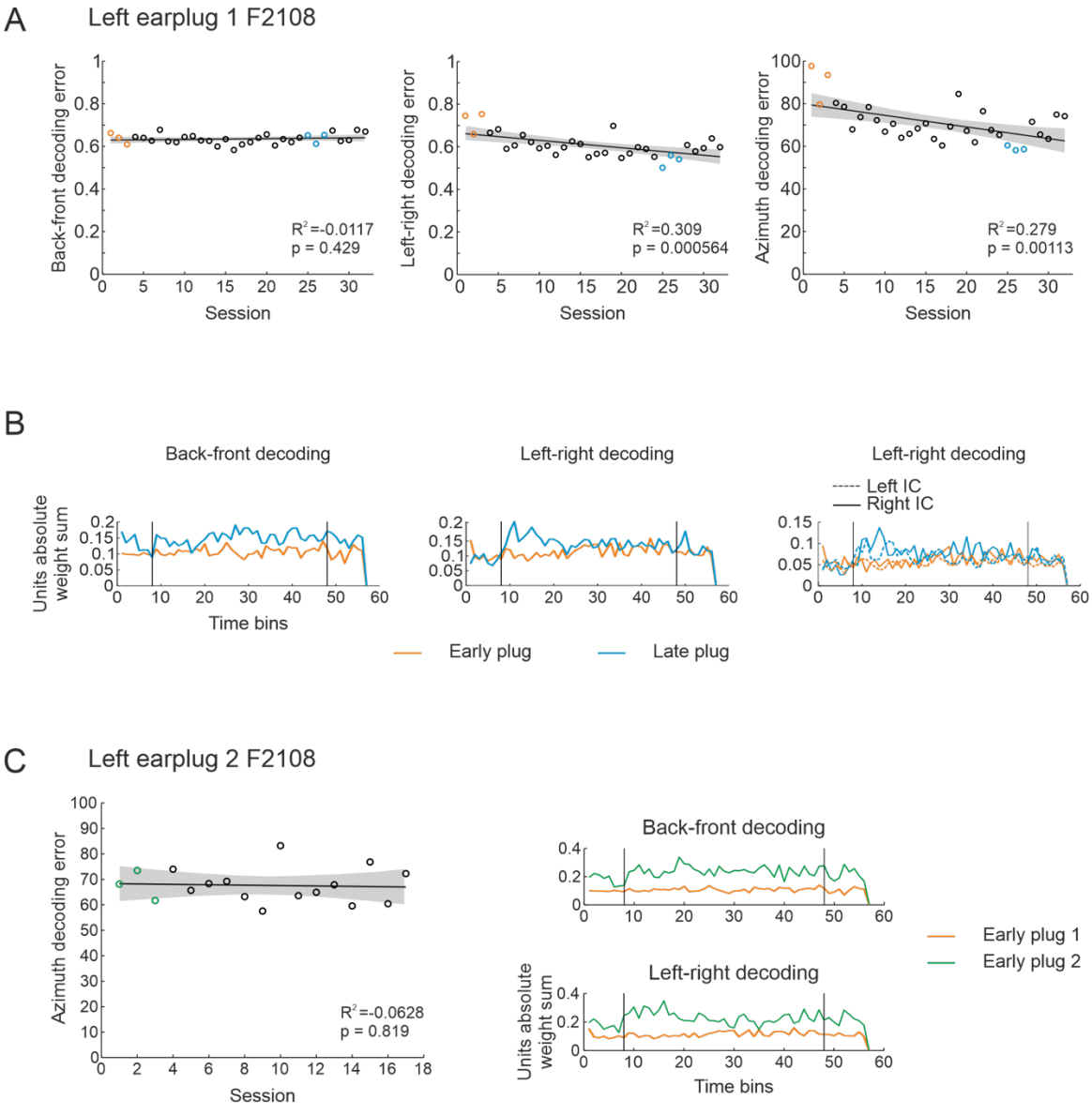

Figure 5-9. Decoding analysis during adaptation to UCHL. (A) Regression lines (shaded areas are 95% confidence intervals) and individual decoding error values (RMSE) for each session during adaptation to UCHL in the left ear are plotted for back-front, left-right and azimuth decoding. The data used for training the pattern decoder were recorded bilaterally in the IC of ferret F2108 while it adapted to an earplug inserted in the left ear through training in a sound localisation task. The pattern decoder was trained independently for each session, thus a reduction in the decoding error indicates that the

neural population is more informative about the decoded variable. For each recording session, 1400-ms windows of spiking activity were used to train the decoder, comprising the 1000 ms duration noise burst plus 200ms before and after this, except for the last five sessions in which the sound duration was increased to 2000ms to maximise the improvement in the animal's behavioural performance (thus in those cases the windows were 2400ms long). (B) The sum of units' absolute weights across hemispheres are plotted across time, averaged for three early plug sessions (orange) and three late plug sessions (blue) for the decoding of back-front and left-right positions (left and middle panels, respectively). The sessions used to obtain these results are highlighted in the same colour in panel A. The rightmost panel shows the sum of weights by hemisphere for left-right decoding. (C) Regression line (shaded areas are 95% confident intervals) and individual azimuth decoding error values for each session during adaptation to a second period of adaptation to UCHL in the left ear. For comparability with the first earplug period, 1400-ms windows of activity were used to train the decoder. On the right, sum of units' absolute weight is shown averaged across the first three sessions of both the second earplug period (green) and the first earplug period (orange), as in B, for back-front and left-right decoding.

In animal F2108, a second period of earplugging was performed in the same ear (left ear) to explore whether any neural correlates of a memory trace could be found from the previous learning period. In this period, training was carried out using 2000-ms noise bursts although for comparability with the first period, the decoder was trained using 1400-ms windows. For the re-plugging period, no significant reduction in the decoding error across sessions was observed (Table 5-1, Figure 5-9 C). Interestingly, the intercept was reduced relative to the first earplug period (Table 5-1), indicating a smaller initial decoding error, i.e. a better decoding accuracy at the start of the second earplugging period compared to the first. This was also observed when the training of the decoder was restricted to a 200ms window from sound onset (Supplementary Figure 5-2 C), discarding any direct effects of changes in head movement accuracy during adaptation on IC activity. This resembles the improved initial behavioural performance shown by animals after re-plugging relative to a naïve earplugging. An increase in negative weights in the right IC

was observed at the start of this second earplug period relative to the start of the first period of earplugging, resembling that observed toward the end of the first earplug period and in the pre-plug condition (Supplementary Figure 5-2). Thus, this could be indicating a retention of previous learning in the IC. Inspection of summed absolute weights across time showed an overall increased weight in early plug 2 relative to early plug 1 (Figure 5-9 C) for both left-right and back-front decoding.

For case F2110, a reduction in azimuth decoding error with training was also found, despite data from the left IC only being recorded in this ferret. For comparison, we explored whether we could see this for animal F2108 (plug 1) – for which we have described a similar result with the combined activity of both hemispheres – when the decoder was trained exclusively with data collected from the left IC. Indeed, we found a significant reduction in azimuth decoding error in this animal (fitted regression line slope = -0.46494, $p = 0.0147$) when data from the left IC only were used. To further discard any effects of ferret head movement we repeated the analysis with decoding restricted to a 200ms window from sound onset, before the head movement started, for which we also found a significant improvement in azimuth decoding in both cases (F2110 $p = 0.01$, $R^2 = 0.163$, F2108 left IC only $p < 0.001$, $R^2 = 0.613$).

An important factor to consider is the unequal number of sound presentations per location in the early stages of training relative to late training, due to changes in the proportion of correction and easy trials with learning, which could be affecting the performance of the decoder. To confirm that the observed changes in decoding accuracy were indeed associated with adaptation to UCHL and not confounded by this factor, we repeated the analysis for F2108 and F2110, equalising the number of trials per sound source location and training the decoder using 15 validation runs and we still observed

the same effect (fitted regression lines F2108 slope = -1.6709, p = 0.000148; F2110 slope = -0.8757, p = 0.0231).

The results of the decoding analysis for ferret F2111 were different from those obtained from the other animals. In this case, we did not observe a significant reduction in azimuth decoding error during either a first period of earplugging in the left ear or for a later period of earplugging in the right ear (Table 5-1). Interestingly, this is the same animal that in normal hearing conditions showed an unusually low contralateral preference in the right IC and a higher proportion of ipsilateral units in the left IC relative to other animals. The neural data from F2111 also showed a smaller displacement of the centroid in the left IC population following the insertion of an earplug in the left ear (Figure 5-2). In the decoding analysis, we found that the intercepts of the regression lines fitted to azimuth decoding error across sessions for both earplugging periods in F2111 were smaller than those for animals F2108 and F2110 (Table 5-1). This was the case even for the second earplugging period in F2108, indicating a better initial decoding accuracy. Thus, the induction of UCHL in ferret F2111 did not disrupt sound source location decoding from IC activity as much as in the other animals. Bringing the results from the descriptive and decoding analyses together, it appears that there may have been something abnormal about the IC data in F2111, the probe inserted in the right IC in this animal was the most caudally placed probe and could be reflecting activity from the external cortex.

A key advantage of these experiments, as has been pointed out before, is that they were performed in awake animals engaged in a sound localisation task. This allowed us to directly compare the performance of the decoder with the animals' sound localisation performance to explore whether neural activity in the IC might support the animals'

behaviour. We fitted regression lines to the mean approach-to-target error plotted across sessions for each period of earplugging in each animal (Table 5-2, Figure 5-10, red). The parameters of these lines were compared to those computed for the decoding analysis (Table 5-1, Figure 5-10 black). Indeed, some relationship was found between the animals' behaviour and the accuracy of the decoder. Regarding the behavioural performance during the first period of earplugging in each animal, ferret F2111 showed a reduced intercept (a = 41.445) compared to F2108 and F2110 (F2108 a = 80.653, F2110 a = 70.545), indicating better initial performance in the task following the onset of UCHL, and resembling the result described in the decoding analysis (F2108 a = 79.972, F2110 a = 74.198, F2111 a = 49.82). Consequently, the improvement in performance with training in F2111 was less than in the other ferrets, as shown by the reduced magnitude of the slope (F2108 b = -1.6913, F2110 b = -1.3757, F2111 b = -0.5090) (Figure 5-10), which might explain the absence of a significant reduction in decoding error with training progression in this ferret. Therefore, animals that showed a significant improvement in decoding accuracy with the progression of sessions during a first period of earplugging (F2108 (plug 1) and F2110) also showed the steepest improvement in sound localisation accuracy. Because approach-to-target localization accuracy changes with the duration of the stimulus (Chapter 3 Section 3.2.1.), it is important to perform the decoding analysis over the same duration (1000 ms) used for the behaviour. However, examining the decoding accuracy using a reduced time window is also necessary to determine whether changes in the direction of the head movements relative to the sound source during adaptation were contributing to the improvement in decoding accuracy. As with the long window analysis, we found that when the decoder was trained using a 200ms window after sound onset, without any head movement confounds, a significant reduction in error

was observed for ferrets F2108 (plug 1) and F2110, although the slope was less steep for the short window analysis in the case of F2110 (b = -0.319) (Supplementary Figure 5-3). Although a significant improvement was not observed for F2111 or F2108 (plug 2), these animals also showed less steep slopes in their behavioural performance. However, the decoding error was greater for the model using 200ms than the whole duration (intercept comparison between decoding restricted to 200ms (short) and decoding with the whole duration (long): F2108 plug 1 short = 83.54, long = 79.97; F2108 plug 2 short = 76.04, long = 68.35; F2110 short = 84.22, long = 74.19; F2111 left plug short = 57.37 , long = 49.82; F2111 right plug short =67.21, long = 62.57), indicating that both behaviour and decoding accuracy are influenced by the later parts of the stimulus.

During a second period of earplugging in F2111, in the opposite right ear, we observed a steeper learning slope relative to the period with left ear plugged (F2111 left earplug b = -0.5090, F2111 right earplug b = -1.1336). This may be associated with the increase in sound duration from 1000ms to 2000ms during the right earplugging period to encourage further adaptation in this animal. Despite the steeper behavioural slope, a significant reduction in decoding error was not observed during the right earplugging period in F2111 (Figure 5-10, Supplementary Figure 5-3). Finally, during the second period of left earplugging in F2108, a reduced intercept was observed relative to the first earplugging period for localisation errors (Table 5-2. F2108 left plug 1 a = 80.653; F2108 left earplug 2 a = 41.898), indicative of a memory trace from previous learning, which resembled the result described in the decoding analysis where a difference in intercept was also observed (Table 5-1. F2108 left earplug 1 a = 79.972; F2108 left plug 2 a = 68.355) (Supplementary Figure 5-2, 5-3).

Table 5-2. Parameters of the fitted regression lines for approach-to-target error during adaptation to an earplug.

	y = a + bx				
	R^2	a (intercept)	b (slope)	p_b	tStat (b)
F2108 Left plug 1	0.802	80.653	-1.6913	2.79e-12	$t_{(30)}$= -11.244
F2108 Left plug 2	0.382	41.898	-1.3813	0.00486	$t_{(15)}$= -3.2998
F2110 Left plug	0.658	70.545	-1.3757	1.87e-08	$t_{(29)}$= -7.6685
F2111 Left plug	0.217	41.445	-0.50909	0.0073	$t_{(26)}$= -2.9106
F2111 Right plug	0.474	49.736	-1.1336	0.00017	$t_{(21)}$= -4.5612

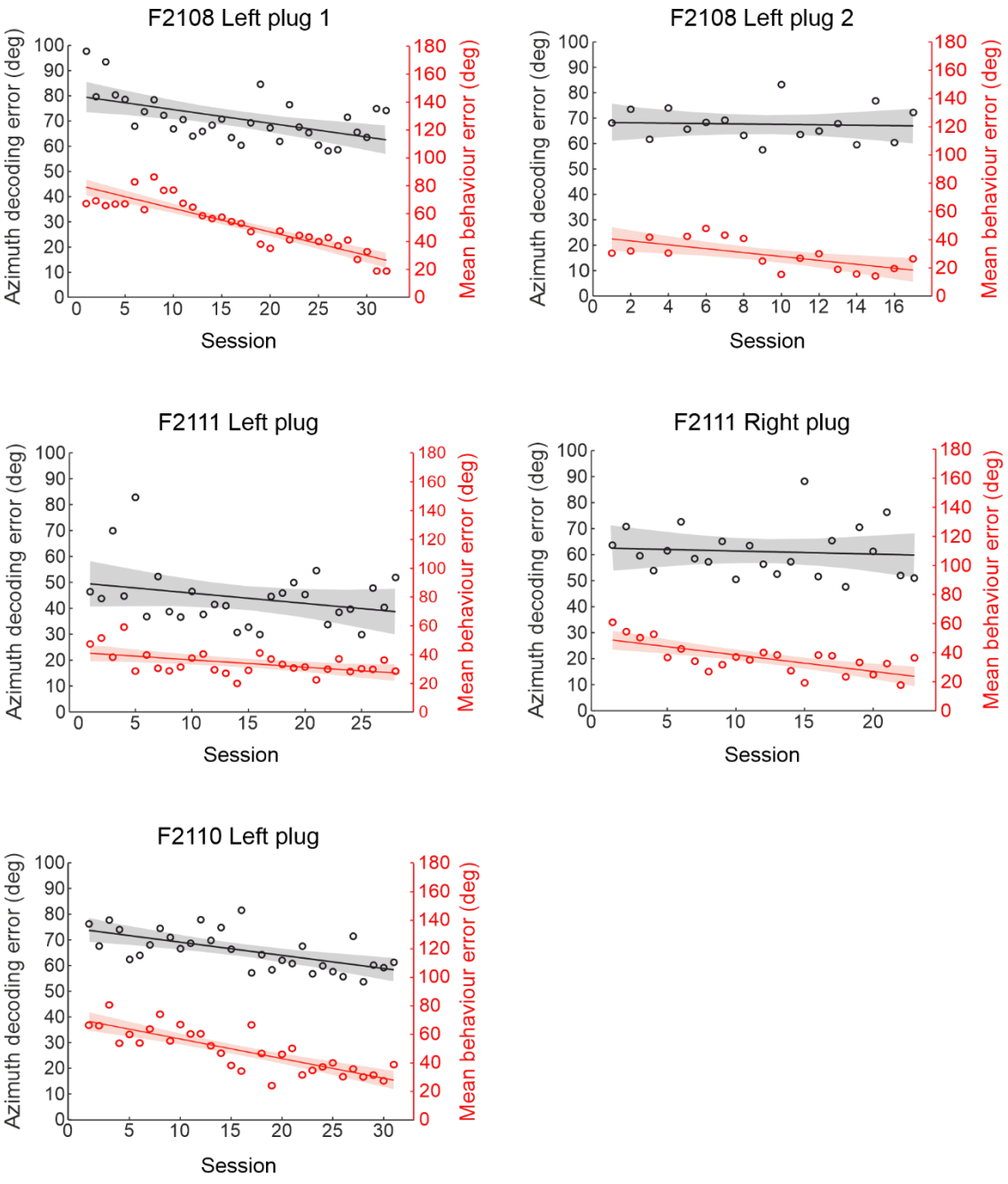

Figure 5-10. Comparison of azimuth decoding in the IC and the behavioural performance of the same ferrets. Regression lines (shaded areas are 95% confident intervals) and individual azimuth decoding error values (RMSE) for each session during adaptation to UCHL in each of the earplugging periods experienced by each animal are shown in black, reflecting the decoder's performance, while regression lines and individual mean unsigned errors are shown in red, reflecting the animals' approach-to-target behaviour.

To conclude the analysis, we compared the accuracy of the population pattern decoder after the earplug was removed with that before the earplug was inserted to explore whether a recovery in decoding accuracy was observed back to preplug levels, as predicted by the animals' behaviour.

We found that the decoder estimated the sound azimuth highly accurately, achieving similar accuracy to preplug performance (Figure 5-11). The decoding of sound position in the left-right axis showed better accuracy compared to decoding of back-front positions. This suggests that despite extensive training in a sound localisation task, which induced changes in the azimuth representation in the IC during UCHL, the restoration of balanced binaural hearing reinstated the dominance of left-right decoding accuracy, which is also indicated by the reappearance of the characteristic contralateral preference. Moreover, the kernels illustrating the weights of the different units across time showed a clear bilateral increase in weighting at sound onset for the decoding of left-right positions, which was also the case prior to earplugging, but which disappeared during UCHL. Altogether, these findings indicate that the sound location code present in the IC before earplug insertion is reinstated after earplug removal, also supported by the lack of aftereffects in the animals' behaviour.

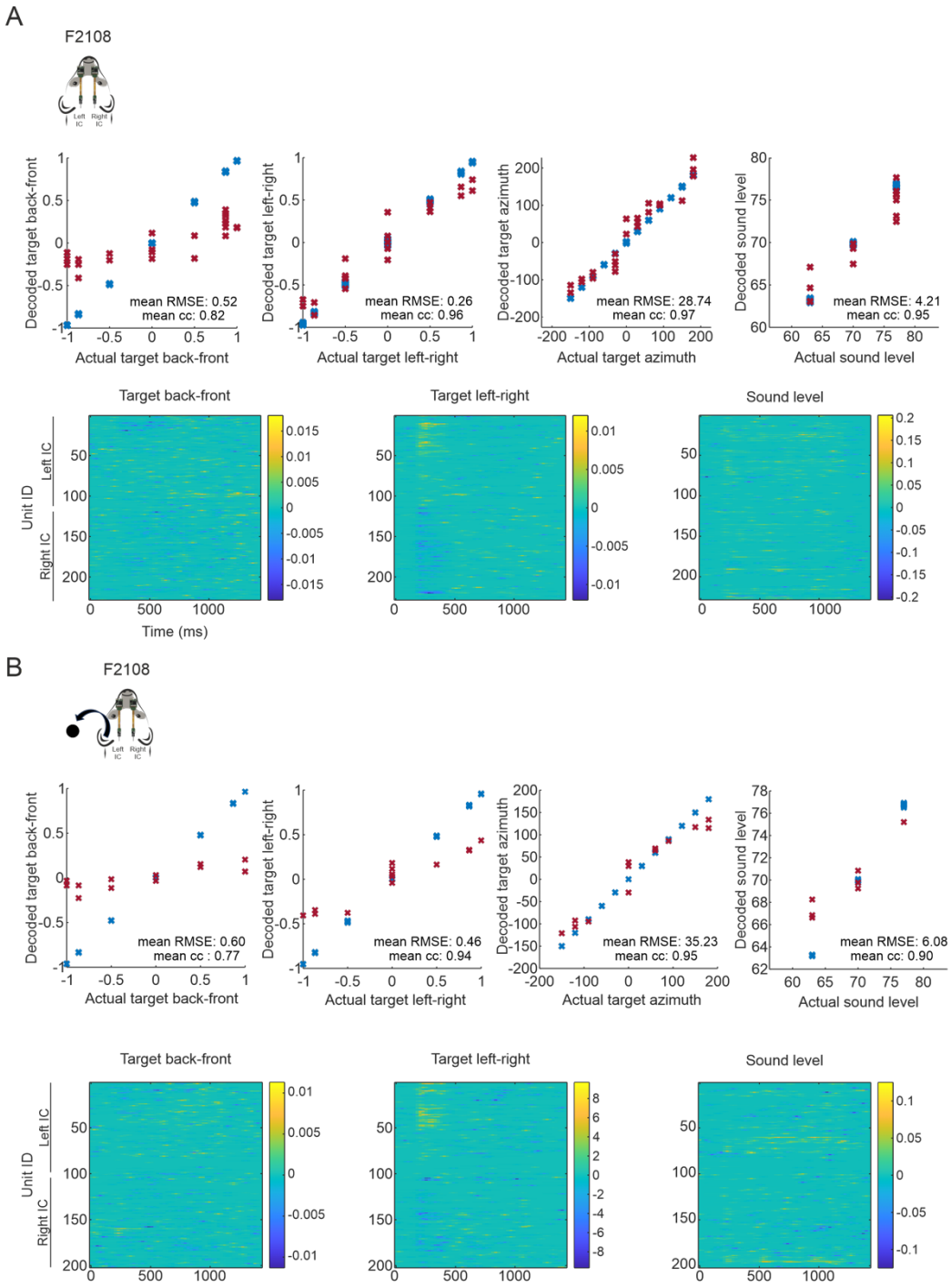

Figure 5-11. Comparison of sound location decoding in the IC between preplug and post-plug removal sessions. (A) Same as Figure 4-8 A-B. (B) Estimates of sound location by a population decoder are plotted against the actual location of the sound sources. The model was trained with data recorded bilaterally in the inferior colliculus of animal F2108 while performing a sound localisation task in after the removal of an earplug from the left ear. Estimates are plotted for the training set (blue) and the testing

set for an example fold. The mean correlation coefficient (cc) and root mean square error (RMSE) across folds are indicated at the bottom of each plot. Estimates are shown for back-front, left-right azimuth and sound level decoding. Kernels are plotted showing the weight of each recorded unit across time, indicating how informative each unit is about the decoded variable at each time bin. Units were sorted by side (left IC – top half of each plot, right IC – bottom half).

5.3. Discussion

Understanding the neural basis of auditory plasticity is crucial for the treatment of hearing disorders. Sound localisation is an invaluable skill, crucial for survival, which is highly sensitive to asymmetric hearing loss. Adaptation of sound localisation to UCHL has been demonstrated during development in ferrets raised with monaural occlusion (Keating et al., 2013; Keating et al., 2015) and in adulthood in ferrets (Kacelnik et al., 2006; Bajo et al., 2010; Bajo et al., 2019; Nodal et al., 2010; Nodal et al., 2012) and humans (Kumpik et al., 2010; Keating et al., 2016).Adult auditory plasticity relies on training in a sound localisation task and a series of lesion and deactivation studies (Bajo et al., 2010; Bajo et al., 2019; Nodal et al., 2010;) have pointed to the AC and its interaction with subcortical structures as the possible underlying neural substrate. In particular, the inferior colliculus in the midbrain has been suggested to play a role in the consolidation of this training-induced learning (Bajo et al., 2010; Bajo et al., 2019). However, recordings in this area are necessary to determine whether neural changes associated with adaptation to UCHL are present there.

In this chapter, we performed electrophysiological recordings bilaterally in the IC in ferrets experiencing UCHL. Recordings were performed while ferrets received daily training to induce adaptation to this condition. This approach allowed us to explore the effect that the induction of UCHL has on the spatial responses in the IC and to track neural changes that might be associated with training-induced plasticity in localisation behaviour.

The induction of UCHL in a cohort of ferrets chronically implanted with recording probes (Neuropixels 1.0) introduced an interaural imbalance, changing the binaural cue values and the monaural spectral cues at the occluded ear. The resulting impairment in localisation accuracy in the azimuthal plane recovered with training, as shown in previous studies (Kacelnik et al., 2006; Bajo et al., 2010; Bajo et al., 2019; Nodal et al., 2010; Nodal et al., 2012) and in Chapter 3. The four ferrets achieved a degree of adaptation within the range observed in non-implanted ferrets, although the localisation accuracy achieved by the end of the earplugging period was within the lower part of the range. Therefore, despite the small lesions and associated gliosis caused by the implanted probes in the IC and the possible restriction of head movement due to carrying a head implant, significant adaptation was still achieved.

Neural activity in the IC was found to be highly affected by UCHL. In the IC contralateral to the plugged ear, neural activity was suppressed in response to self-initiated broadband sounds presented as part of the behavioural training. In contrast, the IC ipsilateral to the plugged ear remained driven by sound, reflecting the predominantly excitatory input from the side of the open ear. This differs from neural responses described in both ICs during normal hearing conditions, which are characterised by sound-induced excitation as reported in Chapter 4, and by previous studies (Aitkin et al., 1984; Day & Delgutte, 2013; Kuwada et al., 2011). In normal conditions, units in the IC show broad spatial sensitivity with a contralateral bias, i.e., a preference for sounds presented in the contralateral hemifield (Aitkin 1984, Day and Delgutte 2013, Kuwada et al 2011), which disappeared with the onset of UCHL.

The characteristic contralateral preference of IC neurons reflects laterality of the inputs from the auditory brainstem (Grothe et al., 2010), including the LSO, a superior

olivary complex nucleus involved in ILD processing. The LSO receives ipsilateral excitatory input and contralateral inhibitory input from the VCN resulting in a subtraction of the firing rates from both ears to compute the ILD. In turn, the LSO sends contralateral excitatory and ipsilateral inhibitory connections to the IC (Grothe et al., 2010). Because the principal effect of the earplugs used is to attenuate the transmission of high-frequency sounds, and therefore to affect ILDs, the observed alteration in IC activity following the induction of UCHL can be explained by the change in firing activity encoding sound intensity in the inputs from the occluded ear, which ultimately disrupts ILD computation. As shown in Figure 5-1, a reduction in the firing rate in the ipsilateral VCN should decrease the excitatory input to the ipsilateral LSO and the inhibitory input to the contralateral LSO, while input from the contralateral VCN would remain intact. As a consequence, a suppression of the ipsilateral LSO and an overexcitation of the contralateral LSO would be expected, producing the opposite effect in the upstream IC due to their contralateral projections. We indeed observed a clear suppression of activity in the IC contralateral to the earplug and a broadening of spatial tuning in the ipsilateral IC, which likely reflects the reduction in inhibitory input from the side of the earplug.

No clear increase in the normalised firing rate was observed relative to pre-plug measurements conditions, reflecting an unchanged excitatory drive from the side of the open ear. However, the monaural occlusion caused by an earplug would not only be expected to affect ILD computations but also the ITD. Any alteration in the firing activity in the VCN will ultimately alter the inputs to the MSO and potentially distort its ITD-dependent firing rate functions. Moreover, the attenuation produced by the earplug is frequency dependent, and thus it also alters the spectral cues in that ear. Therefore,

spectral cues provided by the open ear are the only set of cues unchanged following UCHL.

In normal hearing conditions, sound azimuth can be accurately decoded from activity recorded in the IC, as reported in Chapter 4. Here we extended this approach to explore how sound location encoding is affected by the onset of UCHL and the effect that training has on this. Decoding data recorded bilaterally in the IC following the insertion of an earplug in one ear resulted in a highly degraded decoding accuracy, indicating that IC responses in these conditions were now much less informative about the sound azimuth. Importantly, this decline in decoding performance coincided with a drop in the animals' localisation accuracy. However, in contrast to the behavioural data obtained from ferrets that mostly experienced normal hearing, the pattern decoder was only trained using data recorded during disrupted hearing. Therefore, the poor decoding performance observed in this condition relative to when the decoder was trained with data from animals experiencing normal hearing indicates that the disruption produced by UCHL does not just change the way sound location is encoded in the IC, but rather disrupts activity in the IC, making it uninformative about sound azimuth.

To track whether any changes associated with training-induced plasticity occurred in the IC, we then trained the decoder independently with data obtained from consecutive training sessions. We found that the decoding performance improved as the sessions progressed, indicating that activity in the IC became more informative about sound location with training, probably due to adaptive changes in binaural integration. The magnitude of this improvement was also found to be associated with the ferret's behaviour. A possible plasticity strategy to compensate for the binaural imbalance caused by the sound attenuation in the occluded ear could be reducing the suppression in the

contralateral IC, by decreasing the ipsilateral inhibition or increasing the contralateral excitation. Alternatively, the excitation in the ipsilateral IC could be reduced by increasing the ipsilateral inhibition or by reducing the contralateral excitation, which would contribute to rebalancing both hemispheres. Compensatory changes supporting this hypothesis have been described in the IC following exposure to monaural occlusion by Thornton et al., 2021. In this study, activity was recorded in neurons in the CNIC of young adult chinchillas (~P70) after 6 weeks of exposure to UCHL. They found an elevation of the minimum discharge rate in the CNIC contralateral to the ear that had been plugged, which altered the modulation of discharge rate due to ILD relative to control animals, suggesting a reduction in the suppression of these neurons as an adaptive strategy to UCHL (Thornton et al., 2021). This observation is congruent with our observation indicating that units in the IC contralateral to the plugged ear became more informative about sound location with training as evidenced by the increase of units' weights at the onset of the stimulus in the decoder, although an increase in the normalised firing rate indicative of a reduction of suppression was not observed. In the IC ipsilateral to the plugged ear, we also found an increase in the sharpening of units towards preplug levels, as shown by the reduction in the width of the ERRF. While this adaptive sharpening of spatial tuning could be indicative of a reduction in the excitation/increase in inhibition to these units, it could also reflect increased sensitivity to the intact monaural spectral cues available at the open ear, which has been shown to provide the primary basis for adaptation to UCHL in adult ferrets (Kacelnik, et al., 2006) and humans (Kumpik et al., 2010; Keating et al., 2016)..

An important difference between our experiments and those carried out by Thornton et al., 2021 is that they performed the recordings exclusively following earplug

removal, suggesting that these adaptive changes persist for at least 24-36h after binaural hearing restoration, which was the interval within which recordings were performed. In our experiments, the ferrets' performance in the sound localisation task returned to preplug levels straight after earplug removal, agreeing with what has been reported by previous studies (e.g. Kacelnik et al., 2006). Similarly, we found that the contralateral bias characteristic of these units in normal hearing conditions was restored after earplug removal. Additionally, the performance of the decoder was similar to preplug levels. A very rapid resetting of binaural sensitivity seems unlikely, particularly as Thornton et al. (2021) found that the proportion of binaural responses had declined in animals with UCHL. However, the lack of an after-effect in our behavioural and IC data is consistent with previous studies demonstrating that changes in the relative weighting of binaural and monaural localisation cues accompany adaptation to UCHL (Kacelnik, et al., 2006; Kumpik et al., 2010; Keating et al., 2016). That these context-dependent changes can occur rapidly may be a consequence of performing the neural recordings in awake ferrets while they were engaged in a sound localisation task. This could be contributing to a much faster restoration of preplug activity than when recordings are performed under anaesthesia, as was the case in other studies (Thornton et al., 2021). However, in adult ferrets raised with one ear occluded, Keating et al. (2013) showed that the relative contribution of monaural and binaural spatial cues to the responses of A1 neurons can change even under anaesthesia when a virtual earplug is introduced and removed.

The changes we observed in spatial tuning and in the balance of excitatory and inhibitory responses in the IC were less pronounced when the same ear was re-plugged. This again matches the animals' behaviour, with smaller deficits occurring after re-plugging (as reported in Chapter 3). This suggests that adaptive changes in the IC could

be involved in the consolidation and retrieval of previous learning as suggested by (Bajo et al., 2019) and (Bajo et al., 2010). The presence of such changes would also explain the greater localisation deficit observed when UCHL was switched to the opposite ear (Chapter 3 Section 3.2.5.). Irrespective of whether the plasticity in the IC supports spatial cue reweighting and/or binaural cue remapping, these changes would have to be reversed when all the cues are altered by occluding the other ear.

Both cue reweighting and remapping have been shown to occur in the same individuals depending on the spectral composition of the stimulus (Keating et al., 2013, Keating et al., 2015, Keating et al., 2016). These are therefore not mutually exclusive processes and we have proposed that they might arise at different stages of training (Chapter 3). Thus, reweighting could be an early onset strategy that helps resolve sound localisation in the side ipsilateral to the open ear, while remapping could arise progressively and contribute to the improvement in localisation at other positions. Since adaptation to UCHL is progressive, taking place gradually over several days, and leaves a memory trace (Kacelnik et al., 2006, Bajo et al., 2019), this may be more indicative of a remapping process that would involve recalibrating the altered cues with locations in the azimuth. However, while we observed a compensatory shift in the cluster centroids over the course of behavioural adaptation, this was not sufficient to restore the contralateral preference observed before earplugging. This is perhaps not surprising since complete recalibration of binaural sensitivity would be expected to result in an after-effect following earplug removal, which was not the case.

Studies investigating training-induced auditory plasticity in adulthood have demonstrated the role of the AC and its interaction with subcortical structures as key elements of the neural circuitry involved. While the AC, and A1 in particular, is essential

for the acquisition of this learning (Bajo et al., 2019; Nodal et al., 2010), we have provided the first evidence that compensatory changes take place in the IC, which is consistent with the disruptive effects on adaptation of eliminating auditory corticocollicular neurons (Bajo et al., 2010). Therefore, we hypothesise that changes observed in the IC are derived from the influence of the AC through its downstream connections. This is supported by electrical stimulation studies, which have demonstrated that the AC can modulate neural activity in the IC (Ma & Suga 2001; Yan & Ehret 2002; Zhou & Yen 2005). Optogenetic deactivation of A1 at different stages of learning provided further insight into the role of the AC in auditory plasticity. Bajo et al., 2019 showed that AC is necessary for the initial acquisition of learning, as evidenced by impaired adaptation when AC was inactivated during sound presentation, similar to the changes observed with longer-term inactivation (Nodal et al., 2012) and lesion studies (Nodal et al., 2010). However, after learning without cortical inactivation, subsequent training with AC inactivation showed that animals improved in the same fashion as when the AC was active, indicating that adaptation to further periods of earplugging was no longer dependent on the AC (Bajo et al., 2019). This is indicative of the consolidation of learning taking place somewhere else in the brain. With the results reported in this chapter and the evidence indicating the importance of the cortico-collicular pathway in adaptation to UCHL (Bajo et al., 2010), we hypothesise that the IC is the centre for the consolidation of this learning. Similarly, adaptive changes in the IC appear to play an important role in the facilitation of adaptation when the alteration in spatial cues is experienced again in subsequent periods of UCHL.

To conclude, auditory plasticity during development is crucial for adaptation to changes in the maturing auditory system and, unlike in adulthood, it is driven primarily by sensory experience. Previous studies have investigated the consequences of UCHL at

different stages of development and have linked this condition with maladaptive plasticity leading to perceptual sequelae. In particular, UCHL during development has been shown to lead to a reduced representation of the occluded ear at different levels of the auditory pathway (Popescu & Polley, 2010). In contrast, we have shown in adult ferrets that adaptive changes serve to rebalance both sides (by increasing responses to the occluded ear or decreasing those to the open ear), agreeing with previous findings (Thornton et al., 2021). This work therefore highlights the importance of behavioural training while also suggesting that that key differences may exist between developmental and adult plasticity.

5.4. Appendix

5.4.1. Supplementary figures

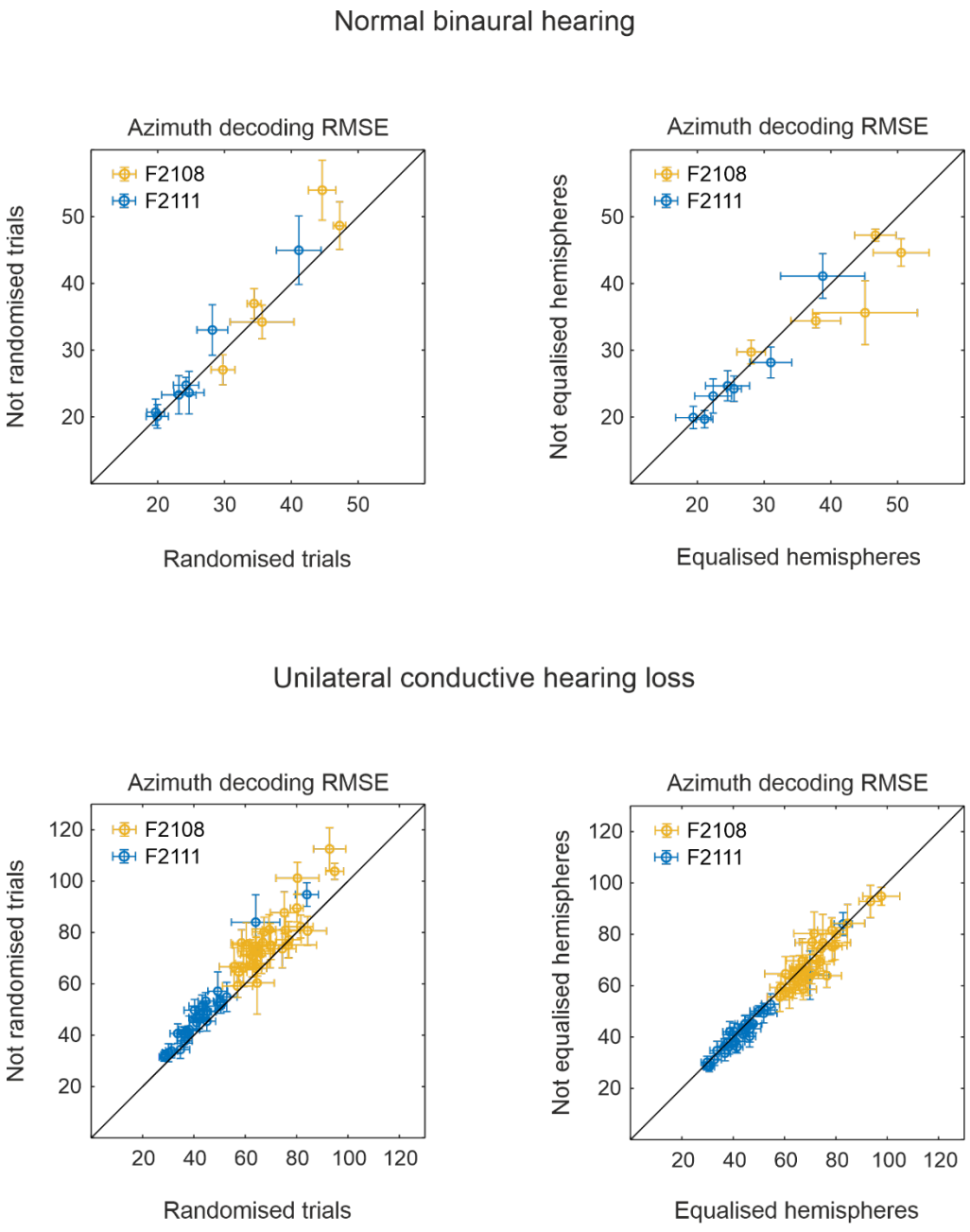

Supplementary Figure 5-1. Effect of trial randomisation and hemisphere equalisation in the decoding analysis in different listening conditions. Azimuth decoding errors are plotted for individual sessions (mean ± SE) recorded in two animals, F2108 and F2111, with data combined from both ICs in normal hearing conditions (top) and in the presence of UCHL (bottom) comparing different decoding approaches. Left panels show comparison of decoding with and without trial randomisation while right panels compare decoding with and without hemisphere equalisation, i.e. equalisation of number of units in each hemisphere. Distance from the diagonal identity line indicates a difference between conditions.

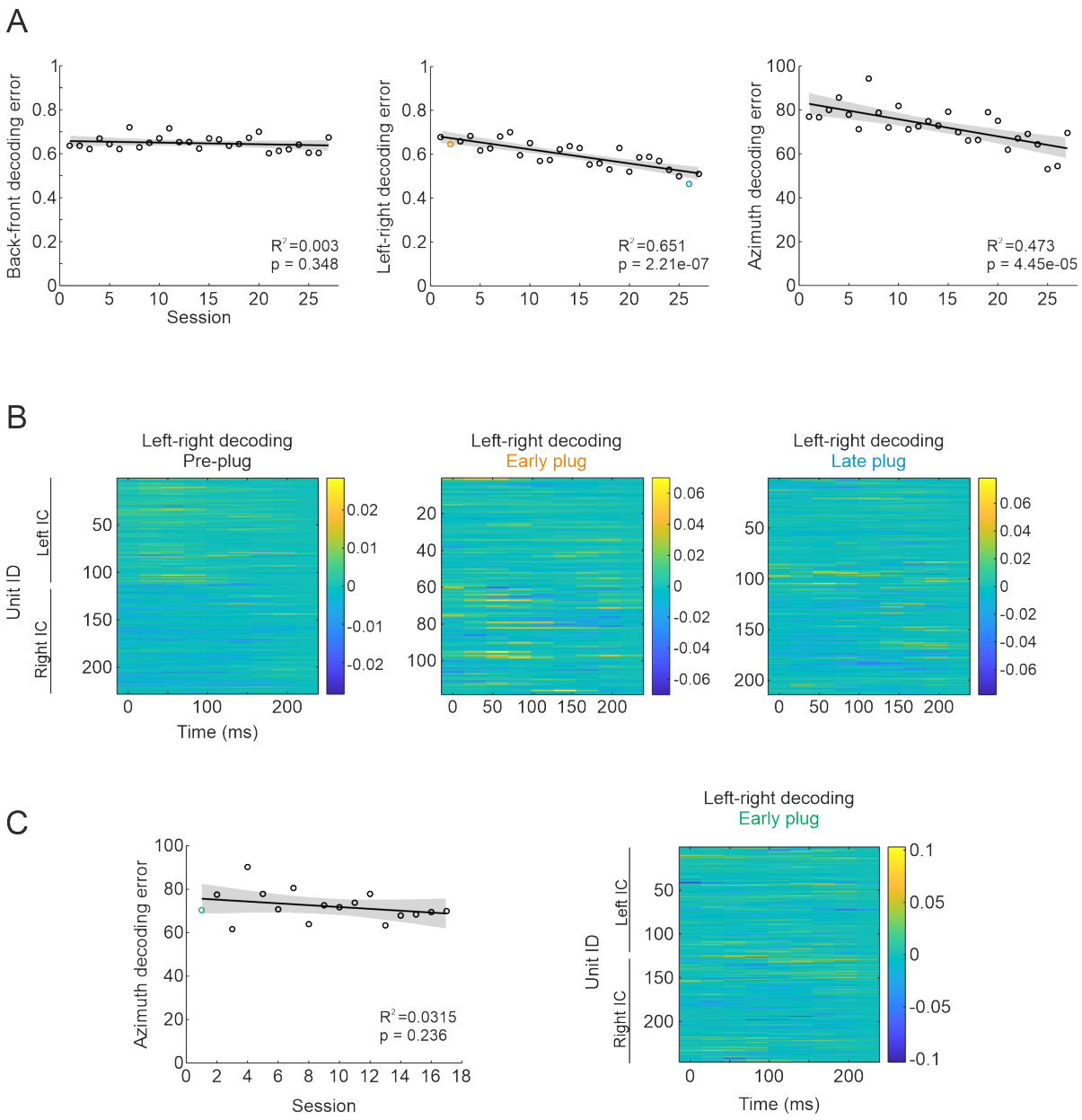

Supplementary Figure 5-2. Decoding analysis in a 200ms window during adaptation to UCHL. (A) Regression lines (shaded areas are 95% confidence intervals) and individual decoding error values (RMSE) for each session during adaptation to UCHL in the left ear are plotted for back-front, left-right and azimuth decoding. The data used for training the pattern decoder were the same as Figure 5-9A but in this case the pattern decoder was trained in a 200-ms window of spiking activity from sound onset (B) Kernels indicating the weight of each IC unit across time are plotted for a 200-ms window binned in 25-ms bins. Weights (colours) indicate how informative each unit is about left-right decoding (blue indicative of left and yellow indicative of right). Kernels are shown for three conditions, from left to right: pre-plug, early plug, and late plug. Early and late plug data were extracted from sessions highlighted in orange and blue in A, respectively. (C) Regression line (shaded areas are 95% confident intervals) and individual azimuth

decoding error values for each session during adaptation to a second period of adaptation to UCHL in the left ear. The data used for training the pattern decoder were the same as Figure 5-9C but in this case the pattern decoder was trained in a 200-ms window of spiking activity from sound onset. On the right, the weights for an early plug session are shown. The data correspond to the session highlighted in green in the left panel.

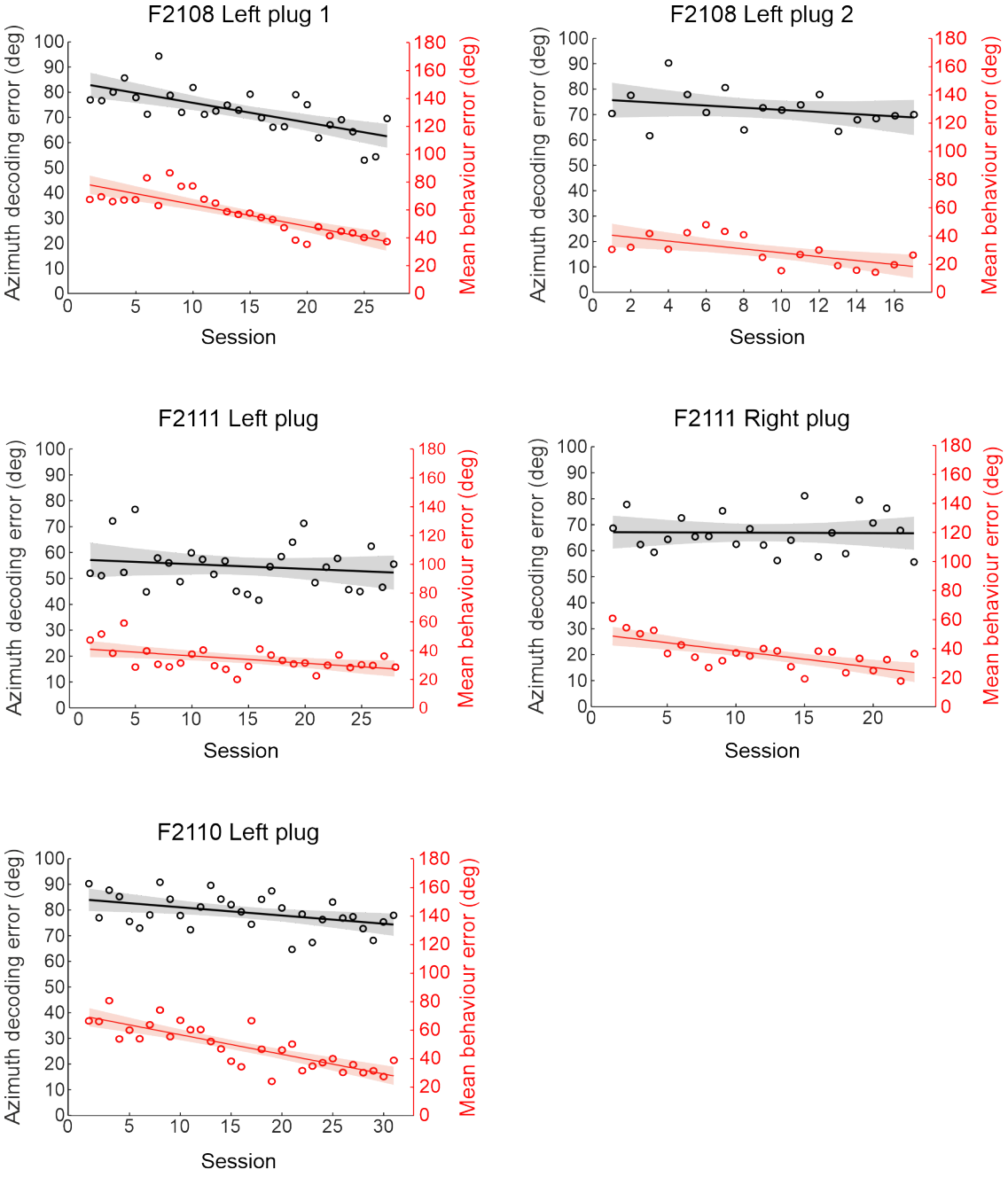

Supplementary Figure 5-3. Equivalent to Figure 5-10 with decoding restricted to a 200ms window after sound onset - comparison of azimuth decoding in the IC and the behavioural performance of the same ferrets. Regression lines (shaded areas are 95% confident intervals) and individual azimuth decoding error values (RMSE) for each session during adaptation to UCHL in each of the earplugging periods experienced by each animal are shown in black, reflecting the decoder's performance, while regression lines and individual mean unsigned errors are shown in red, reflecting the animals' approach-to- target behaviour.

6. FUTURE APPLICATIONS

6.1. Introduction

A significant proportion of the world's population is affected by hearing loss and according to the World Health Organisation, by 2050, 700 million people are projected to suffer from hearing loss requiring hearing rehabilitation. Hearing loss is a disabling condition that greatly impacts the quality of life of people suffering from it, affecting their ability to communicate, especially in noisy environments and, consequently, disrupting their social interactions. Auditory perceptual learning plays a key aspect in the development of future rehabilitation strategies, since it allows adaptation to altered sensory inputs leading to the recovery of perceptual abilities. In particular, the recovery of spatial hearing through behavioural training in sound localisation tasks shown for experimentally induced UCHL is likely to be important for the future treatment of hearing loss affecting the two ears asymmetrically.

To determine the effectiveness of such training as a therapeutic approach, it is necessary to explore the generalisation of the induced learning from experimental conditions to daily life scenarios. Psychophysical studies have traditionally been performed in highly-controlled listening conditions, usually involving the presentation of single bursts of sound against a silent background inside sound-proof rooms. These conditions are far from the acoustic ambience we are exposed to in our daily lives. As

part of Chapter 3, we explored this aspect of learning in ferrets by testing the animals' ability to localise sounds of different bandwidth in the presence of background noise after they had adapted to UCHL. Similar studies will be needed in humans to test whether results obtained in ferrets translate to humans. Nevertheless, the listening conditions that can be tested are highly limited by the experimental setups traditionally used for behavioural studies.

Virtual reality (VR) is a tool that allows the recreation of complex sensory environments using a head display and thus provides an alternative to get rid of the physical constrains of typical laboratory setups. This technology can also be accessed from potentially anywhere in the world, since an appropriate headset is all that is needed to access VR environments. Therefore, this could be used to provide access to training protocols if these were to be implemented as part of an approach for rehabilitating individuals with hearing or other sensory disorders.

In this chapter, we developed a proof of concept for the use of VR for behavioural testing of sound localisation in humans, with the aim of using VR in the future as a tool for performing psychophysical studies to explore adaptation to hearing loss in real-life scenarios. For that, we recreated the testing arena used for studies in ferrets in VR for humans and some preliminary data was collected to measure the ability of humans to localise sounds in a virtual environment. It was intended that training studies would be carried so that results could be included in this thesis, but the restrictions imposed by the COVID-19 pandemic unfortunately meant that this was not possible.

6.2. Sound localisation in virtual reality

6.2.1. The virtual environment

A virtual environment was created using *Unity*® engine, a game developing engine that allows the creation and exploration of 3D environments. In this environment, we created a human replica of the real-life sound localisation testing arena used for ferrets (Figure 2-1). For that, twelve loudspeaker prefabs from the *HQ Acoustic system* package, acquired from the *Unity Asset Store,* were placed along the circumference equidistant from each other and at the same elevation (Figure 6-1). Each of the loudspeaker prefabs was comprised of a *box collider* component, which conferred the object the ability to collide with others allowing interactions, and an *audio source* component, which allowed sound presentation during the task. A blue rectangular User Interface (UI) button component displaying the text 'NEXT' was placed in front of a reference loudspeaker (0 degrees speaker) (Figure 6-1) and was used to trigger the sound presentation for each trial. This made sure that human players/participants were always facing the reference loudspeaker at the start of each trial, playing an equivalent role to the central platform spout in the ferret task.

A key aspect of virtual reality is that it is an immersive experience, and thus the player must be able to explore and interact with the environment. To achieve this, we used an *XR Rig* game object, which contained the elements whose movements were controlled by the player's locomotion. Among these elements, we find the *Main Camera* object, comprised of several components: (1) a camera providing a view of the virtual

environment, acting as the player's eyes, (2) an *Audio Listener* component to allow the player to hear sounds in the environment, and (3) a *Tracked Pose Driver* component, which tracked the movement of the VR headset (Oculus Rift S) worn by the player and applied the position to the virtual camera component, allowing head movements within the virtual environment. Another element in the *XR Rig* was a *Right Hand* object, which tracked the movements of the right-hand controller held by the player during the task and allowed the execution of certain behaviours crucial for the task, such as 'selection of speaker' or 'button pressing'. Finally, we also had a *Ray Interactor*, which rendered a ray associated with the controller, key for the interaction within the environment with distant objects, such as the loudspeakers or the 'NEXT' button.

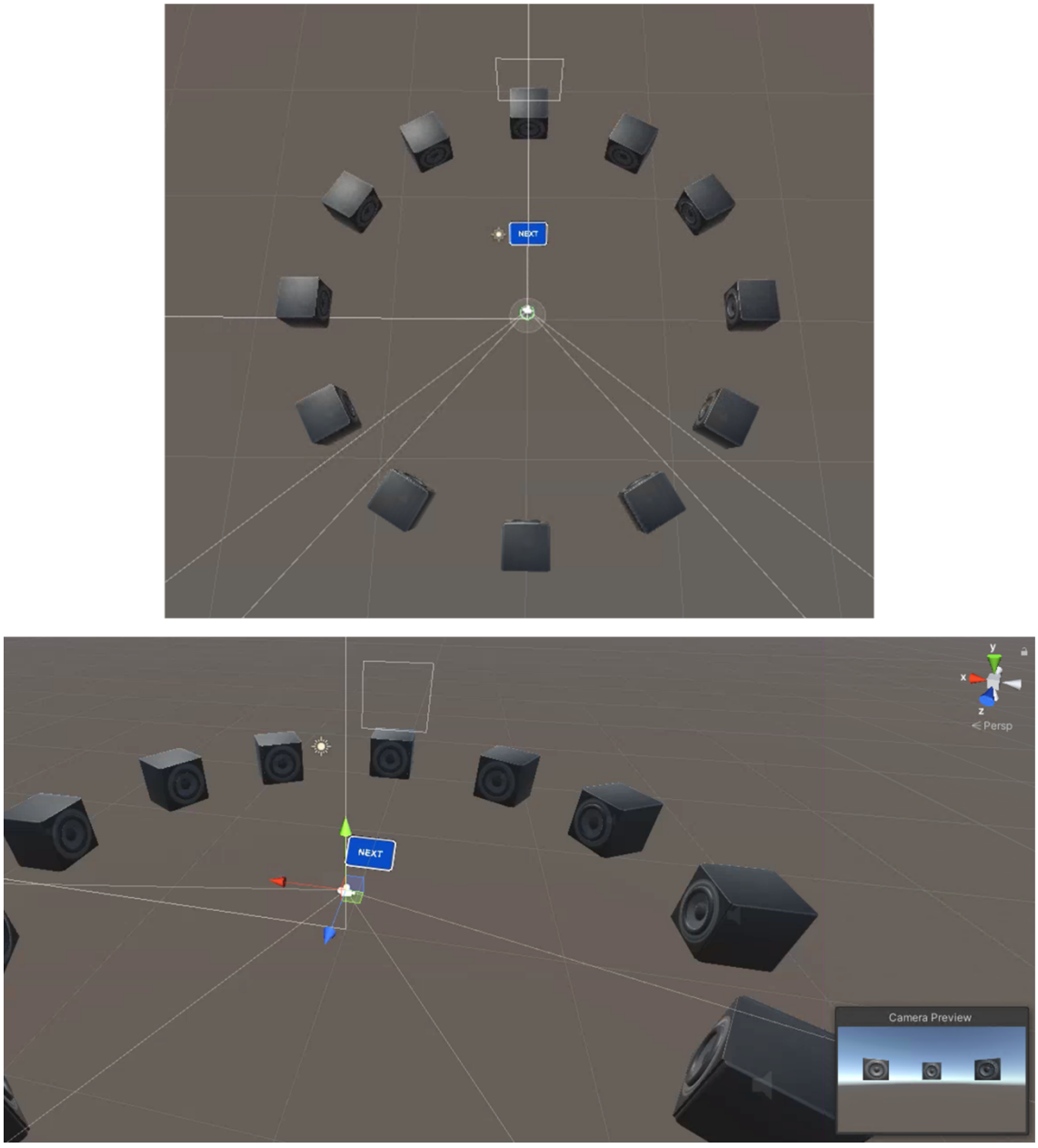

Figure 6-1. Developer view of the virtual environment for sound localisation testing in humans. Top panel shows a top view of the virtual scene containing twelve loudspeakers distributed around the circumference at different azimuths, a button for triggering sound presentation and, in the centre, a 3D object containing the camera and other components manipulated by the player's locomotion. Bottom panel displays the same view but from a different angle. It also shows a camera preview in the bottom right corner which provides the player's point of view.

6.2.2. Virtual sound localisation task programming and execution

The task/game was initialised with a 2D environment displayed on the computer screen consisting of a canvas where the experimenter could specify the parameters for the task variables, such as duration and type of the target sound (Figure 6-2). Sounds were previously synthesised in MATLAB (MathWorks, United States) and imported into Unity. On the action of pressing the button 'PLAY' a change of environment was triggered that transported the player into the 3D virtual sound localisation setup. A change of virtual environment by default destroys the variables created in any prior scene. To conserve the values of the task parameters introduced by the experimenter in the starting screen (2D environment) for determining the experimental conditions, an object *parameters* was created to save them and the function DoNotDestroyOnLoad() was used to keep the object in the 3D environment (see code below). All code was written in Visual Studio using C# programming language.

Code for keeping task parameters:

```
public class DoNotDestroy : MonoBehaviour
{
    void Awake()
    {
        GameObject[] objs = GameObject.FindGameObjectsWithTag("parameters");

        DontDestroyOnLoad(objs[0]);

    }
}
```

Once in the 3D environment, as in the ferret task, the player had to trigger a sound presentation and respond by reporting the location of the source/loudspeaker. No reward

was associated with the task, but feedback was given about the success of the response. The task consisted of 96 trials, i.e., sound presentations, and the location and intensity of the sound were randomised. There were 12 location values (0 to 330°) and 4 intensity values (1, 0.44, 0.2, 0.09, equivalent to 0, -7, -14 and -21 dB relative to the maximum sound level, i.e. setting the computer volume to the maximum value). Thus, each location-intensity combination was presented twice. At the start of the game, the *SequenceGenerator* class was called to generate a list with all location and intensity combinations repeated twice, the order of which was then randomised for trial presentation.



Figure 6-2. Starting screen. Left panel shows three possible actions 'PLAY', which loads the task environment, 'QUIT', which exits the game and 'OPTIONS', which loads the screen shown in the right panel, where the experimenter specifies the parameters of the task, such as duration (in this example 1000ms) and type of stimulus (in this example, broadband noise flattened up to 30kHz), as well as a name for the file created to save the behavioural relevant parameters of the task.

From the player's viewpoint, they found themselves in the centre of a surrounding circumference composed by loudspeakers placed at eye level in the azimuth plane. The player could also see a model of a right hand whose position corresponded to the tracked right-hand controller that they were holding in their own hand. From the hand model, a visible ray was traced with which the player could point at objects. This ray was a *Ray*

Interactor object, which allowed interactions with other objects in the environment, such as the loudspeakers when it collided with the objects' colliders. These interactions triggered changes in the environment, for instance with the interaction of the ray and a speaker's collider, the material of the loudspeaker was changed to 'shiny', so that it was highlighted relative to other loudspeakers (Figure 6-3).

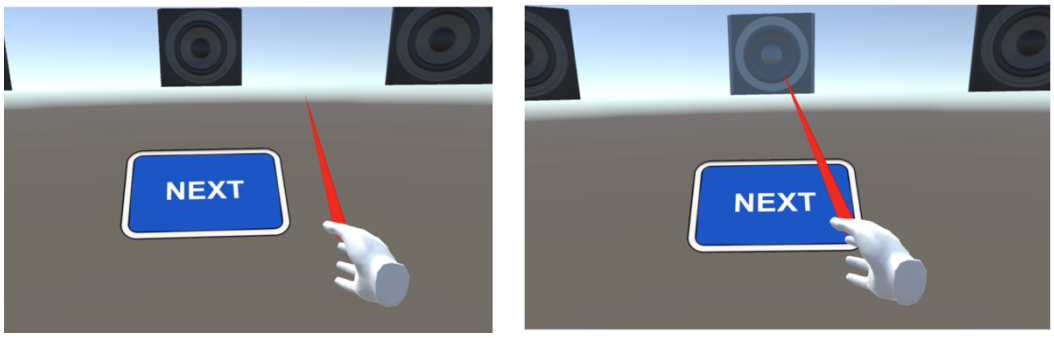

Figure 6-3. Interaction of raycast with a loudspeaker object. Two frames are shown illustrating a change in the loudspeaker object material as a consequence of its interaction/collision with the raycast from the right hand.

Because sound presentation was self-initiated, in order to start the task, the first thing that the participant had to do was to trigger the stimulus presentation. To achieve this, the player had to point at the 'NEXT' button located in front of the 0º speaker and select it by pressing the trigger button in the controller. This action set the variable 'TrigTarg' to true activating the 'TriggerTarget' class, which extracted information about sound location, level and duration for a given trial and activated the corresponding loudspeaker object by calling the 'PlayForTime' method in the 'soundTime' class. For subsequent trials, to activate 'TriggerTarget', i.e., to trigger a sound presentation, two conditions had to be met: that the 'NEXT' button was pressed ('TrigTarg' set to true) and that a response

for the previous trial was given (‘HaveResponse’ set to true) to avoid the player being able to trigger presentation of the same trial repeatedly.

Extract of the code for triggering sound presentation:

```
for (int i = 1; i < Order.Length; i++)
       {

        yield return new WaitUntil(() => HaveResponse == true);//response
        yield return new WaitUntil(() => Trigtarg == true);//button pressed

        CorrespondingLocation = (float)Sequence.GetValue(Order[i], 1); //location
        CorrespondingVol = (float)Sequence.GetValue(Order[i], 2); //level
        HeadTracker = GameObject.Find("HeadTracker");
        Timer = GameObject.Find("Timer");
        Speaker = GameObject.Find(CorrespondingLocation.ToString());
        durSet = GameObject.Find("SetDuration");// sound duration
        float soundurr = float.Parse(dur) / 1000;
        //trigger sound presentation:
        durSet.GetComponent<soundTime>().PlayForTime(soundurr, CorrespondingVol);
       HeadTracker.GetComponent<RecHeadData>().GetHeadData();
        Timer.GetComponent<getTime>().GetStartTime();
        yield return new WaitUntil(() => Triggerer == false);
            trial = i+1;

        }
```

When the trial was initiated and the sound presented, the participant had to respond by indicating the loudspeaker from where they thought the sound originated. To do so, they had to point at the loudspeaker and select it by pressing the trigger button in the controller. This action resulted in a change in the tag of the selected loudspeaker object from ‘untagged’ to ‘selected’, and called the ‘FindSelected’ class, which compared the selected speaker with the target speaker and defined whether the response was correct or incorrect.

Extract of code in 'FindSelected' class:

```
GameObject[] gos;
        gos = GameObject.FindGameObjectsWithTag("Selected");


        if (gos.Length == 0)
        {
            Debug.Log("No game objects are tagged with Selected");
        }

        if (gos.Length > 1)
        {
            Debug.Log("Several game objects were found");
        }
        if (gos.Length == 1)
        {


            SelectedLocation = gos[0].name; //selected speaker
            string TargLocation =
GameObject.Find("TargetTriggerer").GetComponent<TriggerTarget>().CorrespondingLoc
ation.ToString();//target speaker

            //Compare

            if (Int32.Parse(SelectedLocation) == Int32.Parse(TargLocation))
            {

                Response = "Correct!";
                Correctness = 1;

            }
            else
            if(Int32.Parse(SelectedLocation) != Int32.Parse(TargLocation))
            {

                Response = "Try Again!";
                Correctness = 0;
            }

}
```

Selecting a loudspeaker object also called the 'DisplayFeedback' class, which triggered the presentation of dynamic feedback displaying the messages 'Correct!' or 'Try Again!' based on the success of the player's choice (Figure 6-4).

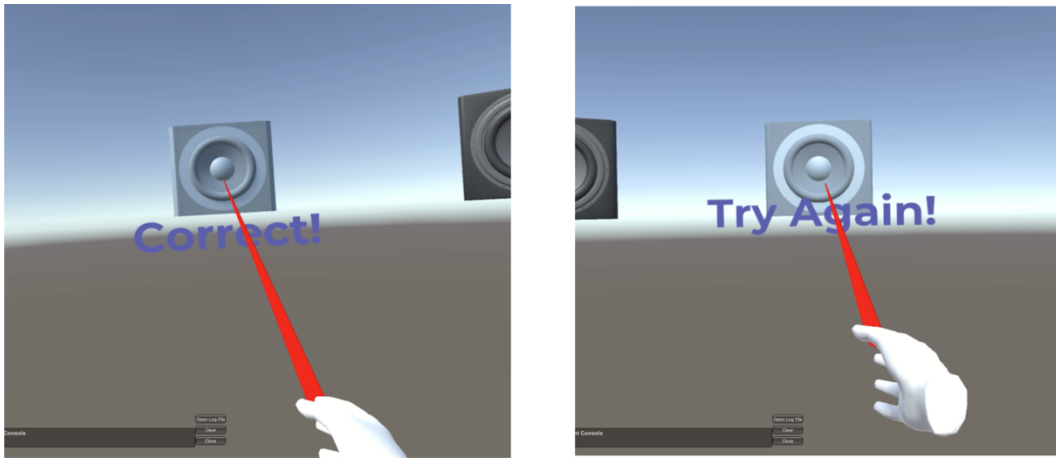

Figure 6-4. Response feedback during the task. Two frames illustrate how feedback is given to inform the player about the success of their response.

Throughout the task, other classes playing different roles were also called, which register certain behavioural parameters that could be analysed offline using MATLAB (Figure 6-5). Some important examples include 'RecHeadData' involved in tracking the movement of the head in the azimuthal plane over the time period from when the sound was presented until a response was given, registering highly precise changes in head orientation (Figure 6-5 A). The class 'getTime' extracted the response times by computing the time elapsed from when the trial was triggered until the response was given. Finally, the class 'writeFile' wrote the relevant behavioural information for each trial (target location, response location, level, sound type, sound duration, head tracking data and response time) in a file in MATLAB script format, which could then be run using MATLAB, generating a structure containing all the information for each trial.

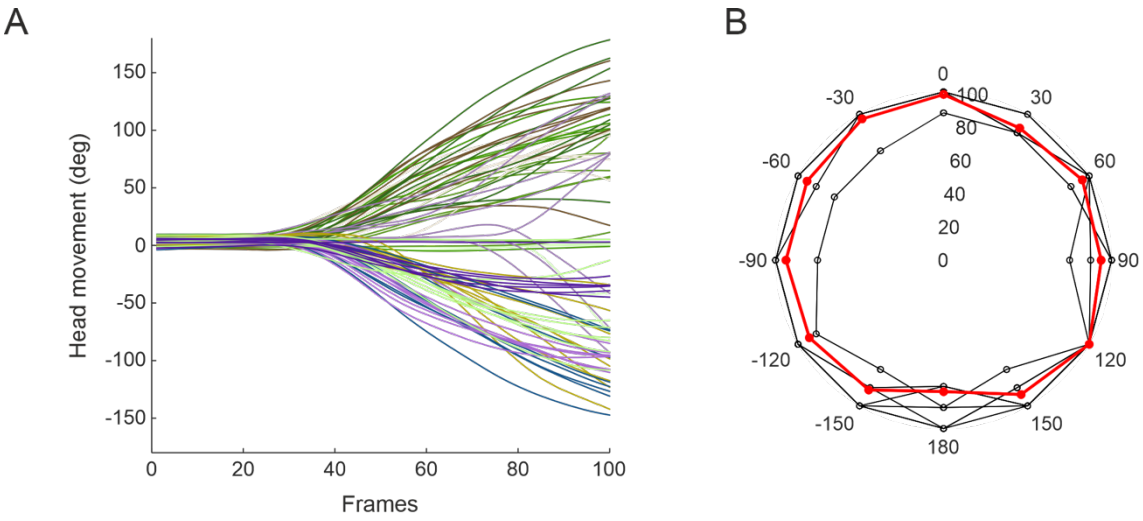

Figure 6-5. Example behavioural data collected from players testing the VR task. (A) Change in head orientation is plotted across time frames for an example participant. Each trace corresponds to an individual trial head movement. Different colours represent different target locations. (B) Percentage of correct responses per azimuth location is shown for individual players (black) (n=6) and for the averaged data (red). Data were collected in a single session for each player.

6.2.3. Real-time sound spatialisation

During the task, sounds were presented to the player through a pair of over ear headphones (Sennheiser HD 650). Listening to closed-field acoustic stimulation using headphones, i.e., sound presentation directly in the ear canals, differs from free-field listening as the signal provides reduced spatial information, due to the absence of congruent binaural and monaural cues. Typically, headphone listening allows the sound to be lateralised, depending on the binaural cues provided without assigning it a specific spatial location. Sound spatialisation can be achieved by filtering the sound so that it is perceived as if it was presented from an external location, creating a virtual acoustic space. This transformation was therefore needed to study sound localisation in a virtual environment. Furthermore, because players in the task were able to freely move their

heads, real-time spatialisation accounting for head movements was necessary to achieve a real feeling of acoustic space inside the 3D environment.

To achieve this, we implemented the 3D-TuneIn wrapper for Unity (Cuevas-Rodríguez et al., 2019) a tool for applying real-time binaural spatialisation in 3D environments created using the Unity engine. This tool convolves sounds with Head-Related Transfer Functions (HRTFs), which characterise the way the external ears, head and torso filter the incoming sound to generate the spatial cues that enable sound sources to be localised. The HRTF for a specific location in the virtual space at each time frame was computed by interpolating HRTFs from an example subject extracted from a database recorded in humans from a limited range of locations. Therefore, HRTFs were not personalised for each participant. However, previous evidence has shown that humans quickly adapt to non-personalised HRTFs (Mendonça et al., 2012; Parseihian & Katz, 2012). In the future, complete personalisation could be achieved by measuring HRTFs for individual participants by placing a microphone in each ear and recording the signal when sound is presented from a range of locations. Alternatively, scaling the HRTFs in frequency can be used to reduce the effects of individual differences in the size of the external ears (Xu & Middlebrooks, 2000).

Additionally, the 3D TuneIn tool also offers the possibility of simulating altered hearing, including hearing loss or the presence of a hearing device. Future studies could take advantage of this property to study adaptation of spatial hearing with training to stimulated hearing loss.

7. GENERAL DISCUSSION

7.1. Overview

Sensory experience calibrates the neural circuits involved in sensory processing allowing them to accommodate changes in inputs or environmental conditions. In adulthood, auditory plasticity is dependent on training and is key for adapting to perturbations in the sensory input, such as hearing loss. Much of the evidence for this has come from the experimental induction of reversible UCHL by monaurally occluding one ear, and this has now been widely used as a model to explore the adaptability of the developing and mature auditory system (Irving & Moore, 2011; Kacelnik et al., 2006; Keating et al., 2016).

Training in a sound localisation task has been shown to lead to the recovery of spatial hearing, which is initially severely disrupted by UCHL, in adult ferrets and humans (Kacelnik et al., 2006; Kumpik et al., 2010). How auditory spatial cues are integrated in the brain to ultimately decode sound source location is still under debate. Furthermore, how this neural representation is affected by UCHL and training-induced adaptation has not previously been addressed. In this study, we used chronic electrophysiological recordings from large numbers of neurons to explore how sound location is decoded in the IC of ferrets, and whether any neural correlates of auditory spatial plasticity could be found in this midbrain structure.

From a clinical point of view, this behavioural training is a potential form of therapeutic intervention to restore spatial hearing in people suffering from hearing loss. In this study, we also behaviourally characterised the persistence and generalisation of this training-induced learning in ferrets, which are key factors for determining its therapeutic value. In the laboratory, behavioural training is traditionally performed under rather unnatural acoustic conditions in which individuals relearn to localise well-isolated target sounds. Characterising whether this learning generalises to more naturalistic listening conditions will determine the value of such training as a potential treatment for individuals with hearing impairments. Moreover, defining how it is retained across time is clinically relevant for conditions such as otitis media with effusion, which usually manifests in a recurrent manner.

7.1.1. Behavioural characterisation of adaptation to UCHL

To explore the retention and retrieval of this learning, we repeatedly exposed a cohort of ferrets to periods of UCHL, by plugging one ear, interspaced with periods of binaural hearing of different duration. Repeated plugging of the same ear always resulted in an initial drop in sound localisation accuracy and thus further training was required in order for the animals to adapt. Nevertheless, this drop in performance was smaller relative to the first earplugging period, which showed the greatest disruption, indicating that learning leaves a 'memory trace', which facilitates adaptation when the same disruption is experienced again (also shown in Kacelnik et al., 2006; Bajo et al; 2019). The magnitude of the initial decrement in localisation accuracy was also positively correlated with the duration of the preceding period of balanced binaural hearing. Examining how

localisation accuracy changed in each hemifield provided insights into the possible processes underlying this adaptation. Sound localisation accuracy on the side ipsilateral to the open ear was found to be conserved across re-plugging periods, suggesting that rapid upweighting of the intact spectral cues provided by that ear provides an adaptation strategy. Evidence that spectral cues can be upweighted almost immediately has also been obtained in human participants wearing an earplug in one ear (Zonooz & Van Opstal, 2019) Further support for cue reweighting was also provided by the lack of overall improvement that we found for the localisation of high-frequency narrowband sounds (1/6-octave bandwidth centred at 15kHz), which do not provide any useful spectral information. By contrast, localisation accuracy on the side ipsilateral to the occluded ear was found to be degraded by re-plugging following a long period of normal hearing. This, together with the finding of progressive improvement at frontal locations in the same hemifield, is indicative of a cue remapping strategy, which would take place gradually. While these observations do not provide direct evidence for the bases for the recovery of sound localisation accuracy, they are consistent with previous findings in humans showing that both strategies can emerge in the same individual depending on the available spatial cues (Keating et al., 2016).

The removal of the earplug resulted in the restoration of pre-plug performance, which is consistent with greater dependence on the unchanged spectral cues available at the open ear. Given the evidence that binaural cue remapping also contributes, however, the lack of an after-effect following earplug removal suggests that adaptation is context specific, with different cues dominating the behaviour of the animals depending on how reliable they are (see Keating et al., 2013 for more direct evidence for this). This agrees with previous evidence demonstrating that humans can adapt to altered spectral cues and

switch between normal and modified cues depending on the context (Carlile & Blackman, 2014; Hofman et al., 1998). In the case of binaural cue alteration, however, a period of learning is required on each occasion that time UCHL is experienced. Moreover, when switching UCHL to the contralateral ear, we found that animals adapted with training, although to a lesser extent than that observed for the other ear. The training-induced changes that enable adaptation to UCHL in one direction could therefore be limiting adaptation in the other direction, which has implications for people experiencing recurrent hearing loss in both ears, as is often the case with otitis media.

We investigated generalisation of learning to untrained conditions by testing the ability of ferrets to localise sounds of different bandwidth in the presence or absence of background noise, with the earplug still in place, after they had adapted using the usual training. We found that learning generalised to untrained narrowband target stimulus (1 octave bandwidth centred at 16 kHz) when it was presented in silence and that the degree of generalisation was positively correlated with the level of adaptation achieved during training. This generalisation was degraded when background noise was present. However, performance was preserved in the presence of background noise when broadband target sounds were used.

In addition to assessing localisation accuracy using approach-to-target behaviour, we also measured the animals' head-orienting responses. We found a similar adaptation in head-orienting behaviour as that observed with the approach-to-target responses, including the retention of learning following re-plugging. Head-orienting movements have been suggested to be dependent on subcortical processing (Isa et al., 2021; Lomber et al., 2001), and so adaptation of this behaviour could be indicative of a downstream transmission of learning. This agrees with the reverse hierarchy theory proposed by

(Ahissar & Hochstein, 2004), which suggests that perceptual learning originates in the cortex and is then guided by top-down influences. Previous evidence has shown that silencing AC impairs adaptation to UCHL, but not the retrieval of previous learning (Bajo et al., 2019), indicating that the AC is necessary for adapting to UCHL, while the retention of this learning is likely occurring somewhere else, probably in a subcortical structure to which the AC projects. This is further supported by prior evidence demonstrating that ablation of the corticocollicular pathway, which connects the AC with the IC, impairs adaptation to UCHL (Bajo et al., 2010). Altogether, these findings implicate the IC, a subcortical structure that receives substantial cortical input, as a possible centre for the consolidation of learning during the adaptation to UCHL.

7.1.2. Sound location encoding in the IC

The IC is a midbrain structure, which receives input from parallel ascending pathways from the brainstem that encode auditory spatial cues (Grothe et al., 2010). Many studies have investigated the spatial sensitivity of IC neurons [e.g. (Chase & Young, 2008; Kuwada et al., 1989)] and some have also proposed models to explain how sound location may be encoded by the IC (Day & Delgutte, 2013; McAlpine et al., 2001). However, these studies have traditionally been performed under anaesthesia [e.g. (Chase & Young, 2008; Dahmen et al., 2010; McAlpine et al., 2001)] and, on some occasions, in head-restrained awake animals [e.g.(Dorkoski et al., 2020; Day & Delgutte, 2013)]. Most of the published literature has also focused on characterising sensitivity to individual spatial cues, with only some studies exploring sound source azimuth tuning, often restricted to the frontal hemifield (e.g. Day & Delgutte, 2013) or the integration of different spatial

cues (Chase & Young, 2008). Furthermore, how neural responses in the IC are affected by the onset of UCHL and whether any changes associated with auditory spatial learning can be found in this structure remains largely unexplored, with only one study describing the effect of exposure to UCHL on IC responses in adult animals (chinchilla) (Thornton et al., 2021).

An innovation of our study is that we chronically implanted a cohort of ferrets (N=3) with high-density recording probes bilaterally in the IC, allowing us to record spiking activity of freely-moving animals while they were engaged in a sound localisation task. We recorded activity in normal hearing conditions and all the way throughout adaption to UCHL, generating an unprecedented set of recordings.

Most of the recordings were performed in the central nucleus of the IC, with some recording sites in the lateral and dorsal cortex of the IC. Most neurons were driven by sound presentation and a wide range of response types was found based on their temporal profiles, with most neurons showing an increased firing rate throughout the duration of the sound presentation. Regarding their spatial sensitivity, neurons tended to show a contralateral preference, exhibiting greater firing rates when sounds were presented in the contralateral side of space, agreeing with that described by previous studies (Aitkin et al., 1984; Day & Delgutte, 2013; Kuwada et al., 2011). The azimuth-rate functions varied greatly in their width, and the spatial tuning of neurons was sharper in awake behaving ferrets than under anaesthesia, agreeing with similar findings in the AC (Mickey & Middlebrooks, 2003). We also observed an effect of task engagement on pre-stimulus activity, which was reduced in the behaving ferrets, but not under anaesthesia, which could be an effect of attention, motivation, or expectation of the trial presentation. Previous studies have also shown that activity in the IC is altered by reward and

behavioural context (Metzger et at., 2006) and that pre-stimulus activity in the IC is even informative of the trial outcome in a sound detection task (Lee et al., 2023). Our findings therefore add to the growing evidence that IC neurons are influenced by the animals' brain state and the behavioural context in which the responses are recorded.

To explore how sound location is decoded by neural responses in the IC, we trained a population pattern decoder to estimate sound azimuth using combined activity from both ICs. Agreeing with previous studies (Day & Delgutte, 2013), we found that sound source location can be accurately decoded from these responses. In particular, IC activity was more informative about stimulus position in the left-right axis than in the back-front axis, which is consistent with a hemispheric two-channel model (McAlpine et al., 2001) by which sound location is computed by comparing the activity of two opposingly tuned populations, the contralaterally tuned ICs. This was further supported by a collapsed two-channel decoder, a variant of the pattern decoder for which the activity of each hemisphere was collapsed into a single spike train, resulting in two opponent single channels. With this decoder, the estimation of sound location in the left-right axis was similar to the population pattern decoder. Nevertheless, decoding the back-front axis was worse in the collapsed model and, overall, azimuth decoding was degraded relative to the population decoder, indicating that further spatial information is likely provided in the pattern of spikes produced by different neurons. The pattern of spikes produced by IC neurons has previously been shown to be important for representing spatial information, with different cues being encoded using different aspects of the spike discharge train, such as the first-spike latency, ongoing spike timing, and discharge rate (Chase & Young, 2008). This indicates that IC neurons may multiplex information from different cues. Multiplexing of different sound features has also been shown in neurons in the AC, by

modulating their firing rate in specific temporal windows (Walker et al., 2011). The multiplexing of different stimulus parameters in the pattern of spikes using different neural codes potentially allows the encoding of sensory features in manner that is invariant to changes in other features.

Our population pattern decoder showed that activity at the onset of the stimulus was the most informative time window about sound location in the left-right axis, which could explain the very low incidence of left-right errors in ferret localisation behaviour under normal hearing conditions, while back-front errors are more common, particularly when the stimulus duration is reduced (Nodal et al., 2008).

7.1.3. Neural correlates of adaptation to UCHL in the IC

We further explored how spatial responses in the IC are affected by the appearance of UCHL and whether any neural changes could be found that might explain the recovery in localisation behaviour. As expected, the induction of UCHL by plugging one ear greatly affected activity in the IC. In the IC contralateral to the plugged ear, neural activity was inhibited by sound, which can be explained by a reduction of excitation from the plugged side altering the balance of ipsilateral inhibition and contralateral excitation. By contrast, neurons in the ipsilateral IC were excited by sound presentation during the behavioural task, and showed a broadening of their spatial tuning, likely reflecting the reduction in inhibition from the plugged side. Therefore, activity in the IC in the presence of UCHL greatly differed from that observed prior to UCHL, which is normally characterised by two opposingly activated populations as we have described before. As a consequence, responses in the IC became less informative about sound source location,

as shown by a reduction in decoding accuracy, coinciding with a drop in the animals' sound localisation performance.

Training the population pattern decoder with data from individual sessions recorded throughout adaptation to UCHL revealed an improvement in the representation of sound location in the IC across sessions, which was also associated with the improvement in localisation accuracy as the animals adapted to the presence of the earplug. This was accompanied by an increase in the units' decoding weight at the onset of the stimulus and an increase in the sharpening of tuning in the IC ipsilateral to the plugged ear, indicative of compensatory changes to UCHL occurring in (or before the level of) the IC. Changes in the IC following exposure to UCHL have previously been described by Thornton et al., 2021, although in this study recordings were exclusively performed after UCHL exposure and in anaesthetised animals. After earplug removal, we found that the contralateral preference of the IC neurons was restored and with that, the sound azimuth decoding accuracy. This is consistent with the lack of aftereffect in the animals' behaviour, with localisation accuracy returning to preplug levels within the first session (Kacelnik et al., 2006).

Following re-plugging, the effects of UCHL in the IC were less pronounced, as shown by a smaller suppression in the contralateral IC and a reduction in the azimuth decoding error, again matching the ferrets' behaviour. This suggests that changes in the IC associated with adaptation to UCHL could be involved in the consolidation and retrieval of learning, as pointed by previous studies (Bajo et al., 2019; Bajo et al., 2010).

Adaptation to UCHL has been shown to be dependent on activity in A1 (Bajo et al., 2010; Nodal et al., 2010) and its descending projection to the IC via the corticocollicular pathway (Bajo et al., 2010). In this study we have shown that changes occur in the IC

responses that correspond to the behavioural plasticity associated with adaptation to UCHL, and we hypothesise that these could be derived from the influence of the AC. The modulation of activity in the IC by the AC as previously been demonstrated by electrical stimulation studies (Jen et al., 1998; Syka & Popelár, 1984; Torterolo et al., 1998). Moreover, adaptation to further earplugging periods was no longer found to be dependent on A1 activity (Bajo et al., 2019), but is associated with corresponding changes in the IC: both the behavioural and neural data reveal a less disruptive effect of repeatedly re-plugging the same ear. We therefore conclude that the IC could be a centre for the consolidation of this learning.

7.2. Future studies

In this study, we have focused on investigating how sound source location is encoded in the IC under normal hearing conditions and how this representation changes as a consequence of monaural hearing loss, which results in the disruption of spatial cues. Moreover, we have shown that compensatory changes occur in the response properties of IC neurons, which occur in parallel with the behavioural adaptation to UCHL. This provides direct, albeit correlative evidence in support of previous studies pointing to the IC as an important element in the circuits involved in this process of training-induced learning. Future work will need to address the challenging question of the relative contributions of spatial cue reweighting and binaural cue remapping to the plasticity observed in the IC. Our observations suggest that cue reweighting may dominant the initial phase of adaptation, while remapping takes place more gradually. However, further electrophysiological recording studies are needed to show whether the same or different

populations of neurons are involved in mediating both types of plasticity and whether the cue multiplexing proposed in the IC by Chase and Young (2008) can be affected by learning.

While we have focused on the auditory midbrain, our findings do not exclude the involvement of other circuits in adaptation to UCHL. We attempted to record simultaneously from both the AC and the IC, but the cortical recordings were much less successful. This is important because greater plasticity was observed in the AC than in the IC following monaural deprivation in rats (Popescu & Polley, 2010). It therefore remains to be seen how cortical response properties change in ferrets during adaptation to UCHL, whether differences exist with the plasticity that we have observed in the IC, and whether this is consistent with top-down cortical influences leading to the establishment of a memory trace in the IC (but not in AC).

Projections from the AC to other subcortical brain regions also need to be assessed. In particular, auditory cortical inputs to the striatum have been shown to be involved in the learning of an auditory discrimination task (Xiong et al., 2015). Selective potentiation of frequency-specific corticostriatal synapses based on the reward contingency can occur throughout learning, with synaptic efficacy reflecting the behavioural performance in the task. Moreover, the response properties of striatal neurons have been shown to be disrupted by developmental hearing loss (Mowery et al., 2017), while inactivation of corticostriatal neurons disrupts auditory perceptual learning (Paraouty & Mowery, 2021). Future studies will therefore be needed to explore whether the corticostriatal projection plays any role in sound localisation plasticity and how this circuit interacts with the corticocollicular pathway to achieve learning.

In this thesis, we also performed behavioural studies in ferrets to further characterise the process of adaptation, specifically investigating the persistence and generalisation of this learning to untrained stimuli. Further studies will be needed in humans to explore whether observations in ferrets are translatable to humans. However, the extent to which generalisation of learning can be assessed is limited by the physical constraints of the experimental setup. To overcome this, as part of my DPhil, we developed a testing setup for humans using virtual reality, which would essentially allow the testing of sound localisation in any listening condition. Future studies will be performed to test how human participants adapt to monaural earplugging in this virtual setup and how that compares to simulated monaural hearing loss. Moreover, the listening conditions can be readily manipulated to more extensively test the generalisation of learning, with unrestricted number of sound sources and sound locations.

Another important advantage offered by this approach is real-time spatialisation of sounds using a head-mounted setup, which allows free head movements and precise tracking of head orienting responses. With this setup, we could address the study of the importance of motor actions in the adaptation to UCHL, widely overlooked in psychophysical studies of sound localisation in humans, which are usually performed with the head restrained by a chin-rest. A study using VR has shown faster and greater adaptation to monaural hearing loss in participants who reported the perceived location of the sound source by reaching toward it rather than naming it, with this improvement thought to be linked to the use of head movements to explore the auditory space (Valzolgher et al., 2020). Other studies have also pointed to the importance of audio-motor integration in sound localisation (Aytekin et al., 2008; Tollin et al., 2005) and in the accommodation of altered cues (Carlile, 2014).

REFERENCES

Agterberg, M. J., Hol, M. K., Van Wanrooij, M. M., Van Opstal, A. J., & Snik, A. F. (2014). Single-sided deafness and directional hearing: contribution of spectral cues and high-frequency hearing loss in the hearing ear. *Front Neurosci*, *8*, 188. https://doi.org/10.3389/fnins.2014.00188

Aharonson, V., & Furst, M. (2001). A model for sound lateralization. *J Acoust Soc Am*, *109*(6), 2840-2851. https://doi.org/10.1121/1.1371756

Ahissar, M., & Hochstein, S. (2004). The reverse hierarchy theory of visual perceptual learning. *Trends Cogn Sci*, *8*(10), 457-464. https://doi.org/10.1016/j.tics.2004.08.011

Aitkin, L. M., Gates, G. R., & Phillips, S. C. (1984). Responses of neurons in inferior colliculus to variations in sound-source azimuth. *J Neurophysiol*, *52*(1), 1-17. https://doi.org/10.1152/jn.1984.52.1.1

Andersen, R. A., Snyder, R. L., & Merzenich, M. M. (1980). The topographic organization of corticocollicular projections from physiologically identified loci in the AI, AII, and anterior auditory cortical fields of the cat. *J Comp Neurol*, *191*(3), 479-494. https://doi.org/10.1002/cne.901910310

Ausili, S. A., & Snapp, H. A. (2023). Contralateral Routing of Signal Disrupts Monaural Sound Localization. *Audiol Res*, *13*(4), 586-599. https://doi.org/10.3390/audiolres13040051

Aytekin, M., Moss, C. F., & Simon, J. Z. (2008). A Sensorimotor Approach to Sound Localization. *Neural Computation*, *20*(3), 603-635. https://doi.org/10.1162/neco.2007.12-05-094

Bajo, V. M., & King, A. J. (2012). Cortical modulation of auditory processing in the midbrain. *Front Neural Circuits*, *6*, 114. https://doi.org/10.3389/fncir.2012.00114

Bajo, V. M., Nodal, F. R., Bizley, J. K., & King, A. J. (2010b). The non-lemniscal auditory cortex in ferrets: convergence of corticotectal inputs in the superior colliculus. *Front Neuroanat*, *4*, 18. https://doi.org/10.3389/fnana.2010.00018

Bajo, V. M., Nodal, F. R., Bizley, J. K., Moore, D. R., & King, A. J. (2007). The ferret auditory cortex: descending projections to the inferior colliculus. *Cereb Cortex*, *17*(2), 475-491. https://doi.org/10.1093/cercor/bhj164

Bajo, V. M., Nodal, F. R., Korn, C., Constantinescu, A. O., Mann, E. O., Boyden, E. S., 3rd, & King, A. J. (2019). Silencing cortical activity during sound-localization training impairs auditory perceptual learning. *Nat Commun*, *10*(1), 3075. https://doi.org/10.1038/s41467-019-10770-4

Bajo, V. M., Nodal, F. R., Moore, D. R., & King, A. J. (2010). The descending corticocollicular pathway mediates learning-induced auditory plasticity. *Nat Neurosci*, *13*(2), 253-260. https://doi.org/10.1038/nn.2466

Bergan, J. F., Ro, P., Ro, D., & Knudsen, E. I. (2005). Hunting increases adaptive auditory map plasticity in adult barn owls. *J Neurosci*, *25*(42), 9816-9820. https://doi.org/10.1523/jneurosci.2533-05.2005

Boffi, J. C., Bathellier, B., Asari, H., & Prevedel, R. (2022). Effective sound localization coding by noisy populations of mouse inferior colliculus neurons revealed by fast volumetric imaging. *bioRxiv*, 2022.2008.2019.504510. https://doi.org/10.1101/2022.08.19.504510

Boudreau, J. C., & Tsuchitani, C. (1968). Binaural interaction in the cat superior olive S segment. *J Neurophysiol*, *31*(3), 442-454. https://doi.org/10.1152/jn.1968.31.3.442

Brainard, M. S., & Knudsen, E. I. (1998). Sensitive periods for visual calibration of the auditory space map in the barn owl optic tectum. *J Neurosci*, *18*(10), 3929-3942. https://doi.org/10.1523/jneurosci.18-10-03929.1998

Brand, A., Behrend, O., Marquardt, T., McAlpine, D., & Grothe, B. (2002). Precise inhibition is essential for microsecond interaural time difference coding. *Nature*, *417*(6888), 543-547. https://doi.org/10.1038/417543a

Campbell, R. A., Doubell, T. P., Nodal, F. R., Schnupp, J. W., & King, A. J. (2006). Interaural timing cues do not contribute to the map of space in the ferret superior colliculus: a virtual acoustic space study. *J Neurophysiol*, *95*(1), 242-254. https://doi.org/10.1152/jn.00827.2005

Carlile, S. (1990). The auditory periphery of the ferret. I: Directional response properties and the pattern of interaural level differences. *J Acoust Soc Am*, *88*(5), 2180-2195. https://doi.org/10.1121/1.400115

Carlile, S. (2014). The plastic ear and perceptual relearning in auditory spatial perception. *Front Neurosci*, *8*, 237. https://doi.org/10.3389/fnins.2014.00237

Carlile, S., Balachandar, K., & Kelly, H. (2014). Accommodating to new ears: The effects of sensory and sensory-motor feedback. *The Journal of the Acoustical Society of America*, *135*(4), 2002-2011. https://doi.org/10.1121/1.4868369

Carlile, S., & Blackman, T. (2014). Relearning auditory spectral cues for locations inside and outside the visual field. *J Assoc Res Otolaryngol*, *15*(2), 249-263. https://doi.org/10.1007/s10162-013-0429-5

Carr, C. E., & Konishi, M. (1988). Axonal delay lines for time measurement in the owl's brainstem. *Proc Natl Acad Sci U S A*, *85*(21), 8311-8315. https://doi.org/10.1073/pnas.85.21.8311

Chase, S. M., & Young, E. D. (2008). Cues for sound localization are encoded in multiple aspects of spike trains in the inferior colliculus. *J Neurophysiol*, *99*(4), 1672-1682. https://doi.org/10.1152/jn.00644.2007

Cherry, E. C. (1953). Some Experiments on the Recognition of Speech, with One and with Two Ears. *The Journal of the Acoustical Society of America*, *25*(5), 975-979. https://doi.org/10.1121/1.1907229

Cuevas-Rodríguez, M., Picinali, L., González-Toledo, D., Garre, C., de la Rubia-Cuestas, E., Molina-Tanco, L., & Reyes-Lecuona, A. (2019). 3D Tune-In Toolkit: An open-source library for real-time binaural spatialisation. *PLoS One*, *14*(3), e0211899. https://doi.org/10.1371/journal.pone.0211899

Dahmen, J. C., Keating, P., Nodal, F. R., Schulz, A. L., & King, A. J. (2010). Adaptation to stimulus statistics in the perception and neural representation of auditory space. *Neuron*, *66*(6), 937-948. https://doi.org/10.1016/j.neuron.2010.05.018

Dahmen, J. C., & King, A. J. (2007). Learning to hear: plasticity of auditory cortical processing. *Curr Opin Neurobiol*, *17*(4), 456-464. https://doi.org/10.1016/j.conb.2007.07.004

Davis, K. A. (2002). Evidence of a functionally segregated pathway from dorsal cochlear nucleus to inferior colliculus. *J Neurophysiol*, *87*(4), 1824-1835. https://doi.org/10.1152/jn.00769.2001

Davis, K. A., Ramachandran, R., & May, B. J. (2003). Auditory processing of spectral cues for sound localization in the inferior colliculus. *J Assoc Res Otolaryngol*, *4*(2), 148-163. https://doi.org/10.1007/s10162-002-2002-5

Day, M. L., & Delgutte, B. (2013). Decoding sound source location and separation using neural population activity patterns. *J Neurosci*, *33*(40), 15837-15847. https://doi.org/10.1523/JNEUROSCI.2034-13.2013

Day, M. L., & Delgutte, B. (2016). Neural population encoding and decoding of sound source location across sound level in the rabbit inferior colliculus. *J Neurophysiol*, *115*(1), 193-207. https://doi.org/10.1152/jn.00643.2015

Delgutte, B., Joris, P. X., Litovsky, R. Y., & Yin, T. C. (1999). Receptive fields and binaural interactions for virtual-space stimuli in the cat inferior colliculus. *J Neurophysiol*, *81*(6), 2833-2851. https://doi.org/10.1152/jn.1999.81.6.2833

Derey, K., Valente, G., de Gelder, B., & Formisano, E. (2016). Opponent Coding of Sound Location (Azimuth) in Planum Temporale is Robust to Sound-Level Variations. *Cereb Cortex*, *26*(1), 450-464. https://doi.org/10.1093/cercor/bhv269

Dorkoski, R., Hancock, K. E., Whaley, G. A., Wohl, T. R., Stroud, N. C., & Day, M. L. (2020). Stimulus-frequency-dependent dominance of sound localization cues across the cochleotopic map of the inferior colliculus. *J Neurophysiol*, *123*(5), 1791-1807. https://doi.org/10.1152/jn.00713.2019

Dosher, B. A., Jeter, P., Liu, J., & Lu, Z.-L. (2013). An integrated reweighting theory of perceptual learning. *Proceedings of the National Academy of Sciences*, *110*(33), 13678-13683. https://doi.org/doi:10.1073/pnas.1312552110

Erulkar, S. D. (1972). Comparative aspects of spatial localization of sound. *Physiol Rev*, *52*(1), 237-360. https://doi.org/10.1152/physrev.1972.52.1.237

Franken, T. P., Joris, P. X., & Smith, P. H. (2018). Principal cells of the brainstem's interaural sound level detector are temporal differentiators rather than integrators. *Elife*, *7*. https://doi.org/10.7554/eLife.33854

Franken, T. P., Roberts, M. T., Wei, L., Golding, N. L., & Joris, P. X. (2015). In vivo coincidence detection in mammalian sound localization generates phase delays. *Nat Neurosci*, *18*(3), 444-452. https://doi.org/10.1038/nn.3948

Glennon, E., Svirsky, M. A., & Froemke, R. C. (2020). Auditory cortical plasticity in cochlear implant users. *Curr Opin Neurobiol*, *60*, 108-114. https://doi.org/10.1016/j.conb.2019.11.003

Gold, J. I., & Knudsen, E. I. (2000a). Abnormal auditory experience induces frequency-specific adjustments in unit tuning for binaural localization cues in the optic tectum of juvenile owls. *J Neurosci*, *20*(2), 862-877. https://doi.org/10.1523/jneurosci.20-02-00862.2000

Gold, J. I., & Knudsen, E. I. (2000b). A site of auditory experience-dependent plasticity in the neural representation of auditory space in the barn owl's inferior colliculus. *J Neurosci*, *20*(9), 3469-3486. https://doi.org/10.1523/jneurosci.20-09-03469.2000

Grothe, B., & Pecka, M. (2014). The natural history of sound localization in mammals--a story of neuronal inhibition. *Front Neural Circuits*, *8*, 116. https://doi.org/10.3389/fncir.2014.00116

Grothe, B., Pecka, M., & McAlpine, D. (2010). Mechanisms of sound localization in mammals. *Physiol Rev*, *90*(3), 983-1012. https://doi.org/10.1152/physrev.00026.2009

Hancock, K. E., & Voigt, H. F. (1999). Wideband inhibition of dorsal cochlear nucleus type IV units in cat: a computational model. *Annals of biomedical engineering*, *27*, 73-87.

Heffner, H. E., & Heffner, R. S. (1990). Effect of bilateral auditory cortex lesions on sound localization in Japanese macaques. *J Neurophysiol*, *64*(3), 915-931. https://doi.org/10.1152/jn.1990.64.3.915

Herbert, H., Aschoff, A., & Ostwald, J. (1991). Topography of projections from the auditory cortex to the inferior colliculus in the rat. *J Comp Neurol*, *304*(1), 103-122. https://doi.org/10.1002/cne.903040108

Higgins, N. C., McLaughlin, S. A., Rinne, T., & Stecker, G. C. (2017). Evidence for cue-independent spatial representation in the human auditory cortex during active listening. *Proc Natl Acad Sci U S A*, *114*(36), E7602-E7611. https://doi.org/10.1073/pnas.1707522114

Hill, D. N., Mehta, S. B., & Kleinfeld, D. (2011). Quality metrics to accompany spike sorting of extracellular signals. *J Neurosci*, *31*(24), 8699-8705. https://doi.org/10.1523/jneurosci.0971-11.2011

Hofman, P. M., Van Riswick, J. G., & Van Opstal, A. J. (1998). Relearning sound localization with new ears. *Nat Neurosci*, *1*(5), 417-421. https://doi.org/10.1038/1633

Hogan, S. C., Stratford, K. J., & Moore, D. R. (1997). Duration and recurrence of otitis media with effusion in children from birth to 3 years: prospective study using monthly otoscopy and tympanometry. *Bmj*, *314*(7077), 350-353. https://doi.org/10.1136/bmj.314.7077.350

Irvine, D. R. F. (2018). Auditory perceptual learning and changes in the conceptualization of auditory cortex. *Hear Res*, *366*, 3-16. https://doi.org/10.1016/j.heares.2018.03.011

Irving, S., & Moore, D. R. (2011). Training sound localization in normal hearing listeners with and without a unilateral ear plug. *Hear Res*, *280*(1-2), 100-108. https://doi.org/10.1016/j.heares.2011.04.020

Isa, T., Marquez-Legorreta, E., Grillner, S., & Scott, E. K. (2021). The tectum/superior colliculus as the vertebrate solution for spatial sensory integration and action. *Curr Biol*, *31*(11), R741-R762. https://doi.org/10.1016/j.cub.2021.04.001

Ito, S., Si, Y., Feldheim, D. A., & Litke, A. M. (2020). Spectral cues are necessary to encode azimuthal auditory space in the mouse superior colliculus. *Nat Commun*, *11*(1), 1087. https://doi.org/10.1038/s41467-020-14897-7

Jeffress, L. A. (1948). A place theory of sound localization. *J Comp Physiol Psychol*, *41*(1), 35-39. https://doi.org/10.1037/h0061495

Jen, P. H., Chen, Q. C., & Sun, X. D. (1998). Corticofugal regulation of auditory sensitivity in the bat inferior colliculus. *J Comp Physiol A*, *183*(6), 683-697. https://doi.org/10.1007/s003590050291

Jenkins, W. M., & Masterton, R. B. (1982). Sound localization: effects of unilateral lesions in central auditory system. *J Neurophysiol*, *47*(6), 987-1016. https://doi.org/10.1152/jn.1982.47.6.987

Jenkins, W. M., & Merzenich, M. M. (1984). Role of cat primary auditory cortex for sound-localization behavior. *J Neurophysiol*, *52*(5), 819-847. https://doi.org/10.1152/jn.1984.52.5.819

Joris, P. X., Carney, L. H., Smith, P. H., & Yin, T. C. (1994). Enhancement of neural synchronization in the anteroventral cochlear nucleus. I. Responses to tones at the characteristic frequency. *J Neurophysiol*, *71*(3), 1022-1036. https://doi.org/10.1152/jn.1994.71.3.1022

Kacelnik, O., Nodal, F. R., Parsons, C. H., & King, A. J. (2006). Training-induced plasticity of auditory localization in adult mammals. *PLoS Biol*, *4*(4), e71. https://doi.org/10.1371/journal.pbio.0040071

Karino, S., Smith, P. H., Yin, T. C., & Joris, P. X. (2011). Axonal branching patterns as sources of delay in the mammalian auditory brainstem: a re-examination. *J Neurosci*, *31*(8), 3016-3031. https://doi.org/10.1523/jneurosci.5175-10.2011

Kasai, M., Ono, M., & Ohmori, H. (2012). Distinct neural firing mechanisms to tonal stimuli offset in the inferior colliculus of mice in vivo. *Neurosci Res*, *73*(3), 224-237. https://doi.org/10.1016/j.neures.2012.04.009

Keating, P., Dahmen, J. C., & King, A. J. (2013). Context-specific reweighting of auditory spatial cues following altered experience during development. *Curr Biol*, *23*(14), 1291-1299. https://doi.org/10.1016/j.cub.2013.05.045

Keating, P., Dahmen, J. C., & King, A. J. (2015). Complementary adaptive processes contribute to the developmental plasticity of spatial hearing. *Nat Neurosci*, *18*(2), 185-187. https://doi.org/10.1038/nn.3914

Keating, P., & King, A. J. (2013). Developmental plasticity of spatial hearing following asymmetric hearing loss: context-dependent cue integration and its clinical implications. *Front Syst Neurosci*, *7*, 123. https://doi.org/10.3389/fnsys.2013.00123

Keating, P., & King, A. J. (2015). Sound localization in a changing world. *Curr Opin Neurobiol*, *35*, 35-43. https://doi.org/10.1016/j.conb.2015.06.005

Keating, P., Nodal, F. R., & King, A. J. (2014). Behavioural sensitivity to binaural spatial cues in ferrets: evidence for plasticity in the duplex theory of sound localization. *Eur J Neurosci*, *39*(2), 197-206. https://doi.org/10.1111/ejn.12402

Keating, P., Rosenior-Patten, O., Dahmen, J. C., Bell, O., & King, A. J. (2016). Behavioral training promotes multiple adaptive processes following acute hearing loss. *Elife*, *5*, e12264. https://doi.org/10.7554/eLife.12264

King, A. J., Bajo, V. M., Bizley, J. K., Campbell, R. A., Nodal, F. R., Schulz, A. L., & Schnupp, J. W. (2007). Physiological and behavioral studies of spatial coding in the auditory cortex. *Hear Res*, *229*(1-2), 106-115. https://doi.org/10.1016/j.heares.2007.01.001

King, A. J., & Hutchings, M. E. (1987). Spatial response properties of acoustically responsive neurons in the superior colliculus of the ferret: a map of auditory space. *J Neurophysiol*, *57*(2), 596-624. https://doi.org/10.1152/jn.1987.57.2.596

King, A. J., Hutchings, M. E., Moore, D. R., & Blakemore, C. (1988). Developmental plasticity in the visual and auditory representations in the mammalian superior colliculus. *Nature*, *332*(6159), 73-76. https://doi.org/10.1038/332073a0

King, A. J., Schnupp, J. W., & Thompson, I. D. (1998). Signals from the superficial layers of the superior colliculus enable the development of the auditory space map in the deeper layers. *J Neurosci*, *18*(22), 9394-9408. https://doi.org/10.1523/jneurosci.18-22-09394.1998

Knudsen, E. I., & Knudsen, P. F. (1985). Vision guides the adjustment of auditory localization in young barn owls. *Science*, *230*(4725), 545-548. https://doi.org/10.1126/science.4048948

Knudsen, E. I., Knudsen, P. F., & Esterly, S. D. (1984). A critical period for the recovery of sound localization accuracy following monaural occlusion in the barn owl. *J Neurosci*, *4*(4), 1012-1020. https://doi.org/10.1523/jneurosci.04-04-01012.1984

Knudsen, E. I., & Mogdans, J. (1992). Vision-independent adjustment of unit tuning to sound localization cues in response to monaural occlusion in developing owl optic tectum. *J Neurosci*, *12*(9), 3485-3493. https://doi.org/10.1523/jneurosci.12-09-03485.1992

Kopp-Scheinpflug, C., Sinclair, J. L., & Linden, J. F. (2018). When Sound Stops: Offset Responses in the Auditory System. *Trends Neurosci*, *41*(10), 712-728. https://doi.org/10.1016/j.tins.2018.08.009

Kumpik, D. P., Kacelnik, O., & King, A. J. (2010). Adaptive reweighting of auditory localization cues in response to chronic unilateral earplugging in humans. *J Neurosci*, *30*(14), 4883-4894. https://doi.org/10.1523/JNEUROSCI.5488-09.2010

Kumpik, D. P., & King, A. J. (2019). A review of the effects of unilateral hearing loss on spatial hearing. *Hear Res*, *372*, 17-28. https://doi.org/10.1016/j.heares.2018.08.003

Kuwada, S., Batra, R., & Stanford, T. R. (1989). Monaural and binaural response properties of neurons in the inferior colliculus of the rabbit: effects of sodium pentobarbital. *J Neurophysiol*, *61*(2), 269-282. https://doi.org/10.1152/jn.1989.61.2.269

Kuwada, S., Bishop, B., Alex, C., Condit, D. W., & Kim, D. O. (2011). Spatial tuning to sound-source azimuth in the inferior colliculus of unanesthetized rabbit. *J Neurophysiol*, *106*(5), 2698-2708. https://doi.org/10.1152/jn.00532.2011

Lee, C. C., & Middlebrooks, J. C. (2011). Auditory cortex spatial sensitivity sharpens during task performance. *Nat Neurosci*, *14*(1), 108-114. https://doi.org/10.1038/nn.2713

Lee, T.-Y., Weissenberger, Y., King, A. J., & Dahmen, J. C. (2023). Midbrain encodes sound detection behavior without auditory cortex. In: eLife Sciences Publications, Ltd.

Linton, P. (2023). Minimal theory of 3D vision: new approach to visual scale and visual shape. *Philos Trans R Soc Lond B Biol Sci*, *378*(1869), 20210455. https://doi.org/10.1098/rstb.2021.0455

Loftus, W. C., Bishop, D. C., & Oliver, D. L. (2010). Differential patterns of inputs create functional zones in central nucleus of inferior colliculus. *J Neurosci*, *30*(40), 13396-13408. https://doi.org/10.1523/jneurosci.0338-10.2010

Lomber, S. G., Payne, B. R., & Cornwell, P. (2001). Role of the superior colliculus in analyses of space: superficial and intermediate layer contributions to visual orienting, auditory orienting, and visuospatial discriminations during unilateral and bilateral deactivations. *J Comp Neurol*, *441*(1), 44-57. https://doi.org/10.1002/cne.1396

Ma, X., & Suga, N. (2001). Corticofugal modulation of duration-tuned neurons in the midbrain auditory nucleus in bats. *Proc Natl Acad Sci U S A*, *98*(24), 14060-14065. https://doi.org/10.1073/pnas.241517098

Macpherson, E. A., & Middlebrooks, J. C. (2002). Listener weighting of cues for lateral angle: the duplex theory of sound localization revisited. *J Acoust Soc Am*, *111*(5 Pt 1), 2219-2236. https://doi.org/10.1121/1.1471898

Malhotra, S., Hall, A. J., & Lomber, S. G. (2004). Cortical control of sound localization in the cat: unilateral cooling deactivation of 19 cerebral areas. *J Neurophysiol*, *92*(3), 1625-1643. https://doi.org/10.1152/jn.01205.2003

McAlpine, D. (2005). Creating a sense of auditory space. *J Physiol*, *566*(Pt 1), 21-28. https://doi.org/10.1113/jphysiol.2005.083113

McAlpine, D., Jiang, D., & Palmer, A. R. (2001). A neural code for low-frequency sound localization in mammals. *Nat Neurosci*, *4*(4), 396-401. https://doi.org/10.1038/86049

Mendonca, C. (2014). A review on auditory space adaptations to altered head-related cues. *Front Neurosci*, *8*, 219. https://doi.org/10.3389/fnins.2014.00219

Mendonça, C., Campos, G., Dias, P., & Santos, J. A. (2013). Learning Auditory Space: Generalization and Long-Term Effects. *PLoS One*, *8*(10), e77900. https://doi.org/10.1371/journal.pone.0077900

Mendonça, C., Campos, G., Dias, P., Vieira, J., Ferreira, J. P., & Santos, J. A. (2012). On the improvement of localization accuracy with non-individualized HRTF-based sounds. *Journal of the Audio Engineering Society*, *60*(10), 821-830.

Merzenich, M. M., & Reid, M. D. (1974). Representation of the cochlea within the inferior colliculus of the cat. *Brain Res*, *77*(3), 397-415. https://doi.org/10.1016/0006-8993(74)90630-1

Metzger, R. R., Greene, N. T., Porter, K. K., & Groh, J. M. (2006). Effects of reward and behavioral context on neural activity in the primate inferior colliculus. *J Neurosci*, *26*(28), 7468-7476. https://doi.org/10.1523/JNEUROSCI.5401-05.2006

Meyers, E. M. (2013). The neural decoding toolbox. *Front Neuroinform*, *7*, 8. https://doi.org/10.3389/fninf.2013.00008

Mickey, B. J., & Middlebrooks, J. C. (2003). Representation of auditory space by cortical neurons in awake cats. *J Neurosci*, *23*(25), 8649-8663. https://doi.org/10.1523/jneurosci.23-25-08649.2003

Middlebrooks, J., & Knudsen, E. (1984). A neural code for auditory space in the cat's superior colliculus. *The Journal of Neuroscience*, *4*(10), 2621-2634. https://doi.org/10.1523/jneurosci.04-10-02621.1984

Middlebrooks, J. C. (2015). Sound localization. *Handb Clin Neurol*, *129*, 99-116. https://doi.org/10.1016/b978-0-444-62630-1.00006-8

Middlebrooks, J. C. (2021). A Search for a Cortical Map of Auditory Space. *J Neurosci*, *41*(27), 5772-5778. https://doi.org/10.1523/jneurosci.0501-21.2021

Middlebrooks, J. C., Clock, A. E., Xu, L., & Green, D. M. (1994). A panoramic code for sound location by cortical neurons. *Science*, *264*(5160), 842-844. https://doi.org/10.1126/science.8171339

Middlebrooks, J. C., Xu, L., Eddins, A. C., & Green, D. M. (1998). Codes for sound-source location in nontonotopic auditory cortex. *J Neurophysiol*, *80*(2), 863-881. https://doi.org/10.1152/jn.1998.80.2.863

Mills, A. W. (1958). On the Minimum Audible Angle. *The Journal of the Acoustical Society of America*, *30*(4), 237-246. https://doi.org/10.1121/1.1909553

Mitchell, D. E., & Maurer, D. (2022). Critical Periods in Vision Revisited. *Annu Rev Vis Sci*, *8*, 291-321. https://doi.org/10.1146/annurev-vision-090721-110411

Mogdans, J., & Knudsen, E. I. (1992). Adaptive adjustment of unit tuning to sound localization cues in response to monaural occlusion in developing owl optic tectum. *J Neurosci*, *12*(9), 3473-3484. https://doi.org/10.1523/jneurosci.12-09-03473.1992

Mogdans, J., & Knudsen, E. I. (1993). Early monaural occlusion alters the neural map of interaural level differences in the inferior colliculus of the barn owl. *Brain Res*, *619*(1-2), 29-38. https://doi.org/10.1016/0006-8993(93)91593-h

Moore, D. R., Hutchings, M. E., King, A. J., & Kowalchuk, N. E. (1989). Auditory brain stem of the ferret: some effects of rearing with a unilateral ear plug on the cochlea, cochlear nucleus, and projections to the inferior colliculus. *J Neurosci*, *9*(4), 1213-1222. https://doi.org/10.1523/jneurosci.09-04-01213.1989

Moore, D. R., & Irvine, D. R. (1981). Plasticity of binaural interaction in the cat inferior colliculus. *Brain Res*, *208*(1), 198-202. https://doi.org/10.1016/0006-8993(81)90632-6

Mowery, T. M., Penikis, K. B., Young, S. K., Ferrer, C. E., Kotak, V. C., & Sanes, D. H. (2017). The Sensory Striatum Is Permanently Impaired by Transient Developmental Deprivation. *Cell Rep*, *19*(12), 2462-2468. https://doi.org/10.1016/j.celrep.2017.05.083

Nakamoto, K. T., Jones, S. J., & Palmer, A. R. (2008). Descending projections from auditory cortex modulate sensitivity in the midbrain to cues for spatial position. *J Neurophysiol*, *99*(5), 2347-2356. https://doi.org/10.1152/jn.01326.2007

Nelken, I., & Young, E. D. (1994). Two separate inhibitory mechanisms shape the responses of dorsal cochlear nucleus type IV units to narrowband and wideband stimuli. *J Neurophysiol*, *71*(6), 2446-2462. https://doi.org/10.1152/jn.1994.71.6.2446

Nodal, F. R., Bajo, V. M., & King, A. J. (2012). Plasticity of spatial hearing: behavioural effects of cortical inactivation. *J Physiol*, *590*(16), 3965-3986. https://doi.org/10.1113/jphysiol.2011.222828

Nodal, F. R., Bajo, V. M., Parsons, C. H., Schnupp, J. W., & King, A. J. (2008). Sound localization behavior in ferrets: comparison of acoustic orientation and approach-to-target responses. *Neuroscience*, *154*(1), 397-408. https://doi.org/10.1016/j.neuroscience.2007.12.022

Nodal, F. R., Doubell, T. P., Jiang, Z. D., Thompson, I. D., & King, A. J. (2005). Development of the projection from the nucleus of the brachium of the inferior colliculus to the superior colliculus in the ferret. *J Comp Neurol*, *485*(3), 202-217. https://doi.org/10.1002/cne.20478

Nodal, F. R., Kacelnik, O., Bajo, V. M., Bizley, J. K., Moore, D. R., & King, A. J. (2010). Lesions of the auditory cortex impair azimuthal sound localization and its recalibration in ferrets. *J Neurophysiol*, *103*(3), 1209-1225. https://doi.org/10.1152/jn.00991.2009

Oertel, D., Wright, S., Cao, X. J., Ferragamo, M., & Bal, R. (2011). The multiple functions of T stellate/multipolar/chopper cells in the ventral cochlear nucleus. *Hear Res*, *276*(1-2), 61-69. https://doi.org/10.1016/j.heares.2010.10.018

Pachitariu, M., Sridhar, S., & Stringer, C. (2023). Solving the spike sorting problem with Kilosort. *bioRxiv*, 2023.2001.2007.523036. https://doi.org/10.1101/2023.01.07.523036

Palmer, A. R., & King, A. J. (1982). The representation of auditory space in the mammalian superior colliculus. *Nature*, *299*(5880), 248-249. https://doi.org/10.1038/299248a0

Paraouty, N., & Mowery, T. M. (2021). Early Sensory Deprivation Leads to Differential Inhibitory Changes in the Striatum During Learning. *Front Neural Circuits*, *15*, 670858. https://doi.org/10.3389/fncir.2021.670858

Paraouty, N., Yao, J. D., Varnet, L., Chou, C. N., Chung, S., & Sanes, D. H. (2023). Sensory cortex plasticity supports auditory social learning. *Nat Commun*, *14*(1), 5828. https://doi.org/10.1038/s41467-023-41641-8

Park, T. J., Grothe, B., Pollak, G. D., Schuller, G., & Koch, U. (1996). Neural delays shape selectivity to interaural intensity differences in the lateral superior olive. *J Neurosci*, *16*(20), 6554-6566. https://doi.org/10.1523/jneurosci.16-20-06554.1996

Parseihian, G., & Katz, B. F. G. (2012). Rapid head-related transfer function adaptation using a virtual auditory environment. *The Journal of the Acoustical Society of America*, *131*(4), 2948-2957. https://doi.org/10.1121/1.3687448

Pecka, M., Brand, A., Behrend, O., & Grothe, B. (2008). Interaural time difference processing in the mammalian medial superior olive: the role of glycinergic inhibition. *J Neurosci*, *28*(27), 6914-6925. https://doi.org/10.1523/jneurosci.1660-08.2008

Polley, D. B., Steinberg, E. E., & Merzenich, M. M. (2006). Perceptual learning directs auditory cortical map reorganization through top-down influences. *J Neurosci*, *26*(18), 4970-4982. https://doi.org/10.1523/JNEUROSCI.3771-05.2006

Popescu, M. V., & Polley, D. B. (2010). Monaural deprivation disrupts development of binaural selectivity in auditory midbrain and cortex. *Neuron*, *65*(5), 718-731. https://doi.org/10.1016/j.neuron.2010.02.019

Radtke-Schuller, S. (2018). *Cyto- and Myeloarchitectural Brain Atlas of the Ferret (Mustela putorius) in MRI Aided Stereotaxic Coordinates*. Springer Cham. https://doi.org/https://doi.org/10.1007/978-3-319-76626-3

Rayleigh, L. (1907). XII. On our perception of sound direction. *The London, Edinburgh, and Dublin Philosophical Magazine and Journal of Science*, *13*(74), 214-232. https://doi.org/10.1080/14786440709463595

Razak, K. A. (2011). Systematic representation of sound locations in the primary auditory cortex. *J Neurosci*, *31*(39), 13848-13859. https://doi.org/10.1523/jneurosci.1937-11.2011

Recanzone, G. H., Schreiner, C. E., & Merzenich, M. M. (1993). Plasticity in the frequency representation of primary auditory cortex following discrimination training in adult owl monkeys. *J Neurosci*, *13*(1), 87-103. https://doi.org/10.1523/jneurosci.13-01-00087.1993

Rhode, W. S., Oertel, D., & Smith, P. H. (1983). Physiological response properties of cells labeled intracellularly with horseradish peroxidase in cat ventral cochlear nucleus. *J Comp Neurol*, *213*(4), 448-463. https://doi.org/10.1002/cne.902130408

Ribic, A. (2020). Stability in the Face of Change: Lifelong Experience-Dependent Plasticity in the Sensory Cortex. *Front Cell Neurosci*, *14*, 76. https://doi.org/10.3389/fncel.2020.00076

Saldaña, E., Feliciano, M., & Mugnaini, E. (1996). Distribution of descending projections from primary auditory neocortex to inferior colliculus mimics the topography of intracollicular projections. *J Comp Neurol*, *371*(1), 15-40. https://doi.org/10.1002/(sici)1096-9861(19960715)371:1<15::Aid-cne2>3.0.Co;2-o

Schnupp, J. W., & Carr, C. E. (2009). On hearing with more than one ear: lessons from evolution. *Nat Neurosci*, *12*(6), 692-697. https://doi.org/10.1038/nn.2325

Schnupp, J. W., & King, A. J. (1997). Coding for auditory space in the nucleus of the brachium of the inferior colliculus in the ferret. *J Neurophysiol*, *78*(5), 2717-2731. https://doi.org/10.1152/jn.1997.78.5.2717

Slattery, W. H., 3rd, & Middlebrooks, J. C. (1994). Monaural sound localization: acute versus chronic unilateral impairment. *Hear Res*, *75*(1-2), 38-46. https://doi.org/10.1016/0378-5955(94)90053-1

Slee, S. J., & Young, E. D. (2014). Alignment of sound localization cues in the nucleus of the brachium of the inferior colliculus. *J Neurophysiol*, *111*(12), 2624-2633. https://doi.org/10.1152/jn.00885.2013

Smith, A. L., Parsons, C. H., Lanyon, R. G., Bizley, J. K., Akerman, C. J., Baker, G. E., Dempster, A. C., Thompson, I. D., & King, A. J. (2004). An investigation of the role of auditory cortex in sound localization using muscimol-releasing Elvax. *Eur J Neurosci*, *19*(11), 3059-3072. https://doi.org/10.1111/j.0953-816X.2004.03379.x

Smith, P. H., Joris, P. X., Carney, L. H., & Yin, T. C. (1991). Projections of physiologically characterized globular bushy cell axons from the cochlear nucleus of the cat. *J Comp Neurol*, *304*(3), 387-407. https://doi.org/10.1002/cne.903040305

Spirou, G. A., & Young, E. D. (1991). Organization of dorsal cochlear nucleus type IV unit response maps and their relationship to activation by bandlimited noise. *J Neurophysiol*, *66*(5), 1750-1768. https://doi.org/10.1152/jn.1991.66.5.1750

Stecker, G. C., Harrington, I. A., & Middlebrooks, J. C. (2005). Location coding by opponent neural populations in the auditory cortex. *PLoS Biol*, *3*(3), e78. https://doi.org/10.1371/journal.pbio.0030078

Strelnikov, K., Rosito, M., & Barone, P. (2011). Effect of audiovisual training on monaural spatial hearing in horizontal plane. *PLoS One*, *6*(3), e18344. https://doi.org/10.1371/journal.pone.0018344

Syka, J., & Popelár, J. (1984). Inferior colliculus in the rat: neuronal responses to stimulation of the auditory cortex. *Neurosci Lett*, *51*(2), 235-240. https://doi.org/10.1016/0304-3940(84)90557-3

Takakusaki, K., Chiba, R., Nozu, T., & Okumura, T. (2016). Brainstem control of locomotion and muscle tone with special reference to the role of the mesopontine tegmentum and medullary reticulospinal systems. *J Neural Transm (Vienna)*, *123*(7), 695-729. https://doi.org/10.1007/s00702-015-1475-4

Terreros, G., & Delano, P. H. (2015). Corticofugal modulation of peripheral auditory responses. *Front Syst Neurosci*, *9*, 134. https://doi.org/10.3389/fnsys.2015.00134

Thompson, G. C., & Masterton, R. B. (1978). Brain stem auditory pathways involved in reflexive head orientation to sound. *J Neurophysiol*, *41*(5), 1183-1202. https://doi.org/10.1152/jn.1978.41.5.1183

Thornton, J. L., Anbuhl, K. L., & Tollin, D. J. (2021). Temporary Unilateral Hearing Loss Impairs Spatial Auditory Information Processing in Neurons in the Central Auditory System. *Front Neurosci*, *15*, 721922. https://doi.org/10.3389/fnins.2021.721922

Tollin, D. J., Populin, L. C., Moore, J. M., Ruhland, J. L., & Yin, T. C. (2005). Sound-localization performance in the cat: the effect of restraining the head. *J Neurophysiol*, *93*(3), 1223-1234. https://doi.org/10.1152/jn.00747.2004

Tollin, D. J., & Yin, T. C. (2005). Interaural phase and level difference sensitivity in low-frequency neurons in the lateral superior olive. *J Neurosci*, *25*(46), 10648-10657. https://doi.org/10.1523/jneurosci.1609-05.2005

Torterolo, P., Zurita, P., Pedemonte, M., & Velluti, R. A. (1998). Auditory cortical efferent actions upon inferior colliculus unitary activity in the guinea pig. *Neurosci Lett*, *249*(2-3), 172-176. https://doi.org/10.1016/s0304-3940(98)00367-x

Trapeau, R., Aubrais, V., & Schönwiesner, M. (2016). Fast and persistent adaptation to new spectral cues for sound localization suggests a many-to-one mapping mechanism. *J Acoust Soc Am*, *140*(2), 879. https://doi.org/10.1121/1.4960568

Valzolgher, C., Verdelet, G., Salemme, R., Lombardi, L., Gaveau, V., Farné, A., & Pavani, F. (2020). Reaching to sounds in virtual reality: A multisensory-motor approach to promote adaptation to altered auditory cues. *Neuropsychologia*, *149*, 107665. https://doi.org/10.1016/j.neuropsychologia.2020.107665

van der Heijden, K., Rauschecker, J. P., de Gelder, B., & Formisano, E. (2019). Cortical mechanisms of spatial hearing. *Nat Rev Neurosci*, *20*(10), 609-623. https://doi.org/10.1038/s41583-019-0206-5

Van Wanrooij, M. M., & Van Opstal, A. J. (2004). Contribution of head shadow and pinna cues to chronic monaural sound localization. *J Neurosci*, *24*(17), 4163-4171. https://doi.org/10.1523/JNEUROSCI.0048-04.2004

Van Wanrooij, M. M., & Van Opstal, A. J. (2005). Relearning sound localization with a new ear. *J Neurosci*, *25*(22), 5413-5424. https://doi.org/10.1523/jneurosci.0850-05.2005

Van Wanrooij, M. M., & Van Opstal, A. J. (2007). Sound localization under perturbed binaural hearing. *J Neurophysiol*, *97*(1), 715-726. https://doi.org/10.1152/jn.00260.2006

Walker, K. M. M., Bizley, J. K., King, A. J., & Schnupp, J. W. H. (2011). Multiplexed and Robust Representations of Sound Features in Auditory Cortex. *The Journal of Neuroscience*, *31*(41), 14565-14576. https://doi.org/10.1523/jneurosci.2074-11.2011

Watson, C. J. G., Carlile, S., Kelly, H., & Balachandar, K. (2017). The Generalization of Auditory Accommodation to Altered Spectral Cues. *Scientific Reports*, *7*(1), 11588. https://doi.org/10.1038/s41598-017-11981-9

Winer, J. A., Larue, D. T., Diehl, J. J., & Hefti, B. J. (1998). Auditory cortical projections to the cat inferior colliculus. *J Comp Neurol*, *400*(2), 147-174.

Woods, T. M., & Recanzone, G. H. (2004). Visually induced plasticity of auditory spatial perception in macaques. *Curr Biol*, *14*(17), 1559-1564. https://doi.org/10.1016/j.cub.2004.08.059

Wright, B. A., & Zhang, Y. (2009). A review of the generalization of auditory learning. *Philosophical Transactions of the Royal Society B: Biological Sciences*, *364*(1515), 301-311. https://doi.org/doi:10.1098/rstb.2008.0262

Xiong, Q., Znamenskiy, P., & Zador, A. M. (2015). Selective corticostriatal plasticity during acquisition of an auditory discrimination task. *Nature*, *521*(7552), 348-351. https://doi.org/10.1038/nature14225

Xu, L., & Middlebrooks, J. C. (2000). Individual differences in external-ear transfer functions of cats. *J Acoust Soc Am*, *107*(3), 1451-1459. https://doi.org/10.1121/1.428432

Yan, J., & Ehret, G. (2002). Corticofugal modulation of midbrain sound processing in the house mouse. *European Journal of Neuroscience*, *16*(1), 119-128. https://doi.org/https://doi.org/10.1046/j.1460-9568.2002.02046.x

Yan, W., & Suga, N. (1998). Corticofugal modulation of the midbrain frequency map in the bat auditory system. *Nat Neurosci*, *1*(1), 54-58. https://doi.org/10.1038/255

Zahorik, P., Bangayan, P., Sundareswaran, V., Wang, K., & Tam, C. (2006). Perceptual recalibration in human sound localization: learning to remediate front-back reversals. *J Acoust Soc Am*, *120*(1), 343-359. https://doi.org/10.1121/1.2208429

Zhou, X., & Jen, P. H. (2005). Corticofugal modulation of directional sensitivity in the midbrain of the big brown bat, Eptesicus fuscus. *Hear Res*, *203*(1-2), 201-215. https://doi.org/10.1016/j.heares.2004.12.008

Zonooz, B., & Van Opstal, A. J. (2019). Differential Adaptation in Azimuth and Elevation to Acute Monaural Spatial Hearing after Training with Visual Feedback. *eNeuro*, *6*(6). https://doi.org/10.1523/ENEURO.0219-19.2019

Zurita, P., Villa, A. E., de Ribaupierre, Y., de Ribaupierre, F., & Rouiller, E. M. (1994). Changes of single unit activity in the cat's auditory thalamus and cortex associated to different anesthetic conditions. *Neurosci Res*, *19*(3), 303-316. https://doi.org/10.1016/0168-0102(94)90043-4